Role of Histone Methyltransferase SET-4 in Developmental Plasticity and Longevity

by

Colin Edward Delaney

A dissertation submitted in partial fulfillment
of the requirements for the degree of
Doctor of Philosophy
(Cell and Developmental Biology)
In the University of Michigan
2017

Doctoral Committee:

Associate Professor Ivan Patrick Maillard, Chair
Assistant Professor Benjamin Allen
Associate Professor Gyorgyi Csankovszki
Adjunct Associate Professor Patrick J Hu
Professor Scott Pletcher

Colin Edward Delaney

cedelane@umich.edu

Orcid ID: 0000-0001-6880-6973

DEDICATION

To my friends and family:

Thank you so much for your support through the difficult times.

I will make it up to you.

ACKNOWLEDGEMENTS

First, I want to thank Patrick Hu for welcoming me in to his laboratory. His enthusiastic support for this project never flagged even when the way forward was unclear. Patrick emphasized experimental rigor, openness about data with the broader community, and a commitment to precision in language. Patrick gave me the space to pursue both science and policy career tracks, even when that meant extended absences from the lab. I benefited greatly from his example.

Second, I thank my committee members, Drs. Ivan Maillard, Gyorgyi Csankovszki, Ben Allen, and Scott Pletcher. Their guidance both during meetings and informally was tremendously valuable in shaping how I approached these projects. I am confident I will benefit from their shared insight both in and out of the lab as my career develops.

Third, I want to thank Drs. Billy Tsai and Diane Fingar, who provided me with additional opportunities to teach. I was fortunate to begin my graduate instructor under an exceptional head GSI, Dr. Brandon Carpenter, whose leadership and grace I tried hard to emulate when I took on the same role. Diane was very open to ideas how best to restructure the course and online resources, and we created a more efficient interface for both instructors and students. I certainly became a better instructor over those three semesters thanks to the example set by Billy, Diane, Brandon, and the faculty instructors in lecture and discussion.

Without my great lab mates, this undertaking would have been greatly diminished. Katie Dumas taught me worms and encouraged me to join the Science, Technology, and Public Policy certificate program, which I have found tremendously enriching. Albert Chen's relentless positivity was a reminder that there is fulfilment in the constant pursuit of personal and professional improvement. Joe Kruempel's encyclopedic knowledge of the scientific literature made for exciting conversations that opened new ways for me to think about science. Titan Shi's steadiness and natural scientific ability was matched only by his lab stewardship and willingness to share our limited resources. Omar Itani's max efficiency set the bar for productivity. Omar's

comfort with positive, negative, and/or confounded data was remarkable. I try to live up to Omar's example every day.

How can I say about Jacqueline Graniel? Jackie worked directly with me as a PREP student for a year, and she has continued to stay involved in the success of my projects for the last two years as well. Along the way, she has become a dear friend and confidante. I am humbled by her generosity, commitment, and acumen, both in the lab and in life. I will always be grateful for her support am excited to see how her promising career unfolds.

I wish to acknowledge my coauthors, collaborators, and advisors. First, I must thank Scott Leiser for hosting me for the final year of my program. He has been generous with his time, space, and reagents, as well as sharing his perspectives on science careers. I thank Stephan Flibotte, Donald Moerman, Manjushe Pande, and Rich McEachin for help with bioinformatics analysis. I thank Ashootosh Tripathi, David Sherman, Erik Anderson, and Xantha Karp for their help optimizing pheromone extractions. Yali Dou, Shirley Lee, and Brian Shay were instrumental in designing and performing functional biochemical assays. Scott Rothbart validated the specificity of anti-histone antibodies. I thank John Kim and his lab, including Natasha Weiser, Amelia Alessi, Mallory Freeberg, and Danny Yang for help with reagents and training.

Throughout my many years at UM I have benefitted from training with exceptional scientists, including Drs, John K. Fink, Shirley Rainier, Xinping Zhao, Peter Hedera, Andrea Todisco, and Maria Mao; Donald Thomas, Debra Tokarz, Melanie Bui, and David Alvarado. As a member of the Geriatrics Center, I received friendship, mentorship, and collaborative engagement from Dr. Bruce Richardson and his current and former lab members, Drs. Faith Strickland, Anura Hewagama, Dipak Patel, Gabriella Gorelik, and Donna Ray. In many ways, I am sharing this dissertation now because of the unwavering support I received from Dr. Raymond Yung. He introduced me to the field of epigenetics and entrusted me with conducting independent research as a technician. My success in Ray's lab was also due to the support I received from Drs. Annabelle Julius, Anjali Desai, and especially Sanjay K. Garg. Sanjay is an exceptional person and friend, and he was the catalyst that allowed us to take our work to the next level. I had the good fortune to work with extremely competent technicians, Erin Harding, Lisa Abernathy, Jianhau Liu, and Genevieve Ray. I thank Dr. Amiya Ghosh, Theresa Mau and Martin O'Brien for their generosity with equipment. It has been my honor to work with you all.

PREFACE

No one wants to live forever. However, everyone prizes their vitality. Sadly, the aging process decreases physical wellbeing and is a major risk factor for the onset of chronic illnesses like metabolic syndrome, atheroschlerosis, cancer, and dementia. Scientific investigations over the last several decades have revealed that the phenomenon of aging is not a stochastic decay but is in fact regulated by signaling pathways activated both systemically and within tissues. These genetic programs are under the control of transcription factors that either activate or inhibit genes associated with longevity. FoxO transcription factor activity is strongly associated with increased wellness and longevity. Insulin-like signaling (IIS) inhibits FoxO activity, and decreasing insulin-like signaling extends lifespan. Importantly, IIS is subject to regulation by environmental stimuli, including diet. As such, understanding how environmental interventions activate conserved FoxO longevity pathways may lead to new knowledge that slows or prevents aging.

FoxO transcription factors operate in nuclei that contain DNA arranged in a complex chromatin architecture. Whether DNA binding sites are accessible depends on chemical modifications to chromatin. This extra layer of transcriptional regulation is known as epigenetics. Although changes in epigenetic modifications have been described in aging and epigenetic patterns are disordered in diseases of aging, remarkably little mechanistic work has shown how these marks contribute to FoxO regulation. It is unknown whether FoxO transcription factors require certain epigenetic partner enzymes to activate longevity genes. This gap in knowledge led to us undertaking investigations to increase our understanding how epigenetic factors promote conserved mechanisms of aging. Like IIS, epigenetic programs are sensitive to environmental perturbations, and intervening in an individual may have multigenerational effects. This work is only one step in a path that may yet lead to a fuller understanding how epigenetic modifications contribute to vitality and to therapies that may show exponential benefits across generational time.

TABLE OF CONTENTS

LIST OF TABLES

LIST OF SUPPLEMENTAL TABLES

LIST OF FIGURES

LIST OF SUPPLEMENTARY FIGURES

ABSTRACT

FoxO transcription factors promote longevity across diverse organisms through upregulation of parallel stress responses. Therefore, understanding how FoxO activity is regulated may provide insights for improving overall vitality in an aging population. Insulin and insulin-like growth factor signaling (IIS) is highly conserved across metazoans and antagonizes FoxO function. Decreasing IIS pathway activity increases lifespan in model organisms and may be conserve in humans. This association between FoxO transcription factors and longevity was first discovered in studies using the free living nematode *Caenorhabditis elegans*. In *C. elegans*, the DAF-2/IIS pathway also influences dauer diapause. Dauer is a state of larval developmental diapause that occurs in response to stressful environmental conditions including population stress perceived through elaboration of a complex pheromone mixture. Mutations that reduce DAF-2/IIS pathway activity arrest as dauers in a manner requiring the FoxO transcription factor DAF-16. When AKT activity is reduced, DAF-16/FoxO translocates to the nucleus, where it is inhibited by EAK-7/TLDC1, a conserved protein of unknown function. *eak-7;akt-1* double mutants always arrest as dauers. We designed a forward genetic screen to discover novel regulators of DAF-16/FOXO by mutagenizing *eak-7;akt-1* worms and looking for suppressors of *eak-7;akt-1* dauer arrest (*seak* mutants). Whole genome sequencing revealed one *seak* mutant strain harbored a mutation in *set-4*, which encodes a conserved histone H4 lysine 20 (H4K20) methyltransferase. SET-4 is required for dauer arrest in both reduced IIS mutant backgrounds and in response to dauer inducing pheromone. SET-4 promotes dauer arrest only in XX hermaphrodites, not XO males, consistent with existing data that SET-4 participates in dosage compensation of X chromosomes. We found that neuron-specific overexpression of *set-4* rescued dauer arrest in *set-4* mutants to a similar extent as the native promoter. SET-4 acts together with DAF-16/FoxO in specific sensory neurons to silence expression of the X-linked insulin-like peptide *ins-9*. Loss of *ins-9* rescues the

dauer-defective phenotype observed in *set-4* mutants in response to pheromone. *ins-9* itself is also sensitive to dauer pheromone. Taken together, these data implicate chromatin remodeling as a novel mechanism that regulates FoxO transcription factor activity. Since epigenetic marks like histone methylation are sensitive to environmental interventions, these findings may lead to new therapies for chronic diseases associated with aging.

Chapter 1

Introduction

Conserved metabolic pathways influence development and longevity

Aging is associated with increased risks of disease, including cardiovascular disease, diabetes, dementia, autoimmunity, frailty, and cancer (Niccoli and Partridge, 2012). Previously, aging was considered a slow stochastic process in which cellular function declines because of accumulation of damaged DNA and proteins. While such molecular phenotypes are some of the hallmarks of aging and attributable to errors in DNA and/or protein synthesis (Lopez-Otin et al., 2013), the accumulation of these defects may also be under the control conserved metabolic pathways. These pathways participate in nutrient-sensing, cellular energy balance, stress responses, and growth factor signaling. Extensive crosstalk exists between these signaling programs that regulate gene expression changes at the level of transcription. In general, signals that indicate low nutrient availability or moderate stress levels combine to promote enhanced stress resistance and longevity. Increased lifespan is also associated with delayed incidence of disease, increasing the quality of life in addition to overall length (Selman and Withers, 2011)

FoxO transcription factors promote longevity and stress resistance

Conserved pathways associated with aging converge on FoxO transcription factors and modulate their activity. FoxO transcription factors are members of the Forkhead superfamily, possessing a Forkhead box DNA binding domain (Kaestner et al., 2000). Forkhead transcription factors have been found in animals, yeast, and fungi. Mammals express four FoxO proteins: FoxO1, FoxO3, FoxO4, and FoxO6 (Greer and Brunet, 2005). The invertebrate model organisms *Drosophila melanogaster* and *Caenorhabditis elegans* express FoxO orthologs from a single locus. All

orthologs bind the same consensus sequence (Liu et al., 2004); however, distinct expression patterns or differentially spliced isoforms may underlie specific effects attributed to FoxO variants (Eijkelenboom and Burgering, 2013).

Animals exhibiting enhanced FoxO transcription factor activity demonstrate increased lifespan. (Bluher et al., 2003; Giannakou et al., 2004; Hwangbo et al., 2004; Kenyon et al., 1993; Yamamoto and Tatar, 2011). This phenomenon may be conserved in humans. Certain FoxO1 and FoxO3A polymorphisms are enriched in centenarians, further supporting the important role of FoxO in longevity (Anselmi et al., 2009; Flachsbart et al., 2009; Li et al., 2009; Willcox et al., 2008).

How do FoxO transcription factors promote longevity? FoxO activity can promote either cell survival or apoptosis depending on upstream environmental cues (Accili and Arden, 2004) and may interact with p53 (Pinkston et al., 2006; Renault et al., 2011). Recent work has linked loss of FoxO with diseases associated with aging. FoxO proteins decrease oxidative stress in osteoblast lineages, promoting the maintenance of skeletal bone integrity, which may reduce age-related frailty and osteoporosis (Ambrogini et al., 2010; Li et al., 2010; Rached et al., 2010). FoxO's role in responding to oxidative stress has also been implicated in Alzheimer's Disease and diabetes (Manolopoulos et al., 2010). The *C. elegans* ortholog DAF-16/FoxO has been shown to prevent cell death due to poly-glutamine aggregations in models of muscular dystrophy and Alzheimer's (Hsu et al., 2003; Oh and Kim, 2013). Ablation of FoxO1, FoxO3, and FoxO4 in mice leads to lymphoma and hemangioma, demonstrating that these transcription factors act as tumor suppressors (Paik et al., 2007).

Insulin and Insulin-like growth factor signaling (IIS) control FoxO activity

Insulin and insulin-like growth factor signaling (IIS) is highly conserved across metazoans and acts to inhibit FoxO activity (Fig. 1.1) (Woods and Rena, 2002). Insulin or insulin-like peptides bind to receptor tyrosine kinases, leading to autophosphorylation of their intracellular kinase domains. This activation recruits the insulin receptor substrate and PI3 kinase, which catalyzes the conversion of phosphatidylinositol (4,5)-bisphosphate (PIP2) into phosphatidylinositol (3,4,5)=triphosphate (PIP3) (Vanhaesebroeck and Alessi, 2000). Signaling proteins possessing

pleckstrin homology domains including PDK and Akt/PKB are then recruited to the plasma membrane. PDK then phosphorylates and activates Akt (Paradis et al., 1999). Activated Akt acts on many substrates containing an RXRXXS/T phosphorylation motif (Obata et al., 2000). After translocating to the nucleus, Akt phosphorylates FoxO transcription factors at multiple conserved consensus sites. Phosphorylation of FoxOs leads to their nuclear export and sequestration in the cytosol (Brunet et al., 1999). Binding of 14-3-3 proteins to phosphorylated FoxO blocks the ability of FoxO to bind DNA and masks the nuclear localization sequence, re-enforcing nuclear exclusion (Brunet et al., 2002; Cahill et al., 2001; Obsilova et al., 2005). Phosphorylation of FoxO by Akt triggers ubiquitination and subsequent degradation (Hu et al., 2004; Huang et al., 2004). Therefore, increased insulin-like signaling suppresses FoxO mediated stress responses and associated longevity.

C. elegans is a model for developmental pathways linked to longevity

Much of the logic of the insulin-like signaling pathway came from epistasis experiments in *C. elegans* using mutant strains that exhibited abnormal rates of entry into an alternative developmental larval state known as dauer (discussed below) (Klass and Hirsh, 1976). Mutations in the *daf-2* gene cause increased rates of dauer arrest and also doubled adult lifespans relative to wild type animals (Kenyon et al., 1993). This greatly enhanced longevity was entirely dependent on the presence of *daf-16*; both *daf-16* and *daf-16;daf-2* mutant strains were found to be short-lived. DAF-2 was later identified as the sole insulin-like growth factor receptor homolog in worms (Kimura et al., 1997), while DAF-16 is the single FoxO transcription factor (Lin et al., 1997; Ogg et al., 1997). Further pathway analysis revealed that the entire IIS pathway is conserved in *C. elegans* (Fig. 1.1) (Engelman et al., 2006).

The simplicity of *C. elegans* is useful for dissecting conserved mechanisms of aging. First, these animals are small but easily manipulated, and can be grown at large numbers. Second, these animals typically live for only two to three weeks. Third, they are highly genetically tractable with mutants available for most genes, including viable *daf-16* null mutants. Many of these mutations produce visible phenotypes that can aid in pathway dissection or forward genetic mutagenesis screens. Importantly, they also exhibit developmental plasticity in conditions of high or low environmental stress that is DAF-16/FoxO dependent.

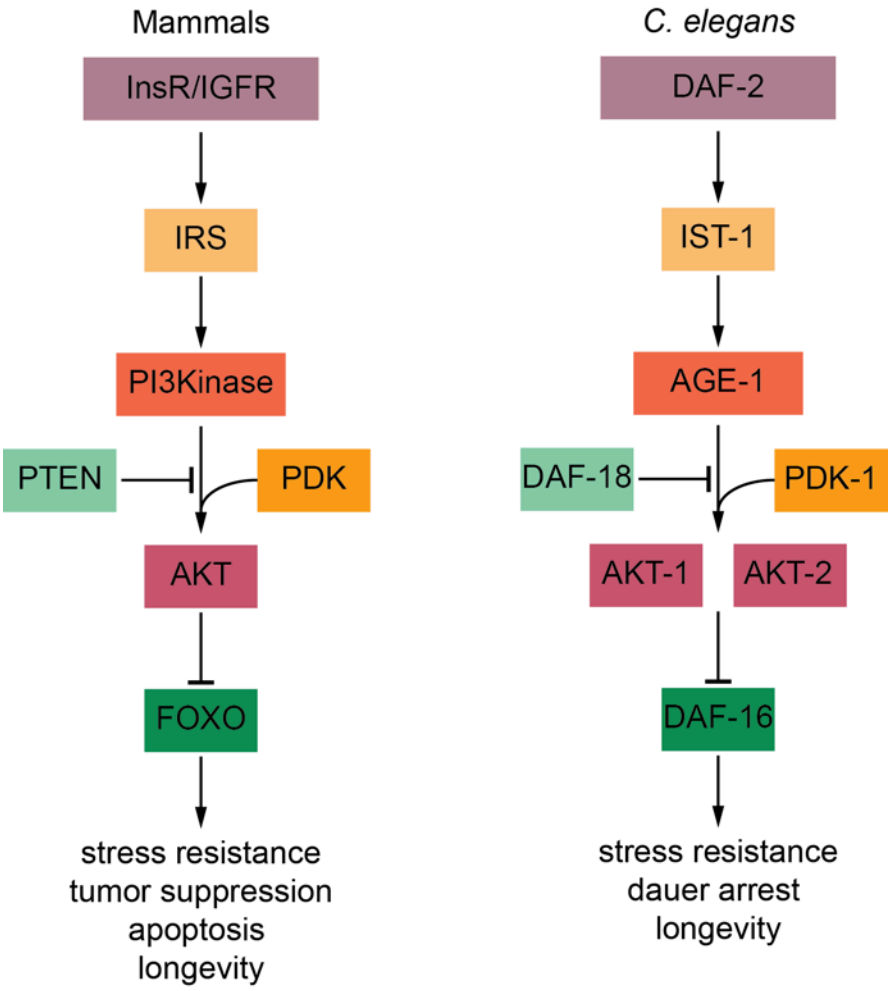

Figure 1.1. Insulin and insulin-like growth factor signaling (IIS) is conserved. The IIS pathways and downstream consequences for mammals and C. elegans are shown. Adapted (Engelman et al., 2006).

Under replete conditions where food is plentiful, *C. elegans* develops from an embryo through four larval stages (L1-L4) to become reproductively mature in two to four days depending on temperature. However, animals that face adverse environmental conditions like high heat, lack of food, or overcrowding will enter a morphologically distinct larval diapause known as dauer (Fig. 1.2) (Cassada and Russell, 1975). Compared to animals continuing reproductive development, dauers have enhanced resistance to stresses. They have a thickened, specialized cuticle to survive harsh environments (Blaxter, 1993) and are protected against endogenous oxidative stress (Honda et al., 2008). During diapause, animals cease feeding, and a buccal plug occludes their constricted pharynx. Dauers develop distinct anatomical features that facilitate dispersal from the undesirable environment. Cuticular ridges called alae allow fast movement (Popham and Webster, 1978) while increased dendritic branching and neuromuscular connections permit dauer-specific behaviors like nictation (Dixon et al., 2008; Schroeder et al., 2013). Dauers generate energy via the glyoxylate pathway, converting stored fat to glucose (Wadsworth and Riddle, 1989). The dauer state can persist for months, far longer than typical adult lifespans (Klass and Hirsh, 1976). Once they sense improved conditions, animals will resume reproductive development at L4 and have a typical adult lifespan.

The decision whether to proceed with reproductive development or arrest as dauers is mediated through multiple sensory inputs. Animals detect an unknown bacterial food signal as well as a mixture of modified ascarosides collectively known as dauer pheromone (Golden and Riddle, 1984; Ludewig and Schroeder, 2013). This pheromone is produced constitutively and may be how animals sense population density. Several different ascaroside derivatives have been found to be active in the pheromone mixture at different potencies (Butcher et al., 2007). In combination with temperature sensing AFD neurons (Mori and Ohshima, 1995), these signals are integrated into a binary choice of developmental fates.

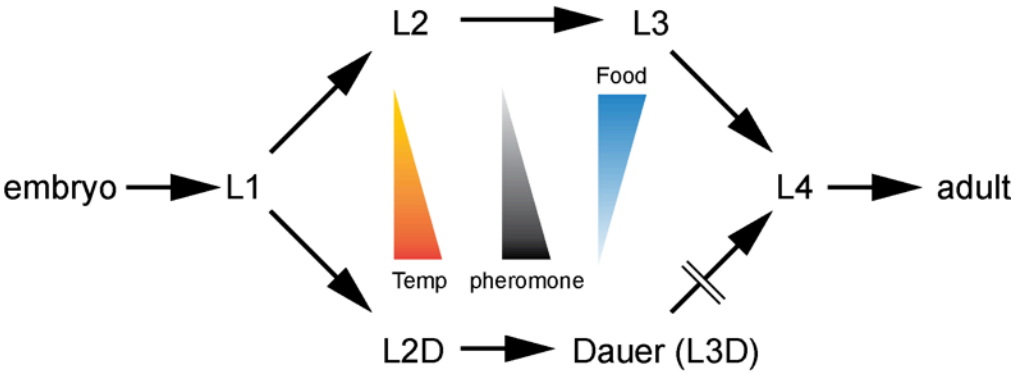

Figure 1.2. *C. elegans* larval development. Animals develop through four larval stages between embryo and adult stages. Under conditions of high temperature, high population density measured by pheromone, and low food, L1s will develop in to L2D larvae and then arrest as dauer larvae. Once conditions improve, dauer larvae will molt into the L4 stage and proceed with reproductive development.

Multiple neuroendocrine signaling pathways transduce environmental cues into developmental strategy (Birnby et al., 2000; Ren et al., 1996; Schackwitz et al., 1996; Thomas et al., 1993; Vowels and Thomas, 1992). The characterization of abnormal dauer formation mutants (daf) has identified two classes of genes that make up components of conserved pathways that control the dauer decision (Fig. 1.3). Mutants that exhibited highly penetrant dauer arrest under permissive conditions were designated dauer-constitutive, or daf-c, while animals that bypassed dauer when animals typically would arrest were dauer defective, or daf-d. The guanylyl cyclase DAF-11 may function most upstream in regulation of dauer arrest via regulation of cGMP gated ion channels TAX-2 and TAX-4 (Birnby et al., 2000; Vowels and Thomas, 1994). DAF-11 also promotes expression of a TGFβ-like signaling pathway ligand *daf-7* that binds to type 1 and type 2 TGFβ receptors DAF-1 and DAF-4, respectively (Estevez et al., 1993; Georgi et al., 1990; Ren et al., 1996). These receptors activate SMAD transcription factors DAF-8, DAF-14, but inhibit the SMAD/SNO-SKI complex of DAF-3 and DAF-5 (da Graca et al., 2004; Park et al., 2010; Tewari et al., 2004). TGFβ and cGMP act in parallel to the IIS pathway but also interact through upregulation of the insulin-like peptide *daf-28* (Li et al., 2003; Ogg et al., 1997). DAF-28 activates DAF-2/IGFR, leading to an AGE-1/PI3Kinase phosphorylation cascade and subsequent phosphorylation cascade of PDK-1, AKT-1 and AKT-2 (Fig. 1.1) (Kimura et al., 1997; Morris et al., 1996; Paradis et al., 1999; Paradis and Ruvkun, 1998). The PTEN tumor suppressor ortholog DAF-18 antagonizes this phosphorylation cascade by dephosphorylating, preventing AKT activation (Gil et al., 1999; Mihaylova et al., 1999; Ogg and Ruvkun, 1998). AKT phosphorylates DAF-16/FoxO, leading to its exclusion from the nucleus and sequestration in the cytosol in a manner dependent on 14-3-3 proteins FTT-2 and PAR-5 (Berdichevsky et al., 2006; Lee et al., 2001; Lin et al., 1997; Lin et al., 2001; Ogg et al., 1997). Importantly, *daf-11/guanylyl cyclase*, *daf-7/TGFβ*, and insulin-like peptide ligands for DAF-2/IGFR are expressed in subsets of sensory neurons that have been shown to be important for dauer arrest (Birnby et al., 2000; Ren et al., 1996; Ritter et al., 2013).

Signals from these conserved genetic pathways converge onto a sterol hormone biosynthesis pathway. The Rieske oxygenase DAF-36 functions upstream of a cytochrome P450 steroid monooxygenase DAF-9 in the synthesis of bile-acid like hormones known as dafachronic acids (DAs) (Gerisch and Antebi, 2004; Gerisch et al., 2001; Jia et al., 2002; Mak and Ruvkun, 2004; Motola et al., 2006; Rottiers et al., 2006). *daf-9* is constitutively expressed in XXX

neuroendocrine cells; however, *daf-9* expression in the hypodermis is reported to dramatically rise in late L2, driving forward the commitment to reproductive development (Schaedel et al., 2012). DAF-12, a nuclear hormone receptor transcription factor distantly related to the vitamin D and thyroid hormone receptors, acts furthest downstream in the dauer decision (Antebi et al., 2000). DAs ligand DAF-12 to promote dauer bypass; unliganded DAF-12 promotes dauer arrest through association with DIN-1 (Ludewig et al., 2004). Animals harboring a *daf-9* null allele are non-conditional dauer unless *daf-12* is also disrupted or if exogenous DA is added to the media (Gerisch et al., 2001; Sharma et al., 2009).

The dauer phenotype can be used as a proxy for IIS regulation of lifespan. Mutations in IIS cause enhanced dauer arrest in a temperature dependent manner. Strong alleles of *daf-2/igfR* are daf-c at 25°C while *akt-1* null alleles develop reproductively at 25°C but arrest at 27°C (Ailion and Thomas, 2000). Disruption of either *daf-2* or *akt-1* enhances longevity (Kenyon et al., 1993; Paradis and Ruvkun, 1998). Loss of *daf-16/foxo* is daf-d, and suppresses either *daf-2* or *akt-1* mediated dauer arrest. Similarly, *daf-16/foxo* mutants fully suppress the lifespan extension of *daf-2* and *akt-1*. Therefore, although dauer arrest is not specific to the IIS pathway, dauer is an easily observed readout of DAF-16/FoxO activity during development. Therefore, genetically manipulating the dauer phenotype is useful for finding novel conserved regulatory inputs on DAF-16/FoxO that may be associated with enhanced stress resistance and longevity.

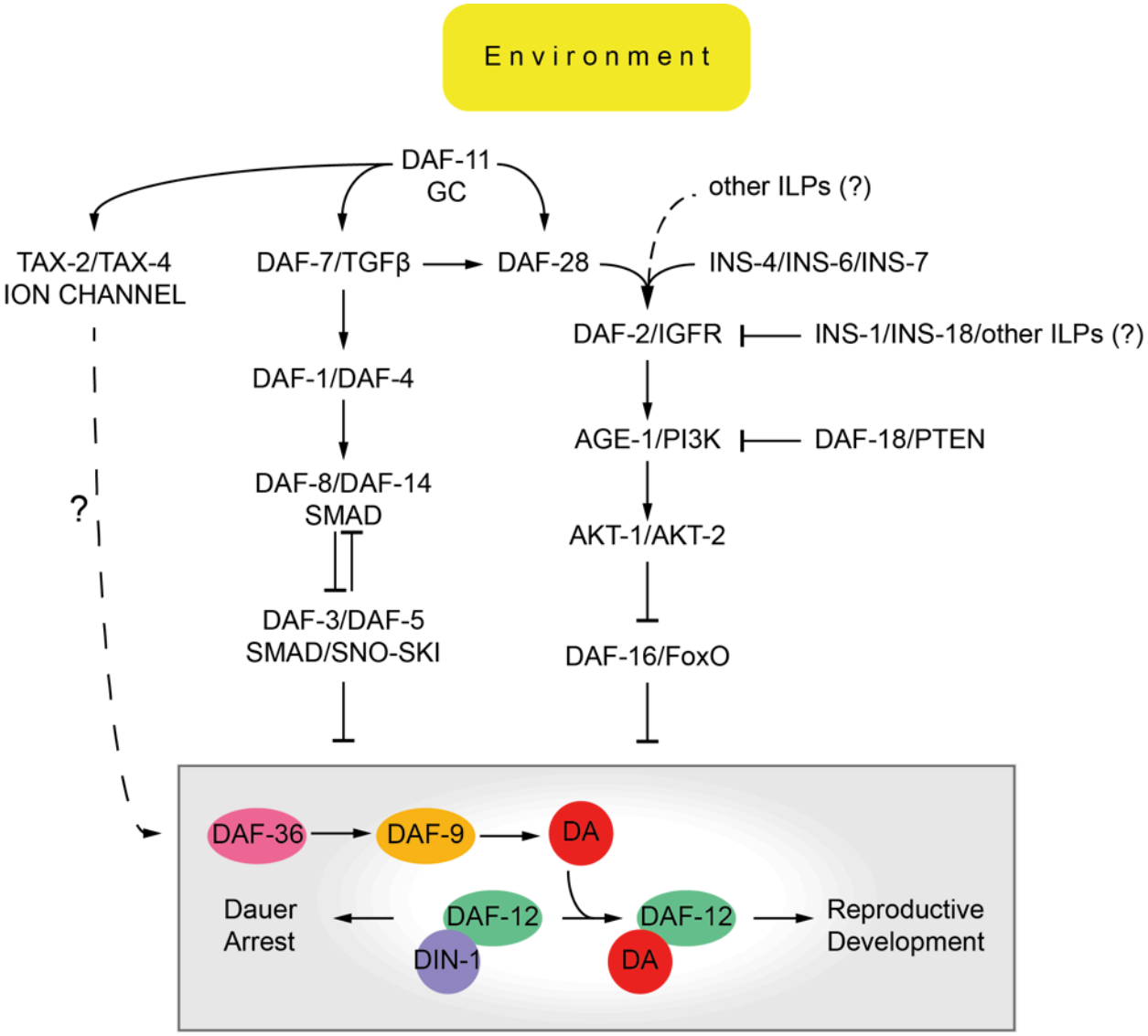

Figure 1.3. Multiple genetic pathways regulate dauer formation. Conserved signal transduction pathways acting in parallel converge on dafachronic acid (DA) hormone biosynthesis (boxed) In the presence of DA, DAF-12 drives reproductive development. In the absence of DA, DAF-12 promotes dauer arrest.

Insulin-like peptides regulate DAF-16/FoxO activity

In contrast to the genetic simplicity of the insulin-like signaling pathway, *C. elegans* expresses 40 insulin-like peptides (ILPs), many times more than either mammals or flies (Lau and Chalasani, 2014). These 40 ILPs are divergent in their structures and functions, and are grouped into subtypes based on their predicted disulfide bonding patterns (Pierce et al., 2001). Type γ ILPs are believed to have the canonical disulfide bonds found in most insulins. Type β ILPs may have one additional disulfide bond, while Type α ILPs may lack the conserved A6-A11 cysteine bridge. The type β INS-1 and type γ INS-18 are most like mammalian insulin, containing a C-peptide between the B- and A-peptides that is cleaved off during maturation. It is believed both INS-1 and INS-18 antagonize DAF-2/IGFR and therefore promote dauer arrest (Hung et al., 2014; Pierce et al., 2001). Type β INS-2 through INS-9 along with DAF-28 have an upstream F-peptide that is cleaved off and lack a C-peptide. Many Type β ILPs have been shown to be DAF-2/IGFR agonists and therefore inhibitors of DAF-16/FoxO (Fig. 1.3) (Hung et al., 2014; Li et al., 2003; Pierce et al., 2001).

ILPs are synthesized in many tissues, and their site of expression may change throughout development (Fernandes de Abreu et al., 2014; Ritter et al., 2013). Because of their number, overlapping expression patterns, and functional redundancy, genetic analysis of the effects of ILPs on DAF-16/FoxO activity has proven difficult to interpret. For example, a *daf-28* loss of function allele causes a weak dauer phenotype, but dauer penetrance can be greatly enhanced in combination with a deletion allele that eliminated three other type β ILPs, *ins-4*, *ins-5*, and *ins-6* (Hung et al., 2014). A systemic investigation recently clarified the roles of some ILPs in development, dauer arrest, longevity, as well as ILP crosstalk (Fernandes de Abreu et al., 2014). What emerges is complex *ins*-to-*ins* signaling across tissues. Both DAF-2/IGFR agonists and antagonists are synthesized in the same amphid sensory neurons, suggesting regulation of IIS is subject to tight control. Downstream of the amphids, *ins-7* expression in the intestine has been hypothesized to coordinate DAF-16/FoxO activity across tissues (Hung et al., 2014; Murphy et al., 2007). There is evidence supporting feedback regulation on agonist *daf-28* and antagonist *ins-18* (Hahm et al., 2009).

ILP expression is also dependent on other developmental signals, including those associated with the dauer decision. *daf-28* expression requires both DAF-11 and DAF-7 ((Li et al., 2003).

Similarly, exposure to dauer pheromone down-regulates *daf-28* and changes the spatial expression of *ins-6* from ASI to ASJ neurons, associated with dauer entry and exit, respectively (Cornils et al., 2011). Both pheromone exposure and disruption of cGMP synthesis has been shown to extend lifespan in *C. elegans* through activation of DAF-16/FoxO (Hahm et al., 2009; Lans and Jansen, 2007; Ludewig et al., 2013). Although the role of pheromone in C. elegans longevity has been questioned (Alcedo and Kenyon, 2004), one component of pheromone also extends lifespan in mice (Park et al., 2014). Unexpectedly, ILPs may also be regulated post-translationally. During dauer both INS-7 and INS-35 produced in the intestine are no longer secreted into the body cavity; rather, they are trafficked into the intestinal lumen and degraded (Matsunaga et al., 2016). Taken together, these data demonstrate ILPs participate in the integration of diverse environmental cues and through the canonical insulin-like signaling pathway regulate DAF-16/FoxO mediated dauer arrest.

Evidence for regulation of DAF-16/FoxO in parallel with DAF-2/IIS

While the upstream signals feeding into insulin-like signaling have proven complex, the mechanism by which the canonical IIS pathway inhibits DAF-16/FoxO is clear. Akt phosphorylates FoxO on conserved motifs, leading to nuclear export of FoxO. Mutation of all four canonical Akt phosphorylation sites leads to DAF-16/FoxO constitutive nuclear localization (Lee et al., 2001; Lin et al., 2001). Surprisingly, however, this nuclear accumulation of DAF-16/FoxO did not lead to a constitutive dauer phenotype nor to enhanced longevity (Lin et al., 2001). Also, knockdown of the 14-3-3 protein *ftt-2* increases DAF-16/FoxO nuclear localization but does not lead to dauer arrest (Li et al., 2007). The suggestion that parallel regulatory mechanisms act on DAF-16/FoxO independently of its subcellular localization was recently substantiated. Physical association between DAF-16/FoxO and the conserved nuclear protein HCF-1 has been shown to decrease transcription of genes associated with the stress response (Li et al., 2008). This association does not alter nuclear localization, consistent with HCF-1 acting in parallel with IIS.

FoxO proteins are extensively modified post-translationally with functional consequences. In addition to phosphorylation by Akt, cytokines can trigger the poly-ubiquitination and subsequent degradation of FoxOs (Hu et al., 2004). Mono-ubiquitination, on the other hand, promotes

FoxO4 nuclear localization and activity (Brenkman et al., 2008; van der Horst et al., 2006). Acetylation has been observed at multiple FoxO lysine residues. Acetylation within the DNA binding domain is associated with decreased activity but not with altered localization (Matsuzaki et al., 2005; Tsai et al., 2007). Acetylation can be reversed by the NAD-dependent lysine deacetylase Sir2, a protein that may promote longevity in model organisms (Ha and Huh, 2011; Viswanathan and Guarente, 2011). The lysine methyltransferase Set9 also methylates mammalian FOXO3 at lysine 271 (Calnan et al., 2012). This modification does not alter FOXO localization but may increase transcriptional activity at the expense of overall stability. Similarly, arginine methylation of DAF-16/FoxO promotes longevity by blocking phosphorylation by AKT (Takahashi et al., 2011).

Epigenetic mechanisms may also be important for DAF-16/FoxO activity. For example, DAF-16/FoxO interacts with the *C. elegans* SWI-SNF chromatin remodeling complex to promote transcription of its target genes (Riedel et al., 2013). Heterochromatin protein 1 (HP1) isoforms can both positively and negatively affect transcription across species (Font-Burgada et al., 2008; Lin et al., 2008; Ogawa et al., 2002; Piacentini et al., 2009). Deleting the HP1 ortholog *hpl-2* enhances dauer arrest in a *daf-2* mutant background under permissive conditions (Meister et al., 2011). Consistent with using dauer as a proxy for DAF-16-mediated longevity, *hpl-2* mutants were modestly long-lived. However, a full understanding of how DAF-16/FoxO interacts with epigenetic modifications is lacking.

EAK pathway proteins act in parallel to IIS mutants to inhibit DAF-16/FoxO

Because of the findings implicating that one or more pathways act in parallel with IIS, we performed a forward genetic screen to identify these novel regulators of nuclear-localized DAF-16/FoxO. *akt-1* mutants arrest as dauers at 27°C but not at 25°C. Therefore, these animals were mutagenized to find enhancers of *akt-1* dauer arrest (*eak* screen) (Hu et al., 2006). Specifically, recovered mutant strains arrested spontaneously at 25°C in combination with an *akt-1* null background. *eak* mutants increase dauer arrest. Six of seven eak mutants have been identified. No combination of *eak* double mutants enhances dauer arrest, suggesting they belong to a single pathway. All identified *eak* genes are expressed in the paired endocrine XXX cells (Alam et al., 2010; Dumas et al., 2010; Hu et al., 2006; Zhang et al., 2008). XXX cells are a site of DAF-9-

mediated dafachronic acid synthesis and are critical to bypassing dauer (Motola et al., 2006). However, XXX cells do not express DAF-16/FoxO (Hu et al., 2006). These data support that the *eak* pathway acts cell-non-autonomously to inhibit DAF-16/FoxO via endocrine signaling.

eak-2 encodes a conserved 3β-hydroxysteroid dehydrogenase known as HSD-1 (Dumas et al., 2010; Patel et al., 2008). Importantly, loss of *hsd-1* does not enhance DAF-16/FoxO localization, linking the *eak* pathway specifically with inhibition of nuclear-localized DAF-16/FoxO. As expected from the design of the *eak* screen, HSD-1 synergizes with reduced insulin signaling in activation of DAF-16/FoxO target genes. This enhancement requires the nuclear hormone receptor/transcription factor DAF-12 in addition to DAF-16. Therefore, the *eak* pathway may act through hormonal signaling.

EAK-7 is unique among EAK pathway members in that it is expressed in multiple tissues, including XXX cells, neurons, and the intestine (Alam et al., 2010). EAK-7 is conserved and possesses an N-terminal myristoylation domain that facilitates membrane association as well as a C-terminal *T*BC- and *L*ysM-*d*omain-*c*ontaining (TLDc) domain. The function of TLDc domains remains obscure. Similar to HSD-1, EAK-7 inhibits nuclear DAF-16. *eak-7* null animals have a weak dauer phenotype at 27ºC that is enhanced by cholesterol deprivation (Alam et al., 2010), consistent with the *eak* pathway interacting with dafachronic acid steroid hormone synthesis pathway in XXX cells. However, when combined with *akt-1* null alleles, the *eak-7;akt-1* double mutant dauer phenotype is fully penetrant at 25°C. Loss of *eak-7* also enhances longevity in a DAF-16/FoxO dependent manner. *eak-7;akt-1* animals live longer than either single mutant, confirming that the eak and IIS pathways act in parallel to inhibit DAF-16/FoxO activity not only in dauer but also in longevity.

EAK-7 is expressed in multiple tissues that co-express DAF-16, suggesting EAK-7 may be the most downstream member of the *eak* pathway identified so far (Alam et al., 2010). Over-expression of an *eak-7::gfp* translational fusion revealed that EAK-7 is localized to the plasma membrane (Alam et al., 2010). Mutation of the myristoylation motif abrogated this localization. However, whether this myristoylation dead mutant was still capable of inhibiting DAF-16/FoxO was ambiguous. Nevertheless, the plasma membrane association of wild type EAK-7 suggests that it cannot act directly on nuclear DAF-16. Therefore, it is plausible that there exist

components of the *eak* pathway further downstream of EAK-7 that are required for inhibition of nuclear-localized DAF-16/FoxO.

Understanding how EAK-7 inhibits DAF-16/FoxO activity may lead to fundamental insights into endocrine control of longevity. The mammalian homolog of EAK-7, TLDc1, is expressed in liver, osteoblasts, and retinal pigment epithelium (Ambrogini et al., 2010; Rached et al., 2010; Su et al., 2004). FoxO transcription factors are expressed in these tissues with potential roles in glucose metabolism and tissue homeostasis. To gain greater insight into parallel regulation of FoxO transcription factors, we once again turned to *C. elegans* genetics to develop our understanding of parallel inputs on DAF-16/FoxO activity.

A genetic screen reveals X-linked gene regulation of DAF-16/FoxO

In order to enhance our understanding of parallel inputs on DAF-16/FoxO activity, we conducted a new forward genetic screen, again using the dauer arrest phenotype as our readout (Dumas et al., 2013). We used *eak-7;akt-1* animals that always arrest as dauers at 25°C because we could target both the *eak* and IIS parallel pathways simultaneously. It is unknown how the *eak* pathway influences DAF-16/FoxO activity in the nucleus, so we reasoned such a screen may provide missing links between EAK-7, situated at the plasma membrane, and nuclear-localized DAF-16/FoxO (Alam et al., 2010). We also may expect to find genes that interact with the IIS pathway that controls DAF-16/FoxO subcellular nuclear localization, as well as genes that act on DAF-16/FoxO in parallel with both IIS and *eak* pathways. We endeavored to discover mutant alleles that suppressed the dauer-constitutive phenotype of *eak-7;akt-1*, (SEAK alleles). We treated P0 animals with the mutagen *N*-ethyl-*N*-nitrosourea (ENU) at the L4 stage and allowed these animals to lay eggs. F1 animals were grown to adulthood, allowed to lay eggs, and their eggs were transferred to 25°C. F2s found to bypass dauer were propagated and the dauer defective (daf-d) phenotypes of these strains were verified in subsequent generations. We sequenced the genomes of the resulting 16 strains as well as performed linkage mapping to find candidate alleles.

Three of sixteen strains had distinct mutations in the conserved protein DPY-21 (Dumas et al., 2013). An independently derived nonsense allele, *e428*, also completely suppressed dauer in both

eak-7;akt-1 compound mutants and *daf-2/igfR* hypomorphs. Intriguingly, *dpy-21* RNAi suppressed *eak-7;akt-1* dauer arrest but not *daf-2* animals. Because certain tissues including neurons and hypodermis are resistant to RNAi (Kamath et al., 2003; Timmons et al., 2001), these data suggest that the *eak* pathway and IIS may promote reproductive development in different tissue types. Loss of *dpy-21* led to robust down-regulation of known DAF-16/FoxO target genes, including *sod-3*, *mtl-1*, and *dod-3*, and knockdown of *dpy-21* decreased DAF-16/FoxO nuclear localization. Taken together, these data suggest that DPY-21 promotes DAF-16/FoxO activity downstream of both the *eak* and IIS pathway in multiple tissue types.

DPY-21 is part of the worm dosage compensation complex (DCC) that equalizes X chromosome gene expression between XO males and XX hermaphrodites (Meyer, 2010). We found evidence that DPY-21 promotes dauer arrest through dosage compensation *per se* because knockdown of other DCC components in *eak-7;akt-1* animals phenocopied loss of *dpy-21* (Dumas et al., 2013). Further, the daf-d phenotype was only observed in hermaphrodites; the male X chromosome is not dosage compensated, and male *eak-7;akt-1* animals continued to arrest normally. We also observed X-linked genes associated with dauer bypass were upregulated 2-fold in a *dpy-21* mutant background while autosomal genes were unchanged. From these data, we concluded that dosage compensation promotes dauer arrest by repressing inhibitors of DAF-16/FoxO activity.

In addition to DPY-21-mediated dauer arrest, two other published SEAK strains contain causative defects on X chromosomes, including a complex rearrangement and duplication that increases gene dosage of *akt-2* (Itani et al., 2016a; Itani et al., 2016b). Such findings implicate X chromosome dosage compensation in the regulation of DAF-16/FoxO during development. Although the genetic programs that establish sex-specific assembly of the DCC and the identity of its components are well-defined, how this complex achieves dosage compensation remains unclear and may involve partner epigenetic effectors (Wells et al., 2012). Further, the specific X-linked genes that cause to the daf-d phenotype associated with DCC disruption have not been rigorously defined. These unanswered questions underlie the rationale for the investigations presented herein.

Summary

Understanding how FoxO transcription factors contribute to stress resistance and increase longevity may contribute to interventions that increase individual vitality and decrease incidence of chronic illness in the population. FoxO transcription factors are controlled by extensive post-translational modification and acted upon by multiple conserved signal transduction pathways to control transcriptional output. In *C. elegans*, insulin-like signaling receives inputs from multiple upstream pathways through the insulin-like peptide milieu that controls the nuclear localization of DAF-16/FoxO. The *eak* pathway acts in parallel with IIS to inhibit nuclear DAF-16/FoxO activity, but the mechanism by which this pathway does this remains unclear.

Others and we have shown that conserved epigenetic proteins can either promote or inhibit DAF-16/FoxO activity (Dumas et al., 2013; Meister et al., 2011). To that end, this dissertation seeks to expand our knowledge of how conserved epigenetic programs influence DAF-16/FoxO activity. We previously showed dosage compensation promotes DAF-16/FoxO activity. However, disrupting the DCC leads to thousands of genes being dysregulated either directly or indirectly (Kramer et al., 2015). In order to clarify the mechanism how dosage compensation promotes dauer arrest, we must interrogate genes believed to partner with the DCC to achieve appropriate gene expression. Intriguingly, one SEAK strain harbored a mutation in the conserved histone methyltransferase *set-4*, which has been implicated in dosage compensation (Wells et al., 2012).

Chapter 2 briefly reviews the principles of dosage compensation across metazoans, focusing on the *C. elegans* DCC, then expands on the dynamics of dosage compensation-associated methylation of histone H4 lysine 20 (H4K20me). Chapter 3 provides clear evidence that the conserved H4K20 methyltransferase SET-4 acts like DCC protein DPY-21 in promoting DAF-16/FoxO activity during development by repressing insulin like peptide production in sensory neurons. Chapter 4 refines our understanding of how SET-4 acts in concert with both upstream stress signals and downstream DAF-16/FoxO feedback to control ILP expression. Finally, chapter 5 explores roles for SET-4 in longevity, implicating H4K20 methylation in multiple conserved mechanisms of aging.

References

Accili, D. and Arden, K. C. (2004). FoxOs at the crossroads of cellular metabolism, differentiation, and transformation. *Cell* 117, 421-426.

Ailion, M. and Thomas, J. H. (2000). Dauer formation induced by high temperatures in Caenorhabditis elegans. *Genetics* 156, 1047-1067.

Alam, H., Williams, T. W., Dumas, K. J., Guo, C., Yoshina, S., Mitani, S. and Hu, P. J. (2010). EAK-7 controls development and life span by regulating nuclear DAF-16/FoxO activity. *Cell Metab* 12, 30-41.

Alcedo, J. and Kenyon, C. (2004). Regulation of C. elegans longevity by specific gustatory and olfactory neurons. *Neuron* 41, 45-55.

Ambrogini, E., Almeida, M., Martin-Millan, M., Paik, J. H., Depinho, R. A., Han, L., Goellner, J., Weinstein, R. S., Jilka, R. L., O'Brien, C. A., et al. (2010). FoxO-mediated defense against oxidative stress in osteoblasts is indispensable for skeletal homeostasis in mice. *Cell Metab* 11, 136-146.

Anselmi, C. V., Malovini, A., Roncarati, R., Novelli, V., Villa, F., Condorelli, G., Bellazzi, R. and Puca, A. A. (2009). Association of the FOXO3A locus with extreme longevity in a southern Italian centenarian study. *Rejuvenation Res* 12, 95-104.

Antebi, A., Yeh, W. H., Tait, D., Hedgecock, E. M. and Riddle, D. L. (2000). daf-12 encodes a nuclear receptor that regulates the dauer diapause and developmental age in C. elegans. *Genes Dev* 14, 1512-1527.

Berdichevsky, A., Viswanathan, M., Horvitz, H. R. and Guarente, L. (2006). C. elegans SIR-2.1 interacts with 14-3-3 proteins to activate DAF-16 and extend life span. *Cell* 125, 1165-1177.

Birnby, D. A., Link, E. M., Vowels, J. J., Tian, H., Colacurcio, P. L. and Thomas, J. H. (2000). A transmembrane guanylyl cyclase (DAF-11) and Hsp90 (DAF-21) regulate a common set of chemosensory behaviors in caenorhabditis elegans. *Genetics* 155, 85-104.

Blaxter, M. L. (1993). Cuticle surface proteins of wild type and mutant Caenorhabditis elegans. *J Biol Chem* 268, 6600-6609.

Bluher, M., Kahn, B. B. and Kahn, C. R. (2003). Extended longevity in mice lacking the insulin receptor in adipose tissue. *Science* 299, 572-574.

Brenkman, A. B., de Keizer, P. L., van den Broek, N. J., Jochemsen, A. G. and Burgering, B. M. (2008). Mdm2 induces mono-ubiquitination of FOXO4. *PLoS One* 3, e2819.

Brunet, A., Bonni, A., Zigmond, M. J., Lin, M. Z., Juo, P., Hu, L. S., Anderson, M. J., Arden, K. C., Blenis, J. and Greenberg, M. E. (1999). Akt promotes cell survival by phosphorylating and inhibiting a Forkhead transcription factor. *Cell* 96, 857-868.

Brunet, A., Kanai, F., Stehn, J., Xu, J., Sarbassova, D., Frangioni, J. V., Dalal, S. N., DeCaprio, J. A., Greenberg, M. E. and Yaffe, M. B. (2002). 14-3-3 transits to the nucleus and participates in dynamic nucleocytoplasmic transport. *J Cell Biol* 156, 817-828.

Butcher, R. A., Fujita, M., Schroeder, F. C. and Clardy, J. (2007). Small-molecule pheromones that control dauer development in Caenorhabditis elegans. *Nat Chem Biol* 3, 420-422.

Cahill, C. M., Tzivion, G., Nasrin, N., Ogg, S., Dore, J., Ruvkun, G. and Alexander-Bridges, M. (2001). Phosphatidylinositol 3-kinase signaling inhibits DAF-16 DNA binding and function via 14-3-3-dependent and 14-3-3-independent pathways. *J Biol Chem* 276, 13402-13410.

Calnan, D. R., Webb, A. E., White, J. L., Stowe, T. R., Goswami, T., Shi, X., Espejo, A., Bedford, M. T., Gozani, O., Gygi, S. P., et al. (2012). Methylation by Set9 modulates FoxO3 stability and transcriptional activity. *Aging (Albany NY)* 4, 462-479.

Cassada, R. C. and Russell, R. L. (1975). The dauerlarva, a post-embryonic developmental variant of the nematode Caenorhabditis elegans. *Dev Biol* 46, 326-342.

Cornils, A., Gloeck, M., Chen, Z., Zhang, Y. and Alcedo, J. (2011). Specific insulin-like peptides encode sensory information to regulate distinct developmental processes. *Development* 138, 1183-1193.

da Graca, L. S., Zimmerman, K. K., Mitchell, M. C., Kozhan-Gorodetska, M., Sekiewicz, K., Morales, Y. and Patterson, G. I. (2004). DAF-5 is a Ski oncoprotein homolog that functions in a neuronal TGF beta pathway to regulate C. elegans dauer development. *Development* 131, 435-446.

Dixon, S. J., Alexander, M., Chan, K. K. and Roy, P. J. (2008). Insulin-like signaling negatively regulates muscle arm extension through DAF-12 in Caenorhabditis elegans. *Dev Biol* 318, 153-161.

Dumas, K. J., Delaney, C. E., Flibotte, S., Moerman, D. G., Csankovszki, G. and Hu, P. J. (2013). Unexpected role for dosage compensation in the control of dauer arrest, insulin-like signaling, and FoxO transcription factor activity in Caenorhabditis elegans. *Genetics* 194, 619-629.

Dumas, K. J., Guo, C., Wang, X., Burkhart, K. B., Adams, E. J., Alam, H. and Hu, P. J. (2010). Functional divergence of dafachronic acid pathways in the control of C. elegans development and lifespan. *Dev Biol* 340, 605-612.

Eijkelenboom, A. and Burgering, B. M. (2013). FOXOs: signalling integrators for homeostasis maintenance. *Nat Rev Mol Cell Biol* 14, 83-97.

Engelman, J. A., Luo, J. and Cantley, L. C. (2006). The evolution of phosphatidylinositol 3-kinases as regulators of growth and metabolism. *Nat Rev Genet* 7, 606-619.

Estevez, M., Attisano, L., Wrana, J. L., Albert, P. S., Massague, J. and Riddle, D. L. (1993). The daf-4 gene encodes a bone morphogenetic protein receptor controlling C. elegans dauer larva development. *Nature* 365, 644-649.

Fernandes de Abreu, D. A., Caballero, A., Fardel, P., Stroustrup, N., Chen, Z., Lee, K., Keyes, W. D., Nash, Z. M., Lopez-Moyado, I. F., Vaggi, F., et al. (2014). An insulin-to-insulin regulatory network orchestrates phenotypic specificity in development and physiology. *PLoS Genet* 10, e1004225.

Flachsbart, F., Caliebe, A., Kleindorp, R., Blanche, H., von Eller-Eberstein, H., Nikolaus, S., Schreiber, S. and Nebel, A. (2009). Association of FOXO3A variation with human longevity confirmed in German centenarians. *Proc Natl Acad Sci U S A* 106, 2700-2705.

Font-Burgada, J., Rossell, D., Auer, H. and Azorin, F. (2008). Drosophila HP1c isoform interacts with the zinc-finger proteins WOC and Relative-of-WOC to regulate gene expression. *Genes Dev* 22, 3007-3023.

Georgi, L. L., Albert, P. S. and Riddle, D. L. (1990). daf-1, a C. elegans gene controlling dauer larva development, encodes a novel receptor protein kinase. *Cell* 61, 635-645.

Gerisch, B. and Antebi, A. (2004). Hormonal signals produced by DAF-9/cytochrome P450 regulate C. elegans dauer diapause in response to environmental cues. *Development* 131, 1765-1776.

Gerisch, B., Weitzel, C., Kober-Eisermann, C., Rottiers, V. and Antebi, A. (2001). A hormonal signaling pathway influencing C. elegans metabolism, reproductive development, and life span. *Dev Cell* 1, 841-851.

Giannakou, M. E., Goss, M., Junger, M. A., Hafen, E., Leevers, S. J. and Partridge, L. (2004). Long-lived Drosophila with overexpressed dFOXO in adult fat body. *Science* 305, 361.

Gil, E. B., Malone Link, E., Liu, L. X., Johnson, C. D. and Lees, J. A. (1999). Regulation of the insulin-like developmental pathway of Caenorhabditis elegans by a homolog of the PTEN tumor suppressor gene. *Proc Natl Acad Sci U S A* 96, 2925-2930.

Golden, J. W. and Riddle, D. L. (1984). ACaenorhabditis elegans dauer-inducing pheromone and an antagonistic component of the food supply. *J Chem Ecol* 10, 1265-1280.

Greer, E. L. and Brunet, A. (2005). FOXO transcription factors at the interface between longevity and tumor suppression. *Oncogene* 24, 7410-7425.

Ha, C. W. and Huh, W. K. (2011). The implication of Sir2 in replicative aging and senescence in Saccharomyces cerevisiae. *Aging (Albany NY)* 3, 319-324.

Hahm, J. H., Kim, S. and Paik, Y. K. (2009). Endogenous cGMP regulates adult longevity via the insulin signaling pathway in Caenorhabditis elegans. *Aging Cell* 8, 473-483.

Honda, Y., Tanaka, M. and Honda, S. (2008). Modulation of longevity and diapause by redox regulation mechanisms under the insulin-like signaling control in Caenorhabditis elegans. *Exp Gerontol* 43, 520-529.

Hsu, A. L., Murphy, C. T. and Kenyon, C. (2003). Regulation of aging and age-related disease by DAF-16 and heat-shock factor. *Science* 300, 1142-1145.

Hu, M. C., Lee, D. F., Xia, W., Golfman, L. S., Ou-Yang, F., Yang, J. Y., Zou, Y., Bao, S., Hanada, N., Saso, H., et al. (2004). IkappaB kinase promotes tumorigenesis through inhibition of forkhead FOXO3a. *Cell* 117, 225-237.

Hu, P. J., Xu, J. and Ruvkun, G. (2006). Two membrane-associated tyrosine phosphatase homologs potentiate C. elegans AKT-1/PKB signaling. *PLoS Genet* 2, e99.

Huang, H., Muddiman, D. C. and Tindall, D. J. (2004). Androgens negatively regulate forkhead transcription factor FKHR (FOXO1) through a proteolytic mechanism in prostate cancer cells. *J Biol Chem* 279, 13866-13877.

Hung, W. L., Wang, Y., Chitturi, J. and Zhen, M. (2014). A Caenorhabditis elegans developmental decision requires insulin signaling-mediated neuron-intestine communication. *Development* 141, 1767-1779.

Hwangbo, D. S., Gershman, B., Tu, M. P., Palmer, M. and Tatar, M. (2004). Drosophila dFOXO controls lifespan and regulates insulin signalling in brain and fat body. *Nature* 429, 562-566.

Itani, O. A., Flibotte, S., Dumas, K. J., Guo, C., Blumenthal, T. and Hu, P. J. (2016a). N-Ethyl-N-Nitrosourea (ENU) Mutagenesis Reveals an Intronic Residue Critical for Caenorhabditis elegans 3' Splice Site Function in Vivo. *G3 (Bethesda)* 6, 1751-1756.

Itani, O. A., Flibotte, S., Dumas, K. J., Moerman, D. G. and Hu, P. J. (2016b). Chromoanasynthetic Genomic Rearrangement Identified in a N-Ethyl-N-Nitrosourea (ENU) Mutagenesis Screen in Caenorhabditis elegans. *G3 (Bethesda)* 6, 351-356.

Jia, K., Albert, P. S. and Riddle, D. L. (2002). DAF-9, a cytochrome P450 regulating C. elegans larval development and adult longevity. *Development* 129, 221-231.

Kaestner, K. H., Knochel, W. and Martinez, D. E. (2000). Unified nomenclature for the winged helix/forkhead transcription factors. *Genes Dev* 14, 142-146.

Kamath, R. S., Fraser, A. G., Dong, Y., Poulin, G., Durbin, R., Gotta, M., Kanapin, A., Le Bot, N., Moreno, S., Sohrmann, M., et al. (2003). Systematic functional analysis of the Caenorhabditis elegans genome using RNAi. *Nature* 421, 231-237.

Kenyon, C., Chang, J., Gensch, E., Rudner, A. and Tabtiang, R. (1993). A C. elegans mutant that lives twice as long as wild type. *Nature* 366, 461-464.

Kimura, K. D., Tissenbaum, H. A., Liu, Y. and Ruvkun, G. (1997). daf-2, an insulin receptor-like gene that regulates longevity and diapause in Caenorhabditis elegans. *Science* 277, 942-946.

Klass, M. and Hirsh, D. (1976). Non-ageing developmental variant of Caenorhabditis elegans. *Nature* 260, 523-525.

Kramer, M., Kranz, A. L., Su, A., Winterkorn, L. H., Albritton, S. E. and Ercan, S. (2015). Developmental Dynamics of X-Chromosome Dosage Compensation by the DCC and H4K20me1 in C. elegans. *PLoS Genet* 11, e1005698.

Lans, H. and Jansen, G. (2007). Multiple sensory G proteins in the olfactory, gustatory and nociceptive neurons modulate longevity in Caenorhabditis elegans. *Dev Biol* 303, 474-482.

Lau, H. E. and Chalasani, S. H. (2014). Divergent and convergent roles for insulin-like peptides in the worm, fly and mammalian nervous systems. *Invert Neurosci* 14, 71-78.

Lee, R. Y., Hench, J. and Ruvkun, G. (2001). Regulation of C. elegans DAF-16 and its human ortholog FKHRL1 by the daf-2 insulin-like signaling pathway. *Curr Biol* 11, 1950-1957.

Li, C. J., Chang, J. K., Chou, C. H., Wang, G. J. and Ho, M. L. (2010). The PI3K/Akt/FOXO3a/p27Kip1 signaling contributes to anti-inflammatory drug-suppressed proliferation of human osteoblasts. *Biochem Pharmacol* 79, 926-937.

Li, J., Ebata, A., Dong, Y., Rizki, G., Iwata, T. and Lee, S. S. (2008). Caenorhabditis elegans HCF-1 functions in longevity maintenance as a DAF-16 regulator. *PLoS Biol* 6, e233.

Li, J., Tewari, M., Vidal, M. and Lee, S. S. (2007). The 14-3-3 protein FTT-2 regulates DAF-16 in Caenorhabditis elegans. *Dev Biol* 301, 82-91.

Li, W., Kennedy, S. G. and Ruvkun, G. (2003). daf-28 encodes a C. elegans insulin superfamily member that is regulated by environmental cues and acts in the DAF-2 signaling pathway. *Genes Dev* 17, 844-858.

Li, Y., Wang, W. J., Cao, H., Lu, J., Wu, C., Hu, F. Y., Guo, J., Zhao, L., Yang, F., Zhang, Y. X., et al. (2009). Genetic association of FOXO1A and FOXO3A with longevity trait in Han Chinese populations. *Hum Mol Genet* 18, 4897-4904.

Lin, C. H., Li, B., Swanson, S., Zhang, Y., Florens, L., Washburn, M. P., Abmayr, S. M. and Workman, J. L. (2008). Heterochromatin protein 1a stimulates histone H3 lysine 36 demethylation by the Drosophila KDM4A demethylase. *Mol Cell* 32, 696-706.

Lin, K., Dorman, J. B., Rodan, A. and Kenyon, C. (1997). daf-16: An HNF-3/forkhead family member that can function to double the life-span of Caenorhabditis elegans. *Science* 278, 1319-1322.

Lin, K., Hsin, H., Libina, N. and Kenyon, C. (2001). Regulation of the Caenorhabditis elegans longevity protein DAF-16 by insulin/IGF-1 and germline signaling. *Nat Genet* 28, 139-145.

Liu, T., Zimmerman, K. K. and Patterson, G. I. (2004). Regulation of signaling genes by TGFbeta during entry into dauer diapause in C. elegans. *BMC Dev Biol* 4, 11.

Lopez-Otin, C., Blasco, M. A., Partridge, L., Serrano, M. and Kroemer, G. (2013). The hallmarks of aging. *Cell* 153, 1194-1217.

Ludewig, A. H., Izrayelit, Y., Park, D., Malik, R. U., Zimmermann, A., Mahanti, P., Fox, B. W., Bethke, A., Doering, F., Riddle, D. L., et al. (2013). Pheromone sensing regulates Caenorhabditis elegans lifespan and stress resistance via the deacetylase SIR-2.1. *Proc Natl Acad Sci U S A* 110, 5522-5527.

Ludewig, A. H., Kober-Eisermann, C., Weitzel, C., Bethke, A., Neubert, K., Gerisch, B., Hutter, H. and Antebi, A. (2004). A novel nuclear receptor/coregulator complex controls C. elegans lipid metabolism, larval development, and aging. *Genes Dev* 18, 2120-2133.

Ludewig, A. H. and Schroeder, F. C. (2013). Ascaroside signaling in C. elegans. *WormBook*, 1-22.

Mak, H. Y. and Ruvkun, G. (2004). Intercellular signaling of reproductive development by the C. elegans DAF-9 cytochrome P450. *Development* 131, 1777-1786.

Manolopoulos, K. N., Klotz, L. O., Korsten, P., Bornstein, S. R. and Barthel, A. (2010). Linking Alzheimer's disease to insulin resistance: the FoxO response to oxidative stress. *Mol Psychiatry* 15, 1046-1052.

Matsunaga, Y., Honda, Y., Honda, S., Iwasaki, T., Qadota, H., Benian, G. M. and Kawano, T. (2016). Diapause is associated with a change in the polarity of secretion of insulin-like peptides. *Nat Commun* 7, 10573.

Matsuzaki, H., Daitoku, H., Hatta, M., Aoyama, H., Yoshimochi, K. and Fukamizu, A. (2005). Acetylation of Foxo1 alters its DNA-binding ability and sensitivity to phosphorylation. *Proc Natl Acad Sci U S A* 102, 11278-11283.

Meister, P., Schott, S., Bedet, C., Xiao, Y., Rohner, S., Bodennec, S., Hudry, B., Molin, L., Solari, F., Gasser, S. M., et al. (2011). Caenorhabditis elegans Heterochromatin protein 1 (HPL-2) links developmental plasticity, longevity and lipid metabolism. *Genome Biol* 12, R123.

Meyer, B. J. (2010). Targeting X chromosomes for repression. *Curr Opin Genet Dev* 20, 179-189.

Mihaylova, V. T., Borland, C. Z., Manjarrez, L., Stern, M. J. and Sun, H. (1999). The PTEN tumor suppressor homolog in Caenorhabditis elegans regulates longevity and dauer formation in an insulin receptor-like signaling pathway. *Proc Natl Acad Sci U S A* 96, 7427-7432.

Mori, I. and Ohshima, Y. (1995). Neural regulation of thermotaxis in Caenorhabditis elegans. *Nature* 376, 344-348.

Morris, J. Z., Tissenbaum, H. A. and Ruvkun, G. (1996). A phosphatidylinositol-3-OH kinase family member regulating longevity and diapause in Caenorhabditis elegans. *Nature* 382, 536-539.

Motola, D. L., Cummins, C. L., Rottiers, V., Sharma, K. K., Li, T., Li, Y., Suino-Powell, K., Xu, H. E., Auchus, R. J., Antebi, A., et al. (2006). Identification of ligands for DAF-12 that govern dauer formation and reproduction in C. elegans. *Cell* 124, 1209-1223.

Murphy, C. T., Lee, S. J. and Kenyon, C. (2007). Tissue entrainment by feedback regulation of insulin gene expression in the endoderm of Caenorhabditis elegans. *Proc Natl Acad Sci U S A* 104, 19046-19050.

Niccoli, T. and Partridge, L. (2012). Ageing as a risk factor for disease. *Curr Biol* 22, R741-752.

Obata, T., Yaffe, M. B., Leparc, G. G., Piro, E. T., Maegawa, H., Kashiwagi, A., Kikkawa, R. and Cantley, L. C. (2000). Peptide and protein library screening defines optimal substrate motifs for AKT/PKB. *J Biol Chem* 275, 36108-36115.

Obsilova, V., Vecer, J., Herman, P., Pabianova, A., Sulc, M., Teisinger, J., Boura, E. and Obsil, T. (2005). 14-3-3 Protein interacts with nuclear localization sequence of forkhead transcription factor FoxO4. *Biochemistry* 44, 11608-11617.

Ogawa, H., Ishiguro, K., Gaubatz, S., Livingston, D. M. and Nakatani, Y. (2002). A complex with chromatin modifiers that occupies E2F- and Myc-responsive genes in G0 cells. *Science* 296, 1132-1136.

Ogg, S., Paradis, S., Gottlieb, S., Patterson, G. I., Lee, L., Tissenbaum, H. A. and Ruvkun, G. (1997). The Fork head transcription factor DAF-16 transduces insulin-like metabolic and longevity signals in C. elegans. *Nature* 389, 994-999.

Ogg, S. and Ruvkun, G. (1998). The C. elegans PTEN homolog, DAF-18, acts in the insulin receptor-like metabolic signaling pathway. *Mol Cell* 2, 887-893.

Oh, K. H. and Kim, H. (2013). Reduced IGF signaling prevents muscle cell death in a Caenorhabditis elegans model of muscular dystrophy. *Proc Natl Acad Sci U S A* 110, 19024-19029.

Paik, J. H., Kollipara, R., Chu, G., Ji, H., Xiao, Y., Ding, Z., Miao, L., Tothova, Z., Horner, J. W., Carrasco, D. R., et al. (2007). FoxOs are lineage-restricted redundant tumor suppressors and regulate endothelial cell homeostasis. *Cell* 128, 309-323.

Paradis, S., Ailion, M., Toker, A., Thomas, J. H. and Ruvkun, G. (1999). A PDK1 homolog is necessary and sufficient to transduce AGE-1 PI3 kinase signals that regulate diapause in Caenorhabditis elegans. *Genes Dev* 13, 1438-1452.

Paradis, S. and Ruvkun, G. (1998). Caenorhabditis elegans Akt/PKB transduces insulin receptor-like signals from AGE-1 PI3 kinase to the DAF-16 transcription factor. *Genes Dev* 12, 2488-2498.

Park, D., Estevez, A. and Riddle, D. L. (2010). Antagonistic Smad transcription factors control the dauer/non-dauer switch in C. elegans. *Development* 137, 477-485.

Park, J. H., Chung, H. Y., Kim, M., Lee, J. H., Jung, M. and Ha, H. (2014). Daumone fed late in life improves survival and reduces hepatic inflammation and fibrosis in mice. *Aging Cell* 13, 709-718.

Patel, D. S., Fang, L. L., Svy, D. K., Ruvkun, G. and Li, W. (2008). Genetic identification of HSD-1, a conserved steroidogenic enzyme that directs larval development in Caenorhabditis elegans. *Development* 135, 2239-2249.

Piacentini, L., Fanti, L., Negri, R., Del Vescovo, V., Fatica, A., Altieri, F. and Pimpinelli, S. (2009). Heterochromatin protein 1 (HP1a) positively regulates euchromatic gene expression through RNA transcript association and interaction with hnRNPs in Drosophila. *PLoS Genet* 5, e1000670.

Pierce, S. B., Costa, M., Wisotzkey, R., Devadhar, S., Homburger, S. A., Buchman, A. R., Ferguson, K. C., Heller, J., Platt, D. M., Pasquinelli, A. A., et al. (2001). Regulation of DAF-2 receptor signaling by human insulin and ins-1, a member of the unusually large and diverse C. elegans insulin gene family. *Genes Dev* 15, 672-686.

Pinkston, J. M., Garigan, D., Hansen, M. and Kenyon, C. (2006). Mutations that increase the life span of C. elegans inhibit tumor growth. *Science* 313, 971-975.

Popham, J. D. and Webster, J. M. (1978). An alternative interpretation of the fine structure of the basal zone of the cuticle of the dauerlarva of the nematode Caenorhabditis elegans (Nematoda). *Can J Zool* 56, 1556-1563.

Rached, M. T., Kode, A., Xu, L., Yoshikawa, Y., Paik, J. H., Depinho, R. A. and Kousteni, S. (2010). FoxO1 is a positive regulator of bone formation by favoring protein synthesis and resistance to oxidative stress in osteoblasts. *Cell Metab* 11, 147-160.

Ren, P., Lim, C. S., Johnsen, R., Albert, P. S., Pilgrim, D. and Riddle, D. L. (1996). Control of C. elegans larval development by neuronal expression of a TGF-beta homolog. *Science* 274, 1389-1391.

Renault, V. M., Thekkat, P. U., Hoang, K. L., White, J. L., Brady, C. A., Kenzelmann Broz, D., Venturelli, O. S., Johnson, T. M., Oskoui, P. R., Xuan, Z., et al. (2011). The pro-longevity gene FoxO3 is a direct target of the p53 tumor suppressor. *Oncogene* 30, 3207-3221.

Riedel, C. G., Dowen, R. H., Lourenco, G. F., Kirienko, N. V., Heimbucher, T., West, J. A., Bowman, S. K., Kingston, R. E., Dillin, A., Asara, J. M., et al. (2013). DAF-16 employs the chromatin remodeller SWI/SNF to promote stress resistance and longevity. *Nature cell biology* 15, 491-501.

Ritter, A. D., Shen, Y., Fuxman Bass, J., Jeyaraj, S., Deplancke, B., Mukhopadhyay, A., Xu, J., Driscoll, M., Tissenbaum, H. A. and Walhout, A. J. (2013). Complex expression dynamics and robustness in C. elegans insulin networks. *Genome Res* 23, 954-965.

Rottiers, V., Motola, D. L., Gerisch, B., Cummins, C. L., Nishiwaki, K., Mangelsdorf, D. J. and Antebi, A. (2006). Hormonal control of C. elegans dauer formation and life span by a Rieske-like oxygenase. *Dev Cell* 10, 473-482.

Schackwitz, W. S., Inoue, T. and Thomas, J. H. (1996). Chemosensory neurons function in parallel to mediate a pheromone response in C. elegans. *Neuron* 17, 719-728.

Schaedel, O. N., Gerisch, B., Antebi, A. and Sternberg, P. W. (2012). Hormonal signal amplification mediates environmental conditions during development and controls an irreversible commitment to adulthood. *PLoS Biol* 10, e1001306.

Schroeder, N. E., Androwski, R. J., Rashid, A., Lee, H., Lee, J. and Barr, M. M. (2013). Dauer-specific dendrite arborization in C. elegans is regulated by KPC-1/Furin. *Curr Biol* 23, 1527-1535.

Selman, C. and Withers, D. J. (2011). Mammalian models of extended healthy lifespan. *Philos Trans R Soc Lond B Biol Sci* 366, 99-107.

Sharma, K. K., Wang, Z., Motola, D. L., Cummins, C. L., Mangelsdorf, D. J. and Auchus, R. J. (2009). Synthesis and activity of dafachronic acid ligands for the C. elegans DAF-12 nuclear hormone receptor. *Mol Endocrinol* 23, 640-648.

Su, A. I., Wiltshire, T., Batalov, S., Lapp, H., Ching, K. A., Block, D., Zhang, J., Soden, R., Hayakawa, M., Kreiman, G., et al. (2004). A gene atlas of the mouse and human protein-encoding transcriptomes. *Proc Natl Acad Sci U S A* 101, 6062-6067.

Takahashi, Y., Daitoku, H., Hirota, K., Tamiya, H., Yokoyama, A., Kako, K., Nagashima, Y., Nakamura, A., Shimada, T., Watanabe, S., et al. (2011). Asymmetric arginine dimethylation determines life span in C. elegans by regulating forkhead transcription factor DAF-16. *Cell Metab* 13, 505-516.

Tewari, M., Hu, P. J., Ahn, J. S., Ayivi-Guedehoussou, N., Vidalain, P. O., Li, S., Milstein, S., Armstrong, C. M., Boxem, M., Butler, M. D., et al. (2004). Systematic interactome mapping and genetic perturbation analysis of a C. elegans TGF-beta signaling network. *Mol Cell* 13, 469-482.

Thomas, J. H., Birnby, D. A. and Vowels, J. J. (1993). Evidence for parallel processing of sensory information controlling dauer formation in Caenorhabditis elegans. *Genetics* 134, 1105-1117.

Timmons, L., Court, D. L. and Fire, A. (2001). Ingestion of bacterially expressed dsRNAs can produce specific and potent genetic interference in Caenorhabditis elegans. *Gene* 263, 103-112.

Tsai, K. L., Sun, Y. J., Huang, C. Y., Yang, J. Y., Hung, M. C. and Hsiao, C. D. (2007). Crystal structure of the human FOXO3a-DBD/DNA complex suggests the effects of post-translational modification. *Nucleic Acids Res* 35, 6984-6994.

van der Horst, A., de Vries-Smits, A. M., Brenkman, A. B., van Triest, M. H., van den Broek, N., Colland, F., Maurice, M. M. and Burgering, B. M. (2006). FOXO4 transcriptional activity is regulated by monoubiquitination and USP7/HAUSP. *Nat Cell Biol* 8, 1064-1073.

Vanhaesebroeck, B. and Alessi, D. R. (2000). The PI3K-PDK1 connection: more than just a road to PKB. *Biochem J* 346 Pt 3, 561-576.

Viswanathan, M. and Guarente, L. (2011). Regulation of Caenorhabditis elegans lifespan by sir-2.1 transgenes. *Nature* 477, E1-2.

Vowels, J. J. and Thomas, J. H. (1992). Genetic analysis of chemosensory control of dauer formation in Caenorhabditis elegans. *Genetics* 130, 105-123.

---- (1994). Multiple chemosensory defects in daf-11 and daf-21 mutants of Caenorhabditis elegans. *Genetics* 138, 303-316.

Wadsworth, W. G. and Riddle, D. L. (1989). Developmental regulation of energy metabolism in Caenorhabditis elegans. *Dev Biol* 132, 167-173.

Wells, M. B., Snyder, M. J., Custer, L. M. and Csankovszki, G. (2012). Caenorhabditis elegans dosage compensation regulates histone H4 chromatin state on X chromosomes. *Molecular and cellular biology* 32, 1710-1719.

Willcox, B. J., Donlon, T. A., He, Q., Chen, R., Grove, J. S., Yano, K., Masaki, K. H., Willcox, D. C., Rodriguez, B. and Curb, J. D. (2008). FOXO3A genotype is strongly associated with human longevity. *Proc Natl Acad Sci U S A* 105, 13987-13992.

Woods, Y. L. and Rena, G. (2002). Effect of multiple phosphorylation events on the transcription factors FKHR, FKHRL1 and AFX. *Biochem Soc Trans* 30, 391-397.

Yamamoto, R. and Tatar, M. (2011). Insulin receptor substrate chico acts with the transcription factor FOXO to extend Drosophila lifespan. *Aging Cell* 10, 729-732.

Zhang, Y., Xu, J., Puscau, C., Kim, Y., Wang, X., Alam, H. and Hu, P. J. (2008). Caenorhabditis elegans EAK-3 inhibits dauer arrest via nonautonomous regulation of nuclear DAF-16/FoxO activity. *Dev Biol* 315, 290-302.

Chapter 2

Links between dosage compensation and histone H4 lysine 20 methylation

Abstract

Eukaryotes employ many epigenetic programs that act synergistically and in parallel to coordinate gene expression. Chromatin may be modified at the level of DNA, the nucleosome, higher order chromosomal loops, and local or chromosome-wide levels of compaction. A special case of chromosome level regulation of gene expression is dosage compensation, a phenomenon observed in many metazoans that equalizes gene expression between biological sexes. Skewed dosage compensation is associated with degenerative diseases and loss of embryonic viability. Different classes of metazoans achieve dosage compensation through distinct mechanisms. *Caenorhabditis elegans* employs a specialized condensin-like dosage compensation complex (DCC) that is only active in hermaphrodites and decreases by half the gene expression from each of two hermaphrodite X chromosomes to match transcription output with XO males. While the composition of the complex is well understood, how the DCC achieves dosage compensation is not fully understood. There is growing evidence that dosage compensation in metazoans requires epigenetic modifiers, especially those associated with histone H4 lysine 20 methylation (H4K20me). In this chapter, we examine the principles underlying dosage compensation and H4K20 methylation states, the gaps in knowledge regarding these epigenetic programs, and the emerging direct and indirect links between H4K20 dynamics and dosage compensation.

Introduction

To preserve cellular identity and genomic integrity, eukaryotes employ chemical and structural modifications to chromatin that do not alter DNA sequences. These epigenetic programs form an important layer of control over cell proliferation, differentiation, and transcriptional activity. Multiple epigenetic mechanisms exist, including microRNA mediated heterochromatin formation (Emmerth et al., 2010), DNA methylation, histone tail modifications, and nuclear organization of chromatin. Aging leads to skewed epigenetic patterns that may underlie changes in cellular transcriptomes and differentiation states (Feser and Tyler, 2011; Tsurumi and Li, 2012; Zhan et al., 2007). Total histone protein may also decrease with aging (Dang et al., 2009). Therefore, organismal aging may be regulated at the level of the nucleosome.

Nucleosomes consist of approximately 146 base pairs of DNA wrapped twice around a core octamer of two copies each of histones H2A, H2B, H3, and H4 (Fig. 2.1) (Luger et al., 1997). Histone proteins are highly basic, facilitating interaction with negatively charged DNA. Each of these histones possesses N-terminal tails projecting away from the nucleosome core. These tails can be extensively modified by methylation, phosphorylation, acetylation, sumoylation, crotonylation, and ubiquitination (Margueron et al., 2005; Tan et al., 2011). Acetylation promotes transcription by decreasing the net positive charge of nucleosomes, leading to less tight binding of DNA to the histone core (Berger, 2007). Aging is associated with increased histone tail acetylation (Dang et al., 2009; Kawahara et al., 2009). In contrast, the role of histone methylation in aging is less clear. Histone methylation can either promote or inhibit gene activation depending on the location of the mark. Methylation of H3 lysine 4 (H3K4me), H3K36, and H3K79 are considered gene activating, while H3K9, H3K27, and H4K20 mark heterochromatin (Barski et al., 2007; Lan and Shi, 2009). Repressive marks facilitate heterochromatin formation through distinct mechanisms. For example, heterochromatin protein 1 (HP1) binds to adjacent sites of H3K9 trimethylation (H3K9me3), compacting the chromatin (Nishibuchi and Dejardin, 2017). H4K20 methylation increases chromatin compaction through stronger interaction between the modified H4 tail and the neighboring histone (Davey et al., 2002; Dorigo et al., 2004; Luger et al., 1997). Lysine methyltransferases contain the Su(var), Enhancer of zeste, and Trithorax-domain (SET domain) and modify histone tails (Xiao et al., 2003).

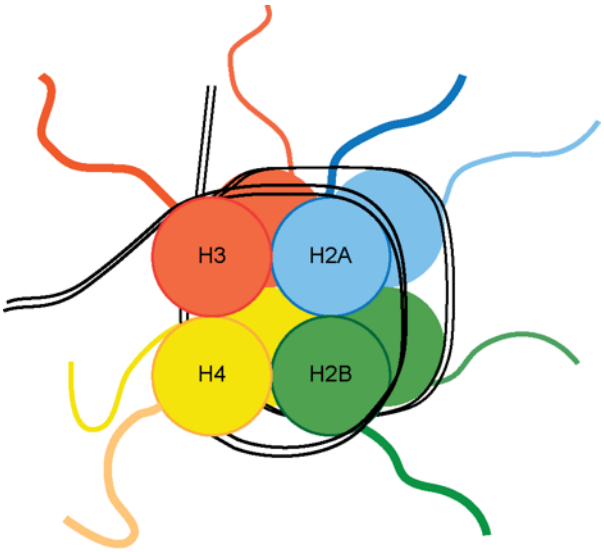

Figure 2.1. Schematic representation of the nucleosome. The nucleosome consists of a core octamer made up of two copies of H2A, H2B, H3, and H4 histones. DNA (black lines) wraps around the histone core twice. N- terminal histone tails project out from the core and can be extensively modified. Histone modifications control the strength of DNA-histone interactions as well as interactions between nucleosomes.

In addition to local nucleosome modifications, chromosome-level regulation of gene expression is critical for maintenance of gene expression. Three-dimensional chromatin architecture controls gene expression. Many heterochromatic regions are directed toward the nuclear periphery through interactions with the nuclear lamina (Towbin et al., 2012), and stereotypical chromosome loops are formed that bring *cis*-acting regulatory sequences into close proximity to their target genes (Kadauke and Blobel, 2009). CTCF proteins interacting with cohesins define the boundaries of these loops to define regulatory 'neighborhoods' that activate tissue-specific gene programs and reinforce silencing of inappropriate genes (Dowen et al., 2014). Finally, the special case of sex chromosome gene dosage is striking. Most autosomal aneuploidies are deleterious. Humans with trisomy 21 are viable but have Down's Syndrome, characterized not only by impaired cognitive development but also early onset of diseases associated with aging, including cardiovascular disease and dementia (Hayes et al., 2017; Lautarescu et al., 2017). However, sex chromosomes tolerate imbalance between homogametic (XX) and heterogametic sexes (XY or XO) through the equalization of X chromosome expression between the sexes, a phenomenon known as dosage compensation. Although mechanistically distinct across metazoans, dosage compensation is required for embryonic viability (Belote and Lucchesi, 1980; Hodgkin, 1987; Plenefisch et al., 1989). In parallel to dosage compensation, X-linked gene expression is also upregulated globally to match hemizygous transcriptional output that of 2N autosomes (Deng et al., 2011; Ka et al., 2016).

Disruption of dosage compensation is linked to many pathologies associated with aging. For example, women suffering from Alzheimer's Disease demonstrate skewed X chromosome inactivation (SXCI) (Bajic et al., 2015), and X chromosome aneuploidy was detected in brain tissue from Alzheimer's patients than in unaffected controls (Yurov et al., 2014). Similarly, SXCI was significantly enriched in somatic tissue of young patients presenting with high-grade glioma, indicating that maintenance of dosage compensation may protect against certain cancers (Li et al., 2013). Given that maintenance of dosage compensation is also associated with long life (Gentilini et al., 2012), it is important to understand how this phenomenon promotes conserved longevity pathways. This chapter seeks to briefly establish the principles underlying dosage compensation, focusing on the free-living nematode *Caenorhabditis elegans*, then elaborate more fully on the dynamics of dosage compensation-associated H4 lysine 20 methylation, and

finally discuss the evidence linking these two epigenetic mechanisms in the regulation of gene expression.

Dosage compensation

The evolution of sex chromosomes created the risk of deleterious gene expression imbalances between homo- and heterogametic sexes. Dosage compensation addresses this risk by equalizing gene expression of sex chromosomes between genders in many types of metazoans. In principle this phenomenon is conserved in worms, flies, and mammals--but perhaps not in birds (Julien et al., 2012; Wolf and Bryk, 2011)--yet the mechanism of achieving correct X chromosome gene dosage in different species is distinct, suggesting dosage compensation evolved independently in multiple animal lineages (Fig. 2.2).

In placental mammals, random X inactivation completely silences one of the sex chromosomes stochastically using noncoding *Xist* RNA that binds in *cis* to the X to be silenced and recruits the Polycomb Repressive Complex 2 to deposit H3K27me3. This leads the increase of other heterochromatic marks including DNA hypermethylation, H3K9me3, and H4K20me3 (Robert Finestra and Gribnau, 2017; Wutz, 2011).

In *Drosophila melanogaster*, a multi-subunit complex known as the male-specific lethal complex (MSL) assembles only on male X chromosomes. The MSL promotes two-fold upregulation of the male X to match female gene dosage through recruitment of MOF acetyltransferase that hyperacetylates histone H4K16 (Birchler, 2016).

As compared to *Drosophila*, *C. elegans* achieves dosage compensation through a mechanism at once similar, in that a multi-subunit complex assembles on sex chromosomes, and opposite, both in terms of affected gender and consequences for gene expression. A specialized 10 member condensin-like dosage compensation complex (DCC) assembles only in XX hermaphrodites and reduces gene expression on both X chromosomes by approximately half (Meyer, 2010). Gender specificity is achieved through hermaphrodite-specific expression of DCC gene *sdc-2* (Dawes et al., 1999), the expression of which is repressed by the X-linked male specifying *xol-1* gene (Miller et al., 1988). SDC-2, in turn, represses male development and is required for DCC assembly on the two hermaphrodite X chromosomes (Dawes et al., 1999). Dosage compensation

promotes X chromosome compaction; impairment of dosage compensation increases the volume the X chromosome occupies in the nucleus without affecting autosomes (Lau et al., 2014).

The DCC binds to the X chromosome at recruitment sites on the X (rex) sites that contain a 12 BP consensus sequence known as motif enriched on X (mex) (Jans et al., 2009). These sites are sufficient for DCC binding, as fusion of X sequence containing rex sites and autosomal chromosomes on recruits the DCC to autosomal regions (Ercan et al., 2009). Despite there being only ~100 rex sites on X, DCC binding then spreads across the X to dox sites (dependent on X) to achieve repression across the entire X chromosome. The result is a depletion of RNA Polymerase II binding to X-linked promoters (Kruesi et al., 2013).

Recent work has suggested that nuclear organization may play a role in DCC-mediated repression. X chromosomes are only weakly associated with the nuclear lamina in *C. elegans*, in contrast to autosomes, which show strong anchoring on both chromosome ends (Ikegami et al., 2010). While hermaphrodite X chromosomes are randomly organized, the male X associates with nuclear pores in a manner dependent on rex sites (Sharma and Meister, 2015). Nuclear pore proximity is associated with active gene transcription, so preventing this nuclear positioning may be important for DCC inhibition of hermaphrodite X chromosomes.

Remarkably, whether a gene is dosage compensated or escapes DCC regulation may be independent of local DCC binding. Therefore, the DCC may not be sufficient for dosage compensation; rather, it may require other epigenetic modifiers to achieve X chromosome compaction and reduced gene expression (Meyer, 2010). For example, recently it was shown that H3K9 methyltransferases are required for X chromosome compaction and stereotypical localization away from the transcriptionally active nuclear center (Snyder et al., 2016). Knockdown of these methyltransferases impaired dosage compensation, providing evidence that the DCC partners with enzymes that promote heterochromatin formation.

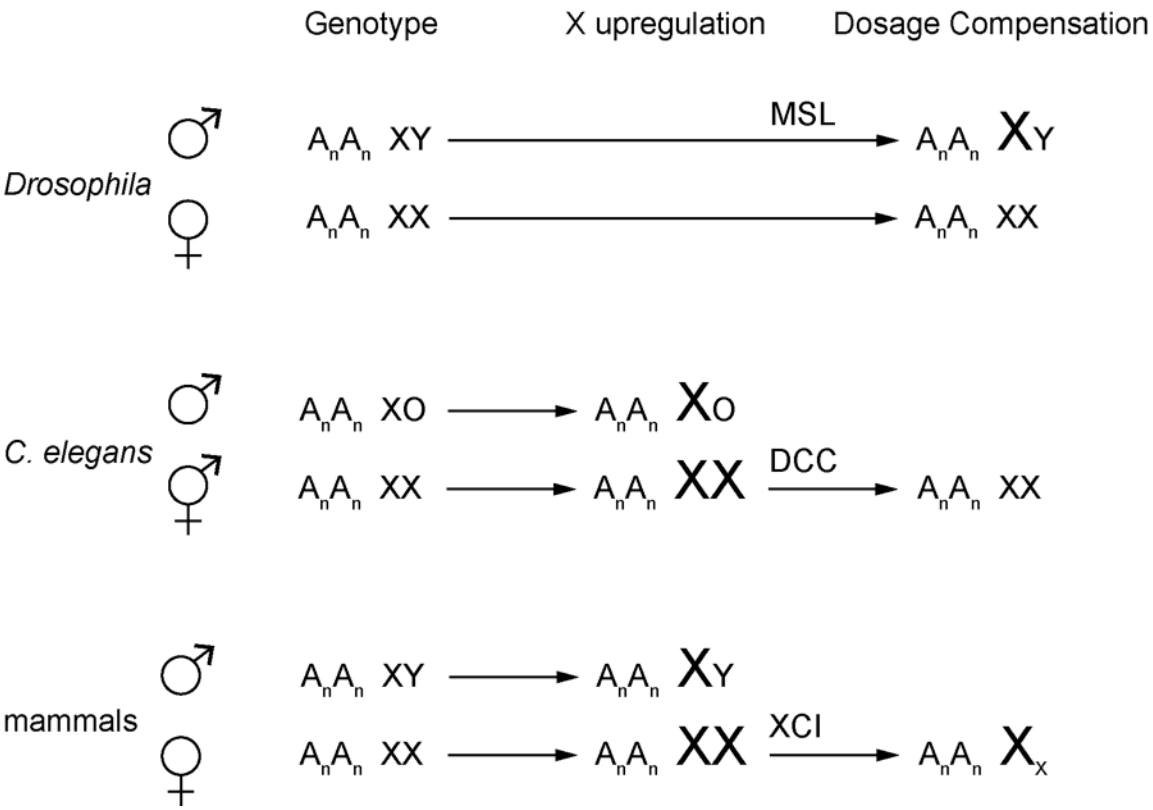

Figure 2.2. X chromosome regulation balances output with autosomes and between sexes. Divergent animals show distinct X chromosome dosage compensation. *Drosophila* upregulates the single male X chromosome to match females via the MSL complex. *In C. elegans* and mammals, global upregulation of the X chromosome balances hemizygous X chromosome gene expression with diploid autosome. In XX animals, this upregulation is followed by repression of X chromosome gene expression to match male X gene dosage. The dosage compensation complex (DCC) mediates dosage compensation in *C. elegans*. Random X chromosome inactivation (XCI) silences one X chromosome in mammals.

Histone H4 Lysine 20 methylation

Lysine 20 is typically the only lysine on histone H4 that is methylated in eukaryotes (van Nuland and Gozani, 2016). Despite being described first in 1969 (DeLange et al., 1969), understanding how these marks participate in epigenetic regulation of development and longevity remains incomplete. Below I discuss the roles attributed to each methylation state of H4K20, the enzymes believed to establish or remove these marks, and current gaps in knowledge regarding this highly conserved epigenetic regulator of genomic integrity. Data is summarized in Table 1.1.

Monomethylation of H4K20 plays a key role in cell cycle regulation (Wu and Rice, 2011). H4K20me1 is enriched on mitotic nucleosomes and is bound by condensin II subunits N-CAPG2 and N-CAPD3 in M-phase (Liu et al., 2010). This modification is reported to recruit 53BP1 to sites of double-strand breaks (Dulev et al., 2014; Hartlerode et al., 2012) and protects against DNA damage in replicating cells (Li et al., 2016). PHF8 is believed to demethylate H4K20me1 (Liu et al., 2010; Qi et al., 2010), while PR-SET7(SETD8) catalyzes K20 monomethylation in mammals and is required for embryonic viability past the 8-cell stage (Nishioka et al., 2002; Oda et al., 2009). In *C. elegans*, animals deficient in the PR-SET7 ortholog SET-1 grow in to sterile adults (Terranova et al., 2002). Similarly, *Drosophila* animals deficient in PR-SET7 die at the second instar larval stage, although whether loss of H4K20me1 is responsible for this lethal phenotype associated with loss of the methyltransferase has become controversial (McKay et al., 2015; Shi et al., 2007).

H4K20me1 is associated with actively transcribed genes (Barski et al., 2007), yet also may contribute to transcriptional repression due to recruitment of both euchromatic and heterochromatin-inducing proteins and modifications. For example, H4K20me1 is bound by the polycomb protein L3MBTL1, promoting compaction and is necessary for higher methylation states of H4K20, which are associated with gene repression (Kalakonda et al., 2008). Similarly, H4K20me1 was recently identified in budding yeast, and it is enriched in heterochromatic regions (Edwards et al., 2011). Mutants deficient in H4K20me1 experienced de-repression of subtelomeric genes as well as reporters located near telomeres and the silent mating type locus. In contrast, H4K20me1 also recruits the MSL complex in flies that promotes H4K16 acetylation and the release of transcriptional pausing of RNA polymerase II (Kapoor-Vazirani and Vertino, 2014). In addition to decreased global H4K20me1 levels, loss of PR-Set7 is also associated with

increased markers of senescence including increased p16/Ink4A expression, increased ribosome biogenesis and nucleolar activity in addition to (Tanaka et al., 2017). Brains of mice that experience accelerated senescence also show decreased K20 monomethylation (Wang et al., 2010).

Like monomethylated H4K20, dimethylated H4K20 is attributed a role in the DNA damage response, and its presence is cell cycle dependent. H4K20me2 is enriched in interphase/G1 cells during which time it constitutes 80% or more of total H4 (Schotta et al., 2008; Yang et al., 2008) and does not display focal enrichment in the genome (Schotta et al., 2004). Also like H4K20me1, dimethylated H4K20 is reported to recruit 53BP1 to sites of DNA damage (Botuyan et al., 2006). Similarly, fission yeast checkpoint protein Crb2 localizes to sites of DNA damage in a H4K20me2 dependent fashion (Greeson et al., 2008). Local increase of H4K20 dimethylation at double stranded DNA breaks in mammalian cells is dependent on the methyltransferase MMSET (Pei et al., 2011) and this interaction is stymied by the lysine demethylase JMJD2A (Mallette et al., 2012). Although loss of dimethylated H4K20 is tolerated in flies and worms, mice deficient in the dimethylase SUV420H1 die perinatally and demonstrate genome instability (Schotta et al., 2008). The loss of both H4K20me2 and H4K20me3 leads to genome-wide DNA damage in these mice. This phenotype may be due to a loss of chromatin compaction; both recombinant nucleosomes marked with either me2 or me3 condense chromatin fibers to a greater degree than unmodified nucleosomes (Lu et al., 2008).

In mammals H4K20 trimethylation is enriched in regions of constitutive heterochromatin, including pericentromeric and telomeric regions, while in the fission yeast *Schizosaccharomyces pombe*, it is broadly distributed (Sanders et al., 2004). Observations in mammalian cells suggest that H3K9me3 may be necessary for subsequent H4K20me3 (Schotta et al., 2004). Consistent with these data, the putative H4K20 trimethylase SUV420H2 contains a chromoshadow motif that facilitates its recruitment to constitutive heterochromatin marked by H3K9me3 through interactions with HP1 (Souza et al., 2009; Wang et al., 2017). H4K20me3 may antagonize H4 acetylation, and vice versa, consistent with H4K20 methylation being associated with chromatin compaction and transcriptional repression (Sarg et al., 2004; Serrano et al., 2013). H4K20me3 promotes RNA polymerase II pausing, perhaps through depletion of H4K16 acetylation (Kapoor-Vazirani et al., 2011). A functional and physical relationship between PR-SET7 and histone

deacetylase (HDAC) SirT2 was recently described, demonstrating that de-acetylation of H4K16 promotes H4K20 methylation to maintain genomic integrity (Serrano et al., 2013). Intriguingly, in contrast to mice deficient in the dimethylase SUV420H1, mice lacking SUV420H2 and associated H4K20me3 lack obvious developmental defects (Schotta et al., 2008), suggesting that H4K20me3 is not essential for maintenance of genomic integrity during normal development. Trimethylation of H4K20 has not been ascribed a major role in cell cycle regulation, but increased H4K20me2 may be associated with replication errors in S-phase (Beck et al., 2012).

H4K20 trimethylation is disordered in cancer progression. Greater trimethylation levels in tumors correlated with good prognosis in colon cancer (Benard et al., 2014). Loss of RB tumor suppressor proteins causes a dramatic loss of genomic stability perhaps due to decreased trimethylated H4K20me3 at constitutive heterochromatic regions (Gonzalo et al., 2005). Further, lung carcinoma tissues showed depleted H4K20me3 that was associated with either disease progression or reduced survival (Van Den Broeck et al., 2008). Similar depletion of H4K20me3 is found in breast cancer cell lines and increased cell invasion in breast cancer tissues (Shinchi et al., 2015; Tryndyak et al., 2006). H4K20me3 loss at repetitive DNA was also observed in liver tumorogenesis (Pogribny et al., 2006). In contrast, greater tumor trimethylation was positively correlated with bladder cancer mortality (Schneider et al., 2011) and may be associated with aggressive prostate cancer (Vieira et al., 2015).

H4K20me3 is enriched in aged mammalian tissues while other H4K20 methylation states do not change with age (Sarg et al., 2002). This enrichment was also observed in fibroblasts derived from Hutchinson-Gilford Progeria Syndrome patients, whose cells manifest defects in nuclear lamin leading to loss of heterochromatin and appear to experience accelerated aging and early death (Shumaker et al., 2006). This increase in trimethylation may occur as cells exit the cell cycle. Conversely, H4K20me3 is inversely related to pluripotency. During embryonic development H4K20me3 selectively represses the pluripotency marker homologs Oct-25 in *Xenopus* and Oct-4 in mice (Nicetto et al., 2013). H4K20me3 is not maintained in preimplantation murine embryos, recovering only in mid-gestation (Eid et al., 2016; Wongtawan et al., 2011). Deposition of H4K20me3 prevents telomere elongation and recombination (Benetti et al., 2007), and induced pluripotent stem cells from both young and old donors demonstrate decreased trimethylation as they acquire increased “stem-ness” (Marion et al., 2009). Taken

together, these findings suggest H4K20me3 is associated with both aged and differentiated tissues.

Recent work suggests that another interpretation of increased H4K20me3 during aging is a mark of cellular quiescence. Consistent with this alternative interpretation, oocytes derived from middle-aged mice show depleted dimethylation in compared to young sexually mature mice, potentially through conversion to H4K20me3 (Manosalva and Gonzalez, 2010). Quiescent macrophages must undergo selective demethylation of H4K20me3 to fully activate the proinflammatory immune response, mediated by the demethylase PHF2 (Stender et al., 2012). Further, in primary human fibroblasts induced into quiescence via contact inhibition, both H4K20me2 and H4K20me3 levels increased, promoting chromatin compaction, while other histone modifications remained unchanged (Evertts et al., 2013). Loss of the Suv4-20 enzymes increased the proportion of fibroblasts in S-phase, suggesting these proteins are required to maintain quiescence. In a separate study, senescent cells resistant to oxidative stress-induced apoptosis also demonstrated increased Suv420H2 protein coupled to increased global H4K20me3 and decreased MOF acetyltransferase and associated H4K16 acetylation (Sanders et al., 2013). The crustacean *Artemia* undergoes developmental diapause in unfavorable environments that can persist for years, and this extreme quiescent phenomenon requires the H4K20 trimethylase SETD4 (Dai et al., 2017). Demethylation of H4K20me3 in mouse neurons is required for the acquisition of new memories and spatial learning, consistent with its role in transcriptional inhibition (Wang et al., 2015). H4K20 trimethylation patterns are among the heterochromatic marks regulating proliferative potential of neural stem progenitor cells in the subventricular zone and are altered in the common glial cell cancer glioblastoma multiforme (Rhodes et al., 2016). Taken together, these reports link H4K20 trimethylation with the repression of both cellular proliferation and plasticity.

H4K20 Modification	Bound by	Functional roles
H4K20me1	Condensins L3MBTL1 53BP1 MBTD1(TIP60)	Cell cycle regulation (M phase) Cell proliferation DNA damage response Chromosome condensation Embryonic viability Transcription activation Dosage compensation
H4K20me2	53BP1 MBTD1(TIP60) JMJD2A Crb2	Postnatal viability DNA damage response Chromatin condensation Cell cycle regulation (G1 phase)
H4K20me3	?	Constitutive heterochromatin Cell cycle exit Quiescence/senescence Aging Chromatin compaction Diapause

Table 2.1. Binding partners and functions attributed to distinct H4K20 methylation states.

Enzymes responsible for higher order methylation of H4K20

In mammals, dimethylation and trimethylation are believed to be performed by the structurally similar SUV420H1 and SUV420H2, respectively, both of which potentially recognize both histone and non-histone substrates (Jorgensen et al., 2013; Weirich et al., 2016). In contrast, flies and worms possess a single ortholog homologous to both enzymes (SUV4-20 and SET-4, respectively) that are required for both di- and tri-methylation (Vielle et al., 2012; Yang et al., 2008), while Set9 is required for all H4K20 methylation states in *S. pombe* (Sanders et al., 2004). This conservation suggests either that these *Drosophila* and *C. elegans* homologs enzymes perform both methylation reactions or that they are dimethylases that provide a required substrate for subsequent trimethylation performed by one or more trimethylases. Although both conversion to di- and/or tri-methylation requires a monomethylated substrate, evidence in mouse embryonic fibroblasts suggests SUV420H2 does not require a dimethylated intermediate to trimethylate H4K20, nor does SUV420H2 rescue H4K20me2 in cells lacking SUV420H1 (Schotta et al., 2008). However, independent reports using *in vitro* functional assays suggest that the SET domain of both SUV420H enzymes is limited to dimethylation (Southall et al., 2014; Weirich et al., 2016; Wu et al., 2013). These findings may indicate that trimethylation kinetics do

not allow for *in vitro* detection, that undescribed domains outside the SET domain may provide additional regulation of enzymatic specificity, and/or enzymes other than the SUV4-20 methyltransferases perform trimethylation. Recent studies have implicated several conserved non-suv4-20 enzymes in H4K20 trimethylation, including SETD4, SMYD5, and SMYD3 (Dai et al., 2017; Foreman et al., 2011; Kidder et al., 2017; Stender et al., 2012). Although these findings have not been independently validated, such data suggest that multiple enzymes may be responsible for deposition of H4K20me3 depending on tissue type and/or developmental time.

Remarkably, little progress has been made in identifying H4K20 demethylases that target di- and tri-methylated residues. PHF8 is established as a H4K20me1 demethylase (Liu et al., 2010; Qi et al., 2010). Only one report suggests that the histone demethylase JMJD2A binds H4K20me2, but this association may not lead to dimethylation (Mallette et al., 2012). Similarly, only a single publication suggests PHF2 demethylates H4K20me3 in macrophages (Stender et al., 2012); however, many reports identify PHF2 as a H3K9me2 demethylase associated with increased adipogenesis (Kim et al., 2014; Lee et al., 2014; Okuno et al., 2013). A recently described neuron-specific splice variant of LSD1 (LSD1n) involved in brain development can demethylate both H4K20me1 and H4K20me2 *in vitro* while changes in H4K20me3 methylation were not reported (Wang et al., 2015; Zibetti et al., 2010).

Organism	H4K20 Modification	Methyltransferase(s)	Demethylase
S. pombe	me1	Set9	?
	me2		
	me3		
C. elegans	me1	SET-1	?
	me2	SET-4	?
	me3		
Drosophila	me1	PR-SET7	?
	me2	SUV4-20	?
	me3		
mammals	me1	PR-SET7/SETD8	PHF8
	me2	SUV420H1 (SUV420H2?)	?
	me3	SUV420H2, SMYD3, SMYD5, MMSET	PHF2?

Table 2.2. Enzymes associated with distinct H4K20 methylation states in model organisms.

Crosstalk between dosage compensation and H4K20 methylation

Emerging evidence has linked the establishment of dosage compensation on X chromosomes with X-specific patterns of H4K20 methylation in *C. elegans*. Independent groups have shown H4K20me1 is deposited on the X in embryos after establishment of dosage compensation (Custer et al., 2014; Kramer et al., 2015). Although a direct physical interaction between DCC components and H4K20 methyltransferases were not observed in *C. elegans* (Csankovszki et al., 2009), condensin II proteins have been shown to bind H4K20me1 in a different system (Liu et al., 2010). Further, intact dosage compensation is associated with an enrichment of H4K20me1 in both mammals and *C. elegans* (Kelsey et al., 2015; Vielle et al., 2012). In worms this enrichment occurs at the expense of H4K20me3 levels, which are depleted on X relative to autosomes. Disruption of the DCC eliminates the imbalance of monomethylation between sex chromosomes and autosomes.

Despite the observed depletion of H4K20me3 on X, both SET-1 and SET-4 activity may be required for dosage compensation (Webster et al., 2013; Wells et al., 2012). Loss of either SET-1 or SET-4 led to X-specific decondensation similar to that observed in DCC disruption (Lau et al., 2014). Recently, Webster et al. demonstrated that both dosage compensation and histone H4 lysine 20 methylation have important metabolic consequences during development (Webster et al., 2013). Animals deficient in TOR complex 2 (TORC2) have delayed development, decreased brood size and increased fat content (Soukas et al., 2009). Knockdown of DCC components including *dpy-21* rescued these phenotypes, as did RNAi against both known H4K20 methyltransferases *set-1* and *set-4* (Webster et al., 2013). Importantly, a role for H4K20 dimethylation in dosage compensation and X chromosome compaction remains undescribed (Fig. 2.3).

In addition to direct regulation of H4K20 methylation states, dosage compensation may interact with H4K20 indirectly through distinct chromatin modifications. Like SET-4, the HDAC SIR-2.1 may participate in dosage compensation, and H4K16 deacetylation promotes the establishment of H4K20 methylation (Lau et al., 2014; Serrano et al., 2013; Wells et al., 2012). H3K9 methylation promotes dosage compensation (Snyder et al., 2016), and previous evidence in mammals suggests that H3K9me3 promotes H4K20me3 deposition (Schotta et al., 2004; Souza et al., 2009).

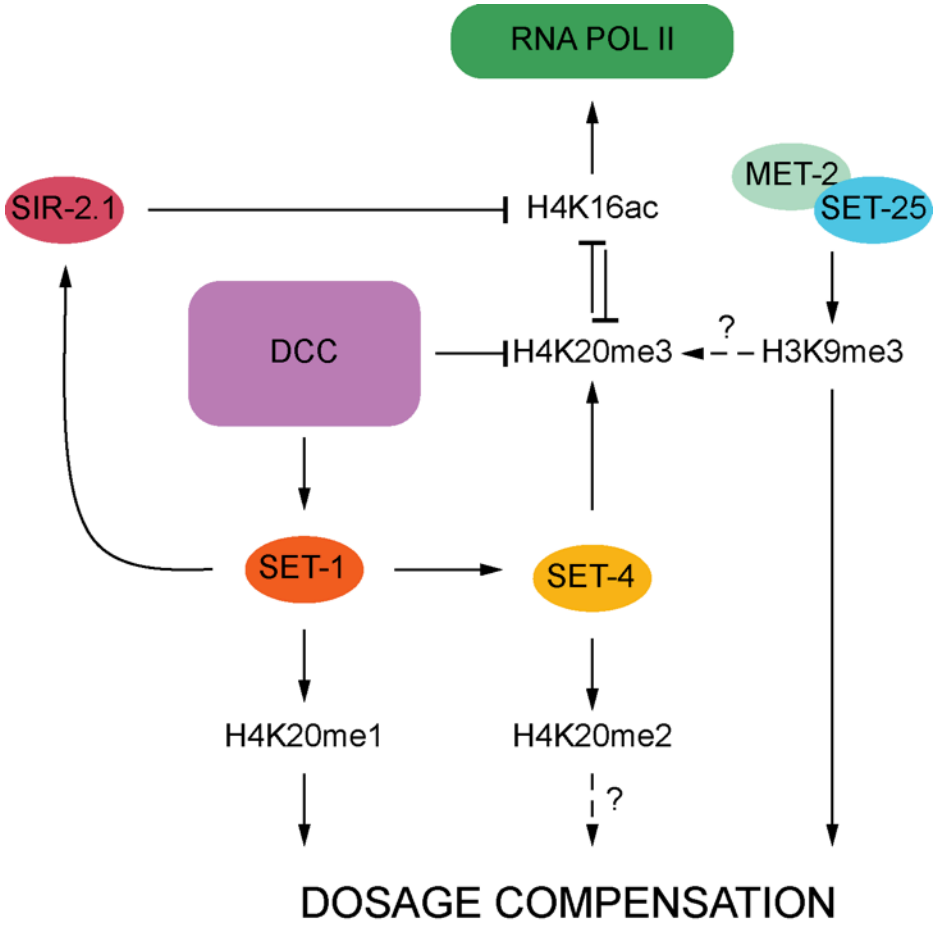

Figure 2.3. The *C. elegans* dosage compensation complex (DCC) interacts with H4K20 modifications to achieve dosage compensation. Binding of the DCC promotes H4K20me1 enrichment on the X chromosome and depletes H4K20me3, but both SET-1 and SET-4 may promote dosage compensation. SET-1 activity promotes H4K16 deacetylation by SIR-2.1. Proteins are represented as shapes while histone modifications are text. Plausible relationships for which direct evidence is lacking are indicated with dashed lines and question marks.

Summary

The epigenetic code permits highly complex regulation over gene expression in cells and tissues across differentiation states. These chemical modifications occur at multiple levels, ranging from the DNA itself, the nucleosome, higher order chromatin structure, to chromosome-wide compaction and nuclear positioning. At the level of chromatin, activating and repressive marks, including H4K16 acetylation and H4K20 methylation, respectively, compete for occupancy among many other post-translational histone modifications, while at the level of the chromosome, dosage compensation employs multiple epigenetic mechanisms to equalize gene expression between the sexes within a species. While this phenomenon is conserved, the mechanisms employed to achieve dosage compensation are remarkably distinct, suggesting dosage compensation evolved independently in distantly related metazoans.

In *C. elegans* the components of the dosage compensation complex are known and how dosage compensation is achieved has been extensively studied. Yet, the interplay between the DCC and partner epigenetic effectors and its consequences for development is only now becoming apparent. In Chapter 3, we expand the link between DPY-21 and SET-4 activity in controlling distinct developmental fates in *C. elegans* larvae in response to environmental stress.

References

Bajic, V., Mandusic, V., Stefanova, E., Bozovic, A., Davidovic, R., Zivkovic, L., Cabarkapa, A. and Spremo-Potparevic, B. (2015). Skewed X-chromosome inactivation in women affected by Alzheimer's disease. *J Alzheimers Dis* 43, 1251-1259.

Barski, A., Cuddapah, S., Cui, K., Roh, T. Y., Schones, D. E., Wang, Z., Wei, G., Chepelev, I. and Zhao, K. (2007). High-resolution profiling of histone methylations in the human genome. *Cell* 129, 823-837.

Beck, D. B., Burton, A., Oda, H., Ziegler-Birling, C., Torres-Padilla, M. E. and Reinberg, D. (2012). The role of PR-Set7 in replication licensing depends on Suv4-20h. *Genes Dev* 26, 2580-2589.

Belote, J. M. and Lucchesi, J. C. (1980). Male-specific lethal mutations of Drosophila melanogaster. *Genetics* 96, 165-186.

Benard, A., Goossens-Beumer, I. J., van Hoesel, A. Q., de Graaf, W., Horati, H., Putter, H., Zeestraten, E. C., van de Velde, C. J. and Kuppen, P. J. (2014). Histone trimethylation at H3K4, H3K9 and H4K20 correlates with patient survival and tumor recurrence in early-stage colon cancer. *BMC Cancer* 14, 531.

Benetti, R., Gonzalo, S., Jaco, I., Schotta, G., Klatt, P., Jenuwein, T. and Blasco, M. A. (2007). Suv4-20h deficiency results in telomere elongation and derepression of telomere recombination. *J Cell Biol* 178, 925-936.

Berger, S. L. (2007). The complex language of chromatin regulation during transcription. *Nature* 447, 407-412.

Birchler, J. A. (2016). Parallel Universes for Models of X Chromosome Dosage Compensation in Drosophila: A Review. *Cytogenet Genome Res* 148, 52-67.

Botuyan, M. V., Lee, J., Ward, I. M., Kim, J. E., Thompson, J. R., Chen, J. and Mer, G. (2006). Structural basis for the methylation state-specific recognition of histone H4-K20 by 53BP1 and Crb2 in DNA repair. *Cell* 127, 1361-1373.

Csankovszki, G., Collette, K., Spahl, K., Carey, J., Snyder, M., Petty, E., Patel, U., Tabuchi, T., Liu, H., McLeod, I., et al. (2009). Three distinct condensin complexes control C. elegans chromosome dynamics. *Curr Biol* 19, 9-19.

Custer, L. M., Snyder, M. J., Flegel, K. and Csankovszki, G. (2014). The onset of C. elegans dosage compensation is linked to the loss of developmental plasticity. *Dev Biol* 385, 279-290.

Dai, L., Ye, S., Li, H. W., Chen, D. F., Wang, H. L., Jia, S. N., Lin, C., Yang, J. S., Yang, F., Nagasawa, H., et al. (2017). SETD4 Regulates Cell Quiescence and Catalyzes the Trimethylation of H4K20 during Diapause Formation in Artemia. *Mol Cell Biol* 37.

Dang, W., Steffen, K. K., Perry, R., Dorsey, J. A., Johnson, F. B., Shilatifard, A., Kaeberlein, M., Kennedy, B. K. and Berger, S. L. (2009). Histone H4 lysine 16 acetylation regulates cellular lifespan. *Nature* 459, 802-807.

Davey, C. A., Sargent, D. F., Luger, K., Maeder, A. W. and Richmond, T. J. (2002). Solvent mediated interactions in the structure of the nucleosome core particle at 1.9 a resolution. *J Mol Biol* 319, 1097-1113.

Dawes, H. E., Berlin, D. S., Lapidus, D. M., Nusbaum, C., Davis, T. L. and Meyer, B. J. (1999). Dosage compensation proteins targeted to X chromosomes by a determinant of hermaphrodite fate. *Science* 284, 1800-1804.

DeLange, R. J., Fambrough, D. M., Smith, E. L. and Bonner, J. (1969). Calf and pea histone IV. II. The complete amino acid sequence of calf thymus histone IV; presence of epsilon-N-acetyllysine. *J Biol Chem* 244, 319-334.

Deng, X., Hiatt, J. B., Nguyen, D. K., Ercan, S., Sturgill, D., Hillier, L. W., Schlesinger, F., Davis, C. A., Reinke, V. J., Gingeras, T. R., et al. (2011). Evidence for compensatory upregulation of expressed X-linked genes in mammals, Caenorhabditis elegans and Drosophila melanogaster. *Nat Genet* 43, 1179-1185.

Dorigo, B., Schalch, T., Kulangara, A., Duda, S., Schroeder, R. R. and Richmond, T. J. (2004). Nucleosome arrays reveal the two-start organization of the chromatin fiber. *Science* 306, 1571-1573.

Dowen, J. M., Fan, Z. P., Hnisz, D., Ren, G., Abraham, B. J., Zhang, L. N., Weintraub, A. S., Schuijers, J., Lee, T. I., Zhao, K., et al. (2014). Control of cell identity genes occurs in insulated neighborhoods in mammalian chromosomes. *Cell* 159, 374-387.

Dulev, S., Tkach, J., Lin, S. and Batada, N. N. (2014). SET8 methyltransferase activity during the DNA double-strand break response is required for recruitment of 53BP1. *EMBO Rep* 15, 1163-1174.

Edwards, C. R., Dang, W. and Berger, S. L. (2011). Histone H4 lysine 20 of Saccharomyces cerevisiae is monomethylated and functions in subtelomeric silencing. *Biochemistry* 50, 10473-10483.

Eid, A., Rodriguez-Terrones, D., Burton, A. and Torres-Padilla, M. E. (2016). SUV4-20 activity in the preimplantation mouse embryo controls timely replication. *Genes Dev* 30, 2513-2526.

Emmerth, S., Schober, H., Gaidatzis, D., Roloff, T., Jacobeit, K. and Buhler, M. (2010). Nuclear retention of fission yeast dicer is a prerequisite for RNAi-mediated heterochromatin assembly. *Dev Cell* 18, 102-113.

Ercan, S., Dick, L. L. and Lieb, J. D. (2009). The C. elegans dosage compensation complex propagates dynamically and independently of X chromosome sequence. *Curr Biol* 19, 1777-1787.

Evertts, A. G., Manning, A. L., Wang, X., Dyson, N. J., Garcia, B. A. and Coller, H. A. (2013). H4K20 methylation regulates quiescence and chromatin compaction. *Mol Biol Cell* 24, 3025-3037.

Feser, J. and Tyler, J. (2011). Chromatin structure as a mediator of aging. *FEBS Lett* 585, 2041-2048.

Foreman, K. W., Brown, M., Park, F., Emtage, S., Harriss, J., Das, C., Zhu, L., Crew, A., Arnold, L., Shaaban, S., et al. (2011). Structural and functional profiling of the human histone methyltransferase SMYD3. *PLoS One* 6, e22290.

Gentilini, D., Castaldi, D., Mari, D., Monti, D., Franceschi, C., Di Blasio, A. M. and Vitale, G. (2012). Age-dependent skewing of X chromosome inactivation appears delayed in centenarians' offspring. Is there a role for allelic imbalance in healthy aging and longevity? *Aging Cell* 11, 277-283.

Gonzalo, S., Garcia-Cao, M., Fraga, M. F., Schotta, G., Peters, A. H., Cotter, S. E., Eguia, R., Dean, D. C., Esteller, M., Jenuwein, T., et al. (2005). Role of the RB1 family in stabilizing histone methylation at constitutive heterochromatin. *Nat Cell Biol* 7, 420-428.

Greeson, N. T., Sengupta, R., Arida, A. R., Jenuwein, T. and Sanders, S. L. (2008). Di-methyl H4 lysine 20 targets the checkpoint protein Crb2 to sites of DNA damage. *J Biol Chem* 283, 33168-33174.

Hartlerode, A. J., Guan, Y., Rajendran, A., Ura, K., Schotta, G., Xie, A., Shah, J. V. and Scully, R. (2012). Impact of histone H4 lysine 20 methylation on 53BP1 responses to chromosomal double strand breaks. *PLoS One* 7, e49211.

Hayes, S. A., Kutty, S., Thomas, J., Johnson, J. T. and Yetman, A. T. (2017). Cardiovascular and general health status of adults with Trisomy 21. *Int J Cardiol*.

Hodgkin, J. (1987). Sex determination and dosage compensation in Caenorhabditis elegans. *Annu Rev Genet* 21, 133-154.

Ikegami, K., Egelhofer, T. A., Strome, S. and Lieb, J. D. (2010). Caenorhabditis elegans chromosome arms are anchored to the nuclear membrane via discontinuous association with LEM-2. *Genome Biol* 11, R120.

Jans, J., Gladden, J. M., Ralston, E. J., Pickle, C. S., Michel, A. H., Pferdehirt, R. R., Eisen, M. B. and Meyer, B. J. (2009). A condensin-like dosage compensation complex acts at a distance to control expression throughout the genome. *Genes Dev* 23, 602-618.

Jorgensen, S., Schotta, G. and Sorensen, C. S. (2013). Histone H4 lysine 20 methylation: key player in epigenetic regulation of genomic integrity. *Nucleic Acids Res* 41, 2797-2806.

Julien, P., Brawand, D., Soumillon, M., Necsulea, A., Liechti, A., Schutz, F., Daish, T., Grutzner, F. and Kaessmann, H. (2012). Mechanisms and evolutionary patterns of mammalian and avian dosage compensation. *PLoS Biol* 10, e1001328.

Ka, S., Ahn, H., Seo, M., Kim, H., Kim, J. N. and Lee, H. J. (2016). Status of dosage compensation of X chromosome in bovine genome. *Genetica* 144, 435-444.

Kadauke, S. and Blobel, G. A. (2009). Chromatin loops in gene regulation. *Biochim Biophys Acta* 1789, 17-25.

Kalakonda, N., Fischle, W., Boccuni, P., Gurvich, N., Hoya-Arias, R., Zhao, X., Miyata, Y., Macgrogan, D., Zhang, J., Sims, J. K., et al. (2008). Histone H4 lysine 20 monomethylation promotes transcriptional repression by L3MBTL1. *Oncogene* 27, 4293-4304.

Kapoor-Vazirani, P., Kagey, J. D. and Vertino, P. M. (2011). SUV420H2-mediated H4K20 trimethylation enforces RNA polymerase II promoter-proximal pausing by blocking hMOF-dependent H4K16 acetylation. *Mol Cell Biol* 31, 1594-1609.

Kapoor-Vazirani, P. and Vertino, P. M. (2014). A dual role for the histone methyltransferase PR-SET7/SETD8 and histone H4 lysine 20 monomethylation in the local regulation of RNA polymerase II pausing. *J Biol Chem* 289, 7425-7437.

Kawahara, T. L., Michishita, E., Adler, A. S., Damian, M., Berber, E., Lin, M., McCord, R. A., Ongaigui, K. C., Boxer, L. D., Chang, H. Y., et al. (2009). SIRT6 links histone H3 lysine 9 deacetylation to NF-kappaB-dependent gene expression and organismal life span. *Cell* 136, 62-74.

Kelsey, A. D., Yang, C., Leung, D., Minks, J., Dixon-McDougall, T., Baldry, S. E., Bogutz, A. B., Lefebvre, L. and Brown, C. J. (2015). Impact of flanking chromosomal sequences on localization and silencing by the human non-coding RNA XIST. *Genome Biol* 16, 208.

Kidder, B. L., Hu, G., Cui, K. and Zhao, K. (2017). SMYD5 regulates H4K20me3-marked heterochromatin to safeguard ES cell self-renewal and prevent spurious differentiation. *Epigenetics Chromatin* 10, 8.

Kim, H. J., Park, J. W., Lee, K. H., Yoon, H., Shin, D. H., Ju, U. I., Seok, S. H., Lim, S. H., Lee, Z. H., Kim, H. H., et al. (2014). Plant homeodomain finger protein 2 promotes bone formation by demethylating and activating Runx2 for osteoblast differentiation. *Cell Res* 24, 1231-1249.

Kramer, M., Kranz, A. L., Su, A., Winterkorn, L. H., Albritton, S. E. and Ercan, S. (2015). Developmental Dynamics of X-Chromosome Dosage Compensation by the DCC and H4K20me1 in C. elegans. *PLoS Genet* 11, e1005698.

Kruesi, W. S., Core, L. J., Waters, C. T., Lis, J. T. and Meyer, B. J. (2013). Condensin controls recruitment of RNA polymerase II to achieve nematode X-chromosome dosage compensation. *Elife* 2, e00808.

Lan, F. and Shi, Y. (2009). Epigenetic regulation: methylation of histone and non-histone proteins. *Sci China C Life Sci* 52, 311-322.

Lau, A. C., Nabeshima, K. and Csankovszki, G. (2014). The C. elegans dosage compensation complex mediates interphase X chromosome compaction. *Epigenetics Chromatin* 7, 31.

Lautarescu, B. A., Holland, A. J. and Zaman, S. H. (2017). The Early Presentation of Dementia in People with Down Syndrome: a Systematic Review of Longitudinal Studies. *Neuropsychol Rev* 27, 31-45.

Lee, K. H., Ju, U. I., Song, J. Y. and Chun, Y. S. (2014). The histone demethylase PHF2 promotes fat cell differentiation as an epigenetic activator of both C/EBPalpha and C/EBPdelta. *Molecules and cells* 37, 734-741.

Li, G., Zhang, Z., Jin, T., Liang, H., Tu, Y., Gong, L., Chen, Z. and Gao, G. (2013). High frequency of the X-chromosome inactivation in young female patients with high-grade glioma. *Diagn Pathol* 8, 101.

Li, Y., Armstrong, R. L., Duronio, R. J. and MacAlpine, D. M. (2016). Methylation of histone H4 lysine 20 by PR-Set7 ensures the integrity of late replicating sequence domains in Drosophila. *Nucleic Acids Res* 44, 7204-7218.

Liu, W., Tanasa, B., Tyurina, O. V., Zhou, T. Y., Gassmann, R., Liu, W. T., Ohgi, K. A., Benner, C., Garcia-Bassets, I., Aggarwal, A. K., et al. (2010). PHF8 mediates histone H4 lysine 20 demethylation events involved in cell cycle progression. *Nature* 466, 508-512.

Lu, X., Simon, M. D., Chodaparambil, J. V., Hansen, J. C., Shokat, K. M. and Luger, K. (2008). The effect of H3K79 dimethylation and H4K20 trimethylation on nucleosome and chromatin structure. *Nat Struct Mol Biol* 15, 1122-1124.

Luger, K., Mader, A. W., Richmond, R. K., Sargent, D. F. and Richmond, T. J. (1997). Crystal structure of the nucleosome core particle at 2.8 A resolution. *Nature* 389, 251-260.

Mallette, F. A., Mattiroli, F., Cui, G., Young, L. C., Hendzel, M. J., Mer, G., Sixma, T. K. and Richard, S. (2012). RNF8- and RNF168-dependent degradation of KDM4A/JMJD2A triggers 53BP1 recruitment to DNA damage sites. *Embo J* 31, 1865-1878.

Manosalva, I. and Gonzalez, A. (2010). Aging changes the chromatin configuration and histone methylation of mouse oocytes at germinal vesicle stage. *Theriogenology* 74, 1539-1547.

Margueron, R., Trojer, P. and Reinberg, D. (2005). The key to development: interpreting the histone code? *Curr Opin Genet Dev* 15, 163-176.

Marion, R. M., Strati, K., Li, H., Tejera, A., Schoeftner, S., Ortega, S., Serrano, M. and Blasco, M. A. (2009). Telomeres acquire embryonic stem cell characteristics in induced pluripotent stem cells. *Cell Stem Cell* 4, 141-154.

McKay, D. J., Klusza, S., Penke, T. J., Meers, M. P., Curry, K. P., McDaniel, S. L., Malek, P. Y., Cooper, S. W., Tatomer, D. C., Lieb, J. D., et al. (2015). Interrogating the function of metazoan histones using engineered gene clusters. *Dev Cell* 32, 373-386.

Meyer, B. J. (2010). Targeting X chromosomes for repression. *Curr Opin Genet Dev* 20, 179-189.

Miller, L. M., Plenefisch, J. D., Casson, L. P. and Meyer, B. J. (1988). xol-1: a gene that controls the male modes of both sex determination and X chromosome dosage compensation in C. elegans. *Cell* 55, 167-183.

Nicetto, D., Hahn, M., Jung, J., Schneider, T. D., Straub, T., David, R., Schotta, G. and Rupp, R. A. (2013). Suv4-20h histone methyltransferases promote neuroectodermal differentiation by silencing the pluripotency-associated Oct-25 gene. *PLoS Genet* 9, e1003188.

Nishibuchi, G. and Dejardin, J. (2017). The molecular basis of the organization of repetitive DNA-containing constitutive heterochromatin in mammals. *Chromosome Res* 25, 77-87.

Nishioka, K., Rice, J. C., Sarma, K., Erdjument-Bromage, H., Werner, J., Wang, Y., Chuikov, S., Valenzuela, P., Tempst, P., Steward, R., et al. (2002). PR-Set7 is a nucleosome-specific methyltransferase that modifies lysine 20 of histone H4 and is associated with silent chromatin. *Mol Cell* 9, 1201-1213.

Oda, H., Okamoto, I., Murphy, N., Chu, J., Price, S. M., Shen, M. M., Torres-Padilla, M. E., Heard, E. and Reinberg, D. (2009). Monomethylation of histone H4-lysine 20 is involved in chromosome structure and stability and is essential for mouse development. *Mol Cell Biol* 29, 2278-2295.

Okuno, Y., Ohtake, F., Igarashi, K., Kanno, J., Matsumoto, T., Takada, I., Kato, S. and Imai, Y. (2013). Epigenetic regulation of adipogenesis by PHF2 histone demethylase. *Diabetes* 62, 1426-1434.

Pei, H., Zhang, L., Luo, K., Qin, Y., Chesi, M., Fei, F., Bergsagel, P. L., Wang, L., You, Z. and Lou, Z. (2011). MMSET regulates histone H4K20 methylation and 53BP1 accumulation at DNA damage sites. *Nature* 470, 124-128.

Plenefisch, J. D., DeLong, L. and Meyer, B. J. (1989). Genes that implement the hermaphrodite mode of dosage compensation in Caenorhabditis elegans. *Genetics* 121, 57-76.

Pogribny, I. P., Ross, S. A., Tryndyak, V. P., Pogribna, M., Poirier, L. A. and Karpinets, T. V. (2006). Histone H3 lysine 9 and H4 lysine 20 trimethylation and the expression of Suv4-20h2 and Suv-39h1 histone methyltransferases in hepatocarcinogenesis induced by methyl deficiency in rats. *Carcinogenesis* 27, 1180-1186.

Qi, H. H., Sarkissian, M., Hu, G. Q., Wang, Z., Bhattacharjee, A., Gordon, D. B., Gonzales, M., Lan, F., Ongusaha, P. P., Huarte, M., et al. (2010). Histone H4K20/H3K9 demethylase PHF8 regulates zebrafish brain and craniofacial development. *Nature* 466, 503-507.

Rhodes, C. T., Sandstrom, R. S., Huang, S. A., Wang, Y., Schotta, G., Berger, M. S. and Lin, C. A. (2016). Cross-species Analyses Unravel the Complexity of H3K27me3 and H4K20me3 in the Context of Neural Stem Progenitor Cells. *Neuroepigenetics* 6, 10-25.

Robert Finestra, T. and Gribnau, J. (2017). X chromosome inactivation: silencing, topology and reactivation. *Curr Opin Cell Biol* 46, 54-61.

Sanders, S. L., Portoso, M., Mata, J., Bahler, J., Allshire, R. C. and Kouzarides, T. (2004). Methylation of histone H4 lysine 20 controls recruitment of Crb2 to sites of DNA damage. *Cell* 119, 603-614.

Sanders, Y. Y., Liu, H., Zhang, X., Hecker, L., Bernard, K., Desai, L., Liu, G. and Thannickal, V. J. (2013). Histone modifications in senescence-associated resistance to apoptosis by oxidative stress. *Redox Biol* 1, 8-16.

Sarg, B., Helliger, W., Talasz, H., Koutzamani, E. and Lindner, H. H. (2004). Histone H4 hyperacetylation precludes histone H4 lysine 20 trimethylation. *J Biol Chem* 279, 53458-53464.

Sarg, B., Koutzamani, E., Helliger, W., Rundquist, I. and Lindner, H. H. (2002). Postsynthetic trimethylation of histone H4 at lysine 20 in mammalian tissues is associated with aging. *J Biol Chem* 277, 39195-39201.

Schneider, A. C., Heukamp, L. C., Rogenhofer, S., Fechner, G., Bastian, P. J., von Ruecker, A., Muller, S. C. and Ellinger, J. (2011). Global histone H4K20 trimethylation predicts cancer-specific survival in patients with muscle-invasive bladder cancer. *BJU Int* 108, E290-296.

Schotta, G., Lachner, M., Sarma, K., Ebert, A., Sengupta, R., Reuter, G., Reinberg, D. and Jenuwein, T. (2004). A silencing pathway to induce H3-K9 and H4-K20 trimethylation at constitutive heterochromatin. *Genes Dev* 18, 1251-1262.

Schotta, G., Sengupta, R., Kubicek, S., Malin, S., Kauer, M., Callen, E., Celeste, A., Pagani, M., Opravil, S., De La Rosa-Velazquez, I. A., et al. (2008). A chromatin-wide transition to H4K20 monomethylation impairs genome integrity and programmed DNA rearrangements in the mouse. *Genes Dev* 22, 2048-2061.

Serrano, L., Martinez-Redondo, P., Marazuela-Duque, A., Vazquez, B. N., Dooley, S. J., Voigt, P., Beck, D. B., Kane-Goldsmith, N., Tong, Q., Rabanal, R. M., et al. (2013). The tumor suppressor SirT2 regulates cell cycle progression and genome stability by modulating the mitotic deposition of H4K20 methylation. *Genes & development* 27, 639-653.

Sharma, R. and Meister, P. (2015). Linking dosage compensation and X chromosome nuclear organization in C. elegans. *Nucleus* 6, 266-272.

Shi, X., Kachirskaia, I., Yamaguchi, H., West, L. E., Wen, H., Wang, E. W., Dutta, S., Appella, E. and Gozani, O. (2007). Modulation of p53 function by SET8-mediated methylation at lysine 382. *Mol Cell* 27, 636-646.

Shinchi, Y., Hieda, M., Nishioka, Y., Matsumoto, A., Yokoyama, Y., Kimura, H., Matsuura, S. and Matsuura, N. (2015). SUV420H2 suppresses breast cancer cell invasion through down regulation of the SH2 domain-containing focal adhesion protein tensin-3. *Exp Cell Res* 334, 90-99.

Shumaker, D. K., Dechat, T., Kohlmaier, A., Adam, S. A., Bozovsky, M. R., Erdos, M. R., Eriksson, M., Goldman, A. E., Khuon, S., Collins, F. S., et al. (2006). Mutant nuclear lamin A leads to progressive alterations of epigenetic control in premature aging. *Proc Natl Acad Sci U S A* 103, 8703-8708.

Snyder, M. J., Lau, A. C., Brouhard, E. A., Davis, M. B., Jiang, J., Sifuentes, M. H. and Csankovszki, G. (2016). Anchoring of Heterochromatin to the Nuclear Lamina Reinforces Dosage Compensation-Mediated Gene Repression. *PLoS Genet* 12, e1006341.

Soukas, A. A., Kane, E. A., Carr, C. E., Melo, J. A. and Ruvkun, G. (2009). Rictor/TORC2 regulates fat metabolism, feeding, growth, and life span in Caenorhabditis elegans. *Genes Dev* 23, 496-511.

Southall, S. M., Cronin, N. B. and Wilson, J. R. (2014). A novel route to product specificity in the Suv4-20 family of histone H4K20 methyltransferases. *Nucleic Acids Res* 42, 661-671.

Souza, P. P., Volkel, P., Trinel, D., Vandamme, J., Rosnoblet, C., Heliot, L. and Angrand, P. O. (2009). The histone methyltransferase SUV420H2 and Heterochromatin Proteins HP1 interact but show different dynamic behaviours. *BMC Cell Biol* 10, 41.

Stender, J. D., Pascual, G., Liu, W., Kaikkonen, M. U., Do, K., Spann, N. J., Boutros, M., Perrimon, N., Rosenfeld, M. G. and Glass, C. K. (2012). Control of proinflammatory

gene programs by regulated trimethylation and demethylation of histone H4K20. *Molecular cell* 48, 28-38.
Tan, M., Luo, H., Lee, S., Jin, F., Yang, J. S., Montellier, E., Buchou, T., Cheng, Z., Rousseaux, S., Rajagopal, N., et al. (2011). Identification of 67 histone marks and histone lysine crotonylation as a new type of histone modification. *Cell* 146, 1016-1028.
Tanaka, H., Takebayashi, S. I., Sakamoto, A., Igata, T., Nakatsu, Y., Saitoh, N., Hino, S. and Nakao, M. (2017). The SETD8/PR-Set7 Methyltransferase Functions as a Barrier to Prevent Senescence-Associated Metabolic Remodeling. *Cell Rep* 18, 2148-2161.
Terranova, R., Pujol, N., Fasano, L. and Djabali, M. (2002). Characterisation of set-1, a conserved PR/SET domain gene in Caenorhabditis elegans. *Gene* 292, 33-41.
Towbin, B. D., Gonzalez-Aguilera, C., Sack, R., Gaidatzis, D., Kalck, V., Meister, P., Askjaer, P. and Gasser, S. M. (2012). Step-wise methylation of histone H3K9 positions heterochromatin at the nuclear periphery. *Cell* 150, 934-947.
Tryndyak, V. P., Kovalchuk, O. and Pogribny, I. P. (2006). Loss of DNA methylation and histone H4 lysine 20 trimethylation in human breast cancer cells is associated with aberrant expression of DNA methyltransferase 1, Suv4-20h2 histone methyltransferase and methyl-binding proteins. *Cancer Biol Ther* 5, 65-70.
Tsurumi, A. and Li, W. X. (2012). Global heterochromatin loss: a unifying theory of aging? *Epigenetics* 7, 680-688.
Van Den Broeck, A., Brambilla, E., Moro-Sibilot, D., Lantuejoul, S., Brambilla, C., Eymin, B., Khochbin, S. and Gazzeri, S. (2008). Loss of histone H4K20 trimethylation occurs in preneoplasia and influences prognosis of non-small cell lung cancer. *Clin Cancer Res* 14, 7237-7245.
van Nuland, R. and Gozani, O. (2016). Histone H4 Lysine 20 (H4K20) Methylation, Expanding the Signaling Potential of the Proteome One Methyl Moiety at a Time. *Mol Cell Proteomics* 15, 755-764.
Vieira, F. Q., Costa-Pinheiro, P., Almeida-Rios, D., Graca, I., Monteiro-Reis, S., Simoes-Sousa, S., Carneiro, I., Sousa, E. J., Godinho, M. I., Baltazar, F., et al. (2015). SMYD3 contributes to a more aggressive phenotype of prostate cancer and targets Cyclin D2 through H4K20me3. *Oncotarget* 6, 13644-13657.
Vielle, A., Lang, J., Dong, Y., Ercan, S., Kotwaliwale, C., Rechtsteiner, A., Appert, A., Chen, Q. B., Dose, A., Egelhofer, T., et al. (2012). H4K20me1 contributes to downregulation of X-linked genes for C. elegans dosage compensation. *PLoS genetics* 8, e1002933.
Wang, C. M., Tsai, S. N., Yew, T. W., Kwan, Y. W. and Ngai, S. M. (2010). Identification of histone methylation multiplicities patterns in the brain of senescence-accelerated prone mouse 8. *Biogerontology* 11, 87-102.
Wang, J., Telese, F., Tan, Y., Li, W., Jin, C., He, X., Basnet, H., Ma, Q., Merkurjev, D., Zhu, X., et al. (2015). LSD1n is an H4K20 demethylase regulating memory formation via transcriptional elongation control. *Nat Neurosci* 18, 1256-1264.
Wang, Y., Wang, Y., Ma, L., Nie, M., Ju, J., Liu, M., Deng, Y., Yao, B., Gui, T., Li, X., et al. (2017). Heterochromatin Protein 1gamma Is a Novel Epigenetic Repressor of Human Embryonic -Globin Gene Expression. *J Biol Chem* 292, 4811-4817.
Webster, C. M., Wu, L., Douglas, D. and Soukas, A. A. (2013). A non-canonical role for the C. elegans dosage compensation complex in growth and metabolic regulation downstream of TOR complex 2. *Development* 140, 3601-3612.

Weirich, S., Kudithipudi, S. and Jeltsch, A. (2016). Specificity of the SUV4-20H1 and SUV4-20H2 protein lysine methyltransferases and methylation of novel substrates. *J Mol Biol* 428, 2344-2358.

Wells, M. B., Snyder, M. J., Custer, L. M. and Csankovszki, G. (2012). Caenorhabditis elegans dosage compensation regulates histone H4 chromatin state on X chromosomes. *Molecular and cellular biology* 32, 1710-1719.

Wolf, J. B. and Bryk, J. (2011). General lack of global dosage compensation in ZZ/ZW systems? Broadening the perspective with RNA-seq. *BMC Genomics* 12, 91.

Wongtawan, T., Taylor, J. E., Lawson, K. A., Wilmut, I. and Pennings, S. (2011). Histone H4K20me3 and HP1alpha are late heterochromatin markers in development, but present in undifferentiated embryonic stem cells. *J Cell Sci* 124, 1878-1890.

Wu, H., Siarheyeva, A., Zeng, H., Lam, R., Dong, A., Wu, X. H., Li, Y., Schapira, M., Vedadi, M. and Min, J. (2013). Crystal structures of the human histone H4K20 methyltransferases SUV420H1 and SUV420H2. *FEBS Lett* 587, 3859-3868.

Wu, S. and Rice, J. C. (2011). A new regulator of the cell cycle: the PR-Set7 histone methyltransferase. *Cell Cycle* 10, 68-72.

Wutz, A. (2011). Gene silencing in X-chromosome inactivation: advances in understanding facultative heterochromatin formation. *Nat Rev Genet* 12, 542-553.

Xiao, B., Wilson, J. R. and Gamblin, S. J. (2003). SET domains and histone methylation. *Curr Opin Struct Biol* 13, 699-705.

Yang, H., Pesavento, J. J., Starnes, T. W., Cryderman, D. E., Wallrath, L. L., Kelleher, N. L. and Mizzen, C. A. (2008). Preferential dimethylation of histone H4 lysine 20 by Suv4-20. *J Biol Chem* 283, 12085-12092.

Yurov, Y. B., Vorsanova, S. G., Liehr, T., Kolotii, A. D. and Iourov, I. Y. (2014). X chromosome aneuploidy in the Alzheimer's disease brain. *Mol Cytogenet* 7, 20.

Zhan, M., Yamaza, H., Sun, Y., Sinclair, J., Li, H. and Zou, S. (2007). Temporal and spatial transcriptional profiles of aging in Drosophila melanogaster. *Genome Res* 17, 1236-1243.

Zibetti, C., Adamo, A., Binda, C., Forneris, F., Toffolo, E., Verpelli, C., Ginelli, E., Mattevi, A., Sala, C. and Battaglioli, E. (2010). Alternative splicing of the histone demethylase LSD1/KDM1 contributes to the modulation of neurite morphogenesis in the mammalian nervous system. *J Neurosci* 30, 2521-2532.

Chapter 3

A histone H4 lysine 20 methyltransferase couples environmental cues to sensory neuron control of developmental plasticity[1]

Abstract

Animals change developmental fates in response to external cues. In the nematode *Caenorhabditis elegans*, unfavorable environmental conditions induce a state of diapause known as dauer by inhibiting the conserved DAF-2 insulin-like signaling (ILS) pathway through incompletely understood mechanisms. We previously established a role for the *C. elegans* dosage compensation protein DPY-21 in the control of dauer arrest and DAF-2 ILS. Here we show that the histone H4 lysine 20 methyltransferase SET-4, which also influences dosage compensation, promotes dauer arrest in part by repressing the X-linked *ins-9* gene, which encodes a new agonist insulin-like peptide (ILP) expressed specifically in the paired ASI sensory neurons that are required for dauer bypass. *ins-9* repression in dauer-constitutive mutants requires DPY-21, SET-4, and the FoxO transcription factor DAF-16, which is the main target of DAF-2 ILS. In contrast, autosomal genes encoding major agonist ILPs that promote reproductive development are not repressed by DPY-21, SET-4, or DAF-16/FoxO. Our results implicate SET-4 as a sensory rheostat that reinforces developmental fates in response to environmental cues by modulating autocrine and paracrine DAF-2 ILS.

[1] Originally published in Development (2017 Feb 16 doi: 10.1242/dev.145722 [Epub ahead of print]) with authors listed as Delaney, C.E., Chen, A.T., Graniel, J.V., Dumas, K.J., and Hu, P.J.

Introduction

To maintain evolutionary fitness, organisms must react appropriately to environmental cues. The free-living nematode *Caenorhabditis elegans* has evolved a developmental strategy to optimize survival in changing environments. Under replete conditions, larvae progress through four stages (L1 – L4) to become reproductive adults. In adverse conditions such as overcrowding, heat, or food scarcity, larvae arrest in an alternative stage known as dauer. Adapted for survival in harsh environments, dauers are morphologically, metabolically, and behaviorally distinct from reproductive L3 larvae. Improvement of ambient conditions induces dauer exit and resumption of reproductive development (Fielenbach and Antebi, 2008; Riddle, 1988). The dominant environmental cue that influences dauer arrest is a constitutively elaborated pheromone that indicates population density (Butcher et al., 2008; Golden and Riddle, 1982).

C. elegans dauer arrest has served as a useful paradigm for understanding the molecular basis for developmental plasticity. Genetic analysis has defined four conserved signaling pathways that promote reproductive development in favorable environments. The DAF-11 transmembrane guanylyl cyclase acts in chemosensory neurons to regulate dauer arrest through the cyclic nucleotide-gated channel subunits TAX-2 and TAX-4. Downstream of DAF-11, DAF-2 insulin receptor (InsR) and DAF-7 transforming growth factor-β (TGFβ)-like pathways act in parallel to promote reproductive development by inhibiting the activities of the FoxO transcription factor DAF-16 and the SMAD transcription factor DAF-3, respectively. Distal to DAF-16/FoxO and DAF-3/SMAD, bile-acid-like steroid hormones known as dafachronic acids (DAs) promote reproductive development by regulating the activity of the conserved nuclear receptor DAF-12 (Fielenbach and Antebi, 2008).

While genetic analysis has identified how components of the DAF-11, DAF-2/InsR, DAF-7/TGFβ, and DAF-12 pathways interact to promote reproductive development in favorable conditions (Gottlieb and Ruvkun, 1994; Riddle et al., 1981; Thomas et al., 1993; Vowels and Thomas, 1992), the molecular nature of the upstream events that couple external cues to the activities of these pathways remains poorly understood. Laser ablation experiments demonstrated that the amphid sensory neurons are required for induction of dauer arrest by pheromone (Schackwitz et al., 1996; Vowels and Thomas, 1994). Indeed, the dauer-inhibitory ASI sensory

neurons (Bargmann and Horvitz, 1991) are specific sites of expression of three insulin-like peptides (ILPs) that promote reproductive development through DAF-2/InsR (INS-4, INS-6, and DAF-28) (Chen and Baugh, 2014; Cornils et al., 2011; Hung et al., 2014; Li et al., 2003) as well as the DAF-7 TGFβ-like ligand that promotes reproductive development (Ren et al., 1996; Schackwitz et al., 1996). Furthermore, crude dauer pheromone reduces the expression of DAF-28 and DAF-7 in ASI (Li et al., 2003; Schackwitz et al., 1996), suggesting that pheromone induces dauer arrest at least in part by reducing the expression of agonist ligands in sensory neurons that regulate DAF-2/InsR and TGFβ-like signaling. How pheromone represses these ligands remains a mystery.

We previously reported an unforeseen role for the *C. elegans* dosage compensation protein DPY-21 in promoting dauer arrest through inhibition of the DAF-2/InsR pathway (Dumas et al., 2013). DPY-21 is a component of the condensin-like dosage compensation complex (DCC) that equalizes X-linked gene expression between males and hermaphrodites by binding to both hermaphrodite X chromosomes during embryogenesis and repressing gene expression approximately two-fold (Meyer, 2010; Yonker and Meyer, 2003). Here we show that the conserved histone H4 lysine 20 (H4K20) methyltransferase SET-4, which also influences dosage compensation (Kramer et al., 2015; Vielle et al., 2012; Wells et al., 2012), promotes dauer arrest in a sex-specific manner by synergizing with DAF-16/FoxO to repress *ins-9,* an X-linked gene that encodes an ILP expressed specifically in ASI neurons (Chen and Baugh, 2014; Pierce et al., 2001). These findings reveal a sexually dimorphic role for regulators of histone H4K20 methylation in broadening the dynamic range of sensory responses to environmental cues that control developmental plasticity.

Results

SET-4 acts through DAF-2 ILS to promote dauer arrest in a sex-specific manner

DAF-2/InsR promotes reproductive development by activating a conserved phosphoinositide 3-kinase (PI3K)/Akt pathway to inhibit DAF-16/FoxO (Murphy and Hu, 2013). The conserved protein EAK-7 acts in parallel to AKT-1 to inhibit nuclear DAF-16/FoxO activity (Alam et al.,

2010). In contrast to *eak-7* and *akt-1* single mutants, which develop reproductively, *eak-7;akt-1* double mutant animals arrest as dauers in a DAF-16/FoxO-dependent manner (Alam et al., 2010). To identify new DAF-16/FoxO regulators, we performed a forward genetic screen for *s*uppressors of the *eak-7;akt-1* dauer-constitutive phenotype (*seak*). The first *seak* mutants characterized harbored loss-of-function mutations in the dosage compensation gene *dpy-21* (Dumas et al., 2013). *dpy-21* encodes a conserved component of the condensin-like dosage compensation complex (DCC) that binds to X chromosomes and represses X-linked gene expression (Meyer, 2010; Yonker and Meyer, 2003). One *seak* mutant strain contained a point mutation in *set-4*, which encodes a histone H4K20 methyltransferase homolog that influences dosage compensation (Vielle et al., 2012; Wells et al., 2012). *set-4(dp268)* is predicted to change the conserved SET domain catalytic residue serine 182 (Southall et al., 2014) to phenylalanine (Figure 1A, Figure S1A). In light of our findings on *dpy-21* (Dumas et al., 2013), we tested the possibility that *set-4(dp268)* was the causative *seak* mutation in this strain. After outcrossing removed all but two closely linked single nucleotide variants, *set-4(dp268)* suppressed dauer arrest to a similar extent as two independently derived *set-4* deletions, *n4600* (Andersen and Horvitz, 2007) and *ok1481* (Figure 1B). Furthermore, an integrated single-copy *HA::set-4* transgene rescued dauer arrest in *set-4(n4600)* animals (Figure 1C and S1B). Therefore, SET-4 promotes dauer arrest.

DPY-21 enhances dauer arrest by activating DAF-16/FoxO, indicating that it acts in the DAF-2/InsR pathway to regulate dauer formation (Dumas et al., 2013). To determine whether SET-4 functions in the DAF-2/InsR pathway, we tested the effect of *set-4* mutation on dauer-constitutive phenotypes caused by mutations in the *daf-2/InsR, daf-7/TGFβ,* and *daf-12* pathways. *set-4* mutation suppressed the dauer-constitutive phenotypes of *daf-2(e1368)* mutants (Figure 1C) as well as *akt-1(ok525)* and *eak-7(tm3188)* single mutants, which develop reproductively at 25°C but arrest as dauers at 27°C (Figs. S1C-D) (Ailion and Thomas, 2003; Alam et al., 2010; Hu et al., 2006). In contrast, *set-4* mutation had no effect on the dauer-constitutive phenotypes caused by mutations in *daf-1,* which encodes a Type 1 TGF-β receptor homolog (Georgi et al., 1990), or *daf-8,* which encodes a SMAD homolog (Park et al., 2010) (Figs. 1D and S1E). Similarly, *set-4* mutation did not suppress dauer arrest in animals harboring mutations in *daf-9* or *daf-36,* which encode DA biosynthesis pathway components (Figs. 1E and

S1F) (Gerisch et al., 2001; Jia et al., 2002; Rottiers et al., 2006). Therefore, SET-4 acts specifically in the DAF-2/InsR pathway to promote dauer arrest.

Since previous reports link H4K20 methylation status to dosage compensation (Vielle et al., 2012; Wells et al., 2012), and DPY-21 promotes dauer arrest through dosage compensation (Dumas et al., 2013), we hypothesized that SET-4 may also regulate dauer arrest through dosage compensation. To test this, we determined the effect of *set-4* mutation on the dauer-constitutive phenotype of *eak-7;akt-1* double mutant hermaphrodites and males. If SET-4 promotes dauer arrest through the same mechanism as dosage compensation, then *set-4* mutation should suppress dauer in hermaphrodites but not males, since the DCC is inactive in males (Meyer, 2010). *dpy-21* and *set-4* mutations suppressed the dauer-constitutive phenotype of *eak-7;akt-1* hermaphrodites but did not affect dauer arrest in males (Figure 1F). Therefore, SET-4 may act through dosage compensation to control dauer arrest. We verified the role of SET-4 in dosage compensation by showing that *set-4* mutation suppressed lethality in *xol-1 sex-1* mutant males, which die due to inappropriate activation of dosage compensation (Dawes et al., 1999) (Figure S1G).

In order to determine whether SET-4 plays a role in regulating dauer entry in wild-type animals in response to physiologic stimuli, we tested the ability of dauer pheromone to induce dauer arrest in wild-type and *set-4* mutant animals. Mutation of either *set-4* or *dpy-21* decreased the sensitivity of wild-type animals to pheromone (Figure 1G). Therefore, SET-4 and DPY-21 promote dauer arrest in wild-type animals in response to increases in population density.

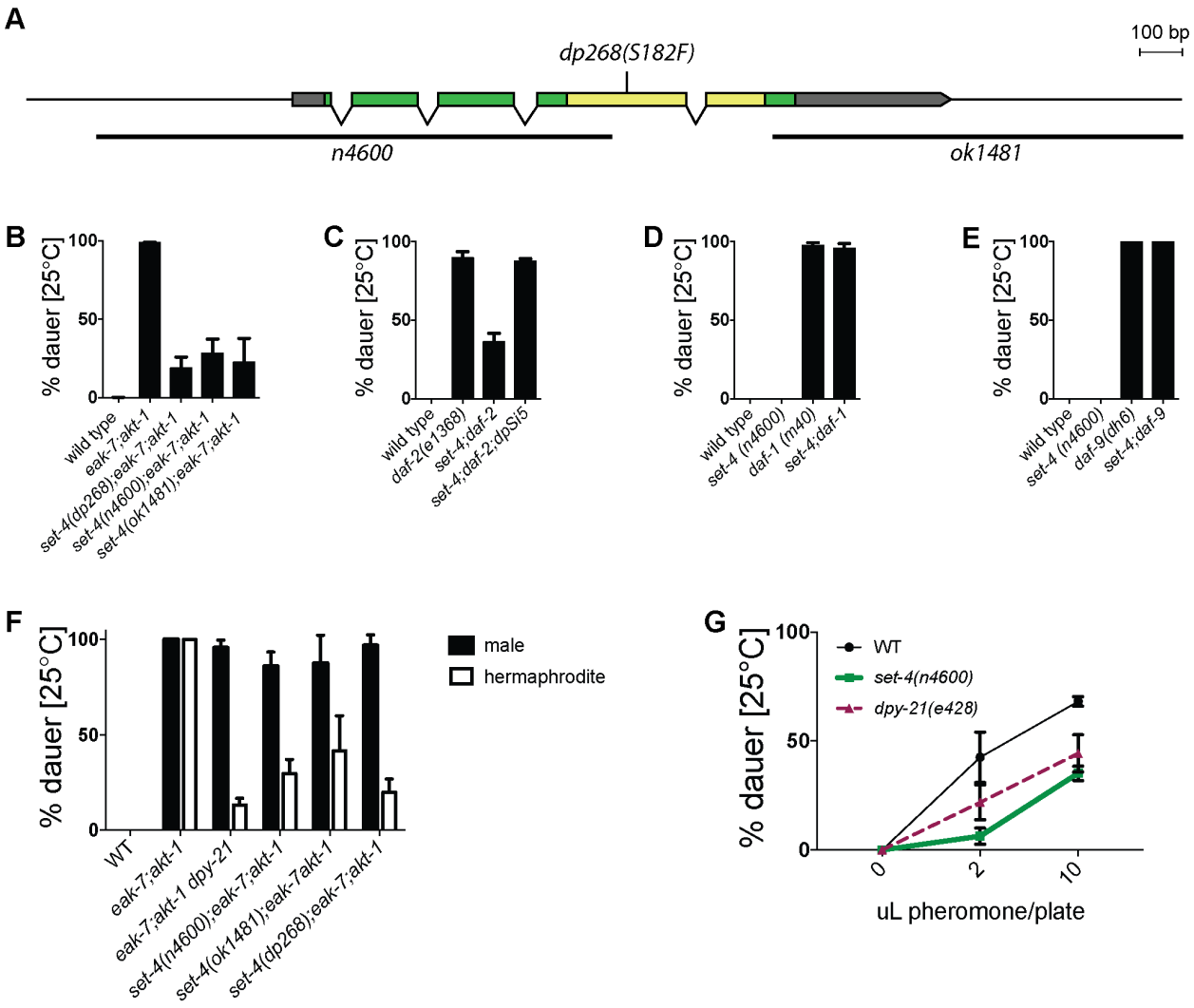

Figure 3.1. SET-4 promotes dauer arrest. (**A**) Schematic of the *set-4* locus and three mutant alleles. Exons are indicated as boxes, separated by introns. Gray, green, and yellow denote untranslated regions, coding sequence, and SET domain coding sequence, respectively. Deletions are indicated by black bars. (**B**) *set-4* mutations suppress the dauer-constitutive phenotype of *eak-7;akt-1* mutants [N (left to right) = 236, 627, 389, 521, 638]. (**C**) *set-4(n4600)* suppresses the dauer-constitutive phenotype of *daf-2(e1368)* mutants and is rescued by the single-copy *set-4* transgene *dpSi5* (N = 913, 1668, 1568, 1785). *set-4* is dispensable for dauer arrest in **(D)** *daf-1(m40)* (N = 2215, 2189, 1816, 1899) and (**E**) *daf-9(dh6)* mutants (N = 1753, 1561, 2188, 2486). (**F**) *set-4* and *dpy-21* mutations suppress dauer arrest in XX hermaphrodites but not XO males (N = 567, 1330, 579, 1003, 1012, 700). (**G**) *set-4* and *dpy-21* mutations attenuate the response of wild-type animals to dauer pheromone [N (0uL, 2uL, 10uL): wild type = 542, 461, 544; *set-4* = 413, 246, 387; *dpy-21* = 334, 220, 275.]. *set-4* vs. wild type: $p < 0.01$ by two-way ANOVA.

SET-4 is a H4K20 methyltransferase

The mammalian SET-4 ortholog SUV420H2 is a H4K20 methyltransferase (Schotta et al., 2004), and *C. elegans* SET-4 promotes H4K20 trimethylation (Vielle et al., 2012; Webster et al., 2013; Wells et al., 2012). We confirmed the requirement of SET-4 for H4K20 di- and trimethylation *in vivo* (Figure 2A). Immunoblots showed no detectable SET-4 protein in *set-4(n4600)* and *set-4(ok1481)* backgrounds, consistent with these being strong loss-of-function alleles. SET-4 protein levels in *set-4(dp268)* are comparable to wild-type (Figure 2A). H4K20me2 and H4K20me3 levels are undetectable in all three *set-4* mutant backgrounds (Figure 2A), suggesting that the S182F substitution in the SET domain abrogates catalytic activity. To test this possibility directly, we purified recombinant wild-type and mutant GST-SET-4 fusion proteins and tested their ability to methylate modified H4 peptides (H4K20me0, H4K20me1, and H4K20me2) *in vitro*. Mass spectrometry analysis revealed that both wild-type GST-SET-4 and GST-SUV420H2 were capable of converting H4K20me1 to H4K20me2 (Figure 2B-C). Consistent with *in vitro* experiments using human SET-4 orthologs SUV420H1 and SUV420H2 (Southall et al., 2014; Wu et al., 2013), methylation was not detected with unmethylated or dimethylated substrates, nor were trimethylated products detected in any assay (Figure 2B-C). It is possible that an enzyme distinct from SET-4 catalyzes H4K20 trimethylation *in vivo.* Alternatively, conversion of H4K20me2 to H4K20me3 by SET-4 *in vivo* may require a cofactor that is absent from our *in vitro* reactions.

GST-SET-4(S182F) did not methylate H4K20me1, indicating that the S182F mutation abolishes catalytic activity (Figure S2). Given that *set-4(dp268)* suppresses dauer to a similar extent as the two deletion alleles (Figure 1B), these data are consistent with SET-4 influencing dauer arrest through its conserved role in methylating H4K20.

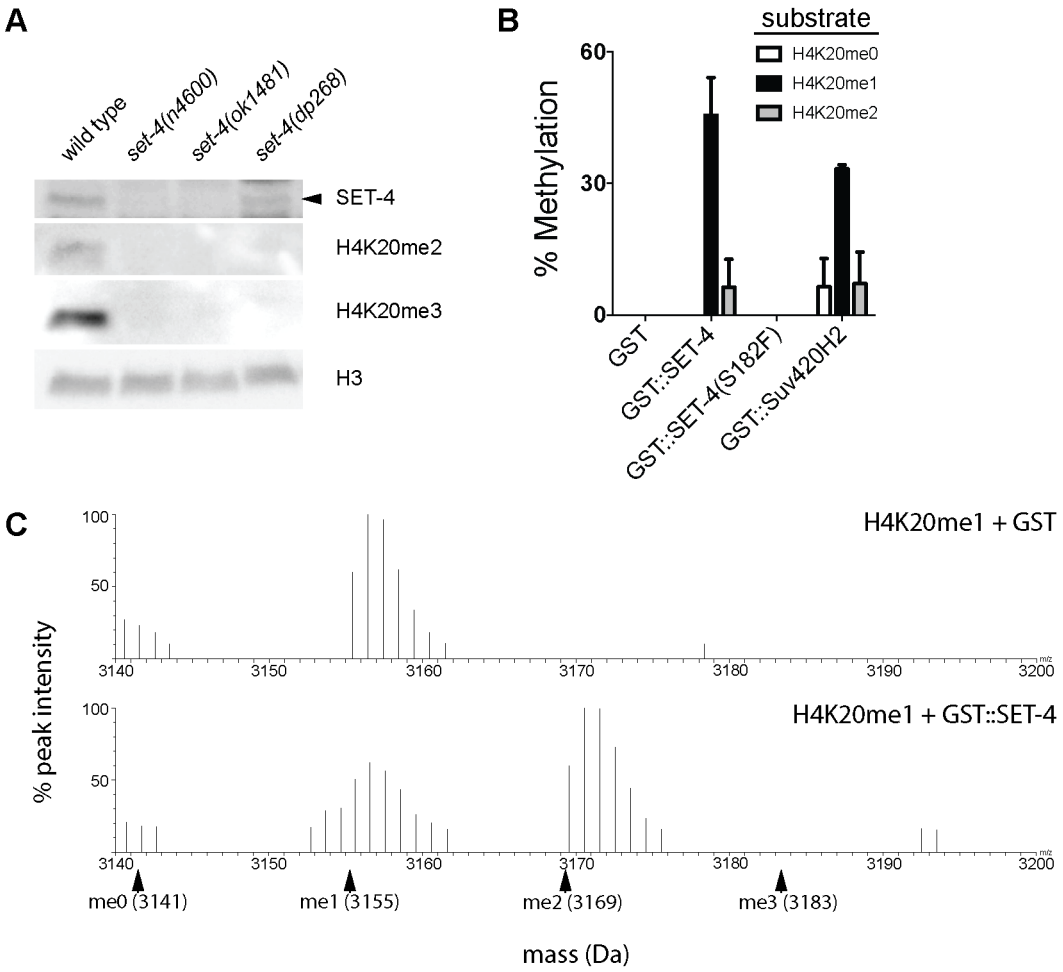

Figure 3.2. SET-4 is a histone H4K20 methyltransferase. (**A**) SET-4 promotes H4K20 methylation *in vivo.* Anti-SET-4, H4K20me2, H4K20me3, and H3 immunoblots of lysates from wild-type and *set-4* mutant animals are shown. SET-4 protein is indicated by the arrowhead. Images are representative of four biological replicates. (**B**) Recombinant GST-SET-4 fusion protein methylates H4K20me1 *in vitro.* Percent methylation of H4K20 peptide substrates by GST proteins fused to wild-type SET-4, mutant SET-4(S182F), or human SET-4 ortholog SUV420H2 is shown. Data represent mean values from three biological replicates. (**C**) MALDI spectra illustrating conversion of H4K20me1 to H4K20me2 by GST-SET-4. Monoisotopic masses (protonated) of peptide substrates are indicated with arrowheads. Spectra are representative of three independent experiments.

SET-4 acts in neurons to promote dauer arrest

To determine where SET-4 is expressed, we generated strains expressing reporter genes under the control of *set-4* regulatory elements. Because two independent C-terminal SET-4::GFP translational fusions failed to rescue dauer arrest in *set-4* mutants, we generated strains expressing a *set-4p::*GFP promoter fusion to determine the spatiotemporal activity of the *set-4* promoter. *set-4p::*GFP transgenic animals expressed GFP broadly in embryos (Figure S3). Post-embryonically, we detected fluorescence predominantly in the head and tail regions of the animal, in a pattern consistent with neuronal expression. To confirm this, we established a transgenic strain that co-expressed *set-4p::*GFP and mCherry driven by the pan-neuronal *rab-3* promoter (Nonet et al., 1997). At all developmental stages interrogated, we observed co-localization of green and red fluorescence (Figure 3A), consistent with somatic *set-4p::*GFP expression being predominantly neuronal. We did not observe significant GFP expression in intestine, body wall muscle, or hypodermis.

As the amphid sensory neurons play a critical role in regulating dauer arrest (Bargmann and Horvitz, 1991; Schackwitz et al., 1996; Vowels and Thomas, 1994), we interrogated them for expression of *set-4p::*GFP. Amphid neurons possess ciliary dendrites that are in directcontact with the environment and can be labeled with the lipophilic dye DiI (Starich et al., 1995). The extent of co-localization of green and red fluorescence in *set-4p::*GFP transgenic animals exposed to DiI (Figure 3B) reveals that the *set-4* promoter is active in amphid sensory neurons as well as in other cells.

To test whether neuronal expression of *set-4* is functionally important for dauer arrest, we generated tissue-specific *set-4* transgenes and tested them for the ability to rescue dauer arrest in *set-4* mutants. The neuronal *rab-3p::set-4* transgene rescued dauer formation to a similar extent as a *set-4* transgene driven by its native promoter (Figure 3C). In contrast, intestine-, hypodermis-, and muscle-specific *set-4* transgenes did not rescue dauer arrest to a greater extent than a transgene expressing the *set-4(dp268)* mutant. Taken together, these data indicate that SET-4 functions in the nervous system to promote dauer arrest.

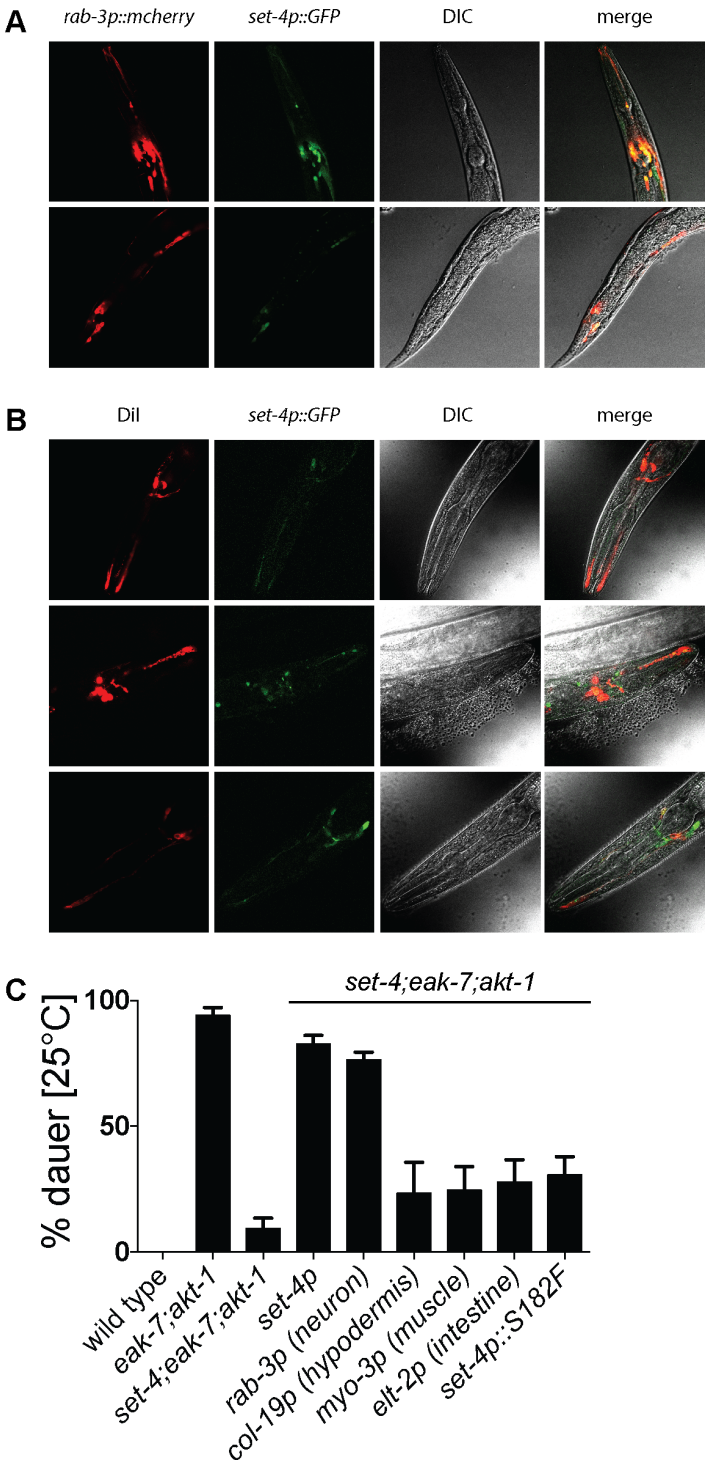

Figure 3.3. *set-4* acts in the nervous system to promote dauer arrest. (**A**) Representative photomicrographs showing colocalization of GFP and mCherry in animals coexpressing *set-4p::gfp* and the pan-neuronal reporter *rab-3p::mcherry* (N = 15). (**B**) Representative photomicrographs showing colocalization of red and green fluorescence in amphid neurons of *set-4p::gfp* transgenic animals exposed to DiI (N = 21). (**C**) Rescue of dauer arrest in *set-4;eak-7;akt-1* mutants by *set-4* transgenes driven by native *set-4* or tissue-specific promoters (N = 2328, 2143, 2058, 662, 811, 705, 936, 516, 541).

Transcriptome-wide influences of DPY-21 and SET-4 on dauer regulation

We previously showed that the DCC component DPY-21 promotes DAF-16/FoxO activity (Dumas et al., 2013). To gain broader insight into how DPY-21 and SET-4 control dauer arrest, we performed whole transcriptome profiling to compare genome-wide regulatory influences (henceforth referred to as the "regulome") of DPY-21 and SET-4 to those of the key transcription factors controlling dauer arrest in *eak-7;akt-1* animals, DAF-16/FoxO and the nuclear receptor DAF-12 (Alam et al., 2010). We identified genes differentially expressed between wild-type and *eak-7;akt-1* double mutant animals [fold change ≥ 1.5 and false discovery rate (FDR) < 0.05]. We then compared the transcriptomes of *eak-7;akt-1* double mutants to those of *eak-7;akt-1* animals harboring mutations in *dpy-21, set-4*, *daf-16/FoxO,* or *daf-12,* and identified genes that are differentially expressed in the opposite direction as in wild-type relative to *eak-7;akt-1* (Table S1). Regulomes were validated by comparison with published data when possible (see below).

We defined the SET-4 dauer regulome by identifying 333 genes common to *set-4(n4600)* and *set-4(dp268)* regulomes (Table S1). Comparison of this gene set with SET-4-regulated genes identified in wild-type embryos and L3 larvae (Kramer et al., 2015) revealed minimal overlap [one gene (MTCE.34) among 94 regulated by SET-4 in embryos, and one gene (B0511.11) among 18 SET-4-regulated genes in L3 larvae]. This lack of concordance could be due to differences in genetic background (*eak-7;akt-1 vs.* wild-type), developmental stage (early L2 larvae *vs.* embryos/L3 larvae), and/or ambient temperature (25°C *vs.* 20°C).

A similar analysis with *eak-7;akt-1 dpy-21* mutants revealed 2,431 genes that comprise the DPY-21 dauer regulome (Table S1). To validate the DPY-21 regulome, we found significant overlap between the set of 700 X-linked genes differentially expressed in *eak-7;akt-1 dpy-21* vs. *eak-7;akt-1* animals with the 374 X-linked genes subject to dosage compensation in embryos (Jans et al., 2009) (119 genes; Figure S4A and Table S2; $p = 2.1e^{-26}$). 308 of 333 genes that comprise the SET-4 dauer regulome (92.5%) are also part of the DPY-21 dauer regulome (Figure 4A and Table S1), suggesting that a functional relationship between DPY-21 and SET-4 may exist in post-embryonic dauer regulation.

The DAF-16/FoxO regulome consists of 2,957 genes (Table S1). This gene set overlapped significantly with both the 469-gene young adult DAF-16/FoxO regulome (Chen et al., 2015) (203 common genes; Figure S4B and Table S3, $p = 3.2e^{-115}$) as well as the 1116-gene dauer regulome defined using *daf-7* TGFβ-like pathway mutants (Liu et al., 2004) (522 common genes; Figure S4C and Table S4, $p < 1e^{-100}$). Furthermore, 65 of the 132 genes regulated by the DAF-7 TGFβ-like pathway that contained at least one upstream DAF-16/FoxO binding motif (Liu et al., 2004) were part of the DAF-16/FoxO regulome [Figure S4D and Table S4 (bolded text), $p = 6.5e^{-42}$]. Most genes in the DAF-16/FoxO regulome (2,282 of 2,957 genes; 77.2%) are also regulated by DAF-12 (Figure 4B and Table S1). Over two-thirds of genes comprising both DAF-16/FoxO (2,041 of 2,957 genes; 69.0%; Table S1) and DAF-12 (1804 of 2556 genes; 70.6%; Table S1) regulomes are concordantly regulated by DPY-21.

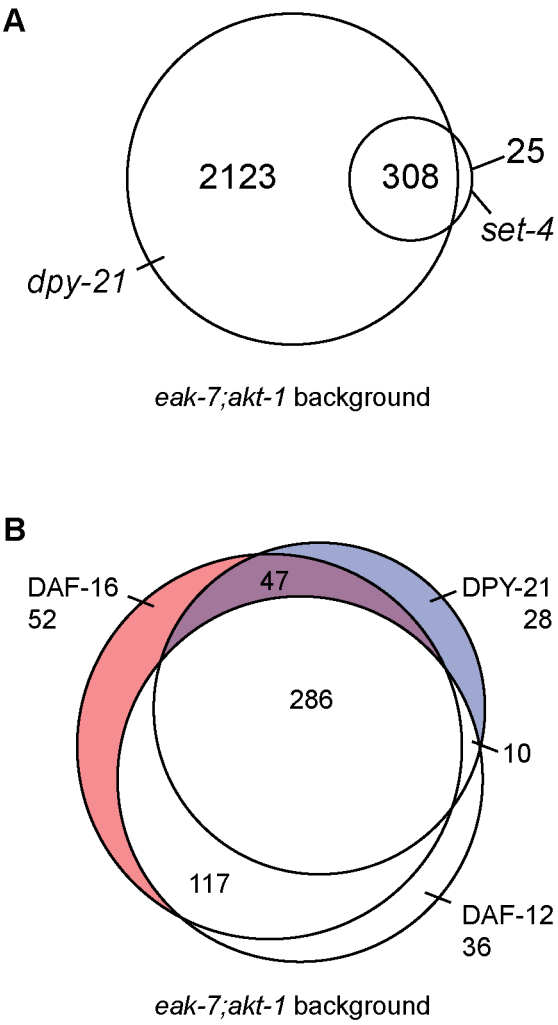

Figure 3.4. Whole transcriptome profiling defines genes coordinately regulated by DPY-21/SET-4 and DAF-16/FoxO. **(A)** Venn diagram of genes regulated by SET-4 and DPY-21. Genes coordinately regulated by SET-4 and DPY-21 are depicted in gray. **(B)** Venn diagram of X-linked genes regulated by DPY-21, DAF-16/FoxO, and DAF-12. 47 genes coordinately regulated by DPY-21 and DAF-16/FoxO but not by DAF-12 are depicted in purple and listed in Table S5. Data represents the aggregate of five biological replicate samples, each from thousands of progeny of no fewer than 200 animals per sample.

The X-linked *ins-9* gene is repressed by DPY-21, SET-4 and DAF-16/FoxO

Based on genetic epistasis experiments (Dumas et al., 2013) (Figure 1), we hypothesized that DPY-21 and SET-4 influence DAF-16/FoxO activity through repression of X-linked genes. Moreover, in light of the neuronal site of action of SET-4 (Figure 3C) and its expression in amphid sensory neurons (Figure 3B), we speculated that key dauer regulatory genes subject to dosage compensation might function in a signaling capacity in the nervous system, upstream of DAF-12. Therefore, we examined the set of X-linked genes common to DPY-21 and DAF-16/FoxO regulomes that were *not* regulated by DAF-12, which acts downstream in the dauer regulatory cascade (Fielenbach and Antebi, 2008; Schaedel et al., 2012). This filtering strategy defined a set of 47 X-linked genes coordinately regulated by DPY-21 and DAF-16/FoxO but not influenced by *daf-12* mutation (Figure 4B; Table S5).

Among these X-linked genes was *ins-9,* which encodes one of 40 *C. elegans* ILPs (Pierce et al., 2001). Transcriptome profiling revealed that *ins-9* is silenced in *eak-7;akt-1* animals in a manner that requires both *daf-16/FoxO* and *dpy-21* (Table S2). We verified this by qPCR; *ins-9* expression was reduced more than 30-fold in *eak-7;akt-1* double mutants compared to wild-type animals (Figure 5A). Full repression required DAF-16/FoxO as well as DPY-21 and SET-4 but was independent of *daf-12*. Notably, a *daf-16/FoxO* null mutation did not restore *ins-9* transcript levels to wild-type levels. Furthermore, mutation of either *dpy-21* or *set-4* increased *ins-9* expression by substantially greater than two-fold (Figure 5A; 7.5-fold increase in *set-4;eak-7;akt-1* vs. *eak-7;akt-1*; 13.5-fold increase in *eak-7;akt-1 dpy-21* vs. *eak-7;akt-1*). Taken together, these observations suggest that DAF-16/FoxO and DPY-21/SET-4 act synergistically to repress *ins-9*.

ins-9 overexpression phenocopies dauer suppression caused by *dpy-21* or *set-4* mutation

INS-9 was an attractive candidate regulator of dauer arrest and DAF-2 ILS, as multiple ILPs have been shown to control dauer arrest through DAF-2/InsR (Cornils et al., 2011; Fernandes de Abreu et al., 2014; Hung et al., 2014; Li et al., 2003; Murphy et al., 2003; Pierce et al., 2001). If derepression of *ins-9* contributes to suppression of *eak-7;akt-1* dauer arrest in dosage

compensation mutants, then *ins-9* overexpression should phenocopy dauer suppression caused by *set-4* or *dpy-21* mutation. We tested this by establishing transgenic strains harboring a polycistronic construct which permitted expression of both *ins-9* and *mNeonGreen* (Shaner et al., 2013) fused to an SL2 leader sequence (Blumenthal, 2005) under the control of native *ins-9* 5' and 3' regulatory elements (*ins-9::SL2::mNG*). In two independent transgenic lines, *ins-9* overexpression (indicated by mNeonGreen detection) suppressed the dauer-constitutive phenotype of *eak-7;akt-1* double mutants (Figure 5B). Therefore, *ins-9* overexpression recapitulated the phenotype caused by *set-4* and *dpy-21* mutations (Dumas et al., 2013) (Figure 1B). These data are consistent with INS-9 acting as an agonist DAF-2/InsR ligand.

ins-9 is expressed specifically in a single pair of amphid neurons

Previous studies using reporters driven by the *ins-9* promoter suggested that *ins-9* is expressed in the ASI and ASJ amphid neurons as well as in additional tissues (Chen and Baugh, 2014; Pierce et al., 2001; Ritter et al., 2013). In contrast, in transgenic L2 larvae expressing *ins-9::SL2::mNG*, we consistently observed green fluorescence solely in one pair of sensory neurons. In animals in which neuronal morphology was discernable, we identified the fluorescent cells as the ASI amphid neurons (Figure 5C). We did not observe fluorescence in more than one pair of amphid neurons in any animal, nor did we detect fluorescence in other neurons or tissues. Since *ins-9::SL2::mNG* contains genomic elements from the *ins-9* locus that are missing from other reporters in the literature (Chen and Baugh, 2014; Pierce et al., 2001; Ritter et al., 2013), these observed patterns of expression are likely to be physiologically relevant.

ins-9 and *akt-2* are required for suppression of dauer arrest by *set-4* mutation

To determine the extent to which *ins-9* derepression contributes to dauer suppression in *set-4* mutants, we tested the ability of *set-4* to suppress the dauer-constitutive phenotype of *daf-2/InsR* mutants in wild-type and *ins-9* loss-of-function backgrounds. We generated strong loss-of-function *ins-9* alleles using CRISPR/Cas9 genome editing (Paix et al., 2015). Two probable null alleles, *dp675* and *dp677*, have nonsense mutations in the F-peptide region of *ins-9* that lies N-

terminal to the functional B and A peptides (Pierce et al., 2001) (Figure S5). Although neither allele induced dauer arrest in a wild-type background, both *ins-9(dp675)* and *ins-9(dp677)* partially rescued dauer arrest in *set-4;daf-2* double mutants (Figure 5D), indicating that dauer suppression caused by *set-4* mutation is due in part to de-repression of *ins-9*.

We previously showed that the X-linked gene *akt-2* is required for dauer suppression caused by *dpy-21* mutation (Dumas et al., 2013). We verified that *akt-2* transcripts increase two-fold in *eak-7;akt-1* double mutants when *set-4* or *dpy-21* is mutated (Figure S6A). Similar to *ins-9* mutation, *akt-2* mutation also partially rescued dauer arrest in animals lacking *set-4* (Figure 5E), and the phenotypic effects of *ins-9* and *akt-2* mutations on dauer arrest may be additive (Figure 5E). However, *set-4;daf-2;ins-9 akt-2* compound mutant animals still did not undergo dauer arrest to the same extent as *daf-2* single mutant animals (Figure 5E), indicating that regulation of additional genes may contribute to dauer arrest.

The autosomal *ins-7* gene contributes to suppression of dauer arrest by *set-4* mutation

As the only X-linked *ins* gene, *ins-9* is the sole *ins* gene subject to direct regulation by dosage compensation or other X-chromosome-specific mechanisms of gene regulation. However, it is conceivable that other *ins* genes could contribute to dauer regulation through indirect effects on their expression. Genes encoding three agonist ILPs, INS-4, INS-6, and DAF-28, are expressed in the ASI sensory neurons and have established roles in inhibiting dauer arrest and promoting reproductive development (Cornils et al., 2011; Hung et al., 2014; Li et al., 2003). To determine whether regulation of *ins-4, ins-6,* and/or *daf-28* contributes to dauer suppression in this context, we measured *ins-4, ins-6,* and *daf-28* transcript levels in wild-type, *eak-7;akt-1* double mutant, and *eak-7;akt-1* triple mutants with reduced DPY-21 or SET-4 activity. None of these genes was repressed in *eak-7;akt-1* double mutants compared to wild-type animals, nor did loss of *set-4* or *dpy-21* cause significant increases in their expression (Figure S6B-D). Therefore, neither DPY-21 nor SET-4 influences dauer arrest through regulation of *ins-4, ins-6,* and *daf-28* expression.

To determine whether other ILPs could contribute to dauer regulation by DPY-21 or SET-4, we searched the set of genes common to DAF-16/FoxO and DPY-21 regulomes for *ins* genes. Seven

ins genes are concordantly regulated by DAF-16/FoxO and DPY-21 based on FPKM counts from whole transcriptome data (Table S6). Two genes encoding putative antagonist ILPs, *ins-20* and *ins-11* (Fernandes de Abreu et al., 2014), are repressed by DAF-16/FoxO and DPY-21; however, an increase in their expression in *dpy-21* mutants would be expected to enhance, rather than suppress, dauer arrest. Similarly, two *ins* genes encoding agonist ILPs, *ins-33* and *ins-35* (Fernandes de Abreu et al., 2014; Michaelson et al., 2010), are induced by DAF-16/FoxO and DPY-21; a decrease in their expression in *dpy-21* mutants would also be expected to enhance dauer arrest if changes in their expression were functionally important in dauer regulation. DAF-16/FoxO and DPY-21 induce the expression of two *ins* genes of unknown function, *ins-16* and *ins-29* (Fernandes de Abreu et al., 2014). Finally, *ins-7,* which encodes an agonist ILP (Murphy et al., 2007; Murphy et al., 2003), is repressed by DAF-16/FoxO and DPY-21 (Murphy et al., 2007; Murphy et al., 2003) (Table S6). As *ins-7* and *ins-9* both encode agonist ILPs, are concordantly regulated by DAF-16/FoxO and DPY-21, and have been shown to influence dauer arrest (Murphy et al., 2007; Murphy et al., 2003) (Figure 5C-E), we tested *ins-7* for a role in promoting reproductive development in *dpy-21* and *set-4* mutants. We verified *ins-7* repression by DAF-16/FoxO, SET-4, and DPY-21 using qPCR (Figure S6E). The *ins-7(tm1907)* deletion allele partially rescued dauer in *set-4;daf-2* animals and may have an additive effect with *ins-9* mutation on dauer suppression (Figure 5F). Thus, SET-4 may influence dauer arrest through both direct repression of X-linked genes such as *ins-9* and *akt-2* and perhaps indirect regulation of autosomal dauer regulatory genes such as *ins-7.*

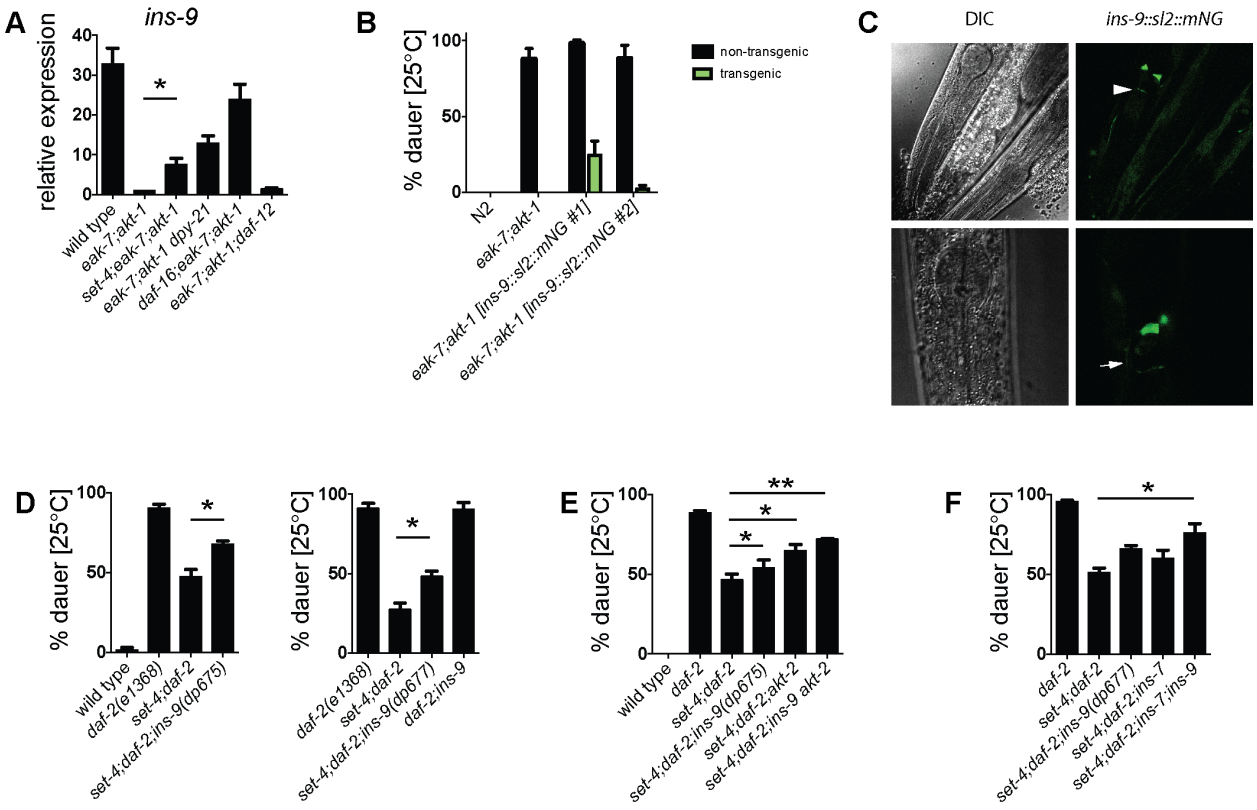

Figure 3.5. SET-4 promotes dauer arrest by repressing the X-linked *ins-9* gene. (**A**) *ins-9* is repressed by DPY-21, SET-4, and DAF-16/FoxO but not DAF-12. Results are the mean and s.e.m. of five experiments. (**B**) *ins-9* overexpression suppresses dauer arrest in *eak-7;akt-1* animals. Non-transgenic (NT) and transgenic (T) progeny of transgenic hermaphrodites are shown. N = 1200, 1522, 718/156 (NT/T), 702/210 (NT/T). (**C**) An *ins-9::SL2::mNG* transgene is expressed specifically in ASI sensory neurons. The arrowhead indicates the top of the nerve ring, and the arrow indicates the ASI axon. Representative images are shown (N = 20). (**D**) Two *ins-9* nonsense mutations partially rescue dauer arrest in *set-4;daf-2* mutants. N = 957, 1205, 1398 (left panel); N = 892, 1028, 897 (right panel). (**E**) *ins-9* and *akt-2* mutations rescue dauer arrest in an additive fashion in *set-4;daf-2* mutants (N = 949, 1281, 1334, 1524, 1333, 1478) (**F**) *ins-9* and *ins-7* mutations rescue dauer arrest in an additive fashion in *set-4;daf-2* mutants (N = 1396, 1251, 754, 827, 1327). *p<0.05, **p<0.01.

Discussion

Although much is known about the conserved signaling pathways that control *C. elegans* dauer arrest, how these pathways are regulated by upstream inputs is poorly understood. In the present study, we have established a framework for understanding how DPY-21 and SET-4 promote dauer arrest in the context of reduced DAF-2 ILS. Specifically, we have discovered that the conserved H4K20 methyltransferase SET-4 acts in the nervous system to promote dauer arrest. It does so in part by synergizing with DAF-16/FoxO to repress the X-linked insulin-like peptide gene *ins-9*. We hypothesize that SET-4 and DPY-21 act similarly to directly repress *ins-9* and *akt-2,* thus attenuating DAF-2 ILS and promoting dauer arrest through activation of DAF-16/FoxO (Figure 6).

Although INS-9 has been predicted to function as an agonist ILP based on both structural models indicating similarity to the agonist ILPs INS-4, INS-6, and DAF-28 (Pierce et al., 2001) and expression changes upon starvation and feeding of larvae (Chen and Baugh, 2014), analysis of existing *ins-9* mutants has not revealed phenotypes consistent with this (Fernandes de Abreu et al., 2014). This may be due to *ins-9(tm3618)* not being a strong loss-of-function allele. In contrast, our analysis of transgenic animals overexpressing *ins-9* (Figure 5B) and mutant animals harboring nonsense *ins-9* alleles (Figure 5D-F) provides the first experimental evidence demonstrating that INS-9 is an agonist ILP.

Several ILPs have been implicated in dauer regulation (Cornils et al., 2011; Fernandes de Abreu et al., 2014; Hung et al., 2014; Li et al., 2003; Murphy et al., 2003; Pierce et al., 2001). However, the mechanistic basis for how environmental cues regulate ILPs remains obscure. The initial events that control dauer arrest through DAF-2 ILS likely take place in the amphid sensory neurons, which are required for dauer formation in response to pheromone (Schackwitz et al., 1996; Vowels and Thomas, 1994). Indeed, genes encoding INS-4, INS-6, and DAF-28, which collectively play a major role in promoting reproductive development through DAF-2 ILS (Cornils et al., 2011; Hung et al., 2014; Li et al., 2003), are expressed in ASI (Chen and Baugh, 2014; Cornils et al., 2011; Hung et al., 2014; Li et al., 2003), and the transcription of *ins-6* and *daf-28* is inhibited by dauer pheromone through unknown mechanisms (Cornils et al., 2011; Li et al., 2003). Our finding that DPY-21 and SET-4 influence dauer arrest in part by repressing the

X-linked *ins-9* gene provides a potential mechanistic link between a dauer-regulatory environmental cue and an ILP expressed in sensory neurons that control the dauer decision.

An intriguing but incompletely understood aspect of dauer morphogenesis is the mechanistic basis for the commitment of larvae to either the reproductive or dauer developmental fate. Assays in which larvae are shifted between favorable and unfavorable conditions at different times after hatching indicate the existence of commitment points beyond which animals develop reproductively or arrest as dauers regardless of ambient conditions (Golden and Riddle, 1984; Schaedel et al., 2012). Commitment to reproductive development correlates temporally with the activation of a feed-forward loop amplifying organismal DA biosynthesis through DA-dependent induction of DAF-9 expression in the hypodermis (Schaedel et al., 2012). However, the XXX cells (Ohkura et al., 2003), thought to be the sole source of DA biosynthesis prior to the commitment point (Schaedel et al., 2012), are not in direct contact with the environment. Therefore, they must receive upstream inputs from sensory neurons that convey information about ambient conditions.

Our finding that DPY-21 and SET-4 synergize with DAF-16/FoxO to repress *ins-9* is consistent with a hypothetical model in which INS-9 may function as a key node in an autocrine feed-forward loop in the ASI sensory neurons that reinforces levels of its own expression in response to changing environments, upstream of DA biosynthesis in the XXX cells and hypodermis. In replete conditions, *ins-9* expression in ASI is expected to lead to activation of DAF-2 ILS and inhibition of DAF-16/FoxO. Since DAF-16/FoxO inhibits *ins-9* expression, decreased DAF-16/FoxO activity would lead to increased *ins-9* expression, which would presumably lead to further activation of DAF-2 ILS and inhibition of DAF-16/FoxO, both in an autocrine fashion in ASI as well as in other cells that express DAF-2/InsR. In the context of increased population density, pheromone would promote *ins-9* repression through DPY-21 and SET-4 and reduce autocrine and paracrine engagement of DAF-2/InsR, resulting in DAF-16/FoxO activation, further repression of *ins-9,* and dauer arrest (Figure 6). The effect of DPY-21 and SET-4 would not be limited to sensory neurons, as they would also act in other cells responding to INS-9 to control their sensitivity to ILPs by repressing *akt-2* (Dumas et al., 2013) (Figures 6 and S6A). In addition, *ins-9* regulation may also be amplified through other ILPs such as INS-7, which

functions in a feed-forward loop in adults to coordinate DAF-16/FoxO activity throughout the animal (Murphy et al., 2007).

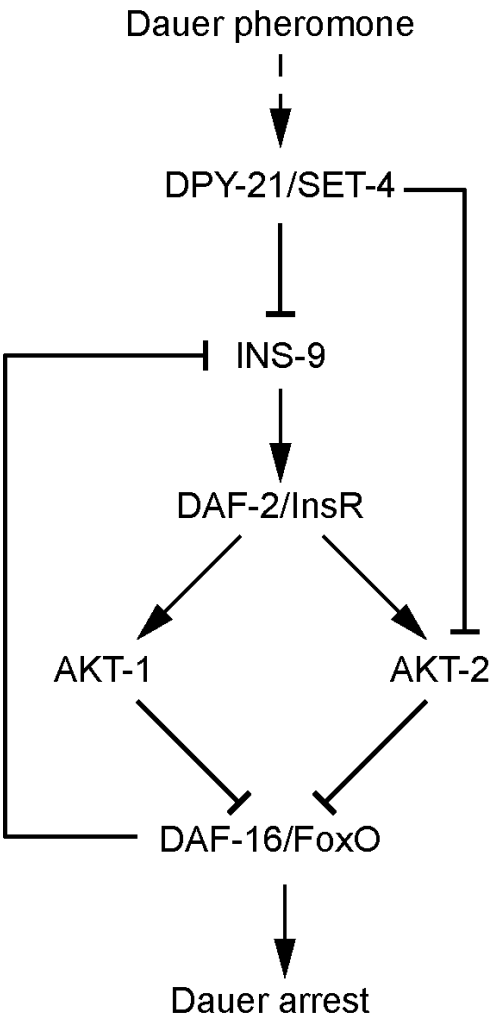

Figure 3.6. Hypothetical model of dauer regulation by pheromone through DPY-21/SET-4 and DAF-2 ILS. DPY-21 and SET-4 act in concert to promote transduction of pheromone cues by repressing X-linked genes encoding the DAF-2/InsR agonist INS-9 and the serine/threonine kinase AKT-2, resulting in increased DAF-16 activation and subsequent dauer arrest.

Materials and Methods

C. elegans strains and maintenance

Mutant alleles are listed in Supplementary Materials and Methods. Compound mutants were generated using standard protocols. All animals were maintained on nematode growth media (NGM) plates seeded with *E. coli* OP50 using standard techniques.

Dauer arrest assays

Dauer arrest assays were performed as previously described (Hu et al., 2006). *daf-9(dh6)* mutant animals were propagated on NGM plates supplemented with 10 nM Δ^7-DA, then transferred to NGM plates for egglays as previously described (Dumas et al., 2013). For male dauer assays, males were crossed to isogenic L4 hermaphrodites, and the gender of dauer progeny was determined after dauer exit.

Dauer pheromone assays

Dauer pheromone was prepared as previously described (Golden and Riddle, 1982; Schroeder and Flatt, 2014). Details are provided in Supplementary Materials and Methods.

Generation of transgenic strains

Details pertaining to the generation of reporter constructs and transgenic strains are provided in Supplementary Materials and Methods.

CRISPR/Cas9-based mutagenesis

ins-9(dp675) and *ins-9(dp677)* were generated using recombinant crRNA and tracrRNA (Dharmacon) and Cas9 (PNA Bio) as described (Paix et al., 2015). See Table S7 for sequences of guide RNAs and repair oligonucleotides.

RNA isolation

Greater than 200 gravid hermaphrodites were allowed to lay eggs for 6 hr at 20°C and then removed. Eggs were transferred to 25°C for 24 hr. Larvae were harvested, washed once in M9 buffer and once in water, and resuspended in TRIzol (Invitrogen). After five sequential freeze-thaws, RNA was extracted using chloroform. Extracted RNA was purified using a Direct-zol RNA Miniprep Kit (Zymo Research).

qPCR

cDNA was synthesized with oligo-dT priming using the SuperScript III First Strand Synthesis Kit (Invitrogen). The equivalent of 10 ng of starting RNA was used as template in a 15 µL reaction using the Quantitect SYBRgreen qPCR Kit (Qiagen). Reactions were performed in a RotorGene 6000 (Corbett Research) and results analyzed using RotorGene 6000 Software (version 1.7). Samples were normalized to *pmp-3* expression prior to comparison between groups (Hoogewijs et al., 2008). See Table S8 for primer sequences. Relative expression was calculated as described (Nolan et al., 2006).

Confocal microscopy

Animals were mounted on slides layered with a thin 3% agarose pad containing 25 mM sodium azide. Images were captured on a Leica Inverted SP5X Confocal Microscope (Leica) using LAS AF software.

RNA-seq analysis

Whole transcriptome profiling was performed by the University of Michigan DNA Sequencing Core as previously described (Chen et al., 2015) using 100 ng input RNA per sample. Samples were barcoded and multiplexed, and 100-nucleotide paired end sequencing was performed using an Illumina HiSeq 2000 sequencer and Version 4 reagents. Five experimental replicates were analyzed. Correlation coefficients between replicates and genotypes are shown in Table S9.

Annotated gene expression data output from CuffDiff v2.2.1 (Trapnell et al., 2013) was read into R version 3.2.1(2015-06-18; The R Foundation for Statistical Computing; http://www.r-project.org/) for six comparisons: *eak-7;akt-1* compared to (1) wild-type, (2) *daf-16(mu86);eak-7;akt-1*, (3) *daf-12;eak-7;akt-1*, (4) set-*4(n4600);eak-7;akt-1*, (5) *set-4(dp268);eak-7;akt-1*, and (6) *dpy-21;eak-7;akt-1*. We filtered genes by the following criteria: (1) status = "OK" for wild-type *vs. eak-7;akt-1,* (2) fold change (FC) ≥ 1.5 or FC ≤ 1/1.5 for wild-type *vs. eak-7;akt-1* and (3) FDR < 0.05 for at least two separate comparisons.

DAF-16 targets were defined as those filtered genes that also met (1) status = "OK" for *eak-7;akt-1 vs. daf-16;eak-7;akt-1*, and (2) FC ≥ 1.5 for *eak-7;akt-1 vs. daf-16;eak-7;akt-1* in the opposite direction as wild-type *vs. eak-7;akt-1*. DPY-21, SET-4, and DAF-12 targets were determined in an analogous fashion. For SET-4, we generated a list of SET-4 targets that showed FC ≥ 1.5 or FC ≤ 1/1.5 for both *set-4* alleles, and a list that showed these changes for either one or both *set-4* alleles. Lists of overlapping targets were then generated from these target lists.

Significance of overlap with dosage-compensated X-linked genes (Jans et al., 2009), strongly regulated dauer genes (Liu et al., 2004), and DAF-16 targets in the *daf-2(e1370)* background (Chen et al., 2015) was calculated using a hypergeometric distribution, assuming 5863 X-linked transcripts and 46233 genome-wide transcripts in *C. elegans* detected in our RNA-seq analysis (by either the UCSCce10 reference transcriptome or *de novo* transcript assembly). If necessary, common WormBase Gene identifiers were downloaded from WormBase version WS250 (intermine.wormbase.org).

Immunoblotting and antibodies

To generate protein lysates, animals were washed in M9, then in sterile water. Pelleted animals were resuspended in equal volumes of worm lysis buffer (Webster et al., 2013), incubated at 85°C for 5 min, then sonicated on ice for two cycles of 30 seconds each at 70% power using a Sonic Dismembrator Model 100 (Fisher Scientific). Homogenates were quantified using a DC™ Protein Quantification Kit (BioRad). 50 µg protein was loaded per lane using Criterion systems (BioRad) and transferred to Immobilon Psq (Millipore). Details pertaining to antibodies are provided in Supplementary Materials and Methods. Membranes were blocked with 5% milk in TBS + 0.5% Tween 20. Antibodies were diluted in Western Blocking Solution (Sigma) prior to incubation with membranes. Blots were washed with TBS + 0.5% Tween 20. Signal was detected by ECL (Pierce).

Histone methyltransferase assay

set-4 cDNAs were amplified from RNA isolated from wild-type or *set-4(dp268)* mutant animals. Human *Suv420H2* cDNA was obtained from Origene. Clones were ligated into pGEX4T1 vector (GE Healthcare). Protein expression was induced overnight at 16°C with 0.1 mM IPTG in BL21-CodonPlus(DE3)-RIPL cells (Agilent Technologies) grown in Terrific Broth (Invitrogen) + 4% glycerol (Sigma). Cells were disrupted using a Sonic Dismembrator Model 100 sonicator (Fisher Scientific), with four cycles of ten one-second on/off pulses of 10-30% intensity. Lysates were cleared by centrifugation at 20,000g for 5 min and incubated with Glutathione-Sepharose beads (GE Healthcare) rotating overnight at 4°C. Expression of recombinant protein was confirmed by Coomassie staining and anti-GST immunoblot. Beads bound to recombinant protein were incubated in 10 mM Tris pH 8.0, 2 µM β-mercaptoethanol, and 7 mM S-adenosylmethionine (Sigma) in the presence of 2 mM substrate peptide corresponding to amino acids 8-30 of *C. elegans* histone H4 (AnaSpec) rotating for 4 hr at 30°C. Reactions were analyzed using a Waters MicroMass MALDI-TOF mass spectrometer and analyzed with MassLynx software. Ratios of peak heights corresponding to reactant and product peptide were calculated to define percent conversion.

Male rescue assay

Mated gravid hermaphrodites were placed on NGM plates to lay eggs for 24 hr at 20°C. Egglayers were removed, and the number of hatchlings and eggs were counted. After 72 hr, the animals were moved to 4°C to slow movement. Male rescue was calculated as the ratio of live males to total eggs laid. Each experiment was performed in triplicate.

Statistics

Two-tailed Student's t-test was used to measure significance in experiments unless otherwise noted. Data is presented as the average and standard error of the means of at least three biological replicates, each replicate performed in triplicate. N's for dauer assays are listed from left to right.

Data availability

Strains are available upon request. Whole transcriptome profiling data are available at GEO with the accession number: GSE89295.

Supplemental Information

Supplemental Materials and Methods

Strains

The following mutant alleles were used: *eak-7(tm3188)* (Alam et al., 2010), *akt-1(ok525)* (Hertweck et al., 2004), *set-4(n4600)* (Andersen and Horvitz, 2007), *set-4(ok1481)*, *daf-2(e1368)* (Kimura et al., 1997), *daf-1(m40)* (Georgi et al., 1990), *daf-9(dh6)* (Gerisch et al., 2001), *dpy-21(e428)* (Yonker and Meyer, 2003), *daf-16(mu86)* (Lin et al., 1997), *daf-12(rh61rh411)* (Antebi et al., 2000), *akt-2(ok393)* (Hertweck et al., 2004), *ins-7(tm1907)* (Murphy et al., 2007), *daf-8(e1393)* ((Park et al., 2010), and *daf-36(k114)* (Rottiers et al., 2006). *set-4(n4600)* and *set-4(ok1481)* were a gift from Gyorgyi Csankovszki.

Reporter constructs and transgenic strains

DNA fragments were amplified and assembled using overlap PCR, and fusion products were cloned into pCRXL-TOPO (Invitrogen). GFP, mCherry, and mNeonGreen were amplified from pPD95.75, pSA120, and pDD268, respectively. The identities of fusion products were verified by Sanger sequencing. To generate the single-copy rescuing transgenic strain *dpSi5*, the 638 bp genomic fragment between *set-4* and the upstream gene C32D5.6 (*set-4p*) was amplified and fused to sequence encoding a HA epitope tag followed by the *set-4* open reading frame (*HA::set-4*) and 350 bp of genomic DNA downstream of *set-4* (*set-4utr*) to create *set-4p::HA::set-4::set-4utr*. Single-copy mosSCI integration of *set-4p::HA::set-4::set-4utr* into strain EG6250 (*cxTi10882*) was performed by Knudra Transgenics as described (Frokjaer-Jensen et al., 2008). The *set-4p::GFP* transcriptional reporter was generated by fusing *set-4p* to GFP and *set-4utr* to create *set-4p::GFP::set-4utr. set-4p::GFP::set-4utr* was mixed with 50 ng μL^{-1} *rol-6(su1006)* (pRF4) or 10 ng μL^{-1} *rab-3p::mcherry::unc-54utr* to a final DNA concentration of 100 ng μL^{-1} or 50 ng μL^{-1}, respectively. For tissue-specific rescue experiments, promoters defined by the Promoterome Project (worfdb.dfci.harvard.edu/promoteromedb) were amplified from wild-type genomic DNA and fused to *HA:set-4:set-4utr.* The sizes of promoter fragments amplified were as follows: *set-4p*: 638 bp; *rab-3p*: 4913bp; *col-19p*: 1321 bp; *myo-3p*: 2006 bp; *elt-2p*: 1988 bp.

Constructs were co-injected with *myo-2p::mcherry::unc-54utr* (pJK343) and pBlueScript at concentrations of 5, 2, and 43 ng μL^{-1}, respectively. To generate the polycistronic *ins-9::SL2::mNG* transgene, a 1939 bp genomic fragment upstream of *ins-9* was fused to *ins-9* and the intercistronic genomic fragment between *gpd-2* and *gpd-3*, mNeonGreen, and a 1017 bp genomic fragment downstream of *ins-9*. 40 ng μL^{-1} *ins-9::SL2::mNG* was mixed with 10 ng μL^{-1} *rab-3p::mcherry::unc-54utr*. Animals were injected as previously described (Mello et al., 1991) using a Leica DMI3000B microscope and Eppendorf FemtoJet pump.

Antibodies

For immunoblotting, both custom anti-SET-4 antisera, generated by immunizing rabbits with a C-terminal SET-4 peptide (NH_3-ENAEPIISEKKTKYELRSRS-COOH) (Pierce), and anti-H4K20me3 antibodies (Abcam #ab78517) were diluted 1:500. Anti-H4K20me2 antibodies (Abcam #ab9052) and anti-histone H3 antibodies (Abcam #ab12079) were diluted 1:2000 and 1:1000, respectively. The specificity of anti-H4K20me2 and anti-H4K20me3 antibodies was verified using competitive peptide-binding arrays. Methodology and results are available at *www.histoneantibodies.com*.

Dauer pheromone preparation

Wild-type animals were washed into a 2.8L Fernbach flask containing 1L S medium to which 25mL of 40X *E. coli* HB101 culture was added. After media clarified, another 25mL of 40X HB101 was added. Four days later, supernatant was filtered through a Buchner funnel, then vacuum filtered through 0.22 μm SteriTop units (Millipore). Clarified supernatant was evaporated to dryness using a V-10 evaporator (Biotage). Solids were extracted three times with 100 mL 100% ethanol, then evaporated. Pheromone was resuspended in ethanol and effective doses determined empirically. 3.5 cm plates containing 2 mL NGM made with Noble Agar (BD) and lacking peptone were treated with 500 μL water containing the indicated volume of pheromone. Once dry, plates were seeded with 20 μL of 6X *E. coli* OP50 in S basal. Dauer assays were performed as above with animals scored after 84 hr at 25°C.

Supplemental Figures

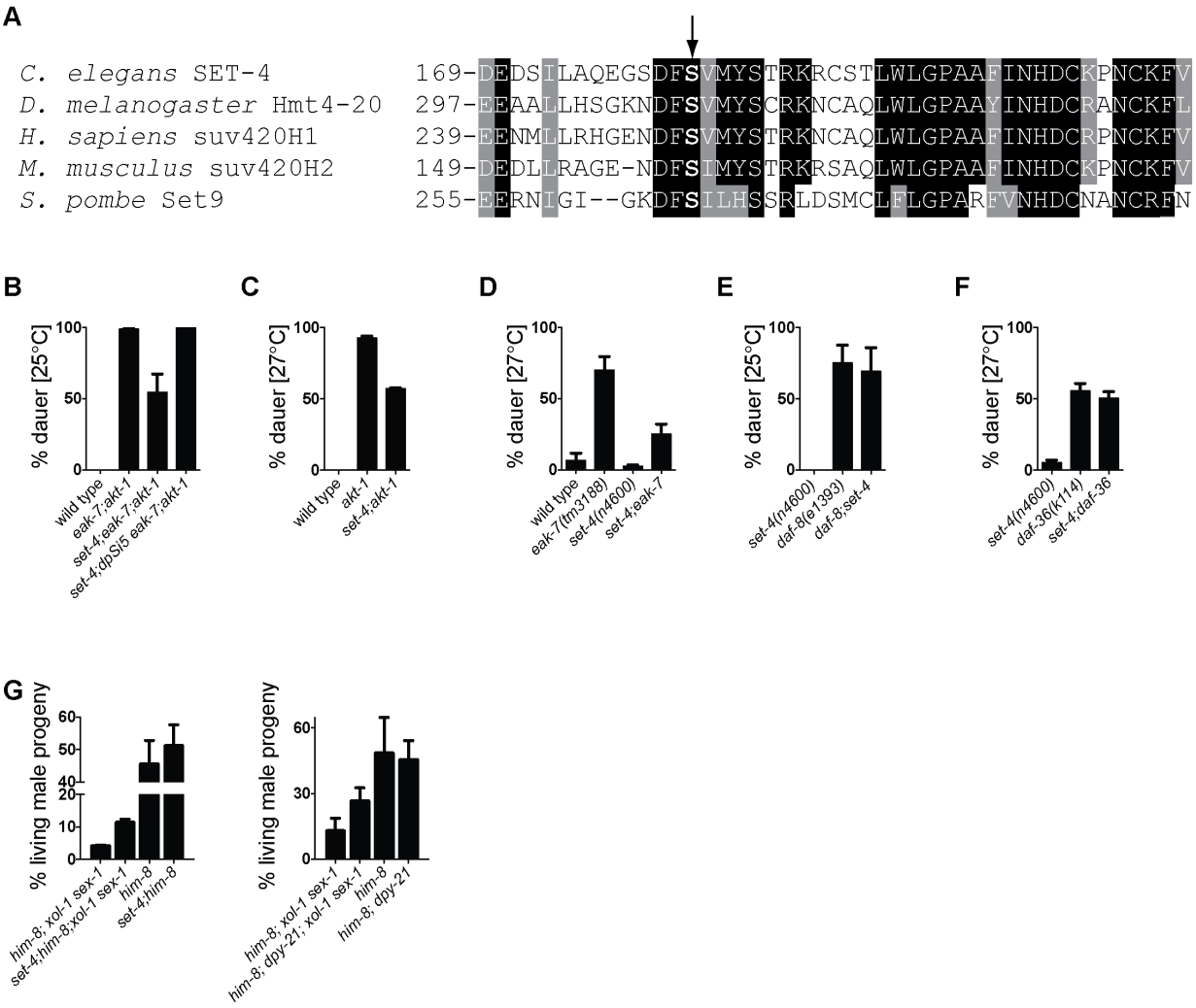

Supplemental Figure 3.S1. SET-4 promotes dauer arrest and participates in dosage compensation. (**A**) Conservation of SET-4 serine 182 within the SET domain. Identical and conserved residues are denoted by black and gray shading, respectively. SET-4 serine 182 is denoted by the arrow. (**B**) The single-copy *set-4* transgene *dpSi5* rescues dauer arrest in *set-4;eak-7;akt-1* animals (N = 720, 1555, 1096, 1351). *set-4* mutation partially suppresses the 27°C dauer-constitutive phenotype of **(C)** *akt-1* (N = 806, 1077, 1121) and (**D**) *eak-7* mutants (N = 409, 472, 379, 318). *set-4* is dispensable for dauer arrest in (**E**) *daf-8* (N = 609, 530, 496) and (**F**) *daf-36* mutants (N = 653, 247, 242). (**G**) *set-4* (N = 4052, 3475, 4486, 3845) and *dpy-21* (N = 3383, 1886, 4171, 3441) mutations rescue viability of *him-8;xol-1 sex-1* mutant males. Data are representative of three biological replicates.

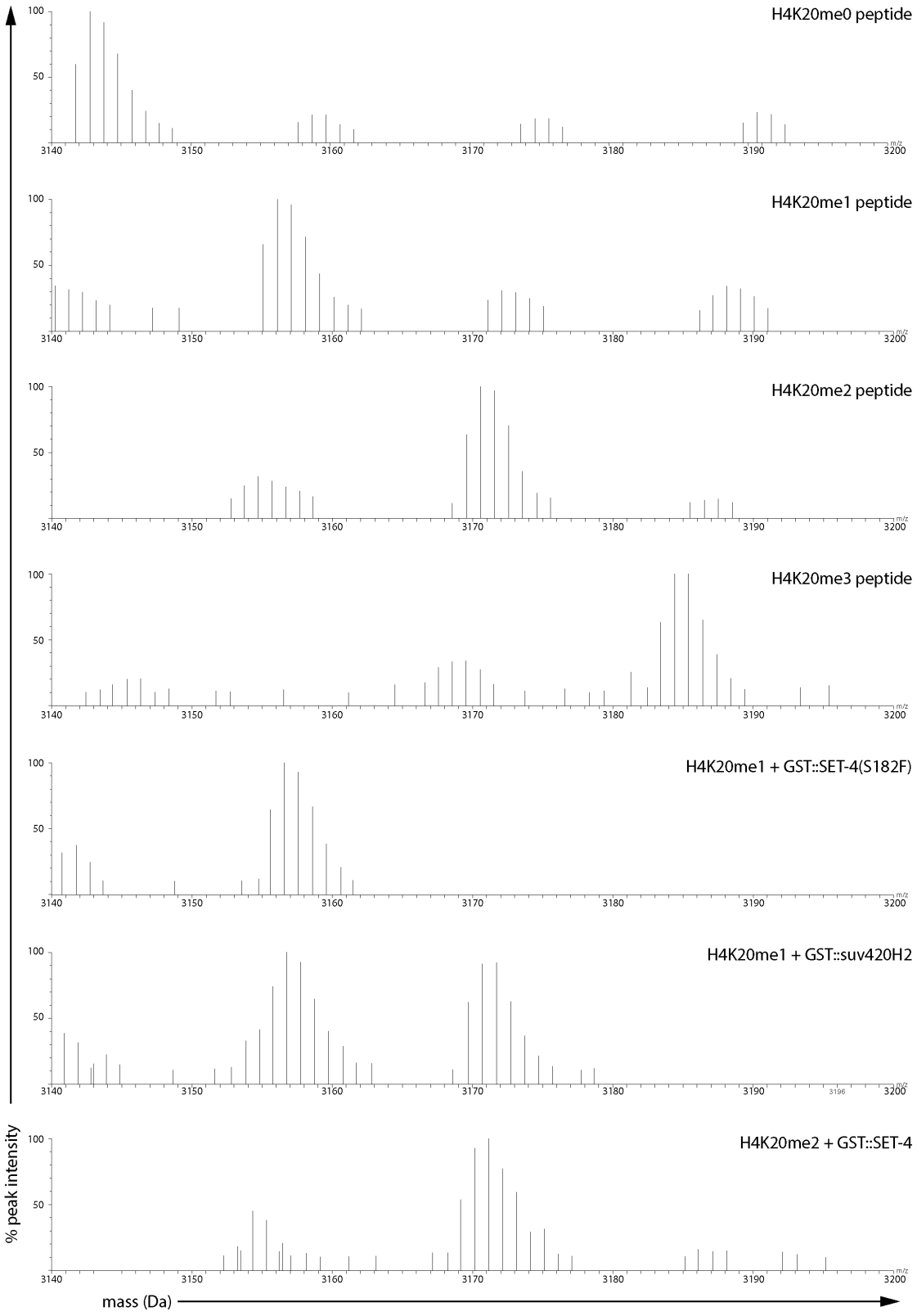

Supplemental Figure 3.S2. **MALDI spectra of methyltransferase assays**. Peptide substrates and GST fusion proteins (if any) are indicated. Data are representative of three independent experiments.

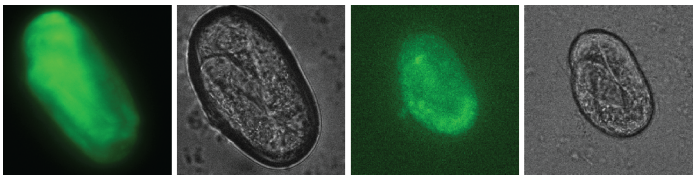

Supplemental Figure 3.S3. *set-4p::gfp* expression in embryos. Embryos from 3 independent transgenic lines were picked from plates and subjected to Nomarski and fluorescent imaging using an Olympus BX61 epifluorescence compound microscope outfitted with a Hamamatsu ORCA ER camera and Slidebook 4.0.1 software. Representative images shown. N = 10

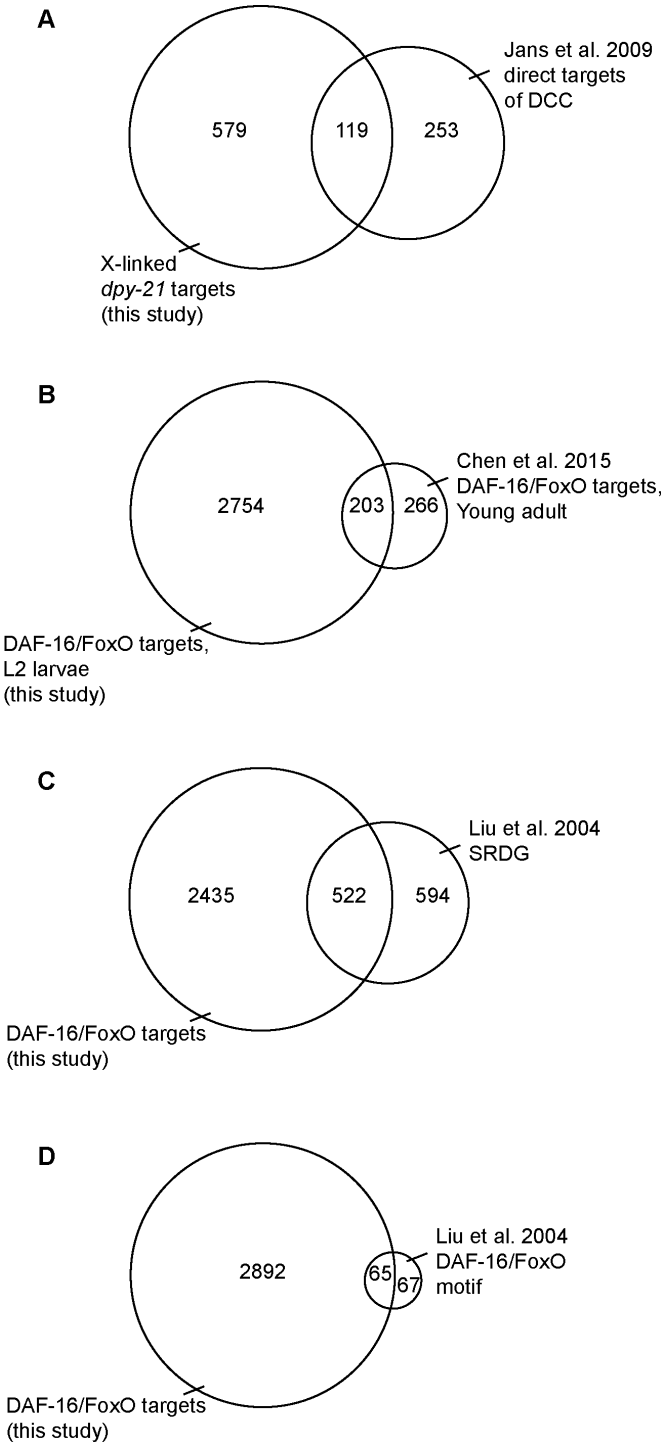

Supplemental Figure 3.S4. **Comparison of whole transcriptome profiling results from this study to published studies**. Venn diagrams depicting significant overlap between (**A**) X-linked genes regulated by *dpy-21* and direct DCC targets (Jans et al., 2009) (overlapping genes listed in Table S2); **(B)** DAF-16/FoxO target genes in L2 larvae and in young adult animals (Chen et al., 2015) (overlapping genes listed in Table S3); (**C**) DAF-16/FoxO target genes in L2 larvae and "strongly regulated dauer genes" (SRDG) (Liu et al., 2004) (overlapping genes listed in Table S4); and (**D**) DAF-16/FoxO target genes in L2 larvae and SRDG containing upstream DAF-16/FoxO binding motifs (Liu et al., 2004) (overlapping genes listed in Table S4).

ins-9

CTTAAATCCATTTGATTTGTCTCAATGGAGCGAAGAAAT**CCT**CCACCGTCAGTATCATCATCA**CCA**CCACCATCACCATGGAAATCGGGCGAGAAGAACCTTGG

MIVTLIVFLVIGLQMAHLSQVSGNNENGFLNPFDLSQWSEEILHRQYHHHHHHHHHGNRARR

dp675

CTTAAATCCATTTGATTTGTCTCAATGGAGCGAAGAAAT**TCTC**TAA**CTGACTAAC**CATCGGGCGAGAAGAACCTTGG

MIVTLIVFLVIGLQMAHLSQVSGNNENGFLNPFDLSQWSEEIL*

dp677

CTTAAATCCATTTGATTTGTCTCAATGGAGCGAAGAAAT**CCT**CCACCGTCAGTATCATCATCA**CCA**CCA**TGGTGATTCTTACCACGACCAGCTA**TAG**GCTGTTGG**
TCTGAAGCCATGTGAAGCTCCGCTACCATAGGCACCGCATGCGAAAAAAAAACAACAGCTATGGTGAGGCAGTTAGATAACCATCGGGCGAGAAGAACCTTGG

MIVTLIVFLVIGLQMAHLSQVSGNNENGFLNPFDLSQWSEEILHRQYHHHHGDSYHDQL*

Supplemental Figure 3.S5. **Schematic of the *ins-9* genomic locus and two mutant alleles generated by CRISPR/Cas9-based genome editing.** Nucleotide sequences encoding wild-type, *dp675,* and *dp677* N-terminal F-peptides and predicted N-terminal protein sequences are shown. Targeted CRISPR/Cas9 PAM sites are indicated in bold enlarged black typeface. The putative RXRR prohormone convertase processing site between the F and B peptides is underlined. Inserted sequences in two mutant alleles are indicated in red bold text, and the resultant in-frame stop codons are shown in red, bold and enlarged typeface.

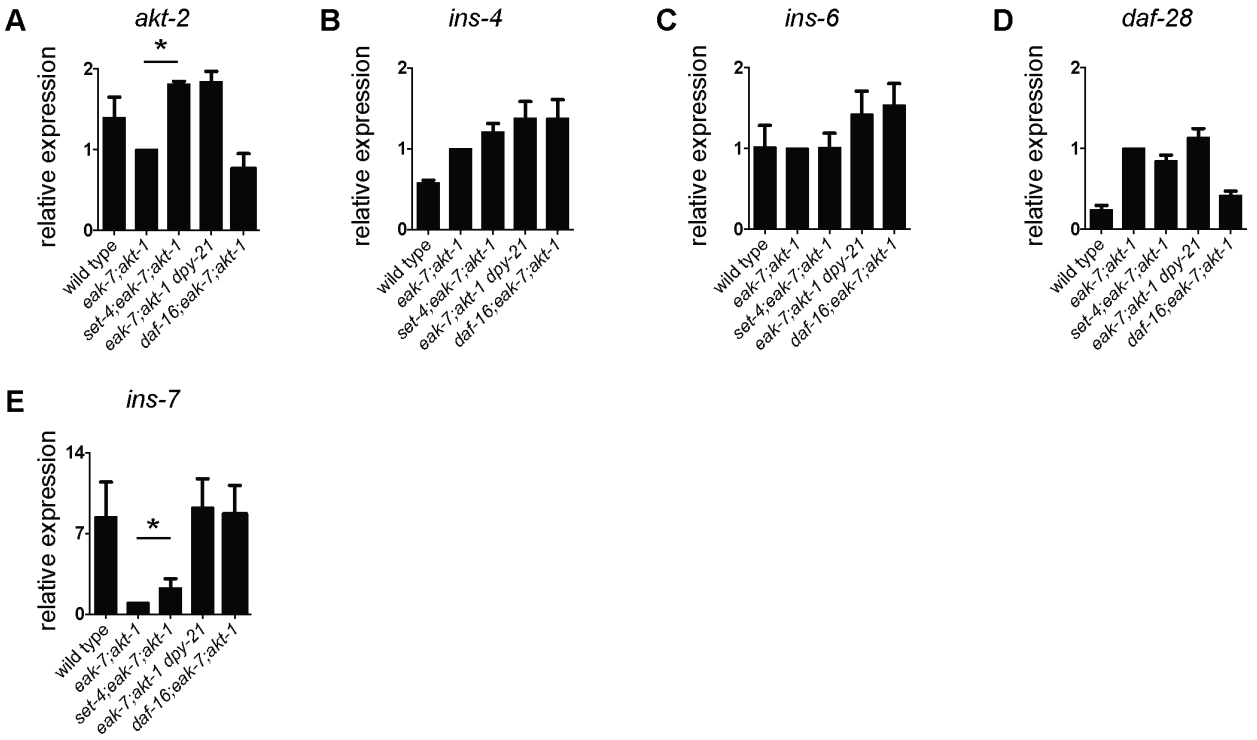

Supplemental Figure 3.S6. Influence of the DCM and DAF-16/FoxO on the expression of *akt-2* and *ins* genes. Transcript levels of (**A**) *akt-2*, (**B**) *ins-4,* (**C**) *ins-6,* (**D**) *daf-28*, and (**E**) *ins-7* in wild-type and mutant strains. Data presented is the mean plus s.e.m of at least three biological replicates.

Supplemental Table 3.1. RNAseq differentially expressed genes. Comparisons between dauer-deficient compound mutant strains and *eak-7;akt-1* background and overlap across regulomes are shown..

Data found on the web:
http://dev.biologists.org/content/develop/suppl/2017/03/22/dev.145722.DC1/DEV145722supp.pdf

Supplemental Table 3.2. Dosage compensated genes. DPY-21 dauer regulome genes previously identified as dosage-compensated genes (Jans et al., 2009).

Wormbase ID	Gene name	NCBI gene ID	Fold Change*
WBGene00007694	C23H4.6	181384	1.536
WBGene00019780	M60.4	187465	1.587
WBGene00001451	flp-8	181583	1.670
WBGene00015948	C18A11.2	182760	1.696
WBGene00007877	C33A11.1	181625	1.510
WBGene00001006	dlg-1	180819	1.529
WBGene00007958	C35C5.9	183231	1.922
WBGene00018257	F41B4.1	180952	1.770
WBGene00001462	flp-19	181260	1.631
WBGene00011154	R09A8.5	187724	1.652
WBGene00006372	syx-2	181505	2.120
WBGene00000277	cab-1	181382	1.758
WBGene00010605	K06G5.1	181531	1.633
WBGene00001674	gpa-12	181157	1.706
WBGene00018175	F38B6.6	185454	1.778
WBGene00014213	ZK1073.1	181689	1.623
WBGene00003517	nac-1	181585	2.100
WBGene00015947	C18A11.1	182759	1.560
WBGene00000072	add-1	180760	1.641
WBGene00006365	syg-1	180555	1.713
WBGene00016894	C53B7.3	180957	1.715
WBGene00003408	mrp-2	180408	2.566
WBGene00020339	ttr-59	188262	1.597
WBGene00001335	erp-1	180667	1.561
WBGene00010059	F54E4.3	181559	1.878
WBGene00004749	sdn-1	181259	1.585
WBGene00001824	hbl-1	180848	1.708
WBGene00008977	iglr-1	184720	2.140
WBGene00018837	F54G2.1	180562	1.682
WBGene00019102	F59C12.3	181718	1.625
WBGene00011880	T21B6.3	181284	2.291
WBGene00006757	unc-18	181030	1.502
WBGene00004719	sad-1	181471	1.923
WBGene00044698	K09F5.6	4363114	2.235
WBGene00006750	unc-10	180990	1.929
WBGene00004033	pkc-2	181166	1.630
WBGene00006068	sto-6	190619	2.236
WBGene00006742	unc-2	180570	2.053
WBGene00001116	dyc-1	181515	1.768

WBGene00006642	tsp-16	192066	1.835
WBGene00007772	egrh-1	181580	1.853
WBGene00002123	inx-1	180968	1.651
WBGene00044061	tbc-12	180556	1.679
WBGene00010329	F59D12.1	181656	1.969
WBGene00004370	rig-3	180958	2.338
WBGene00001708	grk-1	181212	1.801
WBGene00003733	nhx-5	181258	1.788
WBGene00006672	twk-18	181139	2.329
WBGene00006792	unc-58	181224	1.734
WBGene00004727	sax-1	180655	1.539
WBGene00016898	C53C9.2	181031	1.987
WBGene00002991	lin-2	181400	1.763
WBGene00015926	C17H11.6	181076	1.620
WBGene00004862	sma-9	181271	1.694
WBGene00009932	F52D10.6	186110	1.892
WBGene00000103	akt-2	181524	1.658
WBGene00000522	clc-1	181293	2.176
WBGene00020921	W01C8.5	180836	1.613
WBGene00021527	aakg-3	189836	2.674
WBGene00003623	nhr-25	181432	1.855
WBGene00003530	nas-11	180938	1.717
WBGene00001490	frm-3	181346	2.181
WBGene00007944	C34F6.10	181313	1.583
WBGene00001149	bcat-1	181423	1.671
WBGene00003561	ncr-1	180719	1.937
WBGene00003635	nhr-45	180738	1.927
WBGene00002124	inx-2	181318	2.180
WBGene00015294	C01C10.2	182067	2.421
WBGene00020158	T02C5.1	180568	1.692
WBGene00014215	obr-3	181495	1.824
WBGene00007285	C04A11.1	181486	2.479
WBGene00008571	prmn-1	181330	1.650
WBGene00008926	F17H10.2	184623	2.518
WBGene00001441	fkh-9	180670	1.879
WBGene00016866	coel-1	180700	3.026
WBGene00020633	aakg-2	181736	1.762
WBGene00017447	F14B8.5	180965	2.104
WBGene00017898	F28C10.3	180405	2.263
WBGene00009801	F47A4.5	181196	1.902
WBGene00022861	dve-1	180398	1.754
WBGene00008940	F18H3.4	181474	2.149
WBGene00009793	pkn-1	181244	2.013

WBGene00015182	B0416.7	181986	3.052
WBGene00016659	C45B2.2	180877	2.791
WBGene00015177	tmc-2	181161	2.190
WBGene00016423	tag-275	180886	1.719
WBGene00004789	sgk-1	181697	2.724
WBGene00015494	C05E11.3	180730	2.401
WBGene00010701	ent-2	181648	2.204
WBGene00010009	F53H4.4	181675	1.594
WBGene00018374	tag-343	181722	2.095
WBGene00011824	T18D3.7	188577	2.174
WBGene00003986	mct-4	180766	1.908
WBGene00010935	M163.1	181546	2.396
WBGene00020920	set-20	180835	1.950
WBGene00011444	T04F8.6	181354	1.839
WBGene00022200	fard-1	180582	2.036
WBGene00017449	otpl-3	259710	1.933
WBGene00015295	acl-12	181001	2.216
WBGene00017687	ets-4	180927	1.904
WBGene00008951	F19C6.2	181213	2.117
WBGene00020919	set-19	180834	2.325
WBGene00009800	rrc-1	181195	2.546
WBGene00018607	F48E3.8	181010	3.160
WBGene00012261	lpr-3	181295	1.864
WBGene00019518	K08B5.1	187132	2.609
WBGene00011642	T09B9.1	181188	3.814
WBGene00006640	tsp-14	180761	2.428
WBGene00015822	C16B8.2	180680	3.229
WBGene00001690	grd-1	181300	2.502
WBGene00000902	daf-6	181584	3.363
WBGene00007174	mboa-1	181681	4.943
WBGene00007935	C34E11.2	181359	5.672
WBGene00001608	R07B1.8	187649	12.511
WBGene00016662	C45B2.8	180879	4.202
WBGene00016106	C25F6.7	180816	7.304
WBGene00044724	R02E4.3	4363121	9.592
WBGene00002983	lgx-1	180825	12.749
WBGene00018031	F35B3.4	185255	34.952

Supplemental Table 3.3. DAF-16 target genes (Chen). DAF-16 dauer regulome genes previously identified as DAF-16 targets in young adult animals (Chen et al., 2015).

Wormbase ID	Gene name	NCBI gene ID	Fold Change*
WBGene00010614	cri-1	187082	0.097
WBGene00014046	clec-60	191384	2.140
WBGene00000853	cut-6	176520	0.151
WBGene00007131	B0284.1	181902	0.276
WBGene00019021	F57H12.6	177593	0.218
WBGene00007452	C08F11.3	182419	0.079
WBGene00001387	far-3	179785	0.088
WBGene00008390	D1086.3	179907	0.109
WBGene00022546	ZC196.2	191101	0.057
WBGene00015043	cyp-34A8	181850	0.222
WBGene00007440	C08E8.4	182409	0.342
WBGene00009805	F47B8.4	179930	0.115
WBGene00004932	sod-3	181748	0.030
WBGene00000968	dhs-4	172810	0.317
WBGene00001067	dpy-5	172197	84.644
WBGene00017128	E04F6.9	174185	0.198
WBGene00018448	F45D11.1	185779	0.031
WBGene00014047	clec-61	174613	0.133
WBGene00015889	C17C3.3	182714	0.283
WBGene00008482	cut-4	184037	12.155
WBGene00000649	col-73	184366	83.927
WBGene00014030	glb-1	176261	0.092
WBGene00022324	fbxa-26	190756	0.024
WBGene00017698	F22B7.9	176213	0.213
WBGene00013516	Y73F4A.3	177721	0.395
WBGene00011596	T07G12.5	177946	0.256
WBGene00008123	ent-6	178339	3.022
WBGene00022072	cpg-9	177087	5.251
WBGene00001074	dpy-13	177187	80.909
WBGene00019472	cyp-35B1	178803	0.058
WBGene00003473	mtl-1	179060	0.052
WBGene00015041	cyp-34A6	181848	0.182
WBGene00007929	dmd-10	183202	0.186
WBGene00008336	C55A6.7	183836	0.367
WBGene00003096	lys-7	178772	0.228
WBGene00011539	fbxa-135	188184	0.133
WBGene00012398	Y6E2A.4	189374	0.102
WBGene00008301	dct-3	183784	0.203
WBGene00022545	ZC196.1	191100	0.188

WBGene00012399	Y6E2A.5	189376	0.471
WBGene00015223	B0507.6	182013	0.475
WBGene00016052	dod-3	178737	0.160
WBGene00002055	ifc-1	178747	0.392
WBGene00012381	Y2H9A.4	189352	0.388
WBGene00008341	ttr-44	179835	0.453
WBGene00021081	W08A12.4	189288	0.527
WBGene00007833	oac-6	180094	2.441
WBGene00018540	btb-21	185908	3.593
WBGene00017262	F08F3.4	178924	2.789
WBGene00020947	W02F12.2	189124	2.717
WBGene00008793	F14D7.6	184466	3.871
WBGene00007807	C29F3.7	180036	4.771
WBGene00013904	ugt-6	179755	3.616
WBGene00009982	F53F1.4	179822	6.558
WBGene00000734	col-161	179812	39.509
WBGene00009620	fip-5	181237	1.725
WBGene00007812	C29F7.3	181464	1.780
WBGene00018779	F53H8.3	186195	2.021
WBGene00003999	pgp-5	181276	2.373
WBGene00004000	pgp-6	181278	2.701
WBGene00002267	lec-4	175488	0.363
WBGene00010593	gsnl-1	179328	0.351
WBGene00000627	col-50	189050	0.002
WBGene00077701	poml-3	6418581	0.249
WBGene00012959	Y47H10A.3	190008	0.138
WBGene00010135	F55H12.4	186344	0.335
WBGene00011935	scrm-1	173053	0.568
WBGene00010422	H32K16.2	3565869	0.591
WBGene00012140	T28F4.5	172503	0.391
WBGene00007302	C04F12.8	182228	0.541
WBGene00002112	ins-29	3565850	0.544
WBGene00016663	C45E1.4	171885	1.603
WBGene00012961	Y47H10A.5	173091	3.210
WBGene00009964	fip-6	172707	1.502
WBGene00000660	col-85	188672	0.003
WBGene00008842	chil-28	174888	0.007
WBGene00020741	T23F4.3		0.027
WBGene00019311	K02E7.6	173488	0.131
WBGene00001768	gst-20	175008	0.226
WBGene00017135	EEED8.4	173921	0.258
WBGene00018195	btb-16	173674	0.144
WBGene00017247	F08D12.3	3565148	0.490

WBGene00016628	C44B7.6	174125	0.259
WBGene00021797	Y52E8A.4	190188	0.608
WBGene00020329	bath-26	173531	0.204
WBGene00009663	hda-5	174811	0.250
WBGene00013220	ctl-3	175086	0.356
WBGene00018200	btb-17	173673	0.441
WBGene00010322	F59B10.6	174617	0.646
WBGene00007414	C07E3.3	174601	0.402
WBGene00011042	R05H10.1	175144	0.364
WBGene00006464	bath-47	173532	0.471
WBGene00008483	E04D5.4	184038	1.939
WBGene00011888	cutl-15	174426	1.597
WBGene00015894	acdh-2	173940	1.673
WBGene00015829	math-15	182659	5.540
WBGene00009904	F49E12.12	3565627	2.488
WBGene00005552	sri-40	191914	3.163
WBGene00004155	pqn-73	174366	2.794
WBGene00005291	srh-70	188678	6.582
WBGene00015828	math-14	182658	6.273
WBGene00012592	Y38E10A.14	174896	4.612
WBGene00012727	Y39G8B.7	189765	22.443
WBGene00189956	Y34F4.6	13188384	0.045
WBGene00021337	Y34F4.2	175262	0.099
WBGene00021865	fbxa-66	190275	0.129
WBGene00006533	tba-7	176568	0.428
WBGene00022325	fbxa-5	3565750	0.467
WBGene00021339	Y34F4.4	175263	0.600
WBGene00008040	ttr-5	176312	0.480
WBGene00000973	dhs-9	175737	0.435
WBGene00017806	F26A1.8	184948	1.954
WBGene00000932	dao-6	3564991	2.171
WBGene00020551	T17H7.7	175229	8.532
WBGene00022245	acp-6	177407	0.255
WBGene00011424	dhs-31	188051	0.176
WBGene00194646	Y105C5A.1270	13206883	0.258
WBGene00007507	C10C5.3	177767	0.193
WBGene00013633	Y105C5A.8	190873	0.164
WBGene00008028	scl-6	183343	0.655
WBGene00007509	C10C5.5	177769	0.452
WBGene00000535	cpi-1	177372	0.326
WBGene00016877	C52D10.3	3565402	0.568
WBGene00020445	T12B3.2	188439	0.560
WBGene00002013	hsp-12.6	177778	0.189

WBGene00000002	aat-1	177793	0.493
WBGene00016848	klo-1	177557	0.488
WBGene00021156	Y4C6B.2	189355	0.369
WBGene00021872	clec-85	177068	0.608
WBGene00017592	F19C7.2	184678	2.711
WBGene00023486	K08B4.7	259573	1.972
WBGene00012130	T28F3.4		1.919
WBGene00007508	C10C5.4	177768	3.537
WBGene00009895	scl-2	178251	2.571
WBGene00000683	col-109	176988	34.008
WBGene00007930	dmd-11	183203	0.043
WBGene00044201	H39E23.3	3565355	0.075
WBGene00017660	F21C10.11	179293	0.028
WBGene00001852	hil-1	179993	0.098
WBGene00045338	M01B2.13	13216887	0.104
WBGene00010791	sodh-2	179628	0.251
WBGene00013903	ugt-3	191174	0.326
WBGene00020593	ugt-11	178882	0.295
WBGene00005644	srp-3	178672	0.367
WBGene00015042	cyp-34A7	181849	0.149
WBGene00000111	alh-5	178680	0.314
WBGene00005703	sru-40	187650	0.194
WBGene00016046	C24B5.4	182835	0.304
WBGene00015402	C03G6.17	182179	0.419
WBGene00008220	C50B6.7	179813	0.409
WBGene00007835	oac-7	180096	0.567
WBGene00020276	T05H4.15	179030	0.458
WBGene00017082	DC2.5	183970	0.478
WBGene00015393	C03G6.5	179123	0.372
WBGene00015076	B0238.12	178914	0.629
WBGene00005602	srj-14	179124	0.416
WBGene00138721	C54D10.14	13215782	0.191
WBGene00010062	lipl-1	179771	0.625
WBGene00018055	F35F10.5	185310	0.536
WBGene00001591	glc-1	180086	0.416
WBGene00002263	lea-1	3564838	0.288
WBGene00020182	ugt-53	178744	0.610
WBGene00011894	ttr-23	188688	0.637
WBGene00012491	Y20C6A.1	180151	0.268
WBGene00019885	R05D8.7	187608	0.492
WBGene00009840	fbxa-189	185955	0.335
WBGene00012185	W01F3.2	180351	0.499
WBGene00011931	srsx-19	188760	0.445

WBGene00009803	F47B8.2	185895	0.580
WBGene00008296	cdr-2	183779	0.484
WBGene00045401	T26F2.3	6418775	1.631
WBGene00009488	oac-20	185375	2.892
WBGene00013900	ugt-18	179759	1.707
WBGene00009429	F35E12.5	185307	7.848
WBGene00012339	W07G4.5	179791	2.187
WBGene00019565	cyp-35A3	187209	3.605
WBGene00012683	asp-17	180250	5.681
WBGene00011185	R10D12.1	179888	2.976
WBGene00175027	W02F12.8	13213356	2.630
WBGene00019763	galt-1	187430	4.832
WBGene00009857	clec-28	186005	6.149
WBGene00044514	R09E12.9	3896848	9.324
WBGene00019089	clec-206	186582	12.397
WBGene00005018	sqt-3	179693	8.684
WBGene00018616	F48G7.5	178578	4.838
WBGene00020237	phat-4	178812	22.051
WBGene00000756	col-183	184081	0.000
WBGene00009303	lips-8	185178	0.332
WBGene00013975	ZK455.5	191321	0.313
WBGene00020135	aakg-4	187928	0.166
WBGene00001790	gst-42	183911	0.452
WBGene00018466	F45E1.5	185794	0.219
WBGene00015802	flu-2	180883	0.641
WBGene00019780	M60.4	187465	0.366
WBGene00019738	clec-265	180590	0.662
WBGene00004987	spp-2	259714	0.229
WBGene00016407	C34D10.2	181059	0.412
WBGene00000176	aqp-8	180744	1.677
WBGene00019318	K02E10.4	180552	2.901
WBGene00007397	C07A4.2	182351	1.566
WBGene00015355	C02F12.5	180656	1.948
WBGene00043980	F11D5.7	184345	10.033
WBGene00007344	C05E7.2	182266	14.875

Supplemental Table 3.4. DAF-16 target genes (Liu). DAF-16 dauer regulome genes previously identified as strongly regulated dauer genes and whether those genes contain nearby DAF-16 binding sites (Liu et al., 2004).

Wormbase ID[α]	Gene name	NCBI gene ID	Fold Change*
WBGene00010614	**cri-1**	**187082**	**0.097**
WBGene00014046	**clec-60**	**191384**	**2.140**
WBGene00000853	**cut-6**	**176520**	**0.151**
WBGene00007131	**B0284.1**	**181902**	**0.276**
WBGene00019021	**F57H12.6**	**177593**	**0.218**
WBGene00007452	**C08F11.3**	**182419**	**0.079**
WBGene00001387	**far-3**	**179785**	**0.088**
WBGene00008390	**D1086.3**	**179907**	**0.109**
WBGene00022546	**ZC196.2**	**191101**	**0.057**
WBGene00015043	**cyp-34A8**	**181850**	**0.222**
WBGene00007440	**C08E8.4**	**182409**	**0.342**
WBGene00009805	**F47B8.4**	**179930**	**0.115**
WBGene00004932	**sod-3**	**181748**	**0.030**
WBGene00000968	dhs-4	172810	0.317
WBGene00001067	dpy-5	172197	84.644
WBGene00017128	E04F6.9	174185	0.198
WBGene00018448	F45D11.1	185779	0.031
WBGene00014047	clec-61	174613	0.133
WBGene00015889	C17C3.3	182714	0.283
WBGene00008482	cut-4	184037	12.155
WBGene00000649	col-73	184366	83.927
WBGene00014030	glb-1	176261	0.092
WBGene00022324	fbxa-26	190756	0.024
WBGene00017698	F22B7.9	176213	0.213
WBGene00013516	Y73F4A.3	177721	0.395
WBGene00011596	T07G12.5	177946	0.256
WBGene00008123	ent-6	178339	3.022
WBGene00022072	cpg-9	177087	5.251
WBGene00001074	dpy-13	177187	80.909
WBGene00019472	cyp-35B1	178803	0.058
WBGene00003473	mtl-1	179060	0.052
WBGene00015041	cyp-34A6	181848	0.182
WBGene00007929	dmd-10	183202	0.186
WBGene00008336	C55A6.7	183836	0.367
WBGene00003096	lys-7	178772	0.228
WBGene00011539	fbxa-135	188184	0.133
WBGene00012398	Y6E2A.4	189374	0.102
WBGene00008301	dct-3	183784	0.203

WBGene00022545	ZC196.1	191100	0.188
WBGene00012399	Y6E2A.5	189376	0.471
WBGene00015223	B0507.6	182013	0.475
WBGene00016052	dod-3	178737	0.160
WBGene00002055	ifc-1	178747	0.392
WBGene00012381	Y2H9A.4	189352	0.388
WBGene00008341	ttr-44	179835	0.453
WBGene00021081	W08A12.4	189288	0.527
WBGene00007833	oac-6	180094	2.441
WBGene00018540	btb-21	185908	3.593
WBGene00017262	F08F3.4	178924	2.789
WBGene00020947	W02F12.2	189124	2.717
WBGene00008793	F14D7.6	184466	3.871
WBGene00007807	C29F3.7	180036	4.771
WBGene00013904	ugt-6	179755	3.616
WBGene00009982	F53F1.4	179822	6.558
WBGene00000734	col-161	179812	39.509
WBGene00009620	fip-5	181237	1.725
WBGene00007812	C29F7.3	181464	1.780
WBGene00018779	F53H8.3	186195	2.021
WBGene00003999	pgp-5	181276	2.373
WBGene00004000	pgp-6	181278	2.701
WBGene00007855	**C31H5.4**	**172724**	**0.603**
WBGene00012176	**W01C9.2**	**189089**	**0.267**
WBGene00014254	**cyp-13A10**	**174522**	**0.651**
WBGene00016970	**C56E6.2**	**174077**	**0.560**
WBGene00020357	**T08E11.1**	**188287**	**0.380**
WBGene00010945	**chil-13**	**174500**	**0.488**
WBGene00008809	**cyp-13A11**	**184472**	**0.062**
WBGene00003588	**nex-1**	**175714**	**0.335**
WBGene00007132	**B0284.2**	**175567**	**0.313**
WBGene00016612	**C43G2.3**	**183418**	**0.219**
WBGene00016845	**C50F7.5**	**177554**	**0.209**
WBGene00013294	**Y57G11B.1**	**190365**	**0.336**
WBGene00019019	**frpr-10**	**186481**	**0.571**
WBGene00002012	**hsp-12.3**	**177777**	**0.545**
WBGene00019510	**K07H8.10**	**177621**	**1.785**
WBGene00015394	**C03G6.6**	**182169**	**0.012**
WBGene00001712	**grl-3**	**186928**	**0.016**
WBGene00016922	**swt-2**	**183804**	**0.015**
WBGene00018211	**oac-24**	**185503**	**0.015**
WBGene00011948	**T23F1.5**	**180041**	**0.065**
WBGene00008850	**F15B9.6**	**184523**	**0.056**

WBGene00017200	**F07C4.6**	**184131**	**0.279**
WBGene00000723	**col-150**	**181814**	**0.117**
WBGene00018414	**nstp-8**	**178698**	**0.393**
WBGene00017640	**F20D6.11**	**179196**	**0.323**
WBGene00001789	**gst-41**	**179127**	**0.355**
WBGene00018260	**cyp-33C7**	**185589**	**0.540**
WBGene00001770	**gst-22**	**180088**	**3.264**
WBGene00007141	**pitr-4**	**179355**	**3.251**
WBGene00000718	**col-145**	**179297**	**27.509**
WBGene00011763	**T14B1.1**	**181181**	**0.249**
WBGene00010705	**cyp-14A1**	**187183**	**0.195**
WBGene00010706	**cyp-14A2**	**187184**	**0.292**
WBGene00016995	**D1005.1**	**180485**	**0.560**
WBGene00003778	**nnt-1**	**180884**	**0.069**
WBGene00002116	ins-33	189313	0.276
WBGene00008477	clec-17	173111	0.256
WBGene00020397	pcbd-1	188368	0.318
WBGene00007660	C17H1.7	182749	0.236
WBGene00013698	Y106G6D.1	190915	0.646
WBGene00010370	ctg-1	172431	0.525
WBGene00007992	fipr-24	183286	0.127
WBGene00007856	C31H5.5	183103	0.569
WBGene00007739	C26C6.4	182933	0.409
WBGene00020710	T23B3.2	188772	0.666
WBGene00019006	F57B10.9	172369	0.529
WBGene00000138	amx-2	173146	0.591
WBGene00013958	ZK265.6	191277	1.524
WBGene00010111	F55D12.2	172558	1.684
WBGene00020382	T09B4.8	172301	1.757
WBGene00002077	imb-3	3565440	1.558
WBGene00021026	W04C9.4	171636	1.619
WBGene00003062	lpd-6	171886	1.594
WBGene00001234	eif-6	173169	1.588
WBGene00018891	F55F8.3	172224	1.553
WBGene00010582	K05C4.5	173339	1.559
WBGene00021660	Y48G1A.4	171622	1.582
WBGene00004237	ptr-23	173362	1.776
WBGene00016607	C43E11.9	172028	1.689
WBGene00020036	R12E2.11	172008	2.100
WBGene00016653	C44E4.4	172070	1.804
WBGene00020915	nol-5	171901	1.849
WBGene00010644	K07G5.5	187123	2.345
WBGene00000931	dao-5	266845	1.923

WBGene00013895	ZC434.9	172908		1.588
WBGene00008763	F13G3.3	172475		3.574
WBGene00009824	gpdh-1	173272		5.000
WBGene00003664	nhr-74	191723		5.709
WBGene00018786	hmbx-1	171679		4.629
WBGene00004225	ptr-11	171609		7.101
WBGene00020258	T05E7.1	172309		7.793
WBGene00020283	T06A4.3	171668		6.271
WBGene00016329	osr-1	172161		13.913
WBGene00010291	F58H10.1	186556		14.165
WBGene00003548	nas-30	190803		6.288
WBGene00022517	ZC123.1	171671		19.420
WBGene00017068	D2092.8	172380		9.489
WBGene00014184	ZK1025.4	191493		28.846
WBGene00008652	F10D11.6	172635		13.698
WBGene00003552	nas-36	172506		18.038
WBGene00013891	ZC434.3	172903		25.135
WBGene00020033	R12E2.7	172002		21.577
WBGene00008565	F08A8.2	173163		51.546
WBGene00000641	col-65	187138		27.985
WBGene00050875	bah-1	173031		47.561
WBGene00016733	phat-2	172130		35.266
WBGene00020039	R12E2.14	172001		38.594
WBGene00020040	R12E2.15	172000		42.077
WBGene00000631	col-54	185226		55.197
WBGene00016731	C46H11.7	183524		64.298
WBGene00008290	C54C8.2	183769		180.339
WBGene00014182	ZK1025.2	173030		Inf
WBGene00018461	F45D11.16	173480	0.000	
WBGene00000613	col-36	174178		0.003
WBGene00000851	cut-1	174720		0.001
WBGene00020232	T05A8.6	188091		0.011
WBGene00022713	ZK355.3	191298		0.007
WBGene00020503	T14B4.9	188494		0.271
WBGene00019208	lips-14	186750		0.365
WBGene00011673	cyp-13A6	188357		0.252
WBGene00015598	fbxa-163	182398		0.295
WBGene00019906	R05G9R.1	24104792		0.186
WBGene00015597	fbxa-162	182397		0.246
WBGene00022572	ZC239.14	191124		0.379
WBGene00011672	cyp-13A5	188356		0.361
WBGene00017133	EEED8.2	173923		0.292
WBGene00009778	F46C5.1	174411		0.144

WBGene00006367	sym-2	174461	0.494
WBGene00021725	bath-9	173681	0.650
WBGene00009146	F26C11.1	184959	0.471
WBGene00018275	F41C3.11	173816	0.593
WBGene00001755	gst-7	173842	0.390
WBGene00010043	F54C9.7	186225	0.594
WBGene00011052	arrd-11	187635	0.043
WBGene00001753	gst-5	187537	0.556
WBGene00016302	fbxc-7	183113	0.129
WBGene00000372	cyp-13A7	188362	0.632
WBGene00012589	nspe-4	189658	0.313
WBGene00000971	dhs-7	174183	0.389
WBGene00012987	Y48C3A.3	190020	0.566
WBGene00015569	C07D10.5	174209	0.637
WBGene00023407	cex-1	186376	0.615
WBGene00011167	chil-23	187739	0.473
WBGene00001764	gst-16	175009	0.626
WBGene00022867	ZK1240.2	191538	1.647
WBGene00015064	B0228.7	174252	1.797
WBGene00006497	tag-151	173812	1.507
WBGene00008458	E02H1.6	174511	1.684
WBGene00021715	Y49F6B.2	173696	1.563
WBGene00012978	Y48B6A.1	175069	1.579
WBGene00017210	F07E5.5	173564	1.557
WBGene00021074	W07E6.2	173439	1.566
WBGene00020576	T19D12.1	24104905	1.614
WBGene00015941	C18A3.3	173968	1.664
WBGene00021073	nol-1	173437	1.732
WBGene00018271	F41C3.5	173818	1.975
WBGene00009947	F52H3.5	174562	2.240
WBGene00006893	spon-1	174169	2.213
WBGene00019280	K01A2.5	173418	2.991
WBGene00001523	gbh-2	174358	2.180
WBGene00004300	ram-2	174687	2.167
WBGene00013007	Y48E1B.8	175002	5.070
WBGene00004221	ptr-6	173898	3.542
WBGene00012591	nspe-1	189660	2.648
WBGene00004259	pyr-1	174385	5.909
WBGene00022649	ZK84.1	174008	3.241
WBGene00003388	moe-3	174960	5.871
WBGene00001522	gbh-1	174648	6.554
WBGene00004232	ptr-18	174940	7.304
WBGene00003888	osm-8	187684	12.825

WBGene00008500	F01D5.10	184059	9.124
WBGene00017841	F26G1.5	173823	7.284
WBGene00020327	clec-21	188250	9.715
WBGene00003526	nas-7	182368	10.076
WBGene00016805	C50D2.1	173396	14.907
WBGene00014245	ZK1307.2	191559	9.447
WBGene00013171	Y53F4B.25	175163	17.876
WBGene00006947	wrt-1	174223	24.766
WBGene00012032	T26C5.2	174465	35.058
WBGene00007560	C14A4.9	174637	28.280
WBGene00015841	C16C8.2		24.938
WBGene00010760	K10H10.4	175109	11.179
WBGene00012917	Y46G5A.29	174922	36.851
WBGene00000653	col-77	174336	22.853
WBGene00008964	mltn-9	175122	39.426
WBGene00011530	T06D8.10	174717	23.286
WBGene00018573	oac-30	185942	29.006
WBGene00017218	dct-5	184148	31.111
WBGene00005017	sqt-2	173382	79.353
WBGene00005016	sqt-1	174731	92.085
WBGene00015646	mlt-10	173445	82.177
WBGene00004397	rol-6	174397	81.701
WBGene00000606	col-17	173839	92.842
WBGene00007611	C15H7.4	182640	0.082
WBGene00022333	fbxa-27	190764	0.021
WBGene00001242	elo-4	183367	0.341
WBGene00001633	gly-8	176595	0.440
WBGene00020458	fbxa-70	188449	0.380
WBGene00020703	T22F7.4	188758	0.558
WBGene00015518	C06E1.1	176205	0.479
WBGene00000668	col-93	259335	0.259
WBGene00007963	cyp-25A1	183247	0.293
WBGene00000669	col-94	259336	0.326
WBGene00015559	npr-17	176124	0.489
WBGene00011112	R07E5.4	175568	0.434
WBGene00000666	col-91	184269	0.407
WBGene00016219	C29F9.4	175178	0.464
WBGene00000276	byn-1	175968	1.542
WBGene00003577	ndg-4	175582	1.757
WBGene00017356	F10E9.4	184304	1.654
WBGene00020600	T20B12.1	176055	1.723
WBGene00011408	T04A8.6	175614	1.602
WBGene00044318	tag-267	175220	1.638

WBGene00012964	Y48A6B.3	176531	1.790
WBGene00010478	K01G5.5	176504	1.880
WBGene00018241	F40G9.5	185554	2.841
WBGene00011559	umps-1	176453	2.257
WBGene00003887	osm-7	176790	2.645
WBGene00010540	K03H1.5	176404	3.277
WBGene00022180	Y71H2AM.15	175391	3.399
WBGene00001386	far-2	176284	2.821
WBGene00001570	gei-13	176364	14.020
WBGene00015335	acdh-6	182112	8.449
WBGene00015544	C06E8.5	182336	5.086
WBGene00017807	F26A1.9	184949	14.487
WBGene00008655	lips-3	184306	23.560
WBGene00011278	R74.2	175539	44.755
WBGene00001724	grl-15	190707	82.098
WBGene00000665	col-90	176117	95.531
WBGene00000676	col-102	182802	0.001
WBGene00000697	col-123	177823	0.008
WBGene00018143	oac-23	185419	0.019
WBGene00000690	col-116	184617	0.009
WBGene00010528	K03D3.2	186933	0.007
WBGene00019153	H04M03.3	177359	0.019
WBGene00008072	C43F9.4	183414	0.065
WBGene00021183	Y9C9A.16	189421	0.018
WBGene00015999	prmt-4	182806	0.209
WBGene00021585	clec-74	189948	0.263
WBGene00012783	Y43C5A.3	189848	0.266
WBGene00020373	gpx-6	188313	0.215
WBGene00017051	afmd-1	177499	0.253
WBGene00019047	F58E2.3	177110	0.235
WBGene00013882	ZC410.5	177728	0.244
WBGene00020728	T23E1.1	188794	0.336
WBGene00019368	K03H6.2	176959	0.414
WBGene00009077	F23B2.10	184885	0.179
WBGene00000691	col-117	177694	0.276
WBGene00007886	ethe-1	177783	0.295
WBGene00007777	C27D8.1	178226	0.525
WBGene00018547	clec-78	185915	0.432
WBGene00008708	F11E6.4	184358	0.457
WBGene00011171	R09E10.1	177920	0.483
WBGene00011484	T05E11.8	188133	0.550
WBGene00001751	gst-3	177883	0.339
WBGene00019540	K08D12.6	176980	0.416

WBGene00007384	swt-3	177972	0.517
WBGene00021195	Y17G9A.2	177257	0.450
WBGene00001477	fmo-2	177958	0.276
WBGene00016768	cyp-33E1	183602	0.513
WBGene00001975	hmg-5	177543	0.575
WBGene00011021	R05A10.4	187595	0.565
WBGene00009215	thn-2	178187	1.622
WBGene00020981	W03D2.6	177163	1.598
WBGene00011744	T13F2.4	188476	2.783
WBGene00008151	C47E12.7	177853	1.544
WBGene00019164	H06H21.8	186700	1.817
WBGene00010128	F55G11.8	186340	2.355
WBGene00017075	nap-1	177636	1.911
WBGene00014136	ZK896.5	178239	2.176
WBGene00019931	R07C12.1	177179	5.291
WBGene00018470	F45E4.5	185796	2.544
WBGene00010125	dod-22	178247	6.354
WBGene00020688	T22D1.11	177459	4.261
WBGene00010887	M7.12	187458	3.801
WBGene00044620	bus-4	188726	9.913
WBGene00021083	W08E12.2	189291	8.649
WBGene00000005	aat-4	177388	18.601
WBGene00001730	grl-21	177967	5.807
WBGene00009133	bed-3	184940	11.648
WBGene00000699	col-125	178029	9.007
WBGene00016596	C42D4.3	177492	8.153
WBGene00011594	T07G12.3	188242	27.698
WBGene00021084	W08E12.3	177098	19.907
WBGene00010673	K08E7.5	178211	49.792
WBGene00001079	dpy-20	178105	74.576
WBGene00022680	ZK180.6	177219	42.525
WBGene00022725	ZK381.2	191306	100.440
WBGene00001066	dpy-4	178414	76.874
WBGene00015719	C13A2.2	182550	0.000
WBGene00015724	C13A2.7	182555	0.004
WBGene00015725	C13A2.9	182556	0.000
WBGene00015726	C13A2.10	182557	0.000
WBGene00017229	F07G11.2	184157	0.013
WBGene00019526	K08D9.5	187148	0.040
WBGene00015722	C13A2.5	182553	0.000
WBGene00015721	C13A2.4	182552	0.001
WBGene00017230	F07G11.3	184158	0.002
WBGene00019524	K08D9.2	187146	0.024

WBGene00017231	F07G11.4	184159	0.015
WBGene00017819	F26D11.2	184973	0.003
WBGene00015718	C13A2.1	182549	0.018
WBGene00019527	K08D9.6	178760	0.022
WBGene00000731	col-158	179619	0.023
WBGene00017228	F07G11.1	184156	0.007
WBGene00019567	K09D9.9	187211	0.014
WBGene00015723	C13A2.6	182554	0.001
WBGene00009990	F53F4.7	179847	0.086
WBGene00017634	F20D6.2	184723	0.013
WBGene00001718	grl-9	179066	0.006
WBGene00009338	F32G8.2	185211	0.007
WBGene00019851	oac-41	187551	0.014
WBGene00001726	grl-17	183855	0.019
WBGene00005617	srj-32	191944	0.026
WBGene00009988	F53F4.4	186177	0.030
WBGene00015465	C05C8.8	182247	0.051
WBGene00008010	C38D9.2	183313	0.049
WBGene00020871	T28A11.4	189011	0.046
WBGene00015720	C13A2.3	182551	0.080
WBGene00001388	far-4	191633	0.107
WBGene00000722	col-149	179431	0.266
WBGene00019202	H14N18.2	186745	0.037
WBGene00015682	C10G8.3	182502	0.048
WBGene00018406	F44A2.7	185721	0.133
WBGene00021731	Y49G5A.1	190090	0.652
WBGene00010216	F57G8.7	186468	0.332
WBGene00002118	ins-35	180334	0.209
WBGene00010205	F57F5.3	179646	0.219
WBGene00010100	F55C9.3	186291	0.315
WBGene00011004	R04B5.6	179404	0.105
WBGene00019978	hacd-1	178638	0.256
WBGene00010102	F55C9.5	186293	0.307
WBGene00008334	sdz-8	183834	0.203
WBGene00009710	F44G3.10	185758	0.517
WBGene00020748	nhr-221	188826	0.286
WBGene00017363	F10G2.2	184313	0.410
WBGene00019652	K11G9.1	179057	0.315
WBGene00011752	fbxa-2	180091	0.404
WBGene00015397	nhr-149	182174	0.286
WBGene00019648	K11D12.8	187294	0.366
WBGene00016285	C31B8.12	183081	0.421
WBGene00015040	cyp-34A5	181847	0.228

WBGene00008335	C55A6.6	183835	0.273
WBGene00005931	fbxa-199	188182	0.439
WBGene00009600	F40G12.5	185565	0.374
WBGene00020881	T28A11.19	189024	0.531
WBGene00016785	C49G7.7	183621	0.324
WBGene00013078	ttr-25	180210	0.359
WBGene00009804	F47B8.3	185896	0.462
WBGene00019348	K02H11.4	186913	0.423
WBGene00021963	lipl-6	179081	0.596
WBGene00021412	cyp-29A3	189649	0.441
WBGene00003861	oig-3	190105	0.385
WBGene00020941	W02D7.5	189117	0.360
WBGene00022653	ZK105.1	191220	0.416
WBGene00000982	dhs-19	179578	0.497
WBGene00004811	skr-5	180148	0.337
WBGene00008985	F20G2.1	184742	0.563
WBGene00015769	C14C11.7	182612	0.525
WBGene00016860	cyp-33C9	178752	0.567
WBGene00016281	C31B8.4	183078	0.481
WBGene00016101	C25E10.12	182896	0.637
WBGene00019477	K07C11.4	179198	0.575
WBGene00008453	E02A10.3	179722	0.649
WBGene00000599	col-10	179298	0.584
WBGene00011286	ttr-29	187890	0.618
WBGene00008669	acs-14	179330	1.513
WBGene00004910	snf-11	191770	1.554
WBGene00018762	F53E10.6	178728	1.580
WBGene00010080	F55A11.7	179614	1.568
WBGene00015464	C05C8.7	179120	2.040
WBGene00010214	F57G8.5	180097	1.642
WBGene00009993	F53F4.11	179849	1.635
WBGene00000007	aat-6	188421	1.831
WBGene00010627	K07C5.4	179442	1.666
WBGene00001423	fib-1	179999	1.744
WBGene00019117	nhr-144	186627	2.340
WBGene00012058	T26F2.2	179892	1.931
WBGene00017430	F13H6.1	179019	1.575
WBGene00007950	C35A5.6	183224	1.888
WBGene00011090	R07B7.6	179658	2.283
WBGene00022538	ZC190.4	179248	2.748
WBGene00003248	mig-17	179575	2.638
WBGene00011212	R10E8.6	180195	2.564
WBGene00019090	F59A7.2	178682	1.709

WBGene00015758	nhr-155	182602	8.492
WBGene00002259	lbp-7	191701	3.084
WBGene00000003	aat-2	184126	3.073
WBGene00009722	F45D3.2	179716	5.468
WBGene00000373	cyp-14A5	178926	2.595
WBGene00007748	C26E1.2	182940	3.699
WBGene00003763	nlp-25	189877	3.831
WBGene00000726	col-153	179517	6.781
WBGene00016146	C26F1.1	179157	2.909
WBGene00021309	Y32G9B.1	178662	4.570
WBGene00000602	col-13	179452	3.436
WBGene00000728	col-155	186301	4.701
WBGene00001479	fmo-4	179845	10.863
WBGene00022577	nstp-3	191128	10.110
WBGene00010472	cdr-7	24104698	7.969
WBGene00018706	F52F10.2	178644	11.287
WBGene00011624	T08G5.3	179901	18.156
WBGene00000601	col-12	179453	11.645
WBGene00019644	cpt-4	178889	21.546
WBGene00019761	M03F8.1	187429	16.833
WBGene00004230	ptr-16	191750	19.123
WBGene00019754	M03E7.2	178948	13.618
WBGene00015340	C02E7.7	178884	13.597
WBGene00001716	grl-7	179569	29.490
WBGene00007754	C27A7.2	179664	46.841
WBGene00012046	T26E4.4	188930	62.995
WBGene00012346	W08G11.1	180099	44.842
WBGene00007804	C29F3.3	183004	18.305
WBGene00000729	col-156	186439	40.694
WBGene00015339	C02E7.6	178885	38.460
WBGene00003057	lon-3	179673	57.123
WBGene00007806	clec-230	183006	31.044
WBGene00006954	wrt-8	180035	30.675
WBGene00007177	oac-1	181961	55.349
WBGene00000730	col-157	188426	89.265
WBGene00018297	F41F3.3	178856	46.147
WBGene00001691	grd-2	180349	58.566
WBGene00021625	Y47D7A.13	178841	44.047
WBGene00001695	grd-6	24104900	40.262
WBGene00009983	cut-2	179823	66.508
WBGene00010468	K01D12.9	186847	70.682
WBGene00010467	K01D12.8	186846	170.781
WBGene00000737	col-164	180523	0.000

WBGene00019570	K09E2.1	187215	0.011
WBGene00001696	grd-7	191661	0.049
WBGene00009849	F48F7.3	185989	0.063
WBGene00011104	cut-5	187677	0.041
WBGene00017149	EGAP4.1	184049	0.362
WBGene00006534	tba-8	191455	0.394
WBGene00009635	F42F12.3	185670	0.393
WBGene00010504	K02D3.1	186872	0.583
WBGene00007694	C23H4.6	181384	0.547
WBGene00017464	sulp-2	180828	0.416
WBGene00020569	lgc-32	188603	0.429
WBGene00006980	zig-3	192088	0.343
WBGene00000212	asm-2	181323	0.647
WBGene00009813	haly-1	181279	0.625
WBGene00017226	fbxa-53	184154	0.588
WBGene00011108	R07E3.7	187679	0.540
WBGene00007691	C23H4.2	182818	0.180
WBGene00015783	C15B12.1	180921	1.587
WBGene00016714	C46F2.1	183512	2.186
WBGene00019493	catp-5	181067	1.986
WBGene00022200	fard-1	180582	1.636
WBGene00004245	puf-9	180850	1.678
WBGene00010341	glo-3	186637	2.021
WBGene00010521	K03A11.4	186918	1.661
WBGene00008354	gcsh-1	183902	2.180
WBGene00019572	K09E2.3	187217	1.802
WBGene00019779	M60.2	181079	1.884
WBGene00009057	cept-1	184847	2.553
WBGene00015865	C16E9.1	182693	2.096
WBGene00009483	F36G3.2	181192	2.700
WBGene00007811	C29F7.2	181463	3.818
WBGene00017625	cgt-2	181790	3.424
WBGene00010396	H13N06.2	181636	4.270
WBGene00019404	K05B2.4	187017	4.831
WBGene00002067	ifp-1	181182	4.098
WBGene00010835	M03B6.3	181498	8.950
WBGene00015545	C06G1.1	181720	5.591
WBGene00020484	T13C5.3	188473	20.856
WBGene00003554	nas-38	180407	5.776
WBGene00008602	oac-14	181226	6.293
WBGene00019547	K09C4.1	180621	11.718
WBGene00003553	nas-37	181208	18.642
WBGene00044623	bus-8	180821	15.563

WBGene00011077	R07B1.5	187646	16.664
WBGene00017716	F22F4.1	180868	19.560
WBGene00017307	F09F9.2	184263	21.776
WBGene00001703	grd-14	187934	29.375
WBGene00018031	F35B3.4	185255	23.835
WBGene00000746	col-173	180960	43.937
WBGene00010118	F55F3.4	186318	42.509
WBGene00014039	ZK662.2	181660	28.660
WBGene00006950	wrt-4	181664	55.166
WBGene00000755	col-182	187723	52.586
WBGene00000618	col-41	181610	63.306
WBGene00017673	**F21F3.3**	**172106**	**0.004**
WBGene00009345	**F32H2.8**	**185215**	**4.818**
WBGene00018755	**bcmo-2**	**173733**	**0.244**
WBGene00008052	**ctns-1**	**174308**	**0.481**
WBGene00021436	**Y39A3B.1**	**189721**	**11.303**
WBGene00015538	**sams-3**	**177355**	**2.204**
WBGene00019464	**K07B1.4**	**179314**	**0.277**
WBGene00019113	**F59E11.7**	**179277**	**0.211**
WBGene00017312	**pitr-5**	**179104**	**1.693**
WBGene00010360	**fbxa-96**	**186676**	**0.073**
WBGene00001693	**grd-4**	**24104827**	**0.101**
WBGene00022500	**lfi-1**	**180771**	**0.666**
WBGene00009816	**F47B10.5**	**185904**	**2.431**
WBGene00002057	**ifd-1**	**187585**	**2.986**
WBGene00018591	**npax-2**	**185967**	**7.178**
WBGene00002267	**lec-4**	**175488**	**0.363**
WBGene00010593	**gsnl-1**	**179328**	**0.351**

Supplemental Table 3.5. X-linked genes regulated by both DPY-21 and DAF-16, but not regulated by DAF-12.

Wormbase ID	Gene name	NCBI gene ID	Fold Change *daf-16**	Fold Change *dpy-21**
WBGene00000756	col-183	184081	0.000	0.003
WBGene00194674	F23D12.11	13223834	0.276	0.277
WBGene00008350	CE7X_3.2	353483	0.493	0.562
WBGene00000745	col-172	180934	0.441	0.209
WBGene00008462	E02H4.4	183995	0.500	0.502
WBGene00004987	spp-2	259714	0.229	0.550
WBGene00007691	C23H4.2	182818	0.180	0.462
WBGene00000929	dao-3	181065	0.602	0.595
WBGene00006897	ver-4	186632	0.376	0.620
WBGene00018877	aman-1	180749	0.635	0.613
WBGene00009620	fip-5	181237	1.725	1.882
WBGene00020160	igcm-3	180569	1.755	2.403
WBGene00015783	C15B12.1	180921	1.587	1.903
WBGene00010971	R01E6.7	187507	1.598	1.962
WBGene00000176	aqp-8	180744	1.677	2.573
WBGene00019493	catp-5	181067	1.986	2.549
WBGene00015382	C03B1.14	182152	1.781	1.721
WBGene00022200	fard-1	180582	1.636	2.036
WBGene00017449	otpl-3	259710	1.738	1.933
WBGene00015295	acl-12	181001	1.617	2.216
WBGene00016998	D1005.4	183882	1.666	2.160
WBGene00002203	kin-20	181620	1.662	1.985
WBGene00022201	Y71H10B.1	180573	1.656	2.031
WBGene00004245	puf-9	180850	1.678	2.218
WBGene00016660	C45B2.3	183467	2.313	1.520
WBGene00008951	F19C6.2	181213	1.832	2.117
WBGene00019960	ztf-16	180756	1.561	1.617
WBGene00045272	F59C12.4	6418857	1.591	1.751
WBGene00017938	F31A3.3	185135	1.722	2.774
WBGene00018779	F53H8.3	186195	2.021	2.037
WBGene00019572	K09E2.3	187217	1.802	1.988
WBGene00020725	cnp-3	181752	1.847	2.790
WBGene00010336	F59F4.1	181668	2.181	1.541
WBGene00044151	W04G3.12	3896893	2.963	2.449
WBGene00019518	K08B5.1	187132	1.558	2.609
WBGene00019782	M60.7	187467	1.803	1.986
WBGene00019779	M60.2	181079	1.884	2.488
WBGene00015714	C12D12.3	182545	2.016	3.283
WBGene00001468	flr-4	181604	2.710	2.054
WBGene00219376	C28G1.10	13222010	2.045	2.003

WBGene00009852	arrd-24	185991	3.204	2.066
WBGene00206361	K02G10.15	13220381	2.529	3.137
WBGene00011081	R07B1.9	181201	1.779	5.141
WBGene00019404	K05B2.4	187017	4.831	3.231
WBGene00022616	hsd-3	260026	12.275	4.825
WBGene00010118	F55F3.4	186318	42.509	7.732
WBGene00002092	ins-9	3564850	Inf	Inf

Supplemental Table 3.6. Insulin-like peptides regulated by both DPY-21 and DAF-16.

ILP	chromosome	fold change *daf-16**	fold change *dpy-21*[!]	*daf-2* interaction
ins-33	I	0.28	0.30	agonist**
ins-29	I	0.54	0.48	?
ins-20	II	2.65	13.32	antagonist@
ins-11	II	2.49	6.69	antagonist@
ins-16	III	0.03	0.07	?
ins-7	IV	10.83	7.99	agonist***
ins-35	V	0.21	0.27	agonist@
ins-9	X	infinite	infinite	agonist#

**daf-16;eak-7;akt-1* vs. *eak-7;akt-1*
[!]*eak-7;akt-1 dpy-21* vs. *eak-7;akt-1*
@Fernandes de Abreu et al, 2014
**Michaelson et al, 2010
***Murphy et al, 2003
#this study

Supplemental Table 3.7. CRISPR guide sequences and repair oligos.

	Sequence 5' to 3'
ins-9 guide #1	GAUGAUGAUACUGACGGUGG
ins-9 guide #2	GAUUUCCAUGGUGAUGGUGG
ins-9 repair oligo	TTCTTAAATCCATTTGATTTGTCTCAATGGAGCGAAGAAATTC TCTAACTGACTAACCATCGGGCGAGAAGAACCTTGGAAACCG AAAAAATCTACCGCT
dpy-10 guide	GCUACCAUAGGCACCACGAG
dpy-10 repair oligo	CACTTGAACTTCAATACGGCAAGATGAGAATGACTGGAAACC GTACCGCATGCGGTGCCTATGGTAGCGGAGCTTCACATGGC TTCAGACCAACAGCCTAT

Supplemental Table 3.8. qPCR primer sequences.

Gene		Sequence 5' to 3'
akt-2	F	TCGTGATATGAAACTCGAAAATTTGC
	R	ATTCTGGTGTTCCGCAAAAGGTG
daf-28	F	AGTCCGTGTTCCAGGTGTG
	R	TGTTGCGATGTCAATTCCTT
ins-4	F	AAAATCAACTCTCCCGAGCA
	R	GCAATGTCCATGTCCTCTTGT
ins-6	F	CGAGCAAGACGTGTTCCAG
	R	TCGCAATGTCCTTTCCTTCT
ins-9	F	GAAGAAATCCTCCACCGTCA
	R	GTTCTTCTCGCCCGATTTC
ins-7	F	GTTGTGGAAGAAGAATACATTCGTATG
	R	TCTTCACGGCAACATTTTGATG
pmp-3	F	GTTCCCGTGTTCATCACTCAT
	R	ACACCGTCGAGAAGCTGTAGA

Supplemental Table 3.9. RNAseq correlation coefficients between replicates and between strains.

Data found on the web:
http://dev.biologists.org/content/develop/suppl/2017/03/22/dev.145722.DC1/DEV145722supp.pdf

References

Ailion, M. and Thomas, J. H. (2003). Isolation and characterization of high-temperature-induced Dauer formation mutants in Caenorhabditis elegans. *Genetics* 165, 127-144.

Alam, H., Williams, T. W., Dumas, K. J., Guo, C., Yoshina, S., Mitani, S. and Hu, P. J. (2010). EAK-7 controls development and life span by regulating nuclear DAF-16/FoxO activity. *Cell Metab* 12, 30-41.

Andersen, E. C. and Horvitz, H. R. (2007). Two C. elegans histone methyltransferases repress lin-3 EGF transcription to inhibit vulval development. *Development* 134, 2991-2999.

Bargmann, C. I. and Horvitz, H. R. (1991). Control of larval development by chemosensory neurons in Caenorhabditis elegans. *Science* 251, 1243-1246.

Blumenthal, T. (2005). Trans-splicing and operons. *WormBook*, 1-9.

Butcher, R. A., Ragains, J. R., Kim, E. and Clardy, J. (2008). A potent dauer pheromone component in Caenorhabditis elegans that acts synergistically with other components. *Proc Natl Acad Sci U S A* 105, 14288-14292.

Chen, A. T., Guo, C., Itani, O. A., Budaitis, B. G., Williams, T. W., Hopkins, C. E., McEachin, R. C., Pande, M., Grant, A. R., Yoshina, S., et al. (2015). Longevity Genes Revealed by Integrative Analysis of Isoform-Specific daf-16/FoxO Mutants of Caenorhabditis elegans. *Genetics* 201, 613-629.

Chen, Y. and Baugh, L. R. (2014). Ins-4 and daf-28 function redundantly to regulate C. elegans L1 arrest. *Dev Biol* 394, 314-326.

Cornils, A., Gloeck, M., Chen, Z., Zhang, Y. and Alcedo, J. (2011). Specific insulin-like peptides encode sensory information to regulate distinct developmental processes. *Development* 138, 1183-1193.

Dawes, H. E., Berlin, D. S., Lapidus, D. M., Nusbaum, C., Davis, T. L. and Meyer, B. J. (1999). Dosage compensation proteins targeted to X chromosomes by a determinant of hermaphrodite fate. *Science* 284, 1800-1804.

Dumas, K. J., Delaney, C. E., Flibotte, S., Moerman, D. G., Csankovszki, G. and Hu, P. J. (2013). Unexpected Role for Dosage Compensation in the Control of Dauer Arrest, Insulin-Like Signaling, and FoxO Transcription Factor Activity in Caenorhabditis elegans. *Genetics* 194, 619-629.

Fernandes de Abreu, D. A., Caballero, A., Fardel, P., Stroustrup, N., Chen, Z., Lee, K., Keyes, W. D., Nash, Z. M., Lopez-Moyado, I. F., Vaggi, F., et al. (2014). An insulin-to-insulin regulatory network orchestrates phenotypic specificity in development and physiology. *PLoS Genet* 10, e1004225.

Fielenbach, N. and Antebi, A. (2008). C. elegans dauer formation and the molecular basis of plasticity. *Genes Dev* 22, 2149-2165.

Georgi, L. L., Albert, P. S. and Riddle, D. L. (1990). daf-1, a C. elegans gene controlling dauer larva development, encodes a novel receptor protein kinase. *Cell* 61, 635-645.

Gerisch, B., Weitzel, C., Kober-Eisermann, C., Rottiers, V. and Antebi, A. (2001). A hormonal signaling pathway influencing C. elegans metabolism, reproductive development, and life span. *Developmental cell* 1, 841-851.

Golden, J. W. and Riddle, D. L. (1982). A pheromone influences larval development in the nematode Caenorhabditis elegans. *Science* 218, 578-580.

---- (1984). The Caenorhabditis elegans dauer larva: developmental effects of pheromone, food, and temperature. *Dev Biol* 102, 368-378.

Gottlieb, S. and Ruvkun, G. (1994). daf-2, daf-16 and daf-23: genetically interacting genes controlling Dauer formation in Caenorhabditis elegans. *Genetics* 137, 107-120.
Hoogewijs, D., Houthoofd, K., Matthijssens, F., Vandesompele, J. and Vanfleteren, J. R. (2008). Selection and validation of a set of reliable reference genes for quantitative sod gene expression analysis in C. elegans. *BMC Mol Biol* 9, 9.
Hu, P. J., Xu, J. and Ruvkun, G. (2006). Two membrane-associated tyrosine phosphatase homologs potentiate C. elegans AKT-1/PKB signaling. *PLoS Genet* 2, e99.
Hung, W. L., Wang, Y., Chitturi, J. and Zhen, M. (2014). A Caenorhabditis elegans developmental decision requires insulin signaling-mediated neuron-intestine communication. *Development* 141, 1767-1779.
Jans, J., Gladden, J. M., Ralston, E. J., Pickle, C. S., Michel, A. H., Pferdehirt, R. R., Eisen, M. B. and Meyer, B. J. (2009). A condensin-like dosage compensation complex acts at a distance to control expression throughout the genome. *Genes Dev* 23, 602-618.
Jia, K., Albert, P. S. and Riddle, D. L. (2002). DAF-9, a cytochrome P450 regulating C. elegans larval development and adult longevity. *Development* 129, 221-231.
Kramer, M., Kranz, A. L., Su, A., Winterkorn, L. H., Albritton, S. E. and Ercan, S. (2015). Developmental Dynamics of X-Chromosome Dosage Compensation by the DCC and H4K20me1 in C. elegans. *PLoS Genet* 11, e1005698.
Li, W., Kennedy, S. G. and Ruvkun, G. (2003). daf-28 encodes a C. elegans insulin superfamily member that is regulated by environmental cues and acts in the DAF-2 signaling pathway. *Genes Dev* 17, 844-858.
Liu, T., Zimmerman, K. K. and Patterson, G. I. (2004). Regulation of signaling genes by TGFbeta during entry into dauer diapause in C. elegans. *BMC developmental biology* 4, 11.
Meyer, B. J. (2010). Targeting X chromosomes for repression. *Curr Opin Genet Dev* 20, 179-189.
Michaelson, D., Korta, D. Z., Capua, Y. and Hubbard, E. J. (2010). Insulin signaling promotes germline proliferation in C. elegans. *Development* 137, 671-680.
Murphy, C. T. and Hu, P. J. (2013). Insulin/insulin-like growth factor signaling in C. elegans. *WormBook*, 1-43.
Murphy, C. T., Lee, S. J. and Kenyon, C. (2007). Tissue entrainment by feedback regulation of insulin gene expression in the endoderm of Caenorhabditis elegans. *Proc Natl Acad Sci U S A* 104, 19046-19050.
Murphy, C. T., McCarroll, S. A., Bargmann, C. I., Fraser, A., Kamath, R. S., Ahringer, J., Li, H. and Kenyon, C. (2003). Genes that act downstream of DAF-16 to influence the lifespan of Caenorhabditis elegans. *Nature* 424, 277-283.
Nolan, T., Hands, R. E. and Bustin, S. A. (2006). Quantification of mRNA using real-time RT-PCR. *Nat Protoc* 1, 1559-1582.
Nonet, M. L., Staunton, J. E., Kilgard, M. P., Fergestad, T., Hartwieg, E., Horvitz, H. R., Jorgensen, E. M. and Meyer, B. J. (1997). Caenorhabditis elegans rab-3 mutant synapses exhibit impaired function and are partially depleted of vesicles. *The Journal of neuroscience : the official journal of the Society for Neuroscience* 17, 8061-8073.
Ohkura, K., Suzuki, N., Ishihara, T. and Katsura, I. (2003). SDF-9, a protein tyrosine phosphatase-like molecule, regulates the L3/dauer developmental decision through hormonal signaling in C. elegans. *Development* 130, 3237-3248.

Paix, A., Folkmann, A., Rasoloson, D. and Seydoux, G. (2015). High Efficiency, Homology-Directed Genome Editing in Caenorhabditis elegans Using CRISPR-Cas9 Ribonucleoprotein Complexes. *Genetics* 201, 47-54.

Park, D., Estevez, A. and Riddle, D. L. (2010). Antagonistic Smad transcription factors control the dauer/non-dauer switch in C. elegans. *Development* 137, 477-485.

Pierce, S. B., Costa, M., Wisotzkey, R., Devadhar, S., Homburger, S. A., Buchman, A. R., Ferguson, K. C., Heller, J., Platt, D. M., Pasquinelli, A. A., et al. (2001). Regulation of DAF-2 receptor signaling by human insulin and ins-1, a member of the unusually large and diverse C. elegans insulin gene family. *Genes Dev* 15, 672-686.

Ren, P., Lim, C. S., Johnsen, R., Albert, P. S., Pilgrim, D. and Riddle, D. L. (1996). Control of C. elegans larval development by neuronal expression of a TGF-beta homolog. *Science* 274, 1389-1391.

Riddle, D. L. (1988). The Dauer Larva. In *The Nematode Caenorhabditis elegans* (ed. W. B. Wood, editor), pp. 393-412. Plainview (New York): Cold Spring Harbor Laboratory Press.

Riddle, D. L., Swanson, M. M. and Albert, P. S. (1981). Interacting genes in nematode dauer larva formation. *Nature* 290, 668-671.

Ritter, A. D., Shen, Y., Fuxman Bass, J., Jeyaraj, S., Deplancke, B., Mukhopadhyay, A., Xu, J., Driscoll, M., Tissenbaum, H. A. and Walhout, A. J. (2013). Complex expression dynamics and robustness in C. elegans insulin networks. *Genome Res* 23, 954-965.

Rottiers, V., Motola, D. L., Gerisch, B., Cummins, C. L., Nishiwaki, K., Mangelsdorf, D. J. and Antebi, A. (2006). Hormonal control of C. elegans dauer formation and life span by a Rieske-like oxygenase. *Developmental cell* 10, 473-482.

Schackwitz, W. S., Inoue, T. and Thomas, J. H. (1996). Chemosensory neurons function in parallel to mediate a pheromone response in C. elegans. *Neuron* 17, 719-728.

Schaedel, O. N., Gerisch, B., Antebi, A. and Sternberg, P. W. (2012). Hormonal signal amplification mediates environmental conditions during development and controls an irreversible commitment to adulthood. *PLoS Biol* 10, e1001306.

Schotta, G., Lachner, M., Sarma, K., Ebert, A., Sengupta, R., Reuter, G., Reinberg, D. and Jenuwein, T. (2004). A silencing pathway to induce H3-K9 and H4-K20 trimethylation at constitutive heterochromatin. *Genes Dev* 18, 1251-1262.

Schroeder, N. E. and Flatt, K. M. (2014). In vivo imaging of Dauer-specific neuronal remodeling in C. elegans. *Journal of visualized experiments : JoVE*, e51834.

Shaner, N. C., Lambert, G. G., Chammas, A., Ni, Y., Cranfill, P. J., Baird, M. A., Sell, B. R., Allen, J. R., Day, R. N., Israelsson, M., et al. (2013). A bright monomeric green fluorescent protein derived from Branchiostoma lanceolatum. *Nat Methods* 10, 407-409.

Southall, S. M., Cronin, N. B. and Wilson, J. R. (2014). A novel route to product specificity in the Suv4-20 family of histone H4K20 methyltransferases. *Nucleic Acids Res* 42, 661-671.

Starich, T. A., Herman, R. K., Kari, C. K., Yeh, W. H., Schackwitz, W. S., Schuyler, M. W., Collet, J., Thomas, J. H. and Riddle, D. L. (1995). Mutations affecting the chemosensory neurons of Caenorhabditis elegans. *Genetics* 139, 171-188.

Thomas, J. H., Birnby, D. A. and Vowels, J. J. (1993). Evidence for parallel processing of sensory information controlling dauer formation in Caenorhabditis elegans. *Genetics* 134, 1105-1117.

Trapnell, C., Hendrickson, D. G., Sauvageau, M., Goff, L., Rinn, J. L. and Pachter, L. (2013). Differential analysis of gene regulation at transcript resolution with RNA-seq. *Nat Biotechnol* 31, 46-53.

Vielle, A., Lang, J., Dong, Y., Ercan, S., Kotwaliwale, C., Rechtsteiner, A., Appert, A., Chen, Q. B., Dose, A., Egelhofer, T., et al. (2012). H4K20me1 contributes to downregulation of X-linked genes for C. elegans dosage compensation. *PLoS Genet* 8, e1002933.

Vowels, J. J. and Thomas, J. H. (1992). Genetic analysis of chemosensory control of dauer formation in Caenorhabditis elegans. *Genetics* 130, 105-123.

---- (1994). Multiple chemosensory defects in daf-11 and daf-21 mutants of Caenorhabditis elegans. *Genetics* 138, 303-316.

Webster, C. M., Wu, L., Douglas, D. and Soukas, A. A. (2013). A non-canonical role for the C. elegans dosage compensation complex in growth and metabolic regulation downstream of TOR complex 2. *Development* 140, 3601-3612.

Wells, M. B., Snyder, M. J., Custer, L. M. and Csankovszki, G. (2012). Caenorhabditis elegans dosage compensation regulates histone H4 chromatin state on X chromosomes. *Mol Cell Biol* 32, 1710-1719.

Wu, H., Siarheyeva, A., Zeng, H., Lam, R., Dong, A., Wu, X. H., Li, Y., Schapira, M., Vedadi, M. and Min, J. (2013). Crystal structures of the human histone H4K20 methyltransferases SUV420H1 and SUV420H2. *FEBS Lett* 587, 3859-3868.

Yonker, S. A. and Meyer, B. J. (2003). Recruitment of C. elegans dosage compensation proteins for gene-specific versus chromosome-wide repression. *Development* 130, 6519-6532.

Chapter 4

Crosstalk between conserved signal transduction pathways mediates developmental plasticity in response to environmental stress

Abstract

Animals have evolved distinct responses to environmental stimuli to maximize their reproductive fitness. In the free-living nematode *Caenorhabditis elegans*, unfavorable conditions and overpopulation lead to animals' entry into an alternative larval state of diapause known as dauer. Population stress is detected through local concentrations of a complex pheromone mixture, but how pheromone triggers downstream signals to coordinate the dauer decision remains poorly understood. Sensory neurons are required to respond to dauer pheromone and are a major source of neuroendocrine ligands including insulin-like peptides (ILPs), which may activate or inhibit the conserved insulin-like signaling pathway (IIS). IIS promotes reproductive development through inhibition of the transcription factor DAF-16/FoxO. We previously reported that epigenetic modifiers SET-4 and DPY-21 promote dauer arrest through repression of the ILP *ins-9*. Loss of SET-4 or DPY-21 also leads to defects in response to dauer pheromone. Here we show that loss of *ins-9* rescues pheromone-induced dauer arrest in *set-4* mutants. *ins-9* is primarily expressed in ASI sensory neurons, and expression of *set-4* solely in ASI is sufficient to rescue dauer arrest. Dauer arrest in response to pheromone requires DAF-16/FoxO, while pheromone represses *ins-9* expression in a DAF-16/FoxO independent manner. INS-9 and DAF-28 promote reproductive development in parallel, indicating that pheromone signaling engages multiple regulatory pathways that converge on DAF-16/FoxO to promote dauer arrest.

Introduction

How organisms use environmental signals to coordinate their own development to compete and cooperate with others of their species is critical for the fitness of a population. In the free-living nematode *Caenorhabditis elegans*, animals progress through four larval stages (L1 through L4) to reach adulthood (Corsi et al., 2015). They sense population density through detection of a continuously elaborated mixture of ascarosides that collectively are referred to dauer pheromone (Golden and Riddle, 1984a; Golden and Riddle, 1984b; Ludewig and Schroeder, 2013). Pheromone perception is integrated with temperature sensation and certain food signals that may include bacterial fatty acids (Kaul et al., 2014) to control developmental strategy at the transition from L1 to L2 (Fielenbach and Antebi, 2008). Under replete conditions, animals commit to reproductive development. In contrast, when population density reaches a critical tipping point, larvae enter an alternate state of diapause known as dauer (Hu, 2007).

Dauers exhibit many gross morphological differences from non-dauer L3 larvae including constriction of the body and pharynx, the presence of longitudinal ridges called alae, and a thickened cuticle (Blaxter, 1993; Cassada and Russell, 1975). Arrested animals also remodel neuromuscular junctions and exhibit increased dendritic branching (Dixon et al., 2008; Schroeder et al., 2013). These morphological changes may contribute to behaviors associated with dispersal from unfavorable environments. The thickening of the cuticle also creates a buccal plug, leading to cessation of feeding and continued reliance on fatty acid metabolism for energy (Popham, 1979; Wadsworth and Riddle, 1989). Dauers are highly stress-resistant and can persist in diapause far longer than typical adults live as they await improving environmental conditions (Klass and Hirsh, 1976). How pheromone sensing drives the metabolic and anatomical changes associated with dauer arrest remains poorly understood.

C. elegans sense environmental cues through amphid sensory neurons that have dendritic projections exposed to the environment. These amphid neurons are required for proper integration of environmental conditions, resulting in the decision on whether to arrest or proceed with reproductive development (Bargmann and Horvitz, 1991; Birnby et al., 2000; Schackwitz et al., 1996). The paired ASI amphid neurons are a source of neuroendocrine ligands for conserved developmental pathways, including the TGFβ-like pathway and the insulin and insulin-like growth factor signaling (IIS) pathway (Cornils et al., 2011; Hung et al., 2014; Pierce et al., 2001;

Ren et al., 1996). Activation of the insulin receptor DAF-2/IGFR induces a PI3Kinase phosphorylation cascade activating the serine/threonine kinase AKT. AKT phosphorylates the Fork head transcription factor DAF-16/FoxO, leading to its export from the nucleus (Brunet et al., 1999; Lee et al., 2001; Lin et al., 2001). DAF-16/FoxO is a master regulator of stress responses and maintenance of homeostasis and is required for the highly penetrant dauer-constitutive (daf-c) phenotype observed in reduced insulin-signaling mutant animals (Gottlieb and Ruvkun, 1994; Lin et al., 1997; Ogg et al., 1997).

The interaction of pheromone sensing and genetic pathways implicated in promoting reproductive development is complex. Pheromone is known to enhance the *daf-c* phenotype of TGFβ pathway mutants at permissive temperatures (Thomas et al., 1993). Further, pheromone down-regulates expression of the *daf-7*/ TGFβ-like ligand (Ren et al., 1996; Schackwitz et al., 1996). Whether DAF-16/FoxO is required for dauer arrest induced by population stress is less clear. Strains expressing different mutant alleles of *daf-16* showed variable response to dauer pheromone in liquid culture (Gottlieb and Ruvkun, 1994). These animals demonstrated abnormal tissue remodeling as compared to wild type dauers (Vowels and Thomas, 1992).

Insulin-like peptides (ILPs) serve as the ligands for DAF-2/IGFR. *C. elegans* possesses 40 known ILPs with diverse structures and activities (Li et al., 2003; Pierce et al., 2001) For example, DAF-28, INS-4 and INS-6 activate DAF-2/IGFR while INS-1 and INS-18 are believed to be DAF-2 antagonists (Cornils et al., 2011; Hung et al., 2014; Li et al., 2003; Pierce et al., 2001). Many ILPs are synthesized in ASI and may act to coordinate morphological changes in response to environmental conditions at the organismal level (Gruner et al., 2016; Murphy et al., 2007). Attempts have been made to understand the complex interaction(s) of ILPs in development and longevity (Artan et al., 2016; Chen and Baugh, 2014; Fernandes de Abreu et al., 2014); however, contributions of individual ILPs to developmental decisions remain difficult to define using genetics due to functional redundancy and overlapping temporospatial expression patterns (Chen and Baugh, 2014; Pierce et al., 2001; Ritter et al., 2013). Interestingly, certain ILPs expressed in ASI, including DAF-28 and INS-6, have been shown to be responsive to pheromone through an unknown mechanism (Cornils et al., 2011; Li et al., 2003).

We previously demonstrated that the conserved epigenetic regulators DPY-21 and SET-4 promote dauer arrest in response to pheromone and reduced insulin signaling through the

inhibition of INS-9, an incompletely characterized type B ILP expressed primarily in ASI (Delaney et al., 2017). Here we expand our understanding of how pheromone regulates insulin-like signaling and find that *ins-9* is required for dauer bypass in *set-4* mutants, while SET-4 activity in ASI is sufficient to rescue dauer arrest in animals with reduced insulin-like signaling. We show that pheromone-induced dauer arrest requires DAF-16/FoxO. We demonstrate that *ins-9* expression is sensitive to pheromone like other type β ILPs. Pheromone regulates *ins-9* expression itself in a DAF-16/FoxO independent manner. These findings suggest crosstalk between multiple pathways converges on ILP production to control developmental fate in response to population stress.

Results

ins-9 expression in ASI sensory neurons promotes reproductive development

Having previously identified *ins-9* as an X-linked DAF-2/IGFR agonist subject to SET-4 and DPY-21 mediated suppression (Delaney et al., 2017), we asked whether INS-9 was required for the observed defect in dauer formation in response to pheromone in *set-4* mutants. Loss of *ins-9* rescued pheromone-induced dauer arrest in *set-4* animals and enhanced response to pheromone relative to wild type siblings (Fig. 4.1A). *akt-2* was not required for this enhancement of dauer arrest in *set-4* animals (data not shown). This result implicates *ins-9* in promoting reproductive development in replete environments.

INS-9 transgenes were expressed in ASI sensory neurons, which are critical for dauer arrest (Bargmann and Horvitz, 1991; Chen and Baugh, 2014; Pierce et al., 2001). We previously showed the histone methyltransferase SET-4 acts in neurons to promote dauer arrest at least in part through silencing of *ins-9* (Delaney et al., 2017). If SET-4 in ASI is important for dauer regulation, we reasoned that restoring expression of *set-4* in ASI alone should be sufficient to rescue the dauer-defective phenotype caused by *set-4* mutation. We used CRISPR-Cas9 to replace the native *set-4* promoter with the ASI-specific *gpa-4* promoter upstream of the endogenous *set-4* locus (Fig. 4.S1, (Jansen et al., 1999). After outcrossing the resulting *gpa-4p::set-4(dp682)* allele, we found that animals with reduced IIS expressing *set-4* exclusively in ASI underwent dauer arrest at levels comparable to animals expressing *set-4* driven by its native

promoter, and at a significantly greater rate than *set-4* null siblings (Fig. 4.1B). These findings suggest SET-4 promotes dauer arrest in ASI neurons, consistent with its role in repressing *ins-9* expression.

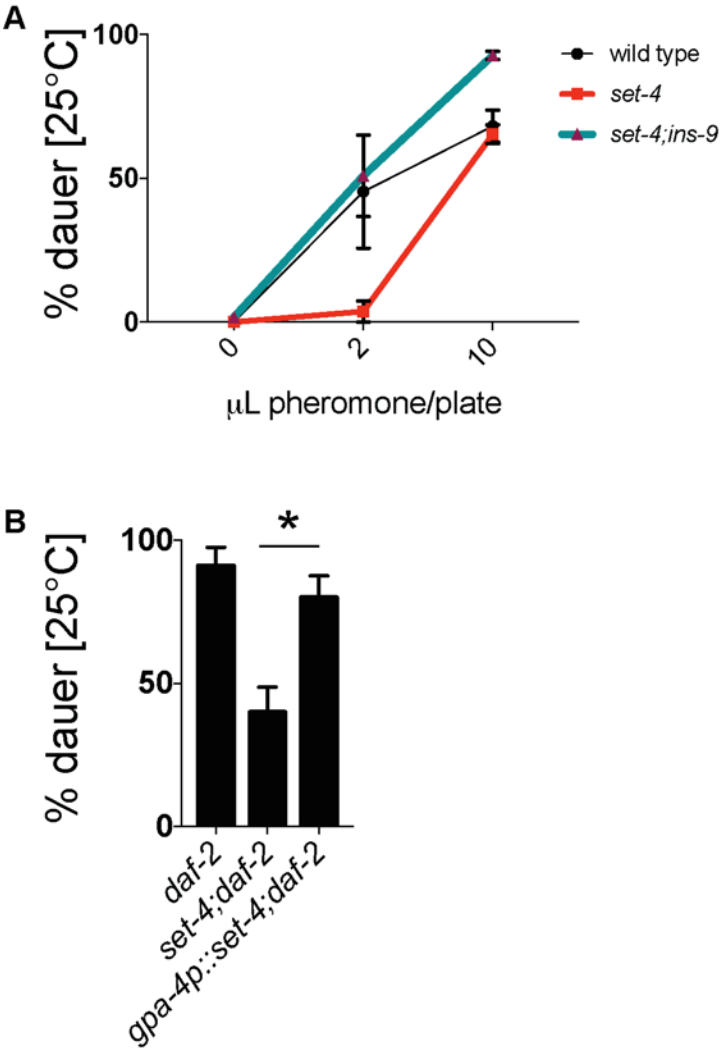

Figure 4.1. SET-4 promotes dauer arrest in ASI sensory neurons upstream of INS-9. (A) Loss of *ins-9* rescues dauer arrest in *set-4* mutants in response to dauer pheromone. Results are the mean and s.e.m. of one experiment performed in duplicate. N (0uL, 2uL, 10uL): wild type = 43, 95, 252; *set-4* =38, 41, 110; *set-4;ins-9* = 119, 70, 57. **(B)** *set-4* expression in ASI specifically is sufficient for dauer arrest. Results are the mean and s.e.m. of 3 experiments. N = 349, 896, 721. *p<0.05

DAF-16 is required for pheromone-induced dauer arrest

Upregulation of *ins-9* expression is predicted to activate DAF-2/IGFR that then inhibits DAF-16/FoxO, promoting reproductive development. Further, DAF-16 is required for silencing of *ins-9* (Delaney et al., 2017). Therefore, we speculated that pheromone-induced dauer arrest may be DAF-16 dependent. Previous results addressing this question were equivocal, owing to modest arrest rates observed in wild type controls (Gottlieb and Ruvkun, 1994; Ogg et al., 1997). We found animals lacking *daf-16* to be far less responsive to dauer pheromone than their wild type siblings (Fig 4.2). Loss of *ins-9* did not rescue this defect in *daf-16* mutants, placing DAF-16/FoxO downstream of *ins-9* expression. These results are consistent with the empirically deduced logic of the insulin-like signaling pathway and suggest that population stress induces dauer arrest in a manner requiring DAF-16 as well as silencing of *ins-9* in ASI sensory neurons.

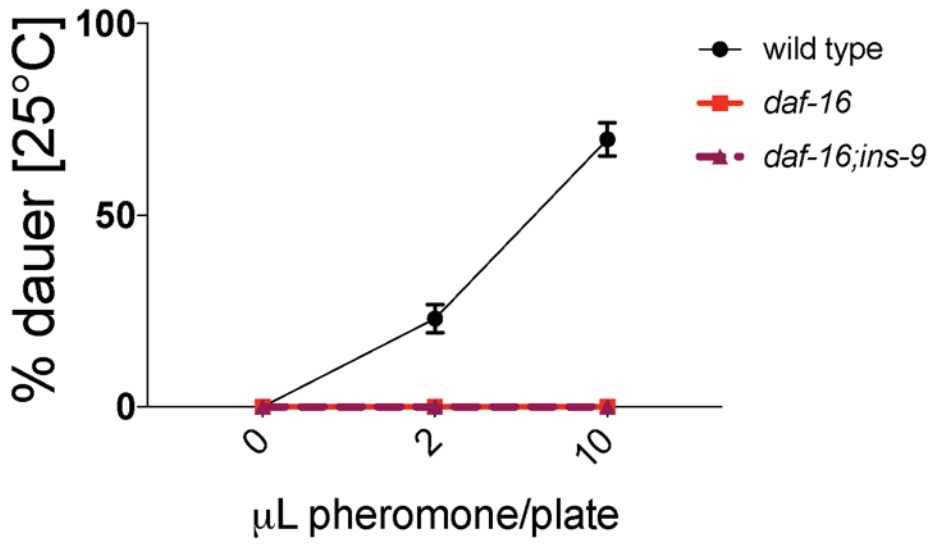

Figure 4.2. DAF-16 is required for response to dauer pheromone. Results are the mean and s.e.m. of one experiment performed in duplicate. N (0uL, 2uL, 10uL): wild type = 168, 183, 253; *daf-16* =179, 191, 141; *daf-16;ins-9* = 171, 170, 127.

ins-9 expression is controlled by dauer pheromone in parallel with DAF-16

To better understand how *ins-9* expression is regulated, we created an single-copy reporter for *ins-9* expression, using CRISPR-Cas9 to insert the operon-like *gpd-2* SL2 sequence coupled to mNeonGreen into the endogenous *ins-9* locus immediately after the stop codon (Blumenthal, 2012; Shaner et al., 2013). The *ins-9::sl2::mNeonGreen(dp690)* reporter allele (henceforth referred to as the *ins-9* reporter) allows the *in vivo* monitoring of expression dynamically via green fluorescence without disrupting *ins-9* activity. Expression was detectable from late L2 to adulthood. Previous reports using extrachromosomal arrays demonstrated that *ins-9* is primarily expressed in ASI with some expression reported in ASJ. Both ASI and ASJ are paired sensory neurons implicated in regulating dauer arrest (Delaney et al., 2017; Pierce et al., 2001). Using the *ins-9* reporter we consistently observed two neurons expressing mNeonGreen; however, sporadically we observed green fluorescence in a third neuron (Fig 4.3A).

Since we observed that *ins-9* expression promotes reproductive development in the context of pheromone or reduced insulin signaling (Delaney et al., 2017), Fig 4.1), we used the *ins-9* reporter to test whether *ins-9* expression itself is regulated by pheromone. Growing reporter animals in the presence of pheromone was sufficient to silence the reporter (Fig 4.3B). Notably, this silencing was independent of DAF-16, as loss of *daf-16* did not rescue mNeonGreen expression in the presence of pheromone. Therefore, it is likely that multiple pathways control *ins-9* expression, including one downstream of dauer pheromone.

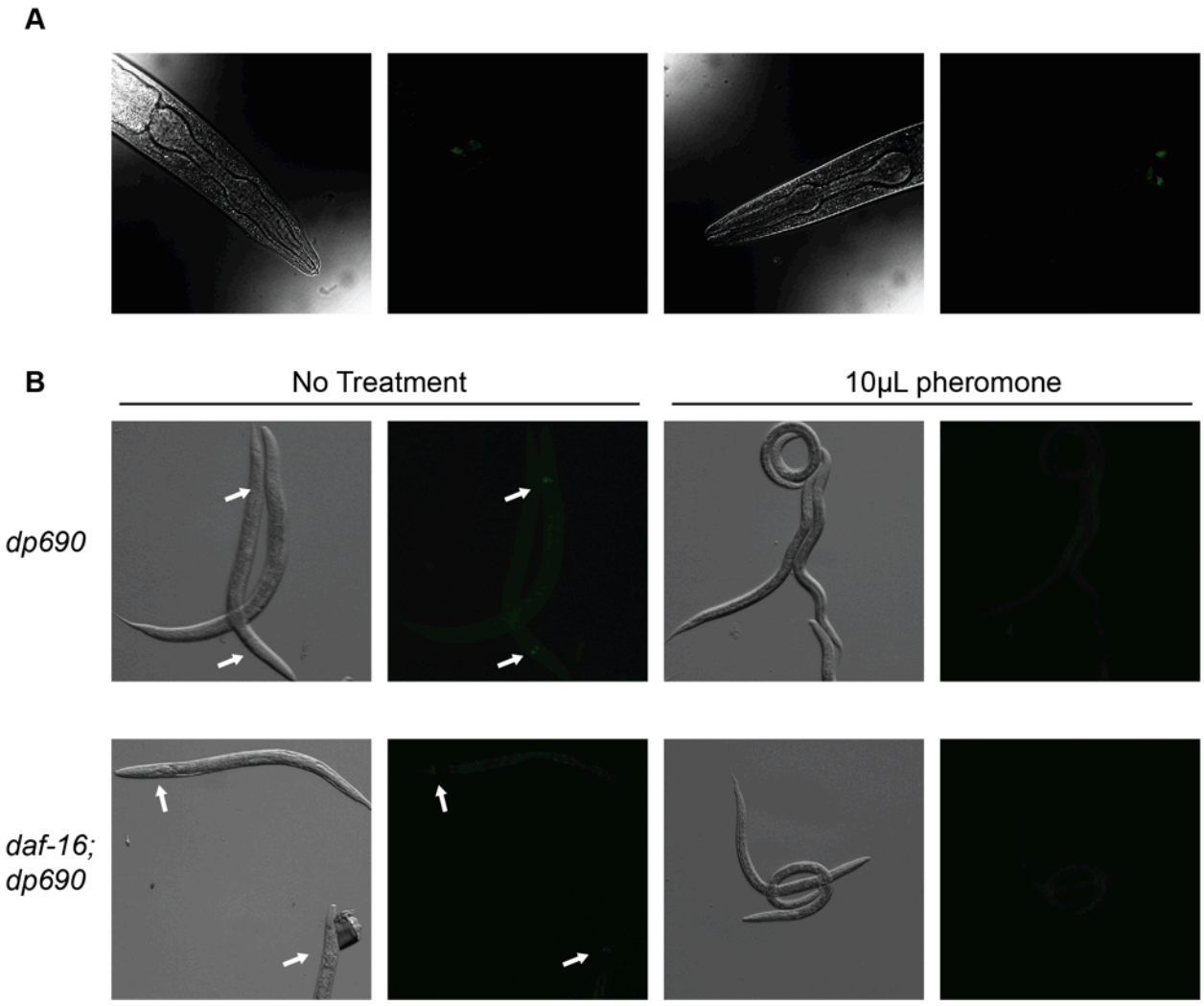

Figure 4.3. *ins-9* is expressed in ASI sensory neurons. (A) Representative images of the single-copy, endogenous locus *ins-9::sl2::mNeonGreen(dp690)* reporter. L4 animals shown. N = 21. (B) *ins-9* reporter animals and daf-16;dp690 animals in the absence and presence of dauer pheromone. Arrows indicate green neurons. N(no treatment) = 12, 13; N(pheromone) = 21, 11.

Pheromone regulates multiple insulin-like peptides in parallel

Previous reports suggest that a major ILP, *daf-28*, is expressed in ASI neurons and is repressed by dauer pheromone. *daf-28* loss of function mutants exhibit low dauer penetrance at 25°C, but *daf-28* mutation in combination with loss of *ins-4*, *ins-5*, and *ins-6*, causes penetrant dauer arrest (Hung et al., 2014). Given that both *ins-9* and *daf-28* are responsive to dauer pheromone, we tested whether *ins-9* augmented *daf-28* dauer arrest like other ILPs. We found a modest but significant increase in dauer arrest in *daf-28;ins-9* animals over *daf-28* single mutants (Fig 4.4). Therefore, these insulins may be regulated in parallel despite both being regulated by pheromone signaling (Li et al., 2003). This is consistent with previous observations that DAF-7/TGF-B-like signaling controls *daf-28* expression while *ins-9* expression is DAF-16/FoxO dependent (Delaney et al., 2017; Honda et al., 2011).

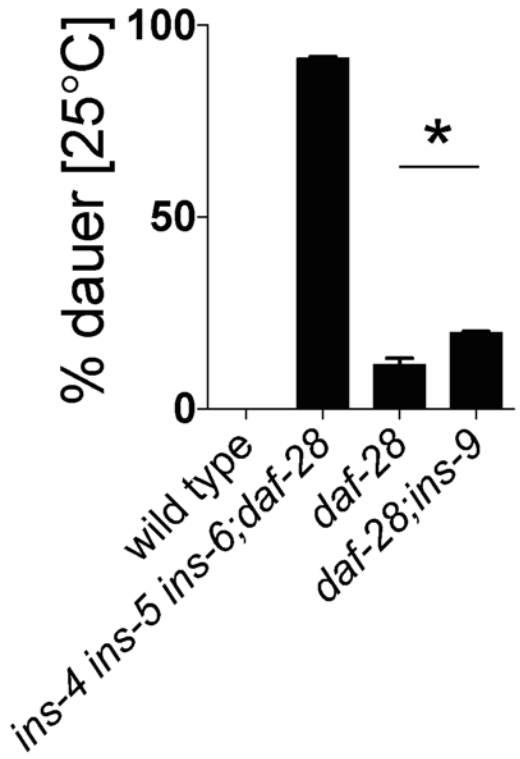

Figure 4.4. *ins-9* acts in parallel with *daf-28*. Results are the mean and s.e.m. of 3 experiments. N = 688, 697, 1018, 792. *p<0.05

Discussion

In the present study we expand on how pheromone signaling mediates developmental strategy through insulin-like signaling. Not only is population stress sufficient to suppress DAF-2/IGFR agonists *daf-28* and *ins-6* (Cornils et al., 2011; Li et al., 2003) but also *ins-9* (Fig. 4.3). Similarly, DAF-16/FoxO is required for diapause in response to dauer pheromone and acts downstream of *ins-9* (Fig. 4.2). We strengthen the evidence that *ins-9* expression promotes reproductive development. We demonstrate that SET-4 activity in ASI, where *ins-9* is expressed, is sufficient for dauer arrest in reduced insulin signaling mutants. We establish that pheromone silences *ins-9* expression in parallel with DAF-16. Taken together with previous findings, these data suggest that multiple inputs converge on insulin-like peptide expression to promote dauer arrest under conditions of perceived population stress.

Animals' perception of their environment dictates which developmental strategy is most appropriate. In *C. elegans*, amphid sensory neuron processes are directly exposed to their environment to sense population density, presence of food, and temperature (Golden and Riddle, 1984a). These environmental cues regulate TGFβ and IIS signaling cascades through mechanisms that remain incompletely understood (Hu, 2007). These inputs converge on the synthesis of steroid hormones known as dafachronic acids (DAs) that promote reproductive development (Gerisch and Antebi, 2004). DA ligands the DAF-12 bile acid-like receptor, which then drives forward reproductive development (Antebi et al., 2000). Dauer pheromone antagonizes DA signaling by repressing *daf-9* expression in the hypodermis that is associated with the commitment to reproductive development. (Schaedel et al., 2012).

The bilaterally paired amphid neuron ASI is known to be a critical regulator of dauer arrest (Ailion and Thomas, 2000; Bargmann and Horvitz, 1991). ASI is the primary site of synthesis of the TGFβ-like DAF-7 (Meisel et al., 2014; Ren et al., 1996; Schackwitz et al., 1996) and is also a primary source for ILP production, including DAF-2 agonists INS-4, INS-6, DAF-28, and INS-9, as well as antagonists INS-1 and INS-18 (Hung et al., 2014; Pierce et al., 2001). Interestingly, unlike *ins-9*, *daf-28* production is independent of DAF-16; rather, *daf-28* is directly dependent on DAF-7/TGFβ, revealing creating crosstalk between the TGFβ and IIS pathways (Li et al., 2003). As a result, in reduced insulin signaling mutants undergoing dauer arrest, *daf-28* expression remains high, arguing that *daf-28* expression may not be sufficient for dauer bypass.

DAF-28 is the only type-β ILP to demonstrate a dauer phenotype as a loss-of-function mutant (Hung et al., 2014). Mutating one of the several putative agonist ILPs in combination with *daf-28* loss of function modestly augments dauer arrest (Hung et al., 2014). However, no findings were reported regarding *ins-9*. While nonsense alleles of *ins-9* have no dauer phenotype, similar to *ins-2* through *ins-8*, we find that loss of *ins-9* increased dauer arrest in *daf-28* mutants to a similar degree as reported for *daf-28* in combination with either *ins-4* or *ins-6* (Fig. 4.4) (Hung et al., 2014). Hung et al. argue that INS-4, INS-6 and DAF-28 promote reproductive development by activating DAF-2 in the intestine, which then relays signals to increase dafachronic acid synthesis. *ins-9* expression, on the other hand, may be regulated in a feed-forward loop within ASI (Delaney et al., 2017), like the DAF-2/IGFR agonist *ins-7* in the intestine (Murphy et al., 2007) and the antagonist *ins-18* in neurons (Matsunaga et al., 2012). Expression of both *daf-28* and *ins-9* is inhibited in the presence of high concentrations of dauer pheromone (Fig. 4.3) (Li et al., 2003). Therefore, multiple signaling networks work in concert and in response to pheromone detection in ASI to coordinate developmental strategy in larvae. Which additional pathways mediate the response of ILPs to pheromone remains to be elucidated.

We have demonstrated that INS-9 is regulated from downstream by DAF-16/FoxO and upstream by pheromone and the epigenetic regulators DPY-21 and SET-4 (Fig. 4.3) (Delaney et al., 2017; Dumas et al.). However, SET-4 and DPY-21 inhibit multiple insulin signaling genes to promote dauer arrest, including neuronally expressed *akt-2* and, possibly indirectly, the ASI- and intestine-expressed *ins-7* (Murphy et al., 2007; Paradis and Ruvkun, 1998). We show that SET-4 acts in ASI to promote dauer arrest (Fig. 4.1B). Given that loss of *ins-9* rescues the dauer-defective phenotype of *set-4* mutants, it is likely that SET-4 promotes dauer arrest in ASI primarily through inhibiting *ins-9*. However, that does not exclude SET-4 acting through inhibition of other IIS genes as well. Similarly, our data places DAF-16 downstream of INS-9 in the dauer decision, but whether DAF-16 is necessary in ASI or whether it acts in downstream tissues like the intestine to coordinate the organismal commitment to dauer remain unclear (Hung et al., 2014; Libina et al., 2003).

Crude pheromone extract has previously been demonstrated to extend longevity of adult animals, and this lifespan extension is dependent on DAF-16/FoxO, implicating that pheromone regulates insulin-like signaling (Kawano et al., 2005; Ludewig et al., 2013). Interestingly, specific

ascarosides present in dauer pheromone extend lifespan in a manner requiring the histone H4 lysine 16 deacetylase SIR-2.1 (Ludewig et al., 2013). H4K16 deacetylation has been reported to promote the establishment of H4K20 trimethylation in mammalian cells (Sarg et al., 2002; Serrano et al., 2013). SET-4 promotes dauer arrest and is required for higher order H4K20 methylation (Delaney et al., 2017; Vielle et al., 2012; Wells et al., 2012). These data are consistent with a model where pheromone may exert its effects through conserved epigenetic regulation of gene expression.

Surprisingly, whether DAF-16/FoxO is required for response to pheromone was unresolved (Gottlieb and Ruvkun, 1994; Ogg and Ruvkun, 1998). We demonstrate that pheromone induced dauer arrest is indeed DAF-16/FoxO dependent (Fig. 4.2). These findings are consistent with pheromone-sensitive ILPs including INS-9 regulating DAF-16/FoxO and more broadly with dauer arrest in *C. elegans* larvae being a useful surrogate for DAF-16/FoxO mediated longevity.

Reduced insulin signaling in metazoans leads to long life (Bluher et al., 2003; Kenyon et al., 1993; Yamamoto and Tatar, 2011). In *C. elegans*, this increased longevity is due in part to downregulation of ILP production (Artan et al., 2016), and is accompanied by a decrease in translation in muscle tissue without compromising muscle mass (Depuydt et al., 2013). Similarly, mammals experiencing reduced insulin-like signaling are long lived and show decreased translation in skeletal muscle in a cell-nonautonomous fashion, suggesting a role for insulin-like growth factor signaling in regulation of tissue homeostasis (Essers et al., 2016). Further, axonal degeneration is delayed or prevented when animals pass through dauer diapause in a manner dependent on increased DAF-16/FoxO activity (Calixto et al., 2012). Therefore, continuing to develop our understanding of conserved mechanisms of insulin-like peptidergic signaling may lead to insights leading to increased years of life free from age-associated diseases like frailty, cancer, diabetes, and dementia.

Materials and Methods

Strains and maintenance.

The following strains were used in this study: *daf-16(mu86)*, *ins-9(dp677)*, *set-4(n4600)*, *akt-2(ok393)*, and *daf-28(tm2804)*. Some strains were provided by the CGC, which is funded by NIH Office of Research Infrastructure Programs (P40 OD010440).

Dauer induction assays

Gravid adults were transferred to fresh NGM plates to lay eggs. Egg layers were then removed and embryos were transferred to 25°C. After 54-60 hr, progeny were scored as dauer or not dauer (i.e. L4/young adult).

Generation of transgenic strains.

CRISPR genome editing was performed using custom crRNA and tracrRNA (Dharmacon) and recombinant Cas9 (PNA Bio) as described (Paix et al., 2015). HDR amplicons were generated by overlap PCR (8 reactions per amplicon in 100 µL reaction volume), purified individually with GeneJet PCR purification columns (Invitrogen), eluted and combined in Buffer QF (Qiagen), precipitated using 0.7 volumes of isopropanol, and resuspended in 10 µL of water. *gpa-4p::set-4(dp682)* was made by targeting the *set-4(n4600)* locus using the crRNA guide sequence 5'-GUAUCUGACUGCGCAUCAUG-3' that overlaps both ends of the *n4600* deletion. The HDR amplicon contained the 1.4 kb upstream of *gpa-4* fused to the 633 bp of *set-4* genomic sequence absent in the *n4600* deletion. For *ins-9::sl2::mNeonGreen(dp690)*, the intergenic sequence between *gpd-2* and *gpd-3* was fused to *mNeonGreen* derived from pDD268 (Dickinson2013). This repair amplicon was inserted between the *ins-9* stop codon and *ins-9* 3' UTR using the crRNA guide sequence 5'-GGUGCCGACAAAUUGUAACC-3'.

Pheromone assays

Crude pheromone extracts were prepared as described (Delaney et al., 2017), with the exception that evaporation steps were carried out using a Savant SC210A SpeedVac Plus with RVT4104 refrigerated vapor trap (Thermo). Effective doses were determined empirically. 500 µL of water containing the indicated volume of pheromone extract were added to 2mL NGM lacking peptone made with Noble Agar (BD) and containing 30 µg/mL streptomycin in 35 mm dishes. 20 µL 6X live OP50 resuspended in S Basal was spotted onto dried plates. Gravid adults were transferred to these plates to lay eggs. After removing egg layers, eggs were transferred to 25°C and scored as dauer or not dauer after 84 hr.

Fluorescence microscopy

Animals were mounted on a 2% agar pad slide and immobilized in a drop of 25mM sodium azide. Detection of green fluorescence was imaged using a Leica M165FC microscope with a (Leica) DFC9000 GT camera and a Lumencor sola light engine fluorescence lamp. Confocal images were acquired using a Leica Inverted SP5X Confocal Microscope (Leica) and LAS AF software.

Supplementary Information

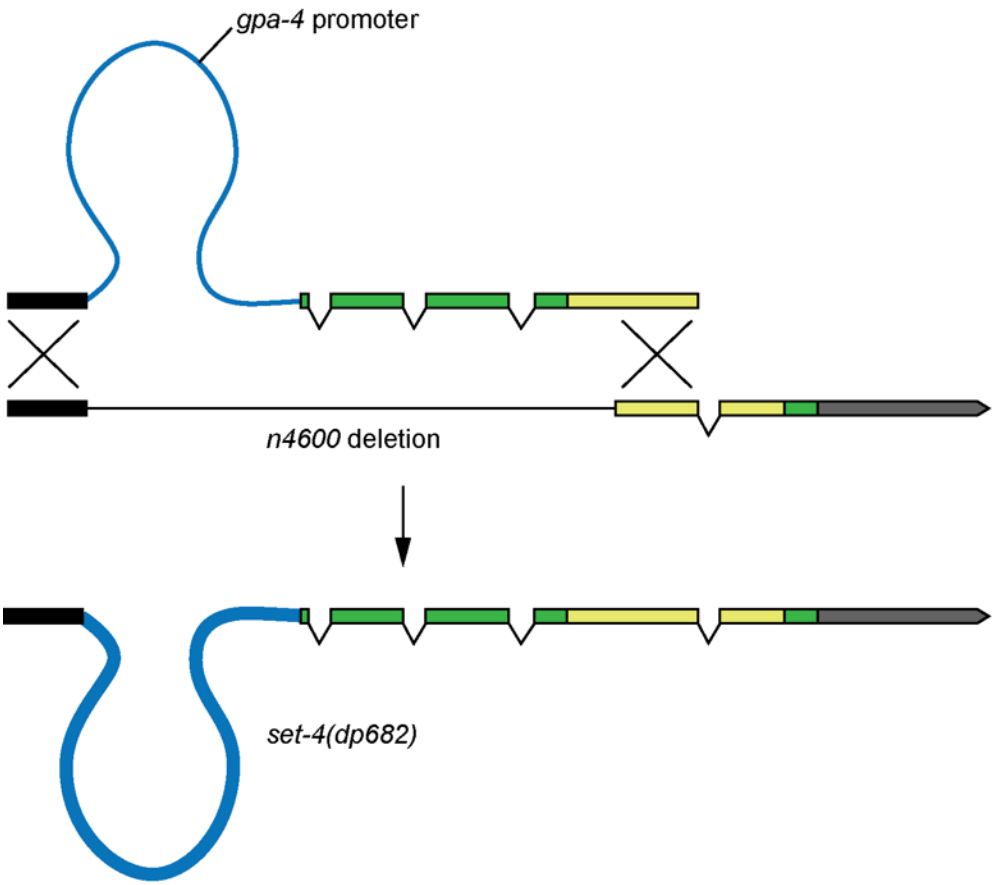

Supplemental Figure 4.S1. Construction of ASI-specific *set-4(dp682)* allele.

References

Ailion, M. and Thomas, J. H. (2000). Dauer formation induced by high temperatures in Caenorhabditis elegans. *Genetics* 156, 1047-1067.

Antebi, A., Yeh, W. H., Tait, D., Hedgecock, E. M. and Riddle, D. L. (2000). daf-12 encodes a nuclear receptor that regulates the dauer diapause and developmental age in C. elegans. *Genes Dev* 14, 1512-1527.

Artan, M., Jeong, D. E., Lee, D., Kim, Y. I., Son, H. G., Husain, Z., Kim, J., Altintas, O., Kim, K., Alcedo, J., et al. (2016). Food-derived sensory cues modulate longevity via distinct neuroendocrine insulin-like peptides. *Genes Dev* 30, 1047-1057.

Bargmann, C. I. and Horvitz, H. R. (1991). Control of larval development by chemosensory neurons in Caenorhabditis elegans. *Science* 251, 1243-1246.

Birnby, D. A., Link, E. M., Vowels, J. J., Tian, H., Colacurcio, P. L. and Thomas, J. H. (2000). A transmembrane guanylyl cyclase (DAF-11) and Hsp90 (DAF-21) regulate a common set of chemosensory behaviors in caenorhabditis elegans. *Genetics* 155, 85-104.

Blaxter, M. L. (1993). Cuticle surface proteins of wild type and mutant Caenorhabditis elegans. *J Biol Chem* 268, 6600-6609.

Bluher, M., Kahn, B. B. and Kahn, C. R. (2003). Extended longevity in mice lacking the insulin receptor in adipose tissue. *Science* 299, 572-574.

Blumenthal, T. (2012). Trans-splicing and operons in C. elegans. *WormBook*, 1-11.

Brunet, A., Bonni, A., Zigmond, M. J., Lin, M. Z., Juo, P., Hu, L. S., Anderson, M. J., Arden, K. C., Blenis, J. and Greenberg, M. E. (1999). Akt promotes cell survival by phosphorylating and inhibiting a Forkhead transcription factor. *Cell* 96, 857-868.

Calixto, A., Jara, J. S. and Court, F. A. (2012). Diapause formation and downregulation of insulin-like signaling via DAF-16/FOXO delays axonal degeneration and neuronal loss. *PLoS Genet* 8, e1003141.

Cassada, R. C. and Russell, R. L. (1975). The dauerlarva, a post-embryonic developmental variant of the nematode Caenorhabditis elegans. *Dev Biol* 46, 326-342.

Chen, Y. and Baugh, L. R. (2014). Ins-4 and daf-28 function redundantly to regulate C. elegans L1 arrest. *Dev Biol* 394, 314-326.

Cornils, A., Gloeck, M., Chen, Z., Zhang, Y. and Alcedo, J. (2011). Specific insulin-like peptides encode sensory information to regulate distinct developmental processes. *Development* 138, 1183-1193.

Corsi, A. K., Wightman, B. and Chalfie, M. (2015). A Transparent window into biology: A primer on Caenorhabditis elegans. *WormBook*, 1-31.

Delaney, C. E., Chen, A. T., Graniel, J. V., Dumas, K. J. and Hu, P. J. (2017). A histone H4 lysine 20 methyltransferase couples environmental cues to sensory neuron control of developmental plasticity. *Development*.

Depuydt, G., Xie, F., Petyuk, V. A., Shanmugam, N., Smolders, A., Dhondt, I., Brewer, H. M., Camp, D. G., 2nd, Smith, R. D. and Braeckman, B. P. (2013). Reduced insulin/insulin-like growth factor-1 signaling and dietary restriction inhibit translation but preserve muscle mass in Caenorhabditis elegans. *Mol Cell Proteomics* 12, 3624-3639.

Dixon, S. J., Alexander, M., Chan, K. K. and Roy, P. J. (2008). Insulin-like signaling negatively regulates muscle arm extension through DAF-12 in Caenorhabditis elegans. *Dev Biol* 318, 153-161.

Dumas, K. J., Delaney, C. E., Flibotte, S., Moerman, D. G., Csankovszki, G. and Hu, P. J. Unexpected Role for Dosage Compensation in the Control of Dauer Arrest, Insulin-Like Signaling, and FoxO Transcription Factor Activity in Caenorhabditis elegans. *Genetics*.

Essers, P., Tain, L. S., Nespital, T., Goncalves, J., Froehlich, J. and Partridge, L. (2016). Reduced insulin/insulin-like growth factor signaling decreases translation in Drosophila and mice. *Sci Rep* 6, 30290.

Fernandes de Abreu, D. A., Caballero, A., Fardel, P., Stroustrup, N., Chen, Z., Lee, K., Keyes, W. D., Nash, Z. M., Lopez-Moyado, I. F., Vaggi, F., et al. (2014). An insulin-to-insulin regulatory network orchestrates phenotypic specificity in development and physiology. *PLoS Genet* 10, e1004225.

Fielenbach, N. and Antebi, A. (2008). C. elegans dauer formation and the molecular basis of plasticity. *Genes Dev* 22, 2149-2165.

Gerisch, B. and Antebi, A. (2004). Hormonal signals produced by DAF-9/cytochrome P450 regulate C. elegans dauer diapause in response to environmental cues. *Development* 131, 1765-1776.

Golden, J. W. and Riddle, D. L. (1984a). ACaenorhabditis elegans dauer-inducing pheromone and an antagonistic component of the food supply. *J Chem Ecol* 10, 1265-1280.

---- (1984b). The Caenorhabditis elegans dauer larva: developmental effects of pheromone, food, and temperature. *Dev Biol* 102, 368-378.

Gottlieb, S. and Ruvkun, G. (1994). daf-2, daf-16 and daf-23: genetically interacting genes controlling Dauer formation in Caenorhabditis elegans. *Genetics* 137, 107-120.

Gruner, M., Grubbs, J., McDonagh, A., Valdes, D., Winbush, A. and van der Linden, A. M. (2016). Cell-Autonomous and Non-Cell-Autonomous Regulation of a Feeding State-Dependent Chemoreceptor Gene via MEF-2 and bHLH Transcription Factors. *PLoS Genet* 12, e1006237.

Honda, Y., Fujita, Y., Maruyama, H., Araki, Y., Ichihara, K., Sato, A., Kojima, T., Tanaka, M., Nozawa, Y., Ito, M., et al. (2011). Lifespan-extending effects of royal jelly and its related substances on the nematode Caenorhabditis elegans. *PLoS One* 6, e23527.

Hu, P. J. (2007). Dauer. *WormBook*, 1-19.

Hung, W. L., Wang, Y., Chitturi, J. and Zhen, M. (2014). A Caenorhabditis elegans developmental decision requires insulin signaling-mediated neuron-intestine communication. *Development* 141, 1767-1779.

Jansen, G., Thijssen, K. L., Werner, P., van der Horst, M., Hazendonk, E. and Plasterk, R. H. (1999). The complete family of genes encoding G proteins of Caenorhabditis elegans. *Nat Genet* 21, 414-419.

Kaul, T. K., Reis Rodrigues, P., Ogungbe, I. V., Kapahi, P. and Gill, M. S. (2014). Bacterial fatty acids enhance recovery from the dauer larva in Caenorhabditis elegans. *PLoS One* 9, e86979.

Kawano, T., Kataoka, N., Abe, S., Ohtani, M., Honda, Y., Honda, S. and Kimura, Y. (2005). Lifespan extending activity of substances secreted by the nematode Caenorhabditis elegans that include the dauer-inducing pheromone. *Biosci Biotechnol Biochem* 69, 2479-2481.

Kenyon, C., Chang, J., Gensch, E., Rudner, A. and Tabtiang, R. (1993). A C. elegans mutant that lives twice as long as wild type. *Nature* 366, 461-464.

Klass, M. and Hirsh, D. (1976). Non-ageing developmental variant of Caenorhabditis elegans. *Nature* 260, 523-525.

Lee, R. Y., Hench, J. and Ruvkun, G. (2001). Regulation of C. elegans DAF-16 and its human ortholog FKHRL1 by the daf-2 insulin-like signaling pathway. *Curr Biol* 11, 1950-1957.
Li, W., Kennedy, S. G. and Ruvkun, G. (2003). daf-28 encodes a C. elegans insulin superfamily member that is regulated by environmental cues and acts in the DAF-2 signaling pathway. *Genes Dev* 17, 844-858.
Libina, N., Berman, J. R. and Kenyon, C. (2003). Tissue-specific activities of C. elegans DAF-16 in the regulation of lifespan. *Cell* 115, 489-502.
Lin, K., Dorman, J. B., Rodan, A. and Kenyon, C. (1997). daf-16: An HNF-3/forkhead family member that can function to double the life-span of Caenorhabditis elegans. *Science* 278, 1319-1322.
Lin, K., Hsin, H., Libina, N. and Kenyon, C. (2001). Regulation of the Caenorhabditis elegans longevity protein DAF-16 by insulin/IGF-1 and germline signaling. *Nat Genet* 28, 139-145.
Ludewig, A. H., Izrayelit, Y., Park, D., Malik, R. U., Zimmermann, A., Mahanti, P., Fox, B. W., Bethke, A., Doering, F., Riddle, D. L., et al. (2013). Pheromone sensing regulates Caenorhabditis elegans lifespan and stress resistance via the deacetylase SIR-2.1. *Proc Natl Acad Sci U S A* 110, 5522-5527.
Ludewig, A. H. and Schroeder, F. C. (2013). Ascaroside signaling in C. elegans. *WormBook*, 1-22.
Matsunaga, Y., Gengyo-Ando, K., Mitani, S., Iwasaki, T. and Kawano, T. (2012). Physiological function, expression pattern, and transcriptional regulation of a Caenorhabditis elegans insulin-like peptide, INS-18. *Biochem Biophys Res Commun* 423, 478-483.
Meisel, J. D., Panda, O., Mahanti, P., Schroeder, F. C. and Kim, D. H. (2014). Chemosensation of bacterial secondary metabolites modulates neuroendocrine signaling and behavior of C. elegans. *Cell* 159, 267-280.
Murphy, C. T., Lee, S. J. and Kenyon, C. (2007). Tissue entrainment by feedback regulation of insulin gene expression in the endoderm of Caenorhabditis elegans. *Proc Natl Acad Sci U S A* 104, 19046-19050.
Ogg, S., Paradis, S., Gottlieb, S., Patterson, G. I., Lee, L., Tissenbaum, H. A. and Ruvkun, G. (1997). The Fork head transcription factor DAF-16 transduces insulin-like metabolic and longevity signals in C. elegans. *Nature* 389, 994-999.
Ogg, S. and Ruvkun, G. (1998). The C. elegans PTEN homolog, DAF-18, acts in the insulin receptor-like metabolic signaling pathway. *Mol Cell* 2, 887-893.
Paix, A., Folkmann, A., Rasoloson, D. and Seydoux, G. (2015). High Efficiency, Homology-Directed Genome Editing in Caenorhabditis elegans Using CRISPR-Cas9 Ribonucleoprotein Complexes. *Genetics* 201, 47-54.
Paradis, S. and Ruvkun, G. (1998). Caenorhabditis elegans Akt/PKB transduces insulin receptor-like signals from AGE-1 PI3 kinase to the DAF-16 transcription factor. *Genes Dev* 12, 2488-2498.
Pierce, S. B., Costa, M., Wisotzkey, R., Devadhar, S., Homburger, S. A., Buchman, A. R., Ferguson, K. C., Heller, J., Platt, D. M., Pasquinelli, A. A., et al. (2001). Regulation of DAF-2 receptor signaling by human insulin and ins-1, a member of the unusually large and diverse C. elegans insulin gene family. *Genes Dev* 15, 672-686.
Popham, R. E. (1979). Psychocultural barriers to successful alcoholism therapy in an American Indian patient. The relevance of Hallowell's analysis. *J Stud Alcohol* 40, 656-676.

Ren, P., Lim, C. S., Johnsen, R., Albert, P. S., Pilgrim, D. and Riddle, D. L. (1996). Control of C. elegans larval development by neuronal expression of a TGF-beta homolog. *Science* 274, 1389-1391.

Ritter, A. D., Shen, Y., Fuxman Bass, J., Jeyaraj, S., Deplancke, B., Mukhopadhyay, A., Xu, J., Driscoll, M., Tissenbaum, H. A. and Walhout, A. J. (2013). Complex expression dynamics and robustness in C. elegans insulin networks. *Genome Res* 23, 954-965.

Sarg, B., Koutzamani, E., Helliger, W., Rundquist, I. and Lindner, H. H. (2002). Postsynthetic trimethylation of histone H4 at lysine 20 in mammalian tissues is associated with aging. *J Biol Chem* 277, 39195-39201.

Schackwitz, W. S., Inoue, T. and Thomas, J. H. (1996). Chemosensory neurons function in parallel to mediate a pheromone response in C. elegans. *Neuron* 17, 719-728.

Schaedel, O. N., Gerisch, B., Antebi, A. and Sternberg, P. W. (2012). Hormonal signal amplification mediates environmental conditions during development and controls an irreversible commitment to adulthood. *PLoS Biol* 10, e1001306.

Schroeder, N. E., Androwski, R. J., Rashid, A., Lee, H., Lee, J. and Barr, M. M. (2013). Dauer-specific dendrite arborization in C. elegans is regulated by KPC-1/Furin. *Curr Biol* 23, 1527-1535.

Serrano, L., Martinez-Redondo, P., Marazuela-Duque, A., Vazquez, B. N., Dooley, S. J., Voigt, P., Beck, D. B., Kane-Goldsmith, N., Tong, Q., Rabanal, R. M., et al. (2013). The tumor suppressor SirT2 regulates cell cycle progression and genome stability by modulating the mitotic deposition of H4K20 methylation. *Genes Dev* 27, 639-653.

Shaner, N. C., Lambert, G. G., Chammas, A., Ni, Y., Cranfill, P. J., Baird, M. A., Sell, B. R., Allen, J. R., Day, R. N., Israelsson, M., et al. (2013). A bright monomeric green fluorescent protein derived from Branchiostoma lanceolatum. *Nat Methods* 10, 407-409.

Thomas, J. H., Birnby, D. A. and Vowels, J. J. (1993). Evidence for parallel processing of sensory information controlling dauer formation in Caenorhabditis elegans. *Genetics* 134, 1105-1117.

Vielle, A., Lang, J., Dong, Y., Ercan, S., Kotwaliwale, C., Rechtsteiner, A., Appert, A., Chen, Q. B., Dose, A., Egelhofer, T., et al. (2012). H4K20me1 contributes to downregulation of X-linked genes for C. elegans dosage compensation. *PLoS genetics* 8, e1002933.

Vowels, J. J. and Thomas, J. H. (1992). Genetic analysis of chemosensory control of dauer formation in Caenorhabditis elegans. *Genetics* 130, 105-123.

Wadsworth, W. G. and Riddle, D. L. (1989). Developmental regulation of energy metabolism in Caenorhabditis elegans. *Dev Biol* 132, 167-173.

Wells, M. B., Snyder, M. J., Custer, L. M. and Csankovszki, G. (2012). Caenorhabditis elegans dosage compensation regulates histone H4 chromatin state on X chromosomes. *Molecular and cellular biology* 32, 1710-1719.

Yamamoto, R. and Tatar, M. (2011). Insulin receptor substrate chico acts with the transcription factor FOXO to extend Drosophila lifespan. *Aging Cell* 10, 729-732.

Chapter 5

Histone methyltransferase SET-4 promotes longevity in *Caenorhabditis elegans*

Abstract

Multiple conserved pathways control aging in metazoans. Several pathways act together and in parallel to control aging, including growth factor signaling, energy/nutrient sensing, and cellular stress responses. Changes in the amount and distribution of epigenetic modifications are also associated with aging. Loss of heterochromatin is a hallmark of aging; however, how specific epigenetic modifications contribute to the aging process is poorly understood. Here we show that the conserved histone H4 lysine 20 methyltransferase SET-4 promotes longevity in *Caenorhabditis elegans*. *set-4* overexpression extends lifespan in parallel with DAF-16/FoxO and causes animals to abstain from feeding. This fasting behavior induces expression of longevity-associated HLH-30 target genes which are required for full lifespan extension. Animals overexpressing *set-4* phenocopy models of dietary restriction, and SET-4 is required for viability in *eat-2* DR mimetics. Overexpression of *set-4* leads to increased H4K20 trimethylation, and H4K20 trimethylation is increased in *eat-2* animals. Taken together, these data support a role for higher order H4K20 methylation in promoting longevity and establish a novel epigenetic model of dietary restriction.

Introduction

Advanced age is strongly associated with the onset of chronic diseases including atherosclerosis, metabolic syndrome, diabetes, and dementia. Understanding the aging process may create new opportunities to prevent or treat these conditions. In recent years, it has become apparent that

organisms ranging from budding yeast to mammals age through conserved mechanisms including energy and nutrient sensing and regulation of growth factor signaling (Lamming, 2016; Mathew et al., 2017; Salminen et al., 2016). In metazoans insulin and insulin-like growth factor signaling activates a PI3-kinase phosphorylation cascade that leads to inhibition of FoxO transcription factors via nuclear exclusion (Brunet et al., 1999; Lee et al., 2001; Lin et al., 2001). Enhanced FoxO activity is associated with increased stress resistance and/or longevity in model organisms, while extreme longevity in humans is associated with FoxO single nucleotide polymorphisms (Anselmi et al., 2009; Bluher et al., 2003; Flachsbart et al., 2009; Kenyon et al., 1993; Li et al., 2003; Willcox et al., 2008; Yamamoto and Tatar, 2011). In parallel with FoxO transcription factor activity, moderate reduction in food intake, known as dietary restriction, is one of the most robust interventions to extend healthy lifespan across taxa (Kennedy et al., 2007). Dietary restriction protects against heart disease, cancer, diabetes and kidney failure in animal models and promotes stress resistance (Berrigan et al., 2005; Guarente and Picard, 2005).

In addition to metabolic perturbations, aging is associated with the loss of genomic integrity (Lopez-Otin et al., 2013). Genome stability is maintained by epigenetic mechanisms including DNA methylation and histone tail modification (Field and Adams, 2016). Skewed chromatin modifications are found in natural aging and in diseases associated with accelerated aging (Imai and Kitano, 1998; Shumaker et al., 2006; Vanyushin et al., 1973; Villeponteau, 1997). Histone tail methylation is highly conserved and contributes to the regulation of gene expression; histone H3 lysine 4 (H3K4), H3K36, and H3K79 methylation are associated with transcriptionally active regions while H3K9, H3K27, and H4K20 methylation typically mark repressed genes and heterochromatin (Davie et al., 2016; Lan and Shi, 2009; Schotta et al., 2004). Previous reports have shown that interventions that facilitate heterochromatin formation or maintenance promote longevity. For example, in the free-living nematode *Caenorhabditis elegans*, perturbing euchromatin-associated H3K4 methylation levels is associated with increased longevity (Greer et al., 2010). Decreased removal of heterochromatic H3K27 methylation also increased lifespan, potentially through maintenance of H3K27 methylation at insulin-like signaling genes (Jin et al., 2011). Disrupting genes that promote synthesis of the methyltransferase co-substrate S-adenosylmethionine (SAM) also promotes longevity (Hansen et al., 2005). Nevertheless, how epigenetic modifications interact with known longevity programs remains poorly understood.

In *C. elegans*, the histone methyltransferase SET-4 is required for both histone H4 lysine 20 di- and tri-methylation (H4K20me2 and H4K20me3, respectively) (Delaney et al., 2017; Vielle et al., 2012; Wells et al., 2012). We recently demonstrated a role for SET-4 in promoting the activity of the FoxO transcription factor DAF-16 in development (Delaney et al., 2017). Here we show that SET-4 promotes longevity in parallel with DAF-16/FoxO through the induction of fasting behavior that phenocopies a dietary restriction regimen. Downstream of decreased food consumption, genes involved in detoxification and fat metabolism are upregulated. H4K20 trimethylation is enriched in larvae undergoing DR, and *set-4* is required for viability in these animals. Overexpression of *set-4* results in H4K20 hypermethylation, consistent with increased catabolism of the methyl donor S-adenosylmethionine. We define a novel model for chronic dietary restriction that can be compared with existing genetic and environmental interventions to define conserved programs that enhance longevity.

Results

H4K20 methyltransferase SET-4 promotes longevity

We previously established a role for SET-4 in promoting DAF-16/FoxO activity in development (Delaney et al., 2017). Since DAF-16/FoxO is a well-described master regulator of lifespan in model organisms (Bluher et al., 2003; Kenyon et al., 1993; Yamamoto and Tatar, 2011), we tested whether SET-4 is required for normal lifespan. We found three independently-derived *set-4* functionally null alleles marginally decreased longevity relative to wild type siblings (Fig 5.1A, Fig. 5.S1A-B). Consistent with SET-4 promoting longevity, overexpression of *HA::set-4* from two independently integrated transgenes, *dpIs7* and *dpIs9*, was sufficient to significantly extend lifespan relative to wild type siblings (Fig 5.1B). The mean lifespan observed in *dpIs7* and *dpIs9* was 24.7 ± 0.55 and 24.6 ± 0.65 days compared to wild type siblings at 21.1 ± 0.40 and 21.2 ± 0.65 days, respectively. Integration of a single copy of *HA::set-4*, *dpIs5*, also extended lifespan, suggesting that the lifespan extension we observed from *set-4* overexpression is physiologically relevant (mean 20.1 ± 0.4 days *dpSi5* vs. 18.6 ± 0.3 days wild type) (Fig. 5.1C). The magnitude of lifespan extension due to *set-4* overexpression was similar to that previously attributed to *set-4* knockdown using RNAi (Greer et al., 2010). We recapitulated the lifespan extension due to *set-4* RNAi (Fig. 5.S1C); however, RNAi may not reproduce findings

in mutants due to incomplete knockdown, differences in tissue sensitivity, bacterial food source, and/or temporal differences. Indeed, we previously observed somatic *set-4* expression is primarily restricted to neurons, which are RNAi resistant (Delaney et al., 2017; Timmons et al., 2001). Taken together, these data suggest SET-4 promotes longevity in *C. elegans*.

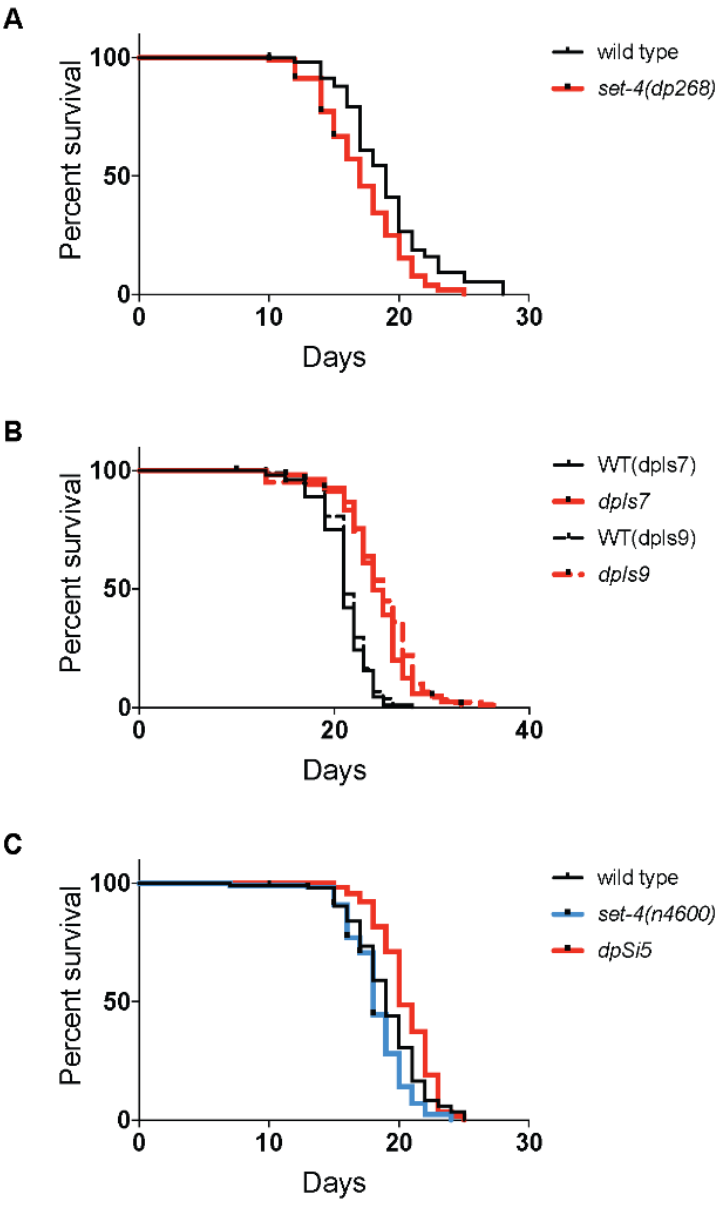

Figure 5.1. SET-4 promotes longevity. (**A**) *set-4* mutants are short-lived relative to wild type siblings. Results are representative of two experiments. P < 0.001. (**B**) overexpression of *HA::set-4* increases longevity relative to wild type siblings. Results are representative of three experiments. P < 0.0001. (**C**) A strain that contains two copies of *set-4* is long-lived relative to wild type siblings. Results are representative of three experiments. P < 0.001. Curves are significant as calculated by the log-rank test.

set-4 promotes longevity independently of DAF-16/FoxO activity

SET-4 is required for dauer arrest when DAF-16/FoxO is activated by reduced insulin-like signaling and/or *eak* pathway mutation (Delaney et al., 2017). We demonstrated *set-4* overexpression rescues dauer arrest in *set-4* mutants, indicating that these integrated transgenes are functional like the single copy insertion strain (Fig. 5.2A) (Delaney et al., 2017). However, we were surprised to observe that *set-4* overexpression promoted longevity in the context of the *daf-16(mu86)* null allele (Fig. 5.2B) or when *daf-16* was inactivated by RNAi (Fig. 5.2C). Therefore, *set-4* overexpression promotes longevity independent of DAF-16/FoxO activity.

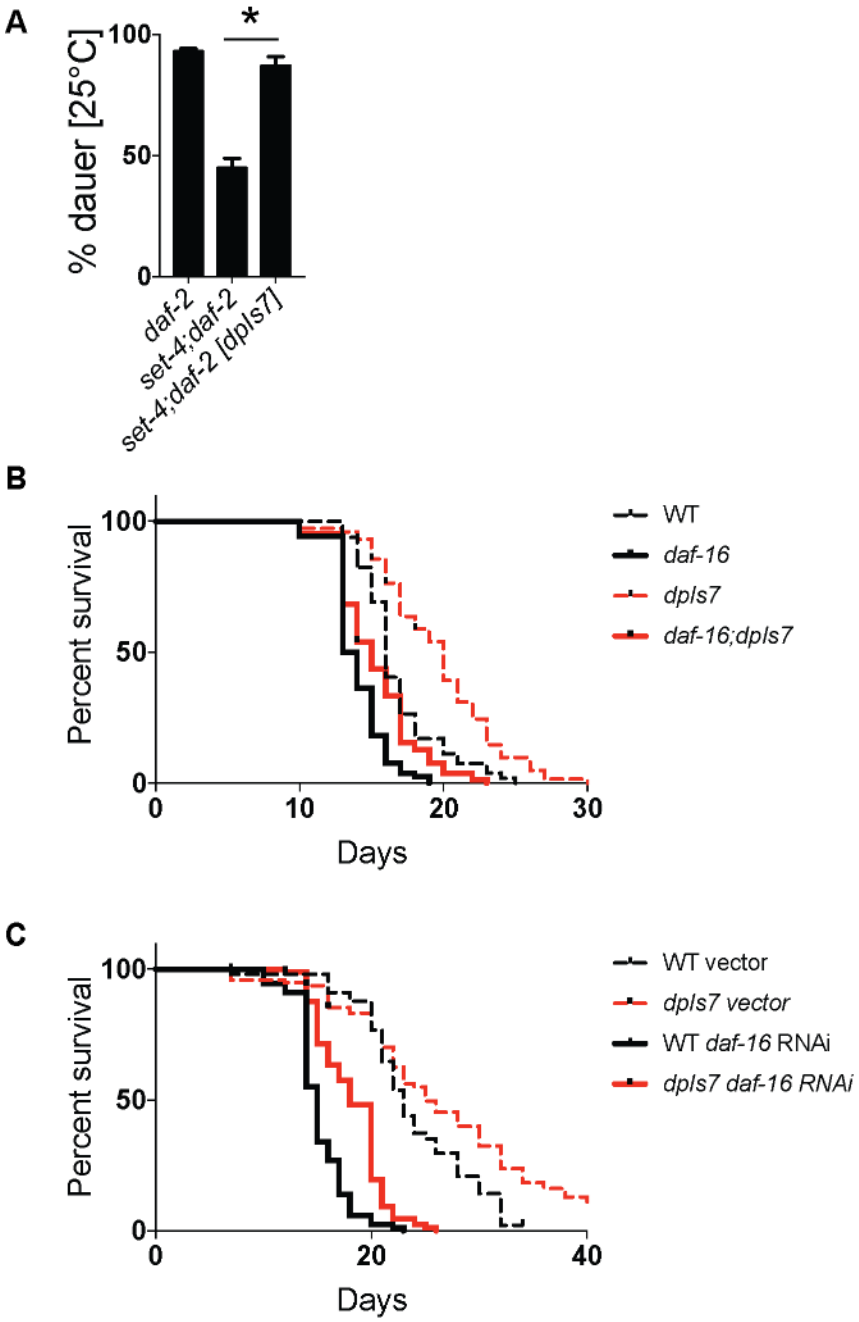

Figure 5.2. *set-4* overexpression extends lifespan independently of DAF-16. (**A**) *set-4* overexpression rescues dauer in *set-4* null animals. Results are the mean and s.e.m. of three experiments. N = 1125, 662, 396. $P < 0.05$ by student's t-test. (**B**) Overexpression of *HA::set-4* increases longevity in the absence of *daf-16*. Results are representative of two experiments. $P < 0.0001$. (**C**) Overexpression of *HA::set-4* increases longevity in the context of *daf-16* RNAi. Results are from one experiment. $P < 0.0001$. Curves are significant as calculated by the log-rank test.

set-4 overexpression induces fasting behavior

Visual examination revealed *set-4* overexpressing strains were smaller, thinner, and more transparent than their wild type siblings as young adults, and they remained so throughout adulthood (Fig. 5.3A). These animals also demonstrated a delay in development most pronounced in the L4 larval stage, delayed onset of egglaying, an extended period of fertility, and fewer progeny overall relative to wild type (Fig 5.3B-C, Fig 5.S2). These phenotypes are similar to those manifested in animals undergoing dietary restriction (DR) (Bishop and Guarente, 2007).

We found this DR-like phenotype intriguing because multiple models of DR extend longevity independently of DAF-16/FoxO, like *set-4* (Lan et al., 2015). Therefore, we investigated the nature of this fasted appearance. SET-4 is expressed primarily in neurons during development (Delaney et al., 2017). A genetic mimetic of DR, *eat-2*, disrupts a nicotinic acetylcholine receptor gene in neurons to decrease the pumping rate of the pharynx. Defective pumping results in *eat-2* animals eating less food throughout life, leading to increased lifespan. We tested whether *set-4* overexpression disrupts normal pharyngeal pumping like *eat-2* mutation (Raizen et al., 1995). Strains overexpressing *set-4* did not demonstrate any defect in pumping rates relative to wild type siblings (Fig 5.3D-E), suggesting a mechanism distinct from a physical defect in feeding. We next examined whether *set-4* overexpressor strains exhibited distinct feeding behaviors. We found fewer young adult animals overexpressing *set-4* to be on food at a given time point compared to wild type siblings (Figs. 5.3F-H), consistent with less feeding behavior. A defect in food perception could explain this behavior; however, raising overexpressor animals on lawns of bacterial food that covered the entire plate did not rescue animal size (Fig 5.3I). Taken together, these data suggest these animals are less inclined to engage in feeding behavior independently of a mechanical or food-sensing defect.

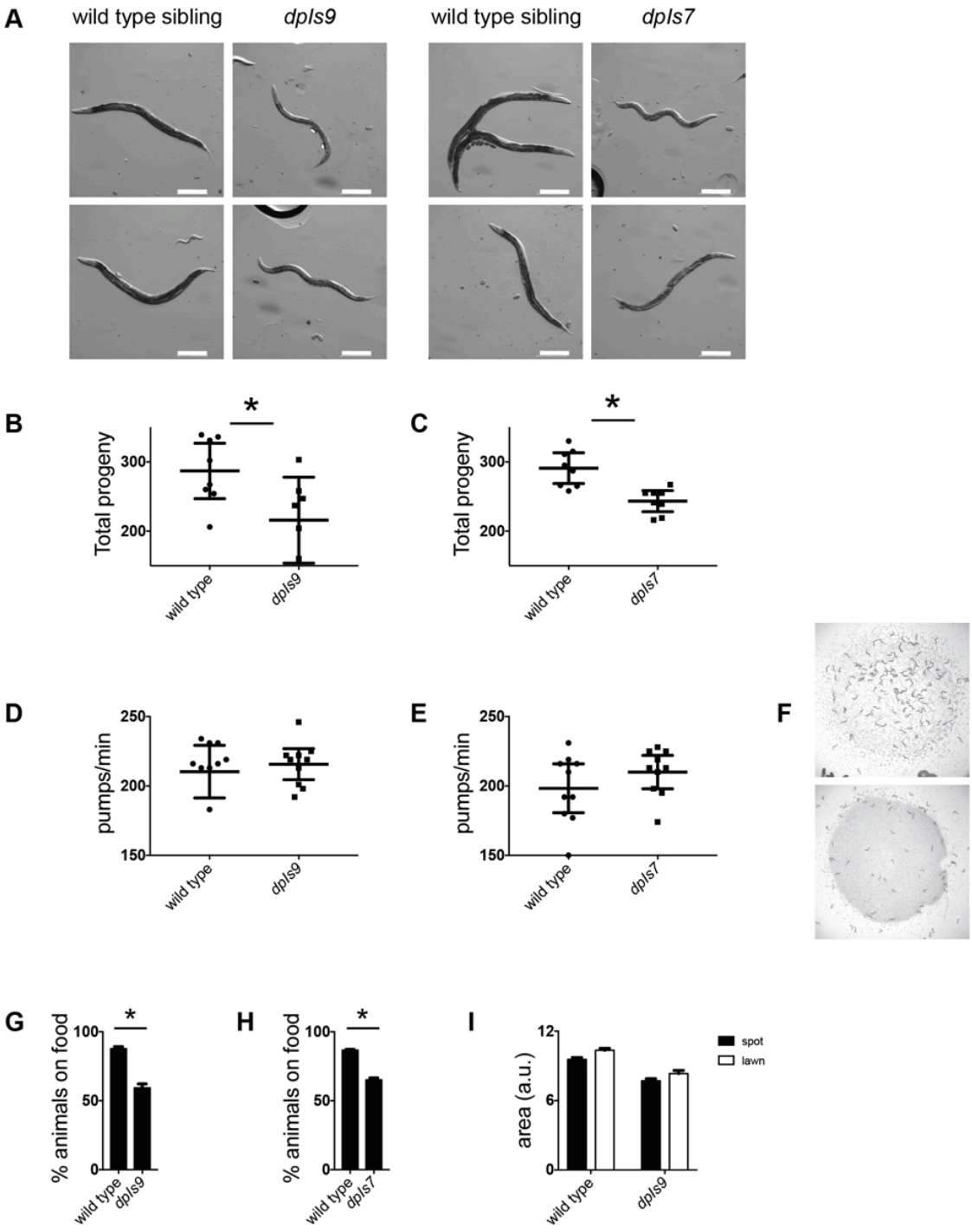

Figure 5.3. *set-4* overexpressors exhibit decreased feeding behavior. (**A**) *set-4* overexpressing strains are smaller than their wild type siblings throughout adulthood. Representative images of day one adults shown. Scale bar = 250 μM. N = 10, 10, 7, 18. (**B**, **C**) *set-4* overexpressors have decreased total fertility. $P < 0.05$, $P < 0.001$, respectively. (**D**, **E**) Overexpressor strains exhibit no defect in pumping rate at young adulthood. (F) *set-4* overexpressors avoid food to a greater extent than wild type siblings. Representative images of young adult animals shown. (**G**, **H**) Quantification of phenotype shown in (F). N (dpIs9) = 1356, 804; N (dpIs7) = 1247, 770. $P < 0.05$, $P < 0.01$, respectively. (**I**) Overexpressing strains raised on bacterial lawns remain smaller than wild type siblings. N = 14, 13, 11, 12.

set-4 overexpression induces fasting response genes

Animals deprived of food upregulate HLH-30 transcription factor activity through down-regulation of the binding site competitor *mxl-3* and upregulation of *hlh-30* expression itself (Lapierre et al., 2013; O'Rourke and Ruvkun, 2013). HLH-30 is required for the induction of genes associated with stress-resistance like the conserved monooxygenase *fmo-2* as well as increased fatty acid metabolism genes like lipases *lipl-2* and *lipl-3* (Leiser et al., 2015; O'Rourke and Ruvkun, 2013). Upregulation of *hlh-30* either through loss of *mxl-3* or through overexpression of *hlh-30* promotes longevity, presumably through *hlh-30* target genes. Similarly, *hlh-30* is required in multiple models of longevity including reduced insulin signaling and dietary restriction (Lapierre et al., 2013). We found *hlh-30* and target gene transcripts were upregulated in *set-4* overexpressing animals, consistent with observations demonstrating these animals engage in fasting behavior (Fig 5.4A). In contrast, neither *mxl-3* nor genes associated with other longevity associated transcription factors were different between overexpressors and wild type siblings. Genes tested include *sod-2* (PHA-4), *sod-3* (DAF-16), *gcs-1* (SKN-1), *alg-2* (DAF-12) and *pat-10* (HSF-1) (An and Blackwell, 2003; Baird et al., 2014; Hochbaum et al., 2011; Honda and Honda, 1999; Panowski et al., 2007).

HLH-30 is required for the upregulation of *lipl-2* and *lipl-3* during fasting (O'Rourke and Ruvkun, 2013). Because *set-4* overexpression promotes fasting behavior, we asked whether *set-4* is necessary for the induction of these fasting response genes. In *set-4* null animals, we found a defect in *lipl-3* expression in both fed and fasted animals (Fig 5.4B). *lipl-2*, on the other hand, was not different between *set-4* and wild type animals in the fed condition but may be less induced in *set-4* animals when fasted (Fig. 5.4C). Preliminary findings show both *lipl-2* and *lipl-3* may be required for longevity in *set-4* overexpressing lines (Figs. 3.4D-E). These data support the hypothesis that HLH-30 promotes longevity through induction of target genes controlling fatty acid metabolism.

Previously, it was established that longevity in a liquid DR regimen required the B isoform of the NRF2 ortholog *skn-1* that is expressed solely in ASI neurons (Bishop and Guarente, 2007). However, those findings were based on overexpression systems and RNAi. Given that *set-4* is expressed primarily in neurons, and that *set-4* expression in ASI is sufficient for dauer arrest (Fig. 4.2) (Delaney et al., 2017), we wanted to test whether *skn-1B* was required for the induction

of HLH-30 target genes observed in *set-4* overexpressors. We used CRISPR-Cas9 to create the *skn-1B*-specific null allele, *skn-1(dp685)* by inserting a stop codon and frameshift in the B-specific exon 1. Preliminary data suggests that *skn-1B* is indeed required for downstream activation of *lipl-2* and *lipl-3* expression (Fig. 5.4F-G).

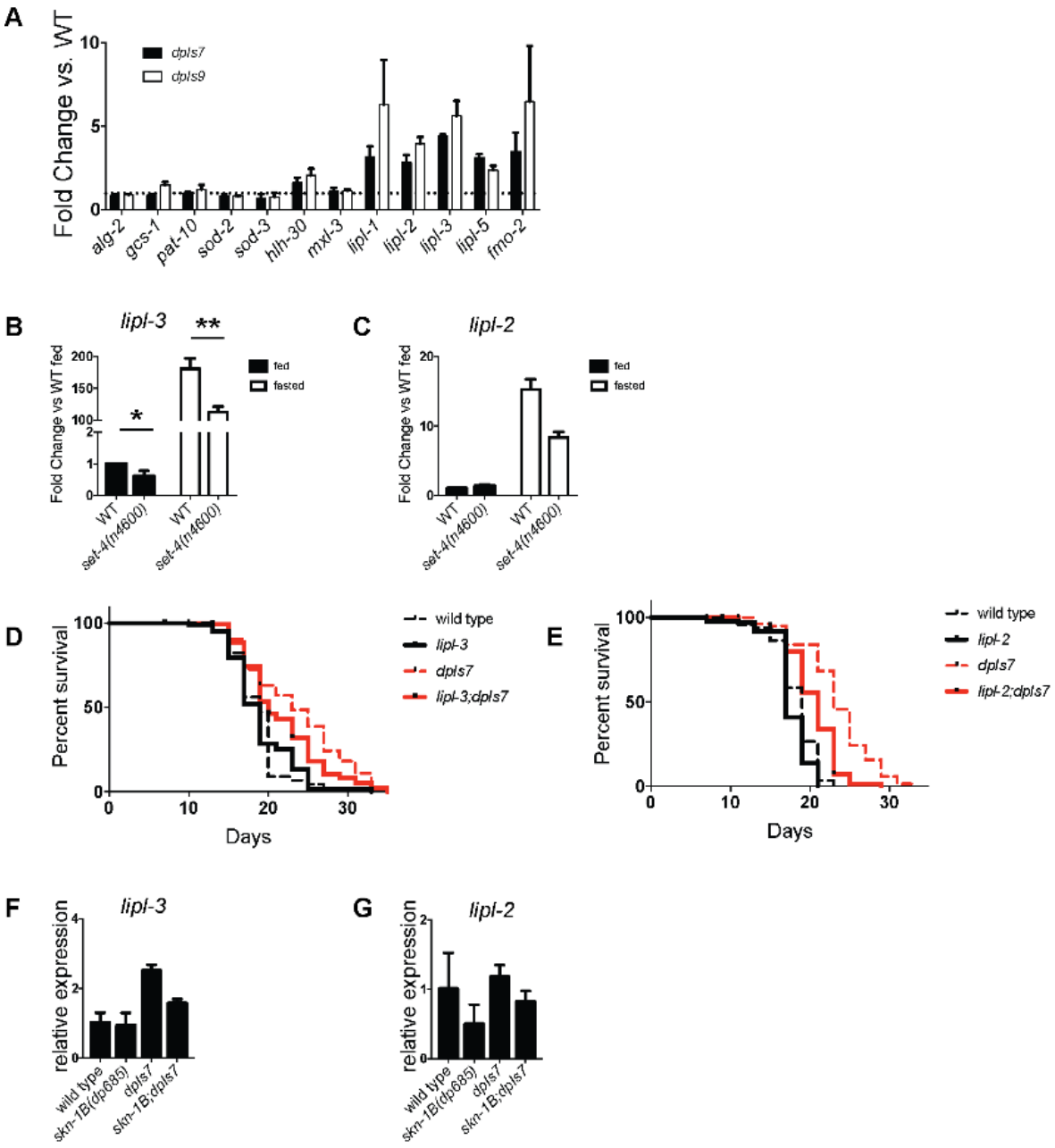

Figure 5.4. *set-4* overexpression activates HLH-30 and fasting response genes. (**A**) Independent transgenic lines demonstrate specific upregulation of genes associated with fasting. Results are the mean and s.e.m. of three experiments. (**B**) *lipl-3* expression requires *set-4* in both fed and fasted conditions. Results are the mean and s.e.m. of three experiments. *P < 0.05, **P < 0.01. (**C**) *lipl-2* expression in fasted conditions may be SET-4 dependent. Results are from one experiment performed in duplicate. (**D**, **E**) Full lifespan extension in *set-4* overexpressors may require both LIPL-3 and LIPL-2. Results shown are one experiment. *dpIs7* vs. *lipl-3;dpIs7* P < 0.05; *dpIs7* vs. *lipl-2;dpIs7* P < 0.0001 by the log-rank test. (F) SKN-1B is required for *lipl-3* induction in *set-4* overexpression. Results are from one experiment performed in duplicate. (G) SKN-1B promotes *lipl-2* expression. Results are from one experiment performed in duplicate.

SET-4 is required for viability in a developmental model of dietary restriction

The epigenetic contribution to longevity in models of dietary restriction remain poorly understood. Because we observed a DR-like phenotype in animals that also demonstrated greater H4K20me3, we asked whether H4K20 methylation was altered in DR animals during development. We observed greater H4K20me3 in *eat-2* L4 larvae to wild type siblings (Fig. 5.5A). Whether H4K20me3 is required for increased longevity in this background could not be addressed because *set-4;eat-2* double mutants were sterile. These animals exhibited a much greater developmental delay compared to *eat-2* single mutants, and while they laid a similar number of eggs as *eat-2*, only rarely did larvae hatch or grow to adulthood. These observations were unexpected because loss of *set-4* does not lead to obvious fertility or growth defects in other genetic backgrounds, including animals with decreased total fertility due to reduced insulin signaling. H4K20 methylation is associated with dosage compensation (Delaney et al., 2017; Lau et al., 2014; Vielle et al., 2012; Wells et al., 2012), but sterility was not due to disruption of dosage compensation because *eat-2;dpy-21* animals were fertile. We then tested whether *set-4* is required for increased longevity in a late-life model of intermittent fasting known as sDR (Greer et al., 2007). Like wild type siblings, animals lacking *set-4* experienced a modest increase in mean life span (Fig. 5.5B). sDR requires DAF-16, but SET-4 promotes longevity in parallel with DAF-16. Therefore, it was not surprising the effect of this DR regimen was not different between wild type animals and *set-4* mutants. Finally, we exposed *eat-2* animals to *set-4* RNAi from hatching throughout life. These animals did not live shorter than *eat-2* animals eating empty vector-expressing bacteria (Fig. 5.5C). In contrast, both *daf-16* and *hlh-30* RNAi shortened the lifespan of both wild type and *eat-2* animals relative to vector only control (data not shown). The fact that *set-4* RNAi did not disrupt *eat-2* lifespan is consistent with *set-4* expression being

restricted to RNAi-resistant neurons post-embryonically (Delaney et al., 2017; Timmons et al., 2001). Taken together, these data implicate SET-4 mediated H4K20 methylation as required for viability in chronically fasted animals during larval development.

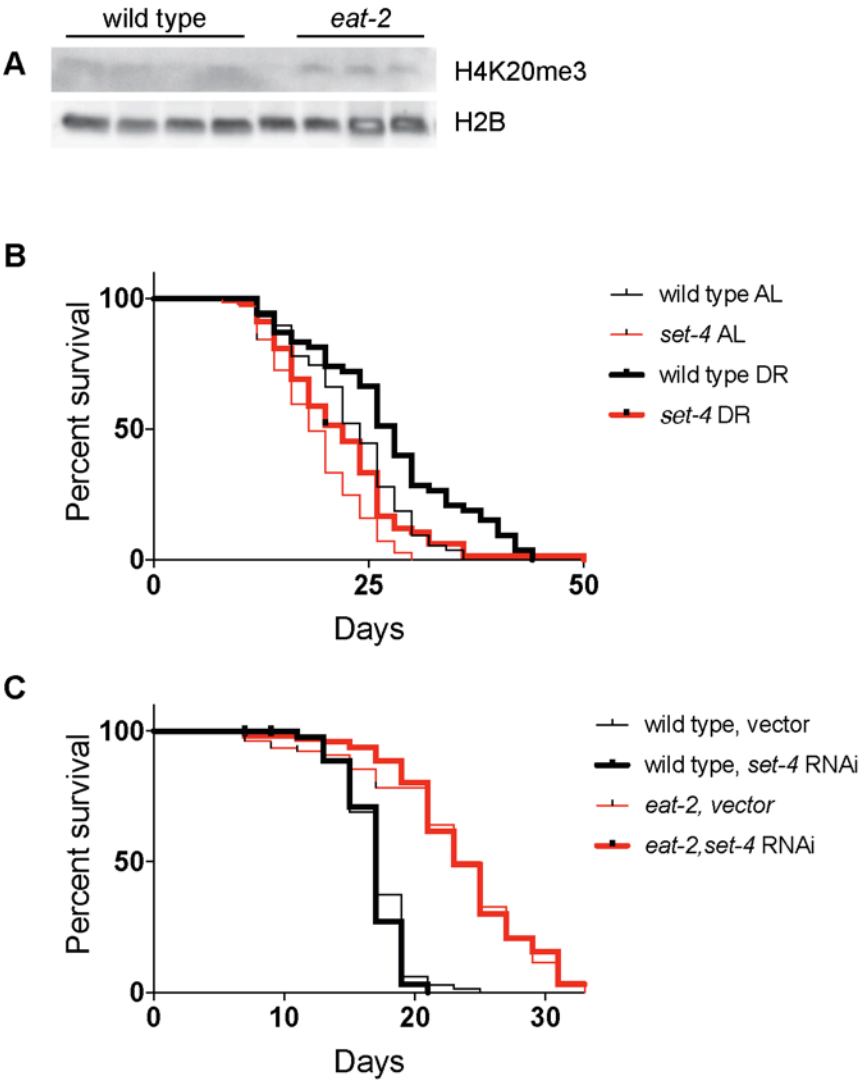

Figure 5.5. H4K20 trimethylation is associated with dietary restriction. (**A**) H4K20 trimethylation is greater in *eat-2* animals compared to wild type siblings. Results show three experiments. (**B**) *set-4* is dispensable for the late-life intermittent fasting model, sDR. Results are from one experiment. For wild type *ad libitum* (AL) vs DR $P < 0.0001$; for *set-4* AL vs. DR, $P < 0.001$. (**C**) *set-4* RNAi does not affect *eat-2* lifespan. Results are from one experiment. Curves are significantly different as calculated by the log-rank test.

Overexpression of *set-4* increases H4K20 methylation

SET-4 is a histone H4 lysine 20 (H4K20) methyltransferase which converts a monomethylated substrate to a dimethylated product and is required for trimethylation as well (Delaney et al., 2017; Vielle et al., 2012; Wells et al., 2012). We wondered whether overexpressing *set-4* alters chromatin state. We used immunofluorescence to detect H4K20 trimethylation in embryos and normalized signal to DAPI nuclear staining. We observed a 71% and 44% increase in H4K20me3 in *dpIs7* and *dpIs9* overexpressor strains, respectively (Fig. 5.6A-B). Methylation reactions require consumption of the methyl donor S-adenosylmethionine (SAM) (Mentch and Locasale, 2016). S-adenosylmethionine synthetase (*sams*) proteins synthesize SAM (Lieber, 2002). Knockdown of *sams-1* also has been shown to increase longevity, delay reproductive development, decrease brood size, and promote food avoiding behavior to a similar degree as *set-4* overexpression (Hansen et al., 2005; Melo and Ruvkun, 2012). Reduction of dietary methionine, an essential metabolic precursor of SAM, has been shown to increase longevity in mammals (Miller et al., 2005; Orentreich et al., 1993). Furthermore, increasing SAM catalysis in *Drosophila* is sufficient to extend lifespan (Obata and Miura, 2015). *sams-1* is X-linked, and we have shown *set-4* promotes silencing of X-linked genes during development (Delaney et al., 2017). W tested whether *set-4* regulates *sams-1* expression. However, *sams-1* mRNA levels were not different between *set-4* overexpressors and wild type siblings (Fig 5.6C). These findings are consistent with *set-4* overexpression leading to increased consumption of SAM through methylation reactions while not affecting SAM synthesis itself.

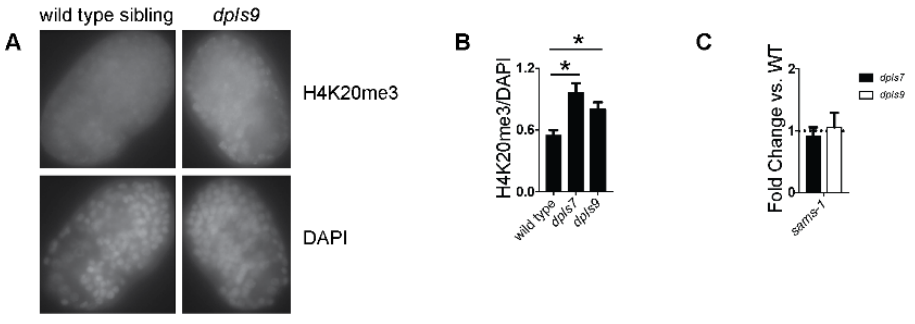

Figure 5.6. *set-4* overexpression increases H4K20 methylation. (**A**) Representative images of embryos stained for H4K20 trimethylation and DAPI. N = 10 each for WT, *dpIs7* and *dpIs9*. (**B**) Quantification of H4K20me3 signal normalized to DAPI, from (A). P < 0.01 by two-sided T test. (**C**) *set-4* overexpression does not affect *sams-1* expression. Results are the mean and s.e.m. of three experiments performed in duplicate.

Discussion

In the present study, we find that increased *set-4* expression promotes longevity through induction of fasting behavior. Accompanying the DR-like phenotype and behavior of these animals is an increase in H4K20 trimethylation in embryos. More methylation would be consistent with increased consumption of the methylation co-factor SAM. Disrupting genes involved in SAM synthesis or increasing SAM catabolism has been linked with food avoidance, decreased brood size and increased longevity (Hansen et al., 2005; Melo and Ruvkun, 2012; Obata and Miura, 2015). Fasting leads to the induction of the longevity-promoting *hlh-30* transcription factor and its target genes which may be required for *set-4* mediated longevity. Finally, we find evidence that H4K20 methylation levels are increased in *eat-2* mutants, while *set-4;eat-2* animals are sterile, suggesting this epigenetic mark may be critical for viability under conditions of dietary restriction during development.

Histone H4 lysine 20 (H4K20) methylation plays an important role in cell cycle control, DNA origin of replication licensing, and promoting double strand break repair (Jorgensen et al., 2013). Different methylation states of H4K20 are associated with different functions that promote genomic integrity in mammals and fission yeast (Botuyan et al., 2006; Sanders et al., 2004; Schotta et al., 2008). H4K20 monomethylation (H4K20me1) enrichment marks active transcription and is important for successful progression through mitosis (Barski et al., 2007; Liu et al., 2010), while H4K20 dimethylation (H4K20me2) marks greater than 80% of histone H4 in G1 phase (Schotta et al., 2008). H4K20me2 is also important for recruiting 53BP1 and associated DNA damage response (DDR) proteins to double strand breaks in both fission yeast and mammalian HeLa cells (Botuyan et al., 2006; Pei et al., 2011). It remains to be tested whether SET-4 promotes longevity through maintenance of genomic integrity by promoting repair of DNA damage.

The role of H4K20 trimethylation (H4K20me3) in maintenance of chromatin is less well understood. In mammalian cells H4K20 trimethylation is concentrated in constitutive heterochromatin in a manner dependent on HP1 and histone H3 lysine 9 trimethylation (Schotta et al., 2004; Souza et al., 2009). H4K20me3 is enriched in aged mammals relative to other histone marks (Sarg et al., 2002). A similar enrichment was observed in fibroblasts derived from progeria patients (Shumaker et al., 2006). However, whether H4K20me3 promotes an aging

phenotype or is a defense response to the progressive loss of heterochromatin remains unclear. Because SET-4 is required for both di- and tri-methylation of H4K20, at present we are unable to parse whether SET-4 promotes longevity through deposition of H4K20 dimethylation, trimethylation, or both.

Signals from multiple tissues control longevity in *C. elegans*, including the intestine, germline, and neurons (Bishop and Guarente, 2007; Chen et al., 2009; Greer et al., 2010; Hsu et al., 2003). SET-4 activity in neurons promotes dauer arrest during development, but in adult animals intestinal DAF-16 is believed to mediate longevity (Libina et al., 2003). Also, *set-4* expression in the soma is detectable only in neurons post-embryonically (Delaney et al., 2017). These observations may explain how SET-4 promotes DAF-16/FoxO activity during development while promoting longevity independently of DAF-16/FoxO (Fig. 5.2B-C). It is unlikely that SET-4 promotes longevity through the germline for two reasons. Despite endogenous *set-4* being expressed in the germline (Jianhao Jiang, personal communication), transgenic constructs like those used in this study typically are silenced in the germline via endogenous RNAi mechanisms (Kelly et al., 1997; Shirayama et al., 2012). Second, one of the two integrated arrays (*dpIs7*) we empirically determined is X-linked, and X chromosome expression is silenced in the germline (Strome et al., 2014).

Dietary restriction can increase lifespan through cell-nonautonomous signaling between neurons and the intestine. The hypoxia inducible factor HIF-1 acts in neurons to upregulate the longevity-promoting flavin monooxygenase FMO-2 in the intestine (Leiser et al., 2015). Similarly, the NRF2 homolog SKN-1 B isoform is expressed exclusively in ASI sensory neurons and is required for increased longevity under a liquid DR regimen (Bishop and Guarente, 2007). We have shown *set-4* is neuronally expressed in larvae, including in sensory neurons, and it functions in ASI to promote dauer arrest (Fig. 4.1B). Also, we showed that *skn-1b* is required for lipase gene expression in *set-4* overexpressing strains (Fig. 5.4). Therefore, it is conceivable that SET-4 acts in neurons to induce a neuron-intestine longevity signal that shifts metabolism towards fatty acid catabolism through induction of HLH-30 activity. Whether this signal stems from locally reduced levels of SAM or results from increased higher order methylation of H4K20 remains unknown. It is conceivable that multiple consequences of methyltransferase activity may contribute to the longevity phenotype.

Multiple lines of evidence suggest the maintenance of heterochromatin promotes longevity. Aging is associated with loss of heterochromatin globally and skewed distribution locally (Oberdoerffer and Sinclair, 2007; Tsurumi and Li, 2012). Decreasing heterochromatin in *Drosophila* dramatically decreases lifespan while increasing heterochromatin formation robustly extends lifespan (Larson et al., 2012). How specific epigenetic modifiers participate in this phenomenon are also becoming clear. For example, sirtuin proteins deacetylate histone H4 lysine 16, which promotes chromatin compaction and the establishment of heterochromatin marks (Sarg et al., 2004; Serrano et al., 2013a). SirT1 has H4K16 deacetylase activity and acts to stabilize the H3K9 trimethylase SUV39H1 protein to maintain genomic integrity at centromeres and telomeres (Bosch-Presegue et al., 2011; Garcia-Cao et al., 2004; Peters et al., 2001; Vaquero et al., 2007). Mammalian studies also suggest H3K9 trimethylation recruits SUV420H2 via HP1 to trimethylate H4K20 in regions of constitutive heterochromatin (Schotta et al., 2004; Souza et al., 2009). H4K20, in turn, antagonizes the acetylation of H4K16 (Sarg et al., 2004; Serrano et al., 2013b). Interrogating the dynamics of these interrelated heterochromatin marks in long-lived model systems may reveal a virtuous cycle that promotes longevity through maintenance of heterochromatin, minimizing genomic damage and transcriptional drift during aging.

Here we describe a novel epigenetic manipulation that recapitulates many of the phenotypes of dietary restriction, most notably long life. Importantly, epigenetic modifications are malleable. Not only are they altered under conditions of environmental toxicity and during aging (Oberdoerffer and Sinclair, 2007; Talens et al., 2012; Tsurumi and Li, 2012), but straightforward interventions like diet can lead to maintenance of heterochromatin-associated marks and down-regulation of inflammation throughout life (Delaney et al., 2013; Delaney et al., 2012). Further investigation into epigenetic interventions that stabilize the genome may lead to more effective therapies for the chronic diseases of aging like rheumatoid arthritis, obesity, and dementia.

Materials and Methods

Worm strains and maintenance

Strains used in this study are as follows: *set-4(n4600)*, *set-4(ok1481)*, *set-4(dp268)*, *daf-16(mu86)*, *lipl-2(tm4324)*, *lipl-3(gk224717)*, *eat-2(ad1116)*, *dpSi5 [set-4p::HA::set-4::set-4utr, unc-119(+,CB)] IV*, *dpEx18 [set-4p::HA::set-4::set-4utr, myo-2p::RFP]*. Animals were propagated on nematode growth media (NGM) plates and fed *E. coli* OP50 using standard techniques.

Generation of transgenic strains

Extrachromosomal arrays were integrated as previously described (Mello et al., 1991) using a Stratalinker 1800 (Stratagene) at 325 μJ/cm^2 x 100. L4 animals with the *dpEx18* array were irradiated, then allowed to lay eggs until food was consumed. Transgenic animals were then singled and propagated. Transgenic animals whose progeny were 100% positive for the myo-2p::RFP marker were considered integrated. Independent integrated transgenic lines were backcrossed ten times prior to analysis. CRISPR mutagenesis was performed as described (Paix et al., 2015) using recombinant Cas9 (PNA Bio) and crRNA and tracrRNA (Dharmacon). *skn-1B* exon 1 was targeted with the crRNA guide sequence 5'-GGCUGCUGGAGCGGUGUUGG-3'. The result is a stop codon after amino acid 22 and a +1 frameshift.

Lifespan Assays

Lifespan assays were performed at 20°C as previously described (Chen et al., 2015). Briefly, young adult (day 0) or day 1 adult animals were transferred to NGM plates seeded with 20X OP50 containing 50 μM 5-fluoro-2'-deoxyuridine (FUDR; Sigma-Aldrich, St. Louis, MO, USA) to control progeny and 10 μg/mL nystatin (Sigma-Aldrich) to inhibit fungal growth. 25 μg/ml carbenicillin was used in sDR plates to attenuate bacterial growth. RNAi experiments were conducted using dsRNA-expressing HT115 bacteria as previously described (Kamath et al., 2001) and included 5 mM IPTG and 25 μg/ml carbenicillin. Completely paralyzed animals that did not respond to prodding were scored as dead and removed. Animals that left the plate or

exploded were censored. Statistical significance was calculated in Prism (GraphPad Software; La Jolla, CA, USA) using the log rank test.

Microscopy

DIC images of animals were taken using a Leica M165FC with a DFC9000 GT camera (Leica). Animal size was calculated in Image J by measuring the area of each animal.

Immunofluorescence

Embryos were fixed and stained with DAPI (1 μg/mL, Thermo D1306) and antibodies against H4K20me3 (1:200, Abcam, ab78517) as previously described (Chuang et al., 1994). Antibody specificity is reported on the Histone Antibodies Database (Rothbart et al., 2015). Anti-mouse FITC (1:100, Jackson ImmunoResearch) secondary antibodies were then applied. Fluorescent images were captured using an Olympus BX61 compound microscope using a 60X oil-immersion objective, a Hamamatsu ORCA ERGA CCD camera, and Slidebook software (Intelligent Imaging Innovations). Mean intensity of antibody signal was measured using Image J and normalized to DAPI signal.

Fertility Assay

Late L4 animals were singled to new plates and allowed to lay eggs at 20°C. Egg-layers were transferred to new plates every 24 hr for 4 days. Living larvae on each plate were then counted to determine total fertility.

Pumping assay

L4 animals were transferred to fresh plates and allowed to recover. Pharyngeal pumps were counted at 120X magnification using the Leica M165FC microscope for 20 sec for each animal, after which the animal was removed from the plate.

Food avoidance assay

Animals were grown on 3cm NGM plates with spotted with 50 μL of 4X concentrated OP50. Young adults were scored as on food or off food, from which the percent feeding was determined.

Fasting assay

Young adult animals were washed in M9 to remove all bacteria, then transferred to plates seeded with OP50 or plates without food. After 6 hr, animals were harvested for RNA as described below.

RNA preparation

Animals were washed three times in M9 buffer, once in water, then resuspended in 500 μL Trizol (Invitrogen). After 5 freeze/thaw cycles, RNA was extracted with chloroform and further purified using the Direct-zol RNA Miniprep Kit (Zymo Research).

Quantitative PCR

cDNA was reverse-transcribed with the SuperScript III First Strand Synthesis Kit (Invitrogen) using dT primers. cDNA was amplified using the Quantitect SYBRgreen qPCR Kit (Qiagen) in a total volume of 15 μL, performed in a RotorGene 6000(Corbett Research). RotorGene 6000 Software (version 1.7) was used to calculate Ct. *pmp-3* was used as a housekeeping gene, and relative expression was calculated using the ΔΔCt method (Hoogewijs et al., 2008; Nolan et al., 2006). Primer sequences are provided in Supplementary Table 5.1.

Western blotting

Gravid adults were dissolved in sodium hypochlorite to release eggs, which were allowed to hatch while rotating overnight in M9 buffer. Synchronized progeny were transferred to NGM

and grown to early L4. Animals were washed thrice in M9, once in water, and then resuspended in one pellet volume of worm lysis buffer (Webster et al., 2013) and frozen at -80°C until use. Protein preparation, transfer, and antibody detection were performed as previously described (Delaney et al., 2017). Briefly, animals were dissolved at 85C for 5 minutes then sonicated on ice for 2 cycles of 30 sec. Lysates were cleared by centrifugation at 21,000g for 15 minutes. Protein concentration was determined using the DC Protein Quantification Kit (BioRad). 50 µg protein per lane was added to Criterion XT gels using XT-MES buffer (BioRad) and transferred to Immobilon Psq PVDF (Millipore). Membranes were incubated with antibodies against H4K20me3 (1:500, Abcam ab78517) or H2B (1:1000, Abcam ab1790), diluted in Western Blocking Solution (Sigma), incubated overnight at 4°C, and washed three times with TBS + 0.5% Tween 20 (TBST). Secondary antibodies conjugated to HRP were applied for at least one hour at room temperature. After three washes with TBST, signal was detected using ECL (Pierce).

Supplementary Information

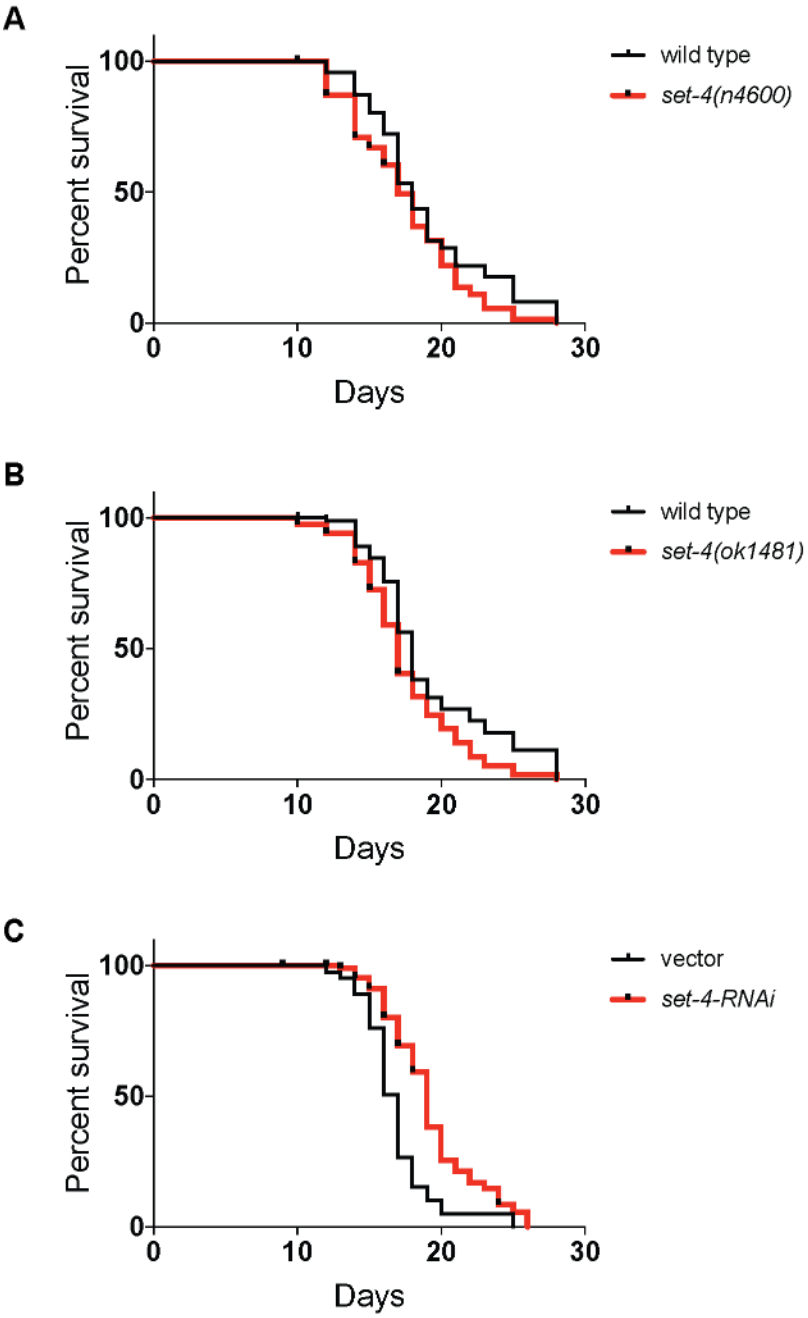

Supplementary Figure 5.S1. SET-4 regulates longevity. (**A**, **B**) *set-4* mutants are short-lived relative to wild type siblings. Results are representative of two experiments. $P < 0.05$. (**C**) RNAi against *set-4* begun at young adulthood extends lifespan. Results are representative of three experiments. $P < 0.0001$. Curves are significant as calculated by the log-rank test.

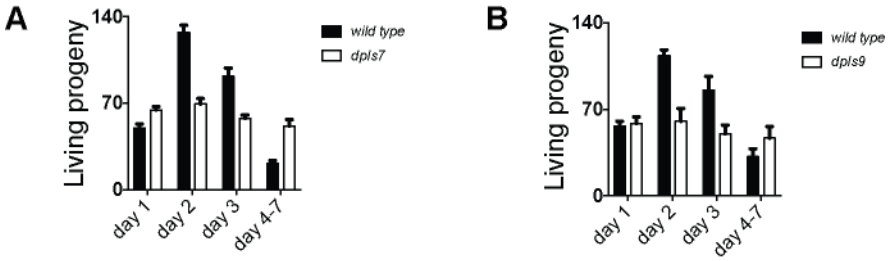

Supplementary Figure 5.S2. Strains overexpressing *set-4* show altered egglaying dynamics. Animals were synchronized at L4 prior to beginning the experiment. (**A**) N = 8 WT, 8 *dpls7*. (B) N = 8 WT, 7 *dpls9.*

Supplemental Table 5.1. qPCR primer sequences.

Gene	Forward primer	Reverse primer
alg-2	TGGTCGATAGGGATCATGG	TCGAGTCGGGATGAACCT
fmo-2	GACGTGGCAGTTGAGCAATC	ACACACGATGAGCTGGCTTT
gcs-1	GGAATGCCTTACGGAGGTC	CGATAGACATGTTTCATCCTTCTTT
hlh-30	GGTGATAATGATCCGGAGGAC	TCTTCGTCGGCGTTCAAT
lipl-1	CGGTTTGCGCTGGACTTA	GAACACGAGTTGCGTTAA
lipl-2	CCCGAATTTGATGGTTGGTA	ATCACAGAGTTCAGCCTC
lipl-3	GCCCGAGCAAAGTGCAGC	CCTTCAAGTTTTTGTGCT
lipl-5	CATATGACTACCCCCCAAATCA	CCATGTTACGTTTGTTTTCCCAAA
mxl-3	ACTCGGATTCTTCCGATGAC	TTCAAGTTCGTTGTGATGTGC
pat-10	ACTCCGACAACATGGCTGA	TGAGTGGCCATGATGTATCC
pmp-3	GTTCCCGTGTTCATCACTCAT	ACACCGTCGAGAAGCTGTAGA
sod-2	TCGACCAGATTATGTCAATGCT	GCATTAATTCTTGTGATTCAGCTC
sod-3	TATTAAGCGCGACTTCGGTTCCCT	CGTGCTCCCAAACGTCAATTCCAA

References

An, J. H. and Blackwell, T. K. (2003). SKN-1 links C. elegans mesendodermal specification to a conserved oxidative stress response. *Genes Dev* 17, 1882-1893.

Anselmi, C. V., Malovini, A., Roncarati, R., Novelli, V., Villa, F., Condorelli, G., Bellazzi, R. and Puca, A. A. (2009). Association of the FOXO3A locus with extreme longevity in a southern Italian centenarian study. *Rejuvenation Res* 12, 95-104.

Baird, N. A., Douglas, P. M., Simic, M. S., Grant, A. R., Moresco, J. J., Wolff, S. C., Yates, J. R., 3rd, Manning, G. and Dillin, A. (2014). HSF-1-mediated cytoskeletal integrity determines thermotolerance and life span. *Science* 346, 360-363.

Barski, A., Cuddapah, S., Cui, K., Roh, T. Y., Schones, D. E., Wang, Z., Wei, G., Chepelev, I. and Zhao, K. (2007). High-resolution profiling of histone methylations in the human genome. *Cell* 129, 823-837.

Berrigan, D., Lavigne, J. A., Perkins, S. N., Nagy, T. R., Barrett, J. C. and Hursting, S. D. (2005). Phenotypic effects of calorie restriction and insulin-like growth factor-1 treatment on body composition and bone mineral density of C57BL/6 mice: implications for cancer prevention. *In Vivo* 19, 667-674.

Bishop, N. A. and Guarente, L. (2007). Two neurons mediate diet-restriction-induced longevity in C. elegans. *Nature* 447, 545-549.

Bluher, M., Kahn, B. B. and Kahn, C. R. (2003). Extended longevity in mice lacking the insulin receptor in adipose tissue. *Science* 299, 572-574.

Bosch-Presegue, L., Raurell-Vila, H., Marazuela-Duque, A., Kane-Goldsmith, N., Valle, A., Oliver, J., Serrano, L. and Vaquero, A. (2011). Stabilization of Suv39H1 by SirT1 is part of oxidative stress response and ensures genome protection. *Mol Cell* 42, 210-223.

Botuyan, M. V., Lee, J., Ward, I. M., Kim, J. E., Thompson, J. R., Chen, J. and Mer, G. (2006). Structural basis for the methylation state-specific recognition of histone H4-K20 by 53BP1 and Crb2 in DNA repair. *Cell* 127, 1361-1373.

Brunet, A., Bonni, A., Zigmond, M. J., Lin, M. Z., Juo, P., Hu, L. S., Anderson, M. J., Arden, K. C., Blenis, J. and Greenberg, M. E. (1999). Akt promotes cell survival by phosphorylating and inhibiting a Forkhead transcription factor. *Cell* 96, 857-868.

Chen, A. T., Guo, C., Itani, O. A., Budaitis, B. G., Williams, T. W., Hopkins, C. E., McEachin, R. C., Pande, M., Grant, A. R., Yoshina, S., et al. (2015). Longevity Genes Revealed by Integrative Analysis of Isoform-Specific daf-16/FoxO Mutants of Caenorhabditis elegans. *Genetics* 201, 613-629.

Chen, D., Thomas, E. L. and Kapahi, P. (2009). HIF-1 modulates dietary restriction-mediated lifespan extension via IRE-1 in Caenorhabditis elegans. *PLoS Genet* 5, e1000486.

Chuang, P. T., Albertson, D. G. and Meyer, B. J. (1994). DPY-27:a chromosome condensation protein homolog that regulates C. elegans dosage compensation through association with the X chromosome. *Cell* 79, 459-474.

Davie, J. R., Xu, W. and Delcuve, G. P. (2016). Histone H3K4 trimethylation: dynamic interplay with pre-mRNA splicing. *Biochem Cell Biol* 94, 1-11.

Delaney, C., Garg, S. K., Fernandes, C., Hoeltzel, M., Allen, R. H., Stabler, S. and Yung, R. (2013). Maternal diet supplemented with methyl-donors protects against atherosclerosis in F1 ApoE(-/-) mice. *PLoS One* 8, e56253.

Delaney, C., Hoeltzel, M., Garg, S. K., Warner, R., Johnson, K. and Yung, R. (2012). Maternal micronutrient supplementation suppresses T cell chemokine receptor expression and function in F1 mice. *J Nutr* 142, 1329-1335.

Delaney, C. E., Chen, A. T., Graniel, J. V., Dumas, K. J. and Hu, P. J. (2017). A histone H4 lysine 20 methyltransferase couples environmental cues to sensory neuron control of developmental plasticity. *Development*.

Dumas, K. J., Guo, C., Shih, H. J. and Hu, P. J. (2013). Influence of steroid hormone signaling on life span control by Caenorhabditis elegans insulin-like signaling. *G3 (Bethesda)* 3, 841-850.

Field, A. E. and Adams, P. D. (2016). Targeting chromatin aging - The epigenetic impact of longevity-associated interventions. *Exp Gerontol*.

Flachsbart, F., Caliebe, A., Kleindorp, R., Blanche, H., von Eller-Eberstein, H., Nikolaus, S., Schreiber, S. and Nebel, A. (2009). Association of FOXO3A variation with human longevity confirmed in German centenarians. *Proc Natl Acad Sci U S A* 106, 2700-2705.

Garcia-Cao, M., O'Sullivan, R., Peters, A. H., Jenuwein, T. and Blasco, M. A. (2004). Epigenetic regulation of telomere length in mammalian cells by the Suv39h1 and Suv39h2 histone methyltransferases. *Nat Genet* 36, 94-99.

Greer, E. L., Dowlatshahi, D., Banko, M. R., Villen, J., Hoang, K., Blanchard, D., Gygi, S. P. and Brunet, A. (2007). An AMPK-FOXO pathway mediates longevity induced by a novel method of dietary restriction in C. elegans. *Curr Biol* 17, 1646-1656.

Greer, E. L., Maures, T. J., Hauswirth, A. G., Green, E. M., Leeman, D. S., Maro, G. S., Han, S., Banko, M. R., Gozani, O. and Brunet, A. (2010). Members of the H3K4 trimethylation complex regulate lifespan in a germline-dependent manner in C. elegans. *Nature* 466, 383-387.

Guarente, L. and Picard, F. (2005). Calorie restriction--the SIR2 connection. *Cell* 120, 473-482.

Hansen, M., Hsu, A. L., Dillin, A. and Kenyon, C. (2005). New genes tied to endocrine, metabolic, and dietary regulation of lifespan from a Caenorhabditis elegans genomic RNAi screen. *PLoS Genet* 1, 119-128.

Hochbaum, D., Zhang, Y., Stuckenholz, C., Labhart, P., Alexiadis, V., Martin, R., Knolker, H. J. and Fisher, A. L. (2011). DAF-12 regulates a connected network of genes to ensure robust developmental decisions. *PLoS Genet* 7, e1002179.

Honda, Y. and Honda, S. (1999). The daf-2 gene network for longevity regulates oxidative stress resistance and Mn-superoxide dismutase gene expression in Caenorhabditis elegans. *FASEB J* 13, 1385-1393.

Hoogewijs, D., Houthoofd, K., Matthijssens, F., Vandesompele, J. and Vanfleteren, J. R. (2008). Selection and validation of a set of reliable reference genes for quantitative sod gene expression analysis in C. elegans. *BMC Mol Biol* 9, 9.

Hsu, A. L., Murphy, C. T. and Kenyon, C. (2003). Regulation of aging and age-related disease by DAF-16 and heat-shock factor. *Science* 300, 1142-1145.

Imai, S. and Kitano, H. (1998). Heterochromatin islands and their dynamic reorganization: a hypothesis for three distinctive features of cellular aging. *Exp Gerontol* 33, 555-570.

Jin, C., Li, J., Green, C. D., Yu, X., Tang, X., Han, D., Xian, B., Wang, D., Huang, X., Cao, X., et al. (2011). Histone demethylase UTX-1 regulates C. elegans life span by targeting the insulin/IGF-1 signaling pathway. *Cell Metab* 14, 161-172.

Jorgensen, S., Schotta, G. and Sorensen, C. S. (2013). Histone H4 lysine 20 methylation: key player in epigenetic regulation of genomic integrity. *Nucleic Acids Res* 41, 2797-2806.

Kamath, R. S., Martinez-Campos, M., Zipperlen, P., Fraser, A. G. and Ahringer, J. (2001). Effectiveness of specific RNA-mediated interference through ingested double-stranded RNA in Caenorhabditis elegans. *Genome Biol* 2, RESEARCH0002.

Kelly, W. G., Xu, S., Montgomery, M. K. and Fire, A. (1997). Distinct requirements for somatic and germline expression of a generally expressed Caernorhabditis elegans gene. *Genetics* 146, 227-238.

Kennedy, B. K., Steffen, K. K. and Kaeberlein, M. (2007). Ruminations on dietary restriction and aging. *Cell Mol Life Sci* 64, 1323-1328.

Kenyon, C., Chang, J., Gensch, E., Rudner, A. and Tabtiang, R. (1993). A C. elegans mutant that lives twice as long as wild type. *Nature* 366, 461-464.

Lamming, D. W. (2016). Inhibition of the Mechanistic Target of Rapamycin (mTOR)-Rapamycin and Beyond. *Cold Spring Harb Perspect Med* 6.

Lan, F. and Shi, Y. (2009). Epigenetic regulation: methylation of histone and non-histone proteins. *Sci China C Life Sci* 52, 311-322.

Lan, J., Zhang, X. and Chen, D. (2015). Molecular mechanisms of dietary restriction in aging-insights from Caenorhabditis elegans research. *Sci China Life Sci* 58, 352-358.

Lapierre, L. R., De Magalhaes Filho, C. D., McQuary, P. R., Chu, C. C., Visvikis, O., Chang, J. T., Gelino, S., Ong, B., Davis, A. E., Irazoqui, J. E., et al. (2013). The TFEB orthologue HLH-30 regulates autophagy and modulates longevity in Caenorhabditis elegans. *Nat Commun* 4, 2267.

Larson, K., Yan, S. J., Tsurumi, A., Liu, J., Zhou, J., Gaur, K., Guo, D., Eickbush, T. H. and Li, W. X. (2012). Heterochromatin formation promotes longevity and represses ribosomal RNA synthesis. *PLoS Genet* 8, e1002473.

Lau, A. C., Nabeshima, K. and Csankovszki, G. (2014). The C. elegans dosage compensation complex mediates interphase X chromosome compaction. *Epigenetics Chromatin* 7, 31.

Lee, R. Y., Hench, J. and Ruvkun, G. (2001). Regulation of C. elegans DAF-16 and its human ortholog FKHRL1 by the daf-2 insulin-like signaling pathway. *Curr Biol* 11, 1950-1957.

Leiser, S. F., Miller, H., Rossner, R., Fletcher, M., Leonard, A., Primitivo, M., Rintala, N., Ramos, F. J., Miller, D. L. and Kaeberlein, M. (2015). Cell nonautonomous activation of flavin-containing monooxygenase promotes longevity and health span. *Science* 350, 1375-1378.

Li, W., Kennedy, S. G. and Ruvkun, G. (2003). daf-28 encodes a C. elegans insulin superfamily member that is regulated by environmental cues and acts in the DAF-2 signaling pathway. *Genes Dev* 17, 844-858.

Libina, N., Berman, J. R. and Kenyon, C. (2003). Tissue-specific activities of C. elegans DAF-16 in the regulation of lifespan. *Cell* 115, 489-502.

Lieber, C. S. (2002). S-Adenosyl-L-methionine and alcoholic liver disease in animal models: implications for early intervention in human beings. *Alcohol* 27, 173-177.

Lin, K., Hsin, H., Libina, N. and Kenyon, C. (2001). Regulation of the Caenorhabditis elegans longevity protein DAF-16 by insulin/IGF-1 and germline signaling. *Nat Genet* 28, 139-145.

Liu, W., Tanasa, B., Tyurina, O. V., Zhou, T. Y., Gassmann, R., Liu, W. T., Ohgi, K. A., Benner, C., Garcia-Bassets, I., Aggarwal, A. K., et al. (2010). PHF8 mediates histone H4 lysine 20 demethylation events involved in cell cycle progression. *Nature* 466, 508-512.

Lopez-Otin, C., Blasco, M. A., Partridge, L., Serrano, M. and Kroemer, G. (2013). The hallmarks of aging. *Cell* 153, 1194-1217.

Mathew, R., Pal Bhadra, M. and Bhadra, U. (2017). Insulin/insulin-like growth factor-1 signalling (IIS) based regulation of lifespan across species. *Biogerontology* 18, 35-53.
Mello, C. C., Kramer, J. M., Stinchcomb, D. and Ambros, V. (1991). Efficient gene transfer in C.elegans: extrachromosomal maintenance and integration of transforming sequences. *Embo J* 10, 3959-3970.
Melo, J. A. and Ruvkun, G. (2012). Inactivation of conserved C. elegans genes engages pathogen- and xenobiotic-associated defenses. *Cell* 149, 452-466.
Mentch, S. J. and Locasale, J. W. (2016). One-carbon metabolism and epigenetics: understanding the specificity. *Ann N Y Acad Sci* 1363, 91-98.
Miller, R. A., Buehner, G., Chang, Y., Harper, J. M., Sigler, R. and Smith-Wheelock, M. (2005). Methionine-deficient diet extends mouse lifespan, slows immune and lens aging, alters glucose, T4, IGF-I and insulin levels, and increases hepatocyte MIF levels and stress resistance. *Aging Cell* 4, 119-125.
Nolan, T., Hands, R. E. and Bustin, S. A. (2006). Quantification of mRNA using real-time RT-PCR. *Nat Protoc* 1, 1559-1582.
O'Rourke, E. J. and Ruvkun, G. (2013). MXL-3 and HLH-30 transcriptionally link lipolysis and autophagy to nutrient availability. *Nat Cell Biol* 15, 668-676.
Obata, F. and Miura, M. (2015). Enhancing S-adenosyl-methionine catabolism extends Drosophila lifespan. *Nat Commun* 6, 8332.
Oberdoerffer, P. and Sinclair, D. A. (2007). The role of nuclear architecture in genomic instability and ageing. *Nat Rev Mol Cell Biol* 8, 692-702.
Orentreich, N., Matias, J. R., DeFelice, A. and Zimmerman, J. A. (1993). Low methionine ingestion by rats extends life span. *J Nutr* 123, 269-274.
Paix, A., Folkmann, A., Rasoloson, D. and Seydoux, G. (2015). High Efficiency, Homology-Directed Genome Editing in Caenorhabditis elegans Using CRISPR-Cas9 Ribonucleoprotein Complexes. *Genetics* 201, 47-54.
Panowski, S. H., Wolff, S., Aguilaniu, H., Durieux, J. and Dillin, A. (2007). PHA-4/Foxa mediates diet-restriction-induced longevity of C. elegans. *Nature* 447, 550-555.
Pei, H., Zhang, L., Luo, K., Qin, Y., Chesi, M., Fei, F., Bergsagel, P. L., Wang, L., You, Z. and Lou, Z. (2011). MMSET regulates histone H4K20 methylation and 53BP1 accumulation at DNA damage sites. *Nature* 470, 124-128.
Peters, A. H., O'Carroll, D., Scherthan, H., Mechtler, K., Sauer, S., Schofer, C., Weipoltshammer, K., Pagani, M., Lachner, M., Kohlmaier, A., et al. (2001). Loss of the Suv39h histone methyltransferases impairs mammalian heterochromatin and genome stability. *Cell* 107, 323-337.
Raizen, D. M., Lee, R. Y. and Avery, L. (1995). Interacting genes required for pharyngeal excitation by motor neuron MC in Caenorhabditis elegans. *Genetics* 141, 1365-1382.
Rothbart, S. B., Dickson, B. M., Raab, J. R., Grzybowski, A. T., Krajewski, K., Guo, A. H., Shanle, E. K., Josefowicz, S. Z., Fuchs, S. M., Allis, C. D., et al. (2015). An Interactive Database for the Assessment of Histone Antibody Specificity. *Mol Cell* 59, 502-511.
Salminen, A., Kaarniranta, K. and Kauppinen, A. (2016). AMPK and HIF signaling pathways regulate both longevity and cancer growth: the good news and the bad news about survival mechanisms. *Biogerontology* 17, 655-680.
Sanders, S. L., Portoso, M., Mata, J., Bahler, J., Allshire, R. C. and Kouzarides, T. (2004). Methylation of histone H4 lysine 20 controls recruitment of Crb2 to sites of DNA damage. *Cell* 119, 603-614.

Sarg, B., Helliger, W., Talasz, H., Koutzamani, E. and Lindner, H. H. (2004). Histone H4 hyperacetylation precludes histone H4 lysine 20 trimethylation. *J Biol Chem* 279, 53458-53464.

Sarg, B., Koutzamani, E., Helliger, W., Rundquist, I. and Lindner, H. H. (2002). Postsynthetic trimethylation of histone H4 at lysine 20 in mammalian tissues is associated with aging. *J Biol Chem* 277, 39195-39201.

Schotta, G., Lachner, M., Sarma, K., Ebert, A., Sengupta, R., Reuter, G., Reinberg, D. and Jenuwein, T. (2004). A silencing pathway to induce H3-K9 and H4-K20 trimethylation at constitutive heterochromatin. *Genes Dev* 18, 1251-1262.

Schotta, G., Sengupta, R., Kubicek, S., Malin, S., Kauer, M., Callen, E., Celeste, A., Pagani, M., Opravil, S., De La Rosa-Velazquez, I. A., et al. (2008). A chromatin-wide transition to H4K20 monomethylation impairs genome integrity and programmed DNA rearrangements in the mouse. *Genes Dev* 22, 2048-2061.

Serrano, L., Martinez-Redondo, P., Marazuela-Duque, A., Vazquez, B. N., Dooley, S. J., Voigt, P., Beck, D. B., Kane-Goldsmith, N., Tong, Q., Rabanal, R. M., et al. (2013a). The tumor suppressor SirT2 regulates cell cycle progression and genome stability by modulating the mitotic deposition of H4K20 methylation. *Genes & development* 27, 639-653.

---- (2013b). The tumor suppressor SirT2 regulates cell cycle progression and genome stability by modulating the mitotic deposition of H4K20 methylation. *Genes Dev* 27, 639-653.

Shirayama, M., Seth, M., Lee, H. C., Gu, W., Ishidate, T., Conte, D., Jr. and Mello, C. C. (2012). piRNAs initiate an epigenetic memory of nonself RNA in the C. elegans germline. *Cell* 150, 65-77.

Shumaker, D. K., Dechat, T., Kohlmaier, A., Adam, S. A., Bozovsky, M. R., Erdos, M. R., Eriksson, M., Goldman, A. E., Khuon, S., Collins, F. S., et al. (2006). Mutant nuclear lamin A leads to progressive alterations of epigenetic control in premature aging. *Proc Natl Acad Sci U S A* 103, 8703-8708.

Souza, P. P., Volkel, P., Trinel, D., Vandamme, J., Rosnoblet, C., Heliot, L. and Angrand, P. O. (2009). The histone methyltransferase SUV420H2 and Heterochromatin Proteins HP1 interact but show different dynamic behaviours. *BMC Cell Biol* 10, 41.

Strome, S., Kelly, W. G., Ercan, S. and Lieb, J. D. (2014). Regulation of the X chromosomes in Caenorhabditis elegans. *Cold Spring Harb Perspect Biol* 6.

Talens, R. P., Christensen, K., Putter, H., Willemsen, G., Christiansen, L., Kremer, D., Suchiman, H. E., Slagboom, P. E., Boomsma, D. I. and Heijmans, B. T. (2012). Epigenetic variation during the adult lifespan: cross-sectional and longitudinal data on monozygotic twin pairs. *Aging Cell* 11, 694-703.

Timmons, L., Court, D. L. and Fire, A. (2001). Ingestion of bacterially expressed dsRNAs can produce specific and potent genetic interference in Caenorhabditis elegans. *Gene* 263, 103-112.

Tsurumi, A. and Li, W. X. (2012). Global heterochromatin loss: a unifying theory of aging? *Epigenetics* 7, 680-688.

Vanyushin, B. F., Nemirovsky, L. E., Klimenko, V. V., Vasiliev, V. K. and Belozersky, A. N. (1973). The 5-methylcytosine in DNA of rats. Tissue and age specificity and the changes induced by hydrocortisone and other agents. *Gerontologia* 19, 138-152.

Vaquero, A., Scher, M., Erdjument-Bromage, H., Tempst, P., Serrano, L. and Reinberg, D. (2007). SIRT1 regulates the histone methyl-transferase SUV39H1 during heterochromatin formation. *Nature* 450, 440-444.

Vielle, A., Lang, J., Dong, Y., Ercan, S., Kotwaliwale, C., Rechtsteiner, A., Appert, A., Chen, Q. B., Dose, A., Egelhofer, T., et al. (2012). H4K20me1 contributes to downregulation of X-linked genes for C. elegans dosage compensation. *PLoS genetics* 8, e1002933.

Villeponteau, B. (1997). The heterochromatin loss model of aging. *Exp Gerontol* 32, 383-394.

Webster, C. M., Wu, L., Douglas, D. and Soukas, A. A. (2013). A non-canonical role for the C. elegans dosage compensation complex in growth and metabolic regulation downstream of TOR complex 2. *Development* 140, 3601-3612.

Wells, M. B., Snyder, M. J., Custer, L. M. and Csankovszki, G. (2012). Caenorhabditis elegans dosage compensation regulates histone H4 chromatin state on X chromosomes. *Molecular and cellular biology* 32, 1710-1719.

Willcox, B. J., Donlon, T. A., He, Q., Chen, R., Grove, J. S., Yano, K., Masaki, K. H., Willcox, D. C., Rodriguez, B. and Curb, J. D. (2008). FOXO3A genotype is strongly associated with human longevity. *Proc Natl Acad Sci U S A* 105, 13987-13992.

Yamamoto, R. and Tatar, M. (2011). Insulin receptor substrate chico acts with the transcription factor FOXO to extend Drosophila lifespan. *Aging Cell* 10, 729-732.

Chapter 6

Conclusions and outstanding questions

Overview

We undertook the investigations presented in this dissertation to begin building fluency in how epigenetic mechanisms participate in DAF-16/FoxO mediated longevity. While the signaling logic of the insulin-like signaling pathway is well understood, how DAF-16/FoxO cooperates with chromatin modifiers remains incompletely understood. Emerging evidence suggests epigenetic mechanisms regulate not only expression of IIS signaling genes but also facilitate FoxO transcription factor binding to promoters. For example, DAF-16/FoxO is known to physically associate with the SWI-SNF chromatin-remodeling complex to promote transcription of target genes (Riedel et al., 2013). FoxO also is re-activated in tumor cells treated with DNA-hypomethylating agents (Thepot et al., 2011). Since DAF-16/FoxO can bind upstream of thousands of genes (Kumar et al., 2015), the epigenetic landscape may play a critical role in defining the stress response programs underlying developmental diapause and extended longevity across taxa. We showed that in *C. elegans* the H4K20 methyltransferase SET-4 promotes DAF-16/FoxO activity through repression of the DAF-2/IGFR agonist INS-9 (Delaney et al., 2017). Intriguingly, H4K20 methylation of the *igf2* locus was different between distinct models of senescence in human embryonic lung fibroblasts, suggesting that H4K20 regulation of insulin-like peptides and FoxO activity may be conserved in mammals (Zhang et al., 2010).

Throughout the preceding chapters we used dauer arrest as a readout of DAF-16/FoxO activity. This alternate developmental fate of *C. elegans* provides an obvious phenotype suitable for screening for new pathway regulators. Interestingly, the SEAK screen produced a disproportionate number of strains featuring direct or mechanistic disruption of X chromosome gene expression (Delaney et al., 2017; Dumas et al., 2013; Itani et al., 2015). In chapters 3 and 4,

we reported how disrupting *set-4* led to a nonlinear increase in expression of the DAF-2/IGFR agonist *ins-9*, suggestive of a novel feedback loop contributing to the dauer decision. Such findings implicate the importance of maintaining chromosome-wide epigenetic programs in preserving developmental plasticity. In chapter 5, we began to explore how SET-4 promotes longevity. That we observed longevity extension in a DAF-16/FoxO independent manner demonstrates the complex role of epigenetic programs in diverse developmental and cellular contexts.

SET-4 acts in a sex-dependent manner to promote dauer arrest

Using an unbiased approach, we isolated animals that failed to arrest as dauers at 25°C despite a genetic background associated with enhanced DAF-16/FoxO activity. Unexpectedly, many strains had mutations in epigenetic modifiers. We identified three strains with mutations in the conserved member of the dosage compensation complex (DCC), DPY-21, as well as the conserved SUV4-20 methyltransferase SET-4 (Delaney et al., 2017; Dumas et al., 2013). After establishing that dosage compensation *per se* promotes dauer arrest in XX hermaphrodites, we found that *set-4* mutant animals demonstrated the same gender-dependent phenotype as dosage compensation knockdown. Both *dpy-21* and *set-4* mutant animals were insensitive to dauer-inducing pheromone, demonstrating the physiological relevance of these epigenetic actors in promoting dauer. Surprisingly, post-embryonic *set-4* expression is restricted to neurons, including sensory neurons which have been shown to be required for dauer arrest (Bargmann and Horvitz, 1991). We confirmed that neuronal expression of SET-4 is functionally relevant (Fig. 3.3C), and restoration of SET-4 solely in the ASI sensory neurons was sufficient for dauer arrest (Fig. 4.2). While DPY-21 acts in several pathways to promote dauer, SET-4 is specific to IIS, allowing us to enrich for genes regulated by dosage compensation that regulate DAF-16/FoxO activity in neurons.

This work was one of the first to implicate histone H4 lysine 20 methylation in regulation of FoxO transcription factor activation. Nevertheless, emerging findings in mammals may indicate that interplay between H4K20 and FoxO is conserved. Expression of the SET-4 ortholog SUV420H2 is dramatically upregulated in osteoblastogenesis, and is required for H4K20me3 (Khani et al., 2017). Knockdown of SUV420H2 in these cells down-regulated markers

associated with osteoblast differentiation. Deficits in osteoblast differentiation are not due to general loss of heterochromatin because inhibition of the H3K27 methyltransferase EZH2 decreases H3K27me3 but accelerates osteoblast differentiation (Dudakovic et al., 2016). Induction of osteoblast differentiation in bone progenitor cell lines was associated with decreased phosphorylation of the insulin receptor β subunit, Akt, and FoxO1 (Dudakovic et al., 2013). FoxO activity has been shown to play a role in reducing oxidative stress in osteoblasts and promoting bone homeostasis (Ambrogini et al., 2010; Li et al., 2010; Rached et al., 2010). Taken together, these findings suggest there may be a link between H4K20 methylation and FoxO activity promoting skeletal bone integrity that warrants further investigation.

INS-9 may represent a novel node integrating upstream and downstream signals during environmental stress

Using transcriptome profiling, we identified the incompletely characterized insulin-like peptide *ins-9* (Delaney et al., 2017). *ins-9* is the only X-linked ILP gene, making it potentially subject to dosage compensation. We found that *ins-9* is expressed primarily in ASI sensory neurons, the origin of many neuroendocrine signals that mediate the dauer decision. Overexpressing *ins-9* was sufficient for dauer bypass in animals that typically arrest at 25°C, while novel null alleles of *ins-9* partially rescued the defect in *set-4;daf-2* animals and completely rescued the *set-4* mutant defect in pheromone response. We demonstrated that DPY-21, SET-4, and DAF-16/FoxO are all necessary for silencing *ins-9*, creating the potential for feedback regulation on DAF-16/FoxO activity. Consistent with a feed-forward model, in *dpy-21* and *set-4* mutant backgrounds *ins-9* expression increased far greater than the two-fold change expected from disruption of dosage compensation. Other ILP regulatory loops have been suggested to play a role in the dauer decision (Hahm et al., 2009; Matsunaga et al., 2012). The decision whether to proceed with reproductive development or arrest as dauers is based on complex environmental stimuli acting through multiple signal transduction pathways and different tissues. Yet the dauer decision is all-or-nothing. Past a certain developmental time, animals become committed to their fate (Schaedel et al., 2012). Feed forward signaling loops involving ILPs like INS-9 may be part of the mechanism through which animals integrate their inputs to commit to alternate developmental strategies.

In addition to providing evidence of DAF-16/FoxO feedback on to *ins-9* expression, we showed that exposure to dauer pheromone also silenced *ins-9* in a DAF-16/FoxO independent manner (Fig. 4.3). *daf-28* expression is believed to be regulated by pheromone like *ins-9*, but these ILPs act in parallel to promote dauer bypass (Fig. 4.4). Therefore, upstream and downstream inputs converge on the *ins-9* gene to repress activation of DAF-2/IGFR. Remarkably, how pheromone promotes dauer arrest is still poorly understood, but it is known that pheromone represses other ASI neuroendocrine signals including *daf-7*, *daf-28*, and *ins-6* (Cornils et al., 2011; Li et al., 2003; Ren et al., 1996). Understanding *ins-9* regulatory dynamics may lead to clarifying how population stress is transduced into the decision to enter diapause.

The purpose of our genetic screen was to find novel regulators of DAF-16/FoxO (Dumas et al., 2013). The discovery of *ins-9* regulatory dynamics demonstrates the utility of our approach. Because *ins-9* null alleles do not have a dauer phenotype, identifying this gene as potentially important in transducing upstream pheromone signals into DAF-16/FoxO activation would be unlikely in an un-sensitized background. We found that SET-4 and DPY-21/DCC are required epigenetic co-factors that partner with DAF-16/FoxO to fully silence *ins-9*. Similarly, the extreme redundancy within the *C. elegans* family of ILPs could easily mask the importance of any one member. The unique position of *ins-9* on the X chromosome was critical for its discovery and subsequent characterization. Taken together, what emerges is an appreciation that chromosomal location and chromosome-wide epigenetic regulatory mechanisms can synergize with conserved signal transduction pathways to control complex developmental fates.

A novel behavioral model of dietary restriction

Having established a role for SET-4 in promoting DAF-16/FoxO activity during development, we asked whether SET-4 also promotes longevity. Previous data using RNAi suggested *set-4* was associated with aging (Greer et al., 2010). Epigenetic modifications are likely to have multiple effects on gene expression that vary in their influence throughout a lifetime. Therefore, it is not necessarily inconsistent that SET-4 may act differently in development and during aging. We sought to clarify this discrepancy using loss of function mutants and overexpression.

In contrast to RNAi data, we found that *set-4* mutant animals live consistently shorter than their wild type siblings (Fig. 5.1A). Animals could be sick or it could be that SET-4 promotes longevity. It remains unclear how loss of *set-4* shortens lifespan. Possible mechanisms include chronic, modest impairment of dosage compensation over time or upregulation of DAF-16 inhibitors during development. Comparative analyses of early and late life *set-4* transcriptomes relative to wild type animals may be informative in clarifying epigenetic influences of longevity.

Consistent with the idea that SET-4 promotes longevity, we observed animals overexpressing *set-4* lived longer than their wild type siblings (Fig. 5.1B). These animals presented a phenotype consistent with dietary restriction. Dietary restriction operates in part through DAF-16/FoxO independent mechanisms, and we confirmed that lifespan extension in *set-4* overexpressors did not require DAF-16/FoxO. These animals lack obvious physiological defects that could decrease food consumption; rather, they manifest food avoiding behavior, choosing to eat less during development. Fasting behavior induces the longevity-associated *hlh-30* transcription factor and its target genes involved in detoxification and fat metabolism. Specifically, lipase activity may be required for longevity in this model (Fig. 5.4D-E).

The induction of downstream longevity programs may occur in a cell-nonautonomous fashion. *set-4* expression is restricted to neurons in the soma and inhibits insulin-like peptide signaling (Delaney et al., 2017). Therefore, it is conceivable that *set-4* mediated alterations of neuronal signals may contribute to longevity. Previous work demonstrated that SKN-1/NRF2 acting in ASI sensory neurons is required for increased lifespan during DR (Bishop and Guarente, 2007). SET-4 expression in ASI is sufficient for dauer arrest (Fig. 4.2). Further, preliminary data indicates that the ASI-specific *skn-1b* isoform was required for lipase expression (Fig. 5.4F-G). Whether SET-4 mediates lifespan extension from sensory neurons, and if SKN-1 is necessary for this extension, remains to be addressed.

SET-4 promotes higher order methylation of H4K20 that is associated with gene silencing and quiescence. Greater methylation of histones leads to catabolism of SAM. Both increased consumption of SAM and reduction in SAM synthesis is known to promote longevity, DR-associated phenotypes, and food avoidance behavior (Hansen et al., 2005; Melo and Ruvkun, 2012; Obata and Miura, 2015). Using this model, we may be able to clarify how metabolite levels in one tissue induce conserved longevity programs in other tissues. Identifying these key

metabolic signals may provide new targets therapeutic interventions for chronic illnesses like obesity and diabetes.

While it remains necessary to confirm whether longevity associated with *set-4* overexpression is due to conserved SET-4 methyltransferase activity, we have isolated strains whose food avoiding behavior leads to phenotypes characteristic of dietary restriction. Comparison with the *eat-2* model at the transcriptional level may provide clues in to which genes modulated by DR are important for longevity (Heestand et al., 2013). The downstream consequences of DR are shared across regimens, but the means of inducing DR are variable and have identified both parallel and interacting signaling pathways for DR-induced longevity (Greer and Brunet, 2009). This disconnect between models may be due to many factors, such as at what developmental stage animals are subjected to DR and whether these animals are cultured in liquid or on solid media. *set-4* overexpressors can be cultivated under identical conditions as *eat-2* animals, eliminating experimental confounds in cross-model analyses. What may emerge is a clearer understanding of the pathways critical for longevity in animals experience lifelong dietary restriction.

CRISPR-Cas9 offers unprecedented genomic precision in evaluating gene function

While conducting the research presented in this dissertation, the discovery and subsequent optimization of CRISPR-Cas9 mediated genome editing greatly enhanced our ability to manipulate the *C. elegans* genome. We benefited from this technological advance and characterized different methods of genome editing. Several vector-based methods as well as a method employing recombinant protein and guide RNA have been described (Dickinson et al., 2015; Farboud and Meyer, 2015; Paix et al., 2015). Although vector-based systems could produce results (as evidenced by the *dpSi6* construct discussed below), we found this method to be highly inefficient. We also observed a high degree of chimerism, where Cas9 became active only in somatic cells, leading to animals possessing the expected phenotype of the *dpy-10* co-injected marker but unable to transmit that phenotype to progeny. As a positive, we did recover an insert that was greater than 5 kb, suggesting this method has similar insert potential as the mosSCI method (Frokjaer-Jensen et al., 2010) in addition to greater flexibility as to where in the genome constructs can be inserted.

In comparison to the vector-based genome editing, we found the Paix/Seydoux method using recombinant Cas9 and RNA in combination with PCR or oligo repair templates to be robust (Paix et al., 2015). Further, we have shown that PCR amplicons up to 3 kb in size can be inserted using this method. That said, homology-directed repair using single-stranded oligo templates of approximately 100 bp we found most efficient. Importantly, PCR-based homology directed repair might allow extrachromosomal arrays to assemble in animals. If the amplicon contains gene-activating regulatory sequences like promoters, false positives are possible.

Despite the relative ease of editing genomes using CRISPR, we observed unexpected confounds in edited strains. We found that CRISPR mutagenesis may lead to multigenerational silencing of the edited locus, consistent with reports using both mosSCI and CRISPR mediated transgenesis (Leopold et al., 2015). When propagating or crossing animals, it is important to select for animals expressing a marker like fluorescence if possible. If no marker or phenotype is present, strains may have to be propagated or outcrossed for several generations prior to an insert to become functional. This phenomenon is likely mediated by endogenous RNAi mechanisms (Leopold et al., 2015; Luteijn et al., 2012; Shirayama et al., 2012) and may be more problematic when inserting fragments containing gene-regulatory information (Alexander Paix, personal communication). Not only is stochastic silencing an issue, off-target cuts elsewhere in the genome remain a potential confound. Good practice, therefore, is to isolate and test several transgenic lines even if they contain genetically identical alleles. These strains should also be outcrossed several times, which in our hands seemed to alleviate locus silencing. When feasible, a reporter showing locus activity should be included, or injected animals should be defective in endogenous RNAi pathways that may participate in silencing. While CRISPR continues to be optimized in worm systems, a role for classical transgenesis will persist due to the limitations of single copy constructs including insert size, reporter detection, and RNAi-mediated silencing.

Generating novel alleles using CRISPR was critical for our understanding of *ins-9*'s emerging role inhibiting DAF-16/FoxO during development. The flexibility and precision of this technology is revolutionizing how we examine specific genes' activities. This work also demonstrated the continuing value of classic mutagenesis screens. The SEAK screen produced a functionally null *set-4* allele, pinpointing an active site residue deemed essential in human orthologs (Southall et al., 2014; Wu et al., 2013). Despite SET-4 being required for H4K20me2

and me3, and that SET-4 promotes dosage compensation, *set-4* null animals have no obvious phenotypes. Surprisingly few genes are differentially expressed between *set-4* mutants and wild type animals (Kramer et al., 2015). Only within the context of reduced insulin-like signaling were we able to begin to understand the role for *set-4* during development. Combining classical genetics, next generation sequencing, and genome editing is likely to greatly accelerate our understanding of genetic and epigenetic regulation of conserved programs in development.

Outstanding Questions

How does pheromone regulate INS-9 activity?

Genetics, stressors, and neuronal ablation have all be used to dissect the dauer developmental paradigm (Hu, 2007). Dauer pheromone has been shown to enhance arrest in daf-c strains at temperatures that permit reproductive development (Thomas et al., 1993). Remarkably, no reports have shown the effects of combining pheromone treatment with selective ablation of sensory neurons. As such, the exact neuronal circuitry required to respond to population stress is not established. Others have shown that ILP production in ASI as well as DAF-7/TGF-β is sensitive to dauer pheromone (Cornils et al., 2011; Li et al., 2003; Ren et al., 1996; Schackwitz et al., 1996), supporting our data implicating ASI in the translation of stress signals into neuroendocrine responses.

INS-9 is a type β ILP made in ASI sensory neurons that promotes reproductive development. It is unique among previously described ILPs to be regulated both by dauer inducing pheromone and DAF-16/FoxO. We established that enhanced DAF-16/FoxO activity silences *ins-9* expression in a manner dependent on dosage compensation effectors DPY-21 and SET-4 (Delaney et al., 2017). However, pheromone silences *ins-9* independently of DAF-16/FoxO. How pheromone acts on the *ins-9* locus remains to be elucidated.

SET-4 is required for pheromone induction of dauer arrest, while *ins-9* ablation rescues the defect in *set-4* mutant animals. Based on these findings, our hypothetical model of *ins-9* regulation shows pheromone acting through SET-4 and DPY-21 to repress *ins-9* (Fig. 3.6). However, it is possible that pheromone and dosage compensation regulate *ins-9* in parallel. We

will cross our endogenous *ins-9* reporter into distinct daf-c and daf-d backgrounds to test whether parallel dauer pathways converge on *ins-9* and whether SET-4 and DPY-21 are required to silence *ins-9* in the presence of pheromone. Similarly, because we can detect the single copy *ins-9* reporter, we can screen for genes important for pheromone-mediated *ins-9* repression. Understanding *ins-9*'s role in the relay of extrinsic signals into morphologically distinct outcomes may clarify the distinct pathways that feed in to insulin-like signaling to promote DAF-16/FoxO longevity.

How does dosage compensation synergize with DAF-16/FoxO to repress *ins-9*?

Maintenance of dosage compensation is important in promoting longevity, while skewing of dosage compensation is associated with diseases of aging (Bajic et al., 2015; Delaney et al., 2017; Gentilini et al., 2012; Yurov et al., 2014). Similarly, IIS pathway repression is an important determinant of overall longevity (Bluher et al., 2003; Kenyon et al., 1993; Yamamoto and Tatar, 2011). In *C. elegans* these seemingly independent regulatory mechanisms intersect during development to promote dauer arrest by repressing X-linked *ins-9* (Delaney et al., 2017; Dumas et al., 2013). How worm dosage compensation is achieved remains unclear, but it is possible that the interplay with DAF-16/FoxO may support certain proposed models. Since the DCC acts over far distances to regulate dosage compensation, other epigenetic partners may be required locally. Our data supports such a model because SET-4, which has previously been associated with dosage compensation, is also required for repression of *ins-9*. The dynamic regulation of DAF-16/FoxO subcellular localization may also inform how dosage compensation works at the level of chromatin architecture. It has been suggested that the DCC prevents association of the X chromosome with regions associated with active transcription near nuclear pores (Sharma and Meister, 2015). DAF-16/FoxO is excluded from the nucleus when IIS is active, presumably by export through nuclear pores. We observed neither dosage compensation nor DAF-16 is sufficient to fully silence INS-9 (Fig. 3.5A). Therefore, in the absence of DAF-16/FoxO the DCC may continue to partially exclude the *ins-9* locus from transcriptionally active perinuclear regions. Disrupting the DCC may permit the *ins-9* locus access to permissive nuclear spaces; however, nuclear DAF-16 can bind the *ins-9* promoter and suppress its transcription (Honda et al., 2011). Examining whether DAF-16/FoxO is enriched in certain subnuclear regions

or if there are changes in DAF-16/FoxO occupancy on the X chromosome in wild type and DCC mutant animals may lead to clarifying how dosage compensation in achieved in *C. elegan*s.

How does EAK-7 inhibit DAF-16/FoxO activity?

One of the potential outcomes of the SEAK screen would be to identify one or more genes that act in the *eak* pathway. EAK proteins act in parallel with IIS to inhibit DAF-16/FoxO without affecting its subcellular location (Alam et al., 2010; Hu et al., 2006). However, the mechanism of this inhibition remains unknown. EAK-7, the most downstream gene identified in the pathway, localizes to the plasma membrane via a myristoylation motif on its N-terminus (Alam et al., 2010). Myristoylation can act both as a membrane anchor as well as an activation switch via intramolecular interactions (Xu et al., 2015).

Using CRISPR, we created myristoylation-dead EAK-7(G2A) mutants (Fig. 6.1A). One of these lines possessed a transmembrane domain on the N-terminus (TM-G2A, *dpSi6*), mimicking the effect of constitutive myristoylation, inserted in a locus on chromosome IV near the cxTi10882 mosSCI insertion site. TM-G2A was sufficient to rescue dauer bypass in *eak-7(tm3188);akt-1* animals at 25°C (Fig. 6.1B). In contrast, the untethered G2A allele, *dp684*, behaved similarly to the null *tm3188* allele when crossed in to an *akt-1* background at 25°C (Fig. 6.1C). These data indicate membrane association is both necessary and sufficient for EAK-7 activity. Therefore, other proteins are likely involved in transducing the signal from EAK-7 to inhibit DAF-16 in the nucleus. Intriguingly, at 27°C, the *dp684* allele may have a stronger dauer phenotype than the *tm3188* allele (Fig. 6.1D). If reproducible, this finding would suggest that the myristoylation-dead EAK-7 might retain binding to proteins important for inhibiting DAF-16/FoxO and sequester them away from their site of action. Future studies using the novel *dp684* allele may provide greater insight into which proteins bind to EAK-7 and how the *eak* pathway inhibits the activity of nuclear DAF-16/FoxO.

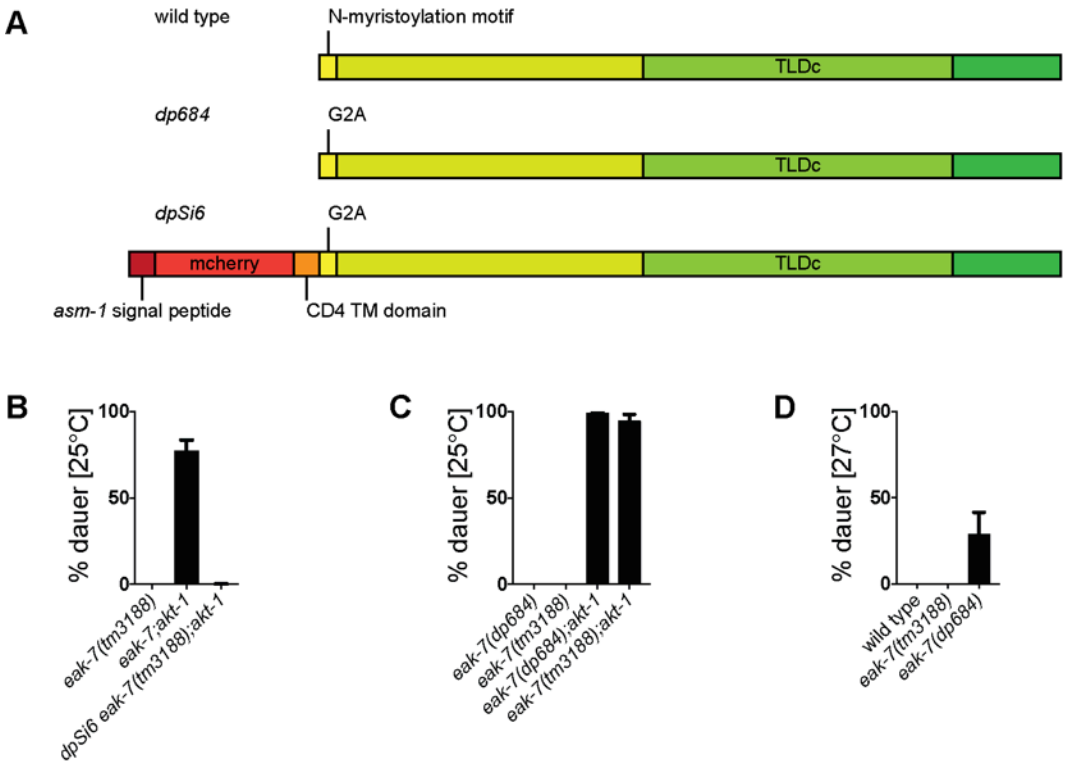

Figure 6.1. EAK-7 membrane association is necessary and sufficient for inhibition of DAF-16/FoxO. (**A**) Schematic of wild type EAK-7 and EAK-7(G2A) mutant protein. (**B**) A transmembrane anchored single-copy transgene encoding myristoylation-dead EAK-7(G2A), *dpSi6*, rescues reproductive development in *eak-7;akt-1* animals. Results are the mean and s.e.m. of three experiments. N = 607, 657, 503. (**C**) The myristoylation-dead *eak-7(dp684)* allele phenocopies the null *eak-7(tm3188)* allele in combination with an *akt-1(ok525)* null allele. Results are the mean and s.e.m. of three experiments. N = 657, 677, 967, 737. (**D**) *eak-7(dp684)* single mutants may arrest at greater rates than the null *eak-7(tm3188)* allele at 27°C on NGM plates containing typical cholesterol levels. Results are a single experiment performed in triplicate. N = 247, 183, 234.

Can we parse whether H4K20 dimethylation or trimethylation of H4K20 is required for dauer arrest?

The dosage compensation complex controls the deposition of H4K20 methylation on the X chromosome. Relative to the autosomes, H4K20me1 is enriched while H4K20me3 is depleted. Loss of dosage compensation rescues the imbalance in H4K20me1 levels (Vielle et al., 2012). Nevertheless, our data along with others suggests that, in addition to SET-1 (monomethylase), SET-4 (di-/tri-methylase) may be required for dosage compensation (Delaney et al., 2017; Lau et al., 2014; Webster et al., 2013; Wells et al., 2012). We confirmed previous data that demonstrated SET-4 is required for both H4K20 di- and tri-methylation (Delaney et al., 2017; Vielle et al., 2012; Wells et al., 2012); however, two possible interpretations of these data are that 1) SET-4 performs both functions, combining the functions of the two closely related mammalian homologs SUV420H1 and SUV420H2, and/or 2) a different lysine methyltransferase performs H4K20 trimethylation yet requires a dimethylated substrate upon which to act. These possibilities are not mutually exclusive, as multiple lysine methyltransferases may act on the same substrate (Greer et al., 2014; Towbin et al., 2012), and these histone methyltransferases may be expressed at different developmental times or tissues in a regulated fashion.

Examining SET-4 orthologs provides conflicting data as to whether SUV4-20 enzymes can trimethylate H4K20. The SET domain of SUV4-20 methyltransferases is highly conserved from fission yeast to mammals, but these homologs display marked differences in number of methyl groups able to be transferred to the lysine substrate. For example, in *Schizosaccharomyces pombe*, Set9 is required for all three methylation states of H4K20 (Sanders et al., 2004; Wang et al., 2009). *Drosophila* SUV4-20, like SET-4, is believed to generate both dimethyllysine and trimethyllysine products with a preference for dimethylation (Yang et al., 2008). However, both fission yeast and fly data are similarly confounded. Because SUV4-20 enzymes are necessary for lower methylation states, attributing trimethylation activity is not possible *in vivo*.

Mammals have two SUV4-20 orthologs with nonredundant roles in development that recognize different consensus binding motifs on histone and non-histone substrates (Schotta et al., 2008; Weirich et al., 2016). Immunofluorescence experiments in mouse embryonic fibroblasts (MEFs) lacking SUV420H1 are deficient in H4K20me2 while H4K20me3 remains intact. Conversely,

MEFs lacking SUV420H2 lack H4K20me3 but retain H4K20me2. Importantly, antibodies to specific histone post-translational modifications sometimes exhibit cross-reactivity with other methylation states of the same residue or even modifications on other histone tails. Nevertheless, these data suggest that SUV420H1 is the mammalian H4K20 dimethylase while SUV420H2 can trimethylated H4K20, and both enzymes act on a monomethylated substrate to generate distinct modifications.

In contrast to these findings, others and we have shown that SET-4 and SUV420H2, like SUV420H1, is limited to dimethylation *in vitro* using mass spectrometry and recombinant peptide substrates (Delaney et al., 2017; Southall et al., 2014; Wu et al., 2013). Importantly, in these *in vitro* assays, truncated human proteins possessing intact SET domains were used for analysis, and only peptide substrates were used. When whole nucleosome substrates were used, truncated versions of both SUV420H1 and SUV420H2 were reported to trimethylate H4K20 (Schotta et al., 2004). We incubated recombinant GST::SET-4 and GST::SUV420H2 with 2.5 µg HeLa nucleosomes for 12 hr at 30°C as described (Delaney et al., 2017). Full length GST::SUV420H2 was capable of increasing trimethylated H4K20 while SET-4 depleted H4K20me1 without generating a detectable trimethylated product (Fig. 6.2). Together with mass spectrometry data, this is consistent with SET-4 being limited to dimethylation.

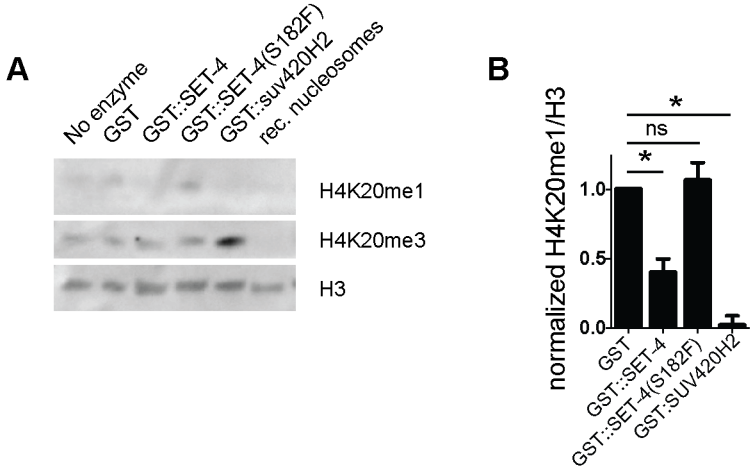

Figure 6.2. SET-4 does not trimethylate H4K20 nucleosomes in vitro. (**A**) Histone methyltransferase assays were performed as described in Delaney *et. al*., 2017 for 12 hr at 30°C. H4K20 modifications were detected with western blotting. (**B**). Quantification of H4K20me1 depletion in (A). Results are the mean and s.e.m of three experiments. $P < 0.05$.

SET-4 is more similar to SUV420H1 than SUV420H2 in the amino acid residues near the catalytic serine. Intriguingly, the side chains of the +1 amino acid adjacent to the catalytic serine in SET-4/SUV420H1 and SUV420H2, valine and isoleucine, respectively, differ by a single methyl group; however, crystallization studies suggest these side chains stabilize protein-histone binding via hydrophobic interactions rather than participate in catalysis (Southall et al., 2014). Crystal structures also suggest that trimethylation function is energetically unfavorable due to hydrogen bonding between the active site serine and the lysine ε-Nitrogen, suggesting that SUV420 enzymes may be limited to dimethylation activity and/or they may require cofactors to gain trimethylase activity. These reports also demonstrated that the analogous residue to SET-4 serine 182 is absolutely required for enzymatic activity in both SUV420H1 and SUV420H2, consistent with our data suggesting *set-4(dp268)* is a functionally null allele (Delaney et al., 2017).

SUV4-20 methyltransferases are most divergent in their post-SET C-terminal domains. These differences may be critical for proper localization and function. SET-4 is unique among its homologs in not possessing an extensive post-SET domain. In contrast, SUV420H2 contains a chromoshadow motif, which directs its localization to constitutive heterochromatin through interactions with HP1 (Smothers and Henikoff, 2000; Souza et al., 2009). Such an interaction may facilitate subsequent trimethylation. Although HP1 is implicated in regulating trimethylation in *Drosophila*, HP1 binding motifs have not been described in other H4K20 methyltransferases (Yang et al., 2008). As such, H4K20me3 is diffuse throughout the nucleus in *S. pombe* rather than concentrated at heterochromatic foci (Sanders et al., 2004). Notably, Set9 requires interaction with a PWWP domain-containing protein, Pdp1, in order to methylate H4K20 (Wang et al., 2009). The Pdp1-binding region of Set9 remains undescribed. Further studies are needed to understand whether SET-4 interacts with other proteins to regulate its function *in vivo*, and if so, whether H4K20 dimethylation and/or trimethylation are required for dauer arrest in response to stressful environmental conditions.

Other conserved proteins have been identified as having trimethylase activity on H4K20, and all identified enzymes have worm homologs (Dai et al., 2017; Foreman et al., 2011; Kidder et al., 2017; Stender et al., 2012). Intriguingly, a recent study into *Artemia* developmental diapause implicated SETD4 in specific trimethylation of a dimethylated H4K20 substrate (Dai et al.,

2017). SETD4 and associated H4K20me3 were required for *Artemia* larval arrest under adverse environmental conditions, analogous to *C. elegans* requiring SET-4. Examining strains deficient in these putative trimethylases may clarify the role of SUV4-20 enzymes like SET-4 in establishing trimethylation of H4K20. Finding ways to parse dimethylation and trimethylation may be critical to resolving the conflicting findings between SET-4 being required for dosage compensation while higher order H4K20 methylation states are depleted on X in a DCC-dependent manner. Separating these two marks may also resolve the role of H4K20me3 enrichment in aging organisms as either a progeric program that promotes senescence or a protective response against genomic stress that puts a brake on inappropriate cell proliferation.

Are other epigenetic enzymes necessary for dauer arrest?

There is evidence that certain epigenetic programs involved in heterochromatin formation contribute to longevity in addition to SET-4. Whether overexpression of SIR-2.1 increases longevity has been controversial due to genetic background (Burnett et al., 2011; Lombard et al., 2011; Viswanathan and Guarente, 2011). Nevertheless, such a finding would be consistent with the established antagonistic role of H4K20 methylation and H4K16 acetylation. Further, knockdown of many histone methyltransferases extends mean lifespan, including the H3K4-targeting Trithorax complex components *set-2* and *ash-2* (Greer et al., 2010; Greer et al., 2011). Unlike H4K20, H3K4 methylation is strongly associated with active gene expression. Similarly, loss of the heterochromatin protein 1 ortholog *hpl-2*, which upregulates germ line gene expression, modestly increases lifespan and augments dauer in animals with enhanced DAF-16/FoxO activity (Meister et al., 2010). However, the roles of epigenetic enzymes in regulation of dauer arrest remains broadly unexplored. Deposition of H4K20 methylation is linked to the establishment of a heterochromatic landscape through the de-acetylation of H4K16 and the trimethylation of H3K9. Further, these marks have been associated with X chromosome regulation (Snyder et al., 2016; Wells et al., 2012). Our data suggests that systematically disrupting genes encoding epigenetic readers, writers and erasers may uncover novel influences on DAF-16/FoxO activity in development and longevity. Indeed, the intermediate dauer phenotype of *set-4;daf-2* double mutants may provide a sensitized background within which to interrogate the contributions of candidate epigenetic modifiers to this model of developmental

plasticity. Findings in this context may lead to greater insight regarding how conserved epigenetic mechanisms regulate FoxO transcription factors in development and longevity.

Summary

We endeavored to understand how epigenetic regulators associated with dosage compensation promote DAF-16/FoxO activity. The work contained within this dissertation demonstrates that SET-4 and DPY-21 synergize with DAF-16 during development to promote dauer diapause through repression of X-linked insulin-like signaling genes, including insulin-like peptide *ins-9*. In answering this basic question, we have opened new avenues of investigation in to the complex regulation of developmental plasticity and longevity. We created new tools with which to explore heretofore-unaddressed gaps in our knowledge regarding the integration of transcription factor activity, chromatin packaging, and environmental cues to produce radically different developmental strategies. These and subsequent findings may contribute to understanding similar interplay in human tissues leading to novel interventions to address chronic diseases of aging.

References

Alam, H., Williams, T. W., Dumas, K. J., Guo, C., Yoshina, S., Mitani, S. and Hu, P. J. (2010). EAK-7 controls development and life span by regulating nuclear DAF-16/FoxO activity. *Cell Metab* 12, 30-41.

Ambrogini, E., Almeida, M., Martin-Millan, M., Paik, J. H., Depinho, R. A., Han, L., Goellner, J., Weinstein, R. S., Jilka, R. L., O'Brien, C. A., et al. (2010). FoxO-mediated defense against oxidative stress in osteoblasts is indispensable for skeletal homeostasis in mice. *Cell Metab* 11, 136-146.

Bajic, V., Mandusic, V., Stefanova, E., Bozovic, A., Davidovic, R., Zivkovic, L., Cabarkapa, A. and Spremo-Potparevic, B. (2015). Skewed X-chromosome inactivation in women affected by Alzheimer's disease. *J Alzheimers Dis* 43, 1251-1259.

Bargmann, C. I. and Horvitz, H. R. (1991). Control of larval development by chemosensory neurons in Caenorhabditis elegans. *Science* 251, 1243-1246.

Bishop, N. A. and Guarente, L. (2007). Two neurons mediate diet-restriction-induced longevity in C. elegans. *Nature* 447, 545-549.

Bluher, M., Kahn, B. B. and Kahn, C. R. (2003). Extended longevity in mice lacking the insulin receptor in adipose tissue. *Science* 299, 572-574.

Burnett, C., Valentini, S., Cabreiro, F., Goss, M., Somogyvari, M., Piper, M. D., Hoddinott, M., Sutphin, G. L., Leko, V., McElwee, J. J., et al. (2011). Absence of effects of Sir2 overexpression on lifespan in C. elegans and Drosophila. *Nature* 477, 482-485.

Cornils, A., Gloeck, M., Chen, Z., Zhang, Y. and Alcedo, J. (2011). Specific insulin-like peptides encode sensory information to regulate distinct developmental processes. *Development* 138, 1183-1193.

Dai, L., Ye, S., Li, H. W., Chen, D. F., Wang, H. L., Jia, S. N., Lin, C., Yang, J. S., Yang, F., Nagasawa, H., et al. (2017). SETD4 Regulates Cell Quiescence and Catalyzes the Trimethylation of H4K20 during Diapause Formation in Artemia. *Mol Cell Biol* 37.

Delaney, C. E., Chen, A. T., Graniel, J. V., Dumas, K. J. and Hu, P. J. (2017). A histone H4 lysine 20 methyltransferase couples environmental cues to sensory neuron control of developmental plasticity. *Development*.

Dickinson, D. J., Pani, A. M., Heppert, J. K., Higgins, C. D. and Goldstein, B. (2015). Streamlined Genome Engineering with a Self-Excising Drug Selection Cassette. *Genetics* 200, 1035-1049.

Dudakovic, A., Camilleri, E. T., Riester, S. M., Paradise, C. R., Gluscevic, M., O'Toole, T. M., Thaler, R., Evans, J. M., Yan, H., Subramaniam, M., et al. (2016). Enhancer of Zeste Homolog 2 Inhibition Stimulates Bone Formation and Mitigates Bone Loss Caused by Ovariectomy in Skeletally Mature Mice. *J Biol Chem* 291, 24594-24606.

Dudakovic, A., Evans, J. M., Li, Y., Middha, S., McGee-Lawrence, M. E., van Wijnen, A. J. and Westendorf, J. J. (2013). Histone deacetylase inhibition promotes osteoblast maturation by altering the histone H4 epigenome and reduces Akt phosphorylation. *J Biol Chem* 288, 28783-28791.

Dumas, K. J., Delaney, C. E., Flibotte, S., Moerman, D. G., Csankovszki, G. and Hu, P. J. (2013). Unexpected role for dosage compensation in the control of dauer arrest, insulin-like signaling, and FoxO transcription factor activity in Caenorhabditis elegans. *Genetics* 194, 619-629.

Farboud, B. and Meyer, B. J. (2015). Dramatic enhancement of genome editing by CRISPR/Cas9 through improved guide RNA design. *Genetics* 199, 959-971.
Foreman, K. W., Brown, M., Park, F., Emtage, S., Harriss, J., Das, C., Zhu, L., Crew, A., Arnold, L., Shaaban, S., et al. (2011). Structural and functional profiling of the human histone methyltransferase SMYD3. *PLoS One* 6, e22290.
Frokjaer-Jensen, C., Davis, M. W., Hollopeter, G., Taylor, J., Harris, T. W., Nix, P., Lofgren, R., Prestgard-Duke, M., Bastiani, M., Moerman, D. G., et al. (2010). Targeted gene deletions in C. elegans using transposon excision. *Nat Methods* 7, 451-453.
Gentilini, D., Castaldi, D., Mari, D., Monti, D., Franceschi, C., Di Blasio, A. M. and Vitale, G. (2012). Age-dependent skewing of X chromosome inactivation appears delayed in centenarians' offspring. Is there a role for allelic imbalance in healthy aging and longevity? *Aging Cell* 11, 277-283.
Greer, E. L., Beese-Sims, S. E., Brookes, E., Spadafora, R., Zhu, Y., Rothbart, S. B., Aristizabal-Corrales, D., Chen, S., Badeaux, A. I., Jin, Q., et al. (2014). A histone methylation network regulates transgenerational epigenetic memory in C. elegans. *Cell Rep* 7, 113-126.
Greer, E. L. and Brunet, A. (2009). Different dietary restriction regimens extend lifespan by both independent and overlapping genetic pathways in C. elegans. *Aging Cell* 8, 113-127.
Greer, E. L., Maures, T. J., Hauswirth, A. G., Green, E. M., Leeman, D. S., Maro, G. S., Han, S., Banko, M. R., Gozani, O. and Brunet, A. (2010). Members of the H3K4 trimethylation complex regulate lifespan in a germline-dependent manner in C. elegans. *Nature* 466, 383-387.
Greer, E. L., Maures, T. J., Ucar, D., Hauswirth, A. G., Mancini, E., Lim, J. P., Benayoun, B. A., Shi, Y. and Brunet, A. (2011). Transgenerational epigenetic inheritance of longevity in Caenorhabditis elegans. *Nature* 479, 365-371.
Hahm, J. H., Kim, S. and Paik, Y. K. (2009). Endogenous cGMP regulates adult longevity via the insulin signaling pathway in Caenorhabditis elegans. *Aging Cell* 8, 473-483.
Hansen, M., Hsu, A. L., Dillin, A. and Kenyon, C. (2005). New genes tied to endocrine, metabolic, and dietary regulation of lifespan from a Caenorhabditis elegans genomic RNAi screen. *PLoS Genet* 1, 119-128.
Heestand, B. N., Shen, Y., Liu, W., Magner, D. B., Storm, N., Meharg, C., Habermann, B. and Antebi, A. (2013). Dietary restriction induced longevity is mediated by nuclear receptor NHR-62 in Caenorhabditis elegans. *PLoS Genet* 9, e1003651.
Honda, Y., Fujita, Y., Maruyama, H., Araki, Y., Ichihara, K., Sato, A., Kojima, T., Tanaka, M., Nozawa, Y., Ito, M., et al. (2011). Lifespan-extending effects of royal jelly and its related substances on the nematode Caenorhabditis elegans. *PLoS One* 6, e23527.
Hu, P. J. (2007). Dauer. *WormBook*, 1-19.
Hu, P. J., Xu, J. and Ruvkun, G. (2006). Two membrane-associated tyrosine phosphatase homologs potentiate C. elegans AKT-1/PKB signaling. *PLoS Genet* 2, e99.
Itani, O. A., Flibotte, S., Dumas, K. J., Guo, C., Blumenthal, T. and Hu, P. J. (2016). N-Ethyl-N-Nitrosourea (ENU) Mutagenesis Reveals an Intronic Residue Critical for Caenorhabditis elegans 3' Splice Site Function in Vivo. *G3 (Bethesda)* 6, 1751-1756.
Itani, O. A., Flibotte, S., Dumas, K. J., Moerman, D. G. and Hu, P. J. (2015). Chromoanasynthetic Genomic Rearrangement Identified in a N-Ethyl-N-Nitrosourea (ENU) Mutagenesis Screen in Caenorhabditis elegans. *G3 (Bethesda)* 6, 351-356.

Kenyon, C., Chang, J., Gensch, E., Rudner, A. and Tabtiang, R. (1993). A C. elegans mutant that lives twice as long as wild type. *Nature* 366, 461-464.
Khani, F., Thaler, R., Paradise, C. R., Deyle, D. R., Kruijthof-de Julio, M., Galindo, M., Gordon, J. A., Stein, G. S., Dudakovic, A. and van Wijnen, A. J. (2017). Histone H4 Methyltransferase Suv420h2 Maintains Fidelity of Osteoblast Differentiation. *J Cell Biochem* 118, 1262-1272.
Kidder, B. L., Hu, G., Cui, K. and Zhao, K. (2017). SMYD5 regulates H4K20me3-marked heterochromatin to safeguard ES cell self-renewal and prevent spurious differentiation. *Epigenetics Chromatin* 10, 8.
Kramer, M., Kranz, A. L., Su, A., Winterkorn, L. H., Albritton, S. E. and Ercan, S. (2015). Developmental Dynamics of X-Chromosome Dosage Compensation by the DCC and H4K20me1 in C. elegans. *PLoS Genet* 11, e1005698.
Kumar, N., Jain, V., Singh, A., Jagtap, U., Verma, S. and Mukhopadhyay, A. (2015). Genome-wide endogenous DAF-16/FOXO recruitment dynamics during lowered insulin signalling in C. elegans. *Oncotarget* 6, 41418-41433.
Lau, A. C., Nabeshima, K. and Csankovszki, G. (2014). The C. elegans dosage compensation complex mediates interphase X chromosome compaction. *Epigenetics Chromatin* 7, 31.
Leopold, L. E., Heestand, B. N., Seong, S., Shtessel, L. and Ahmed, S. (2015). Lack of pairing during meiosis triggers multigenerational transgene silencing in Caenorhabditis elegans. *Proc Natl Acad Sci U S A* 112, E2667-2676.
Li, C. J., Chang, J. K., Chou, C. H., Wang, G. J. and Ho, M. L. (2010). The PI3K/Akt/FOXO3a/p27Kip1 signaling contributes to anti-inflammatory drug-suppressed proliferation of human osteoblasts. *Biochem Pharmacol* 79, 926-937.
Li, W., Kennedy, S. G. and Ruvkun, G. (2003). daf-28 encodes a C. elegans insulin superfamily member that is regulated by environmental cues and acts in the DAF-2 signaling pathway. *Genes Dev* 17, 844-858.
Lombard, D. B., Pletcher, S. D., Canto, C. and Auwerx, J. (2011). Ageing: longevity hits a roadblock. *Nature* 477, 410-411.
Luteijn, M. J., van Bergeijk, P., Kaaij, L. J., Almeida, M. V., Roovers, E. F., Berezikov, E. and Ketting, R. F. (2012). Extremely stable Piwi-induced gene silencing in Caenorhabditis elegans. *Embo J* 31, 3422-3430.
Matsunaga, Y., Gengyo-Ando, K., Mitani, S., Iwasaki, T. and Kawano, T. (2012). Physiological function, expression pattern, and transcriptional regulation of a Caenorhabditis elegans insulin-like peptide, INS-18. *Biochem Biophys Res Commun* 423, 478-483.
Meister, P., Towbin, B. D., Pike, B. L., Ponti, A. and Gasser, S. M. (2010). The spatial dynamics of tissue-specific promoters during C. elegans development. *Genes & development* 24, 766-782.
Melo, J. A. and Ruvkun, G. (2012). Inactivation of conserved C. elegans genes engages pathogen- and xenobiotic-associated defenses. *Cell* 149, 452-466.
Obata, F. and Miura, M. (2015). Enhancing S-adenosyl-methionine catabolism extends Drosophila lifespan. *Nat Commun* 6, 8332.
Paix, A., Folkmann, A., Rasoloson, D. and Seydoux, G. (2015). High Efficiency, Homology-Directed Genome Editing in Caenorhabditis elegans Using CRISPR-Cas9 Ribonucleoprotein Complexes. *Genetics* 201, 47-54.

Rached, M. T., Kode, A., Xu, L., Yoshikawa, Y., Paik, J. H., Depinho, R. A. and Kousteni, S. (2010). FoxO1 is a positive regulator of bone formation by favoring protein synthesis and resistance to oxidative stress in osteoblasts. *Cell Metab* 11, 147-160.

Ren, P., Lim, C. S., Johnsen, R., Albert, P. S., Pilgrim, D. and Riddle, D. L. (1996). Control of C. elegans larval development by neuronal expression of a TGF-beta homolog. *Science* 274, 1389-1391.

Riedel, C. G., Dowen, R. H., Lourenco, G. F., Kirienko, N. V., Heimbucher, T., West, J. A., Bowman, S. K., Kingston, R. E., Dillin, A., Asara, J. M., et al. (2013). DAF-16 employs the chromatin remodeller SWI/SNF to promote stress resistance and longevity. *Nature cell biology* 15, 491-501.

Sanders, S. L., Portoso, M., Mata, J., Bahler, J., Allshire, R. C. and Kouzarides, T. (2004). Methylation of histone H4 lysine 20 controls recruitment of Crb2 to sites of DNA damage. *Cell* 119, 603-614.

Schackwitz, W. S., Inoue, T. and Thomas, J. H. (1996). Chemosensory neurons function in parallel to mediate a pheromone response in C. elegans. *Neuron* 17, 719-728.

Schaedel, O. N., Gerisch, B., Antebi, A. and Sternberg, P. W. (2012). Hormonal signal amplification mediates environmental conditions during development and controls an irreversible commitment to adulthood. *PLoS Biol* 10, e1001306.

Schotta, G., Lachner, M., Sarma, K., Ebert, A., Sengupta, R., Reuter, G., Reinberg, D. and Jenuwein, T. (2004). A silencing pathway to induce H3-K9 and H4-K20 trimethylation at constitutive heterochromatin. *Genes Dev* 18, 1251-1262.

Schotta, G., Sengupta, R., Kubicek, S., Malin, S., Kauer, M., Callen, E., Celeste, A., Pagani, M., Opravil, S., De La Rosa-Velazquez, I. A., et al. (2008). A chromatin-wide transition to H4K20 monomethylation impairs genome integrity and programmed DNA rearrangements in the mouse. *Genes Dev* 22, 2048-2061.

Sharma, R. and Meister, P. (2015). Linking dosage compensation and X chromosome nuclear organization in C. elegans. *Nucleus* 6, 266-272.

Shirayama, M., Seth, M., Lee, H. C., Gu, W., Ishidate, T., Conte, D., Jr. and Mello, C. C. (2012). piRNAs initiate an epigenetic memory of nonself RNA in the C. elegans germline. *Cell* 150, 65-77.

Smothers, J. F. and Henikoff, S. (2000). The HP1 chromo shadow domain binds a consensus peptide pentamer. *Curr Biol* 10, 27-30.

Snyder, M. J., Lau, A. C., Brouhard, E. A., Davis, M. B., Jiang, J., Sifuentes, M. H. and Csankovszki, G. (2016). Anchoring of Heterochromatin to the Nuclear Lamina Reinforces Dosage Compensation-Mediated Gene Repression. *PLoS Genet* 12, e1006341.

Southall, S. M., Cronin, N. B. and Wilson, J. R. (2014). A novel route to product specificity in the Suv4-20 family of histone H4K20 methyltransferases. *Nucleic Acids Res* 42, 661-671.

Souza, P. P., Volkel, P., Trinel, D., Vandamme, J., Rosnoblet, C., Heliot, L. and Angrand, P. O. (2009). The histone methyltransferase SUV420H2 and Heterochromatin Proteins HP1 interact but show different dynamic behaviours. *BMC Cell Biol* 10, 41.

Stender, J. D., Pascual, G., Liu, W., Kaikkonen, M. U., Do, K., Spann, N. J., Boutros, M., Perrimon, N., Rosenfeld, M. G. and Glass, C. K. (2012). Control of proinflammatory gene programs by regulated trimethylation and demethylation of histone H4K20. *Molecular cell* 48, 28-38.

Thepot, S., Lainey, E., Cluzeau, T., Sebert, M., Leroy, C., Ades, L., Tailler, M., Galluzzi, L., Baran-Marszak, F., Roudot, H., et al. (2011). Hypomethylating agents reactivate FOXO3A in acute myeloid leukemia. *Cell Cycle* 10, 2323-2330.

Thomas, J. H., Birnby, D. A. and Vowels, J. J. (1993). Evidence for parallel processing of sensory information controlling dauer formation in Caenorhabditis elegans. *Genetics* 134, 1105-1117.

Towbin, B. D., Gonzalez-Aguilera, C., Sack, R., Gaidatzis, D., Kalck, V., Meister, P., Askjaer, P. and Gasser, S. M. (2012). Step-wise methylation of histone H3K9 positions heterochromatin at the nuclear periphery. *Cell* 150, 934-947.

Vielle, A., Lang, J., Dong, Y., Ercan, S., Kotwaliwale, C., Rechtsteiner, A., Appert, A., Chen, Q. B., Dose, A., Egelhofer, T., et al. (2012). H4K20me1 contributes to downregulation of X-linked genes for C. elegans dosage compensation. *PLoS genetics* 8, e1002933.

Viswanathan, M. and Guarente, L. (2011). Regulation of Caenorhabditis elegans lifespan by sir-2.1 transgenes. *Nature* 477, E1-2.

Wang, Y., Reddy, B., Thompson, J., Wang, H., Noma, K., Yates, J. R., 3rd and Jia, S. (2009). Regulation of Set9-mediated H4K20 methylation by a PWWP domain protein. *Mol Cell* 33, 428-437.

Webster, C. M., Wu, L., Douglas, D. and Soukas, A. A. (2013). A non-canonical role for the C. elegans dosage compensation complex in growth and metabolic regulation downstream of TOR complex 2. *Development* 140, 3601-3612.

Weirich, S., Kudithipudi, S. and Jeltsch, A. (2016). Specificity of the SUV4-20H1 and SUV4-20H2 protein lysine methyltransferases and methylation of novel substrates. *J Mol Biol* 428, 2344-2358.

Wells, M. B., Snyder, M. J., Custer, L. M. and Csankovszki, G. (2012). Caenorhabditis elegans dosage compensation regulates histone H4 chromatin state on X chromosomes. *Molecular and cellular biology* 32, 1710-1719.

Wu, H., Siarheyeva, A., Zeng, H., Lam, R., Dong, A., Wu, X. H., Li, Y., Schapira, M., Vedadi, M. and Min, J. (2013). Crystal structures of the human histone H4K20 methyltransferases SUV420H1 and SUV420H2. *FEBS Lett* 587, 3859-3868.

Xu, M., Xie, L., Yu, Z. and Xie, J. (2015). Roles of Protein N-Myristoylation and Translational Medicine Applications. *Crit Rev Eukaryot Gene Expr* 25, 259-268.

Yamamoto, R. and Tatar, M. (2011). Insulin receptor substrate chico acts with the transcription factor FOXO to extend Drosophila lifespan. *Aging Cell* 10, 729-732.

Yang, H., Pesavento, J. J., Starnes, T. W., Cryderman, D. E., Wallrath, L. L., Kelleher, N. L. and Mizzen, C. A. (2008). Preferential dimethylation of histone H4 lysine 20 by Suv4-20. *J Biol Chem* 283, 12085-12092.

Yurov, Y. B., Vorsanova, S. G., Liehr, T., Kolotii, A. D. and Iourov, I. Y. (2014). X chromosome aneuploidy in the Alzheimer's disease brain. *Mol Cytogenet* 7, 20.

Zhang, W., Ji, W., Yang, L., Xu, Y., Zhang, W. and Zhuang, Z. (2010). [Epigenetic activation of IGF2 during cellular senescence]. *Wei Sheng Yan Jiu* 39, 1-3, 8.